IL
NUOVO CIMENTO
ORGANO DELLA SOCIETÀ ITALIANA DI FISICA
SOTTO GLI AUSPICI DEL CONSIGLIO NAZIONALE DELLE RICERCHE

VOL. II, N. 1 *Serie decima* 1° Luglio 1955

Sull'emissione di fotoni nell'approssimazione di Bloch e Nordsieck.

R. ASCOLI

Istituto di Fisica dell'Università - Torino
Istituto Nazionale di Fisica Nucleare - Sezione di Torino

(ricevuto il 21 Aprile 1955)

Riassunto. — Si esaminano le proprietà caratteristiche dell'emissione di infiniti fotoni che, secondo la trattazione di BLOCH e NORDSIECK, si verifica in ogni processo in cui una particella carica, di impulso iniziale determinato, acquista un impulso finale pure determinato e diverso da quello iniziale. Si trova che, nel caso di carica elettronica, la probabilità che almeno uno di tali fotoni cada nell'intervallo di frequenze che interessa in condizioni sperimentali ordinarie è al più dell'ordine di alcuni centesimi, in accordo con le conclusioni del metodo perturbativo. Non è però escluso che nel caso degli urti nucleari più energici che si hanno nei raggi cosmici tale probabilità possa avvicinarsi all'unità. I risultati dipendono poi fortemente dal valore della carica, e per cariche nucleari la probabilità di emissione di più fotoni risulta notevolmente accresciuta. Nel caso poi di cariche macroscopiche si ha normalmente emissione multipla.

Come è stato dimostrato da BLOCH e NORDSIECK [1], in un processo nel quale una particella carica di impulso iniziale determinato acquista un impulso finale pure determinato e diverso da quello iniziale, vengono emessi, secondo l'elettrodinamica quantistica, infiniti fotoni. Ci proponiamo qui di studiare le

[1] F. BLOCH e A. NORDSIECK: *Phys. Rev.*, **52**, 54 (1937).

proprietà caratteristiche dell'emissione di tali fotoni, e di esaminare sommariamente in quali tipi di fenomeni si possano avere condizioni nelle quali con notevole probabilità più fotoni cadano nel campo di frequenze che interessa sperimentalmente.

Il calcolo di Bloch e Nordsieck presuppone l'uso dell'approssimazione in cui si trascura la reazione del campo elettromagnetico sulle cariche, approssimazione valida quando si prenda in considerazione solo l'interazione con fotoni di energia sufficientemente piccola (in un determinato sistema di riferimento). Il risultato (emissione di infiniti fotoni) mostra che il termine di ordine n della serie perturbativa che dà la matrice S non tende a zero per n tendente ad infinito, se si considera l'interazione con fotoni di energia comunque bassa. Prescindendo qui da eventuali altre cause di non convergenza, la serie stessa è d'altra parte convergente quando se ne calcolino i termini considerando solo l'interazione con fotoni di energia superiore ad un qualsiasi valore k prefissato. Se si considerano i termini della serie come funzioni di k, si può quindi affermare che la serie stessa non è uniformemente convergente rispetto alla variabile k nell'intorno dello zero. Il procedimento da usare quando si voglia trattare l'interazione con fotoni di tutte le energie è quindi il seguente [2]:

a) Trattare con il metodo perturbativo, o con altri metodi, o anche supporre noti dall'esperienza, gli effetti dell'interazione delle particelle cariche con particelle diverse da fotoni e con fotoni di energia superiore ad un valore k_M, scelto in modo che si possa ritener lecito trascurare, in tale studio, l'effetto dell'interazione con fotoni di energia inferiore.

b) Trattare l'interazione con i fotoni di energia inferiore a k_M con il metodo di Bloch e Nordsieck, trascurando cioè la reazione del campo sulle cariche, e supponendo di aver ricavato la distribuzione di queste nel modo indicato in *a*).

Il problema dell'emissione di fotoni di energia sufficientemente bassa da parte di una particella carica, in un processo in cui la sua funzione d'onda varia in modo noto, si può quindi studiare prescindendo dalla natura del processo. Supporremo qui che la particella si possa ritenere puntiforme. In tale caso l'emissione di fotoni di bassa energia dipende solo dagli impulsi iniziale p_μ e finale p'_μ (che supponiamo determinati) della particella stessa ed è per il resto del tutto indipendente dal processo che si considera (scattering da parte di un nucleo, bremsstrahlung, doppia bremsstrahlung, ecc.). La grandezza che ci interessa maggiormente calcolare è il numero medio di fotoni emessi con impulsi compresi in un prefissato campo Δ. Usiamo la formula data da THIRRING

---

[2] Vedi: R. JOST: *Phys. Rev.*, **72**, 815 (1947).

e TOUSCHEK [3], per fotoni di dato vettore di polarizzazione e_μ [4]:

$$\overline{N} = \frac{e^2}{(2\pi)^3} \int_A \mathrm{d}^4k\, \delta(k^2) \left| \frac{(pe)}{(pk)} - \frac{(p'e)}{(p'k)} \right|^2 .$$

Si ricava che il numero medio di fotoni di impulso k_μ e polarizzazione e_μ emessi per unità di volume nello spazio dei vettori $\boldsymbol{k}$ è:

$$\frac{e^2}{(2\pi)^3} \frac{1}{2|\boldsymbol{k}|} \left| \frac{(pe)}{(pk)} - \frac{(p'e)}{(p'k)} \right|^2$$

e il numero medio $\overline{n}(k_\mu, e_\mu)$ di fotoni di impulso k_μ e polarizzazione e_μ emessi per unità di intervallo di energia e di angolo solido è:

$$\overline{n}(k_\mu, e_\mu) = \frac{e^2}{(2\pi)^3} \frac{|\boldsymbol{k}|}{2} \left| \frac{(pe)}{(pk)} - \frac{(p'e)}{(p'k)} \right|^2 . \tag{1}$$

Uno dei sistemi di riferimento nei quali i calcoli sono più semplici è quello di riposo della particella nello stato finale $\boldsymbol{p}' = 0$. Riferendoci a tale sistema scegliamo nullo il potenziale scalare del campo dei fotoni emessi: si ha in tal caso $e_0 = 0$ e

$$\overline{n}(k_\mu, e_\mu) = \frac{e^2}{(2\pi^3)} \frac{|\boldsymbol{k}|}{2} \left| \frac{\boldsymbol{p} \times \boldsymbol{e}}{\boldsymbol{p} \times \boldsymbol{k} - \beta^{-1} |\boldsymbol{p}|\, |\boldsymbol{k}|} \right|^2$$

essendo β la velocità iniziale della particella (in unità $c=1$).

Indichiamo con θ l'angolo dei vettori $\boldsymbol{p}$ e $\boldsymbol{k}$ ed assumiamo come vettori di polarizzazione indipendenti $\boldsymbol{e}_1$ nel piano di $\boldsymbol{p}$ e $\boldsymbol{k}$ ed $\boldsymbol{e}_2$ perpendicolare a tale piano. Si ha:

$$\overline{n}(k_\mu, e_{1\mu}) = \frac{e^2}{(2\pi)^3} \frac{1}{2|\boldsymbol{k}|} \frac{\sin^2\theta}{(\beta^{-1} - \cos\theta)^2} , \qquad \overline{n}(k_\mu, e_{2\mu}) = 0. \tag{2}$$

Segue di qui che nel sistema in cui $\boldsymbol{p}' = 0$:

1) Il vettore di polarizzazione dei fotoni emessi giace nel piano che contiene i vettori $\boldsymbol{p}$ e $\boldsymbol{k}$.

2) Lo spettro dei fotoni emessi in una data direzione (e quindi anche

---

[3] W. THIRRING e B. TOUSCHEK: *Phil. Mag.*, 42, 245 (1951). La formula è stata dedotta nell'ipotesi dell'elettrone classico. Essa vale però anche senza tale ipotesi: vedi J. M. JAUCH e F. ROHRLICH: *Helv. Phys. Acta*, 27, 613 (1954). Tale formula e tutte le successive valgono anche per l'emissione di fotoni in un processo di produzione o distruzione di una coppia di particelle di segno opposto, di impulsi determinati p_μ e p'_μ.

[4] Nelle formule si usano unità di misura per cui $\hbar = 1$, $c = 1$; la carica elettrica viene misurata in unità razionalizzate.

di quelli emessi in tutte le direzioni) è di tipo iperbolico [5]. Risulta quindi un'emissione di infiniti fotoni nell'intervallo di frequenze compreso tra zero ed un qualsiasi valore e vi è un numero medio costante di fotoni per ogni intervallo di frequenze, per cui il rapporto delle frequenze estreme sia costante: il numero medio di fotoni emessi in una direzione che formi un angolo θ con il vettore $\boldsymbol{p}$, per unità di angolo solido e per unità di intervallo logaritmico di energia è:

$$(3) \qquad \bar{n}_1(\theta) = \frac{1}{2}\,\frac{e^2}{(2\pi)^3}\,\frac{\sin^2\theta}{(\beta^{-1}-\cos\theta)^2}\,.$$

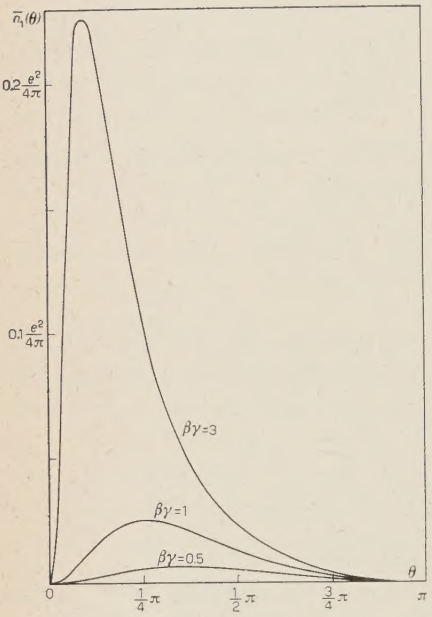

Fig. 1. – Distribuzione angolare dei fotoni emessi per vari valori di $\beta\gamma = |\boldsymbol{p}|/m$, nel sistema in cui $\boldsymbol{p}'=0$. Ascisse: angolo θ formato con il vettore $\boldsymbol{p}$. Ordinate: numero medio di fotoni $\bar{n}_1(\theta)$ per steradiante e per unità di intervallo logaritmico di energia.

3) La distribuzione angolare (indipendente dalla frequenza) è tale che $\bar{n}_1(\theta)$ per $\theta=0$ e per $\theta=\pi$ presenta zeri di 2° ordine e per $\cos\theta=\beta$ presenta un massimo $\frac{1}{2}[e^2/(2\pi)^3]\beta^2\gamma^2$, essendo $\gamma = 1/\sqrt{1-\beta^2}$.

Nel caso non relativistico, $\beta\gamma \ll 1$, il massimo si ha per $\theta \cong \pi/2$ ed è appiattito; la distribuzione angolare segue approssimativamente l'andamento della funzione $\sin^2\theta$.

Nel caso opposto $\beta\gamma \gg 1$ il massimo si ha per $\theta \cong \gamma^{-1}$ ed è tanto più pronunciato quanto più $\beta\gamma$ è elevato. Effettuando l'integrazione rispetto all'angolo solido si conclude che in tal caso il maggior contributo all'emissione di fotoni è dato da quelli il cui impulso forma con il vettore $\boldsymbol{p}$ un angolo dell'ordine di γ^{-1}.

L'andamento della funzione $\bar{n}_1(\theta)$ per vari valori di $\beta\gamma = |\boldsymbol{p}|/m$ è dato in fig. 1.

4) Il numero medio totale $\bar{N}$ di fotoni emessi tra le energie k_m e k_M (nel sistema in cui $\boldsymbol{p}'=0$) è dato da:

$$(4) \qquad \bar{N} = 2\pi \int_{k_m}^{k_M} \mathrm{d}|\boldsymbol{k}| \int_0^{\pi} \mathrm{d}\theta \sin\theta\, \bar{n} = \frac{e^2}{(2\pi)^2} \ln\frac{k_M}{k_m}\left(\frac{1}{\beta}\ln\frac{1+\beta}{1-\beta} - 2\right) =$$

$$= \frac{e^2}{2\pi^2} \ln\frac{k_M}{k_m}\left[\frac{\sqrt{1+(\beta\gamma)^2}}{\beta\gamma}\ln\left(\beta\gamma+\sqrt{1+(\beta\gamma)^2}\right) - 1\right];$$

[5] Questo vale in ogni sistema di riferimento.

$\bar{N}$ è funzione crescente di $\beta\gamma = |\boldsymbol{p}|/m$; per $\beta\gamma \ll 1$ si ha approssimativamente

$$\bar{N} \cong \frac{1}{3}\frac{e^2}{2\pi^2} \ln \frac{k_M}{k_m} (\beta\gamma)^2 ; \tag{5}$$

per $\beta \gg 1$ si ha invece

$$\bar{N} \cong \frac{e^2}{2\pi^2} \ln \frac{k_M}{k_m} (\ln 2\beta\gamma - 1) . \tag{6}$$

In fig. 2 è rappresentato $\bar{N}_1 = \bar{N}/\ln (k_M/k_m)$ in funzione di $\beta\gamma = |\boldsymbol{p}|/m$.

Tenendo poi presente che nell'approssimazione di Bloch e Nordsieck i fotoni sono emessi indipendentemente, la probabilità w_N per l'emissione di N fotoni nel campo di energia considerato è data dalla formula di Poisson:

$$w_N = \frac{\bar{N}^N}{N!} \exp [-\bar{N}] . \tag{7}$$

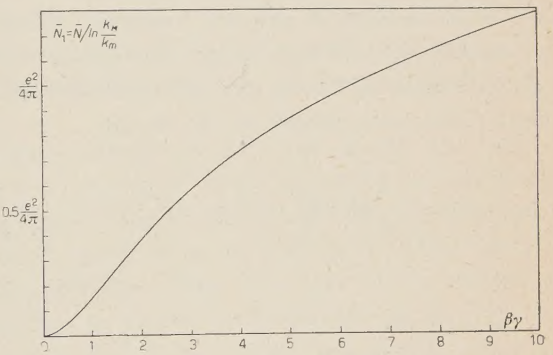

Fig. 2. – Numero medio $\bar{N}_1$ di fotoni emessi, per intervallo logaritmico unitario di energia, da una particella di carica e e impulso iniziale $|\boldsymbol{p}| = \beta\gamma m$, nel sistema di riferimento in cui si arresta.

Queste conclusioni valgono naturalmente solo per l'emissione di fotoni di frequenza sufficientemente bassa perchè si possa applicare l'approssimazione di Bloch e Nordsieck.

Il problema di sapere per quali fotoni sia valida tale approssimazione non si presenta in generale semplice. Sebbene sia desiderabile un esame più approfondito della questione, ci limiteremo qui ad alcune considerazioni sommarie. Poichè l'approssimazione di Bloch e Nordsieck consiste nel trascurare la reazione sulla particella carica dei fotoni di « bassa energia » emessi, si può ritenere che tale approssimazione sia buona allorchè, nel sistema in cui $\boldsymbol{p}' = 0$, la variazione di impulso da essi prodotta sulla particella sia piccola in confronto a quella propria del processo in esame. I risultati che, nella nostra approssimazione, dipendono unicamente dalla variazione totale di impulso $|\boldsymbol{p}| = \beta\gamma/m$ nel sistema in cui $\boldsymbol{p}' = 0$ sono allora poco influenzati da tali fotoni; questo vale in particolar modo nel caso relativistico per il numero totale di fotoni $\bar{N}$, che dipende solo logaritmicamente da $\beta\gamma$. Dove non si richieda grande precisione si può quindi ritener accettabile l'approssimazione di Bloch e Nordsieck per l'emissione di fotoni di impulso $\boldsymbol{k}$

inferiore in modulo almeno alcune volte all'impulso iniziale $\boldsymbol{p}$ della particella carica nel sistema di riferimento in cui si arresta (6).

Passando ora alla discussione dei risultati ottenuti osserviamo innanzitutto che nel caso di particella di carica elettronica ($e^2/2\pi^2 = 1/215$) in condizioni sperimentali ordinarie, cioè quando $\beta\gamma$ vale al più alcune unità e interessano i fotoni emessi in un campo di energie da k_m a k_M per cui $\ln(k_M/k_m)$ vale al più alcune unità, $\overline{N}$ è al massimo dell'ordine di grandezza di alcuni centesimi. Ciò significa che in media, su un centinaio di casi del processo preso in esame ve ne è al più qualcuno in cui si abbia emissione di un altro fotone nel campo di energie che interessa, oltre quelli eventualmente già emessi nel processo considerato. Questo fatto mostra qualitativamente che non vi è una contraddizione tra gli ordinari risultati dati dai primi termini dello sviluppo perturbativo e quelli del metodo di Bloch e Nordsieck. Sempre nelle stesse ipotesi, applicando le considerazioni svolte ad un processo di sezione d'urto σ_0, si ha poi dalla (7) per la sezione d'urto σ_0 del corrispondente processo in cui siano emessi N ulteriori fotoni con energie da k_m a k_M:

$$\sigma_N = \sigma_0 \frac{\overline{N}^N}{N!} \exp[-\overline{N}] \cong \sigma_0 \frac{\overline{N}^N}{N!} = \sigma_0 \frac{1}{N!} \left(\frac{e^2}{4\pi}\right)^N \frac{2^N}{\pi^N} \left(\ln \frac{k_M}{k_m}\right)^N \cdot$$

$$\cdot \left[\frac{\sqrt{1+(\beta\gamma)^2}}{\beta\gamma} \ln\left(\beta\gamma + \sqrt{1+(\beta\gamma)^2}\right) - 1\right]^N,$$

dove si è assunto $e^{-\overline{N}} \cong 1$ essendo nelle ipotesi fatte $\overline{N} \ll 1$. Il risultato conferma innanzitutto il fatto, intuibile col metodo perturbativo, che il rapporto tra la sezione d'urto per un processo in cui siano emessi N fotoni e quella per il corrispondente in cui ne siano emessi $N-1$ è grossolanamente dell'ordine di $1/137$ (7). Il risultato ottenuto mostra però che nel rapporto compare, oltre al fattore numerico costante, un fattore $1/N$ inversamente proporzionale al numero di fotoni emessi, un fattore crescente con l'energia iniziale della particella nel sistema in cui $\boldsymbol{p}' = 0$ (8), ed un fattore dipendente dal campo di frequenze considerato per i fotoni emessi. Quest'ultimo fattore fa sì che, nel

---

(6) Si può giungere a giustificare in modo più preciso questa condizione generalizzando le considerazioni sviluppate da R. JOST (vedi nota (2)), per il caso del doppio effetto Compton; vedi anche W. HEITLER: *The Quantum Theory of Radiation* (Zürich, 1953), p. 229.

(7) W. HEITLER: *The Quantum Theory of Radiation* (Dublin, 1944), p. 181.

(8) Per energie elevate tale fattore cresce logaritmicamente, ed è stato recentemente segnalato, in seguito ad una considerazione più accurata del metodo perturbativo nel caso del doppio effetto Compton, da W. HEITLER: *The Quantum Theory of Radiation* (Zürich, 1953), p. 227.

caso delle energie più elevate che compaiono nei raggi cosmici, la probabilità di processi di ordine maggiore risulti superiore a quella che si ha per energie più basse, in quanto il campo di frequenze dei fotoni che interessano risulta accresciuto.

Esaminiamo ora in quali circostanze $\overline{N}$ possa avere valori dell'ordine dell'unità o maggiori, e quindi si abbia con notevole probabilità l'emissione di uno o più fotoni nel campo di frequenze che si considera.

1) Nel caso di particelle di carica elettronica, aventi nel sistema in cui $\boldsymbol{p}' = 0$ energie relativistiche medie, per cui il fattore dipendente da $\beta\gamma$ nella (4) sia dell'ordine dell'unità, è $\overline{N} \geqslant 1$ se $k_M/k_m \gtrsim e^{215}$. Ammettendo anche che la particella sia un nucleone, e che si possa assumere $k_M = 10^9$ eV, si ha: $k_m \gtrsim 3 \cdot 10^{-85}$ eV. Questo significa che per poter rivelare in media anche uno solo degli infiniti fotoni emessi per ogni processo del tipo considerato, occorrerebbe poter disporre di mezzi atti a rivelare fotoni di energia dell'ordine di 10^{-85} eV. È chiaro che la considerazione di fotoni di tali energie è priva di ogni significato fisico (9).

Queste considerazioni si applicano a maggior ragione per energie non relativistiche. Si osservi inoltre che anche i fenomeni elettromagnetici più energici che si riscontrano nei raggi cosmici raramente si differenziano da quelli sopra esaminati, perchè è improbabile che il valore di $\beta\gamma$ nel sistema di riposo finale superi alcune unità; in tali casi il fenomeno viene osservato da un sistema di laboratorio in cui l'impulso finale ha un valore molto elevato $\beta_i'\gamma_i' m$, quindi in tale sistema di riferimento l'energia dei fotoni emessi nel sistema in cui $\boldsymbol{p}' = 0$ può risultare al più moltiplicata per γ_i'. Assumendo però per γ_i' valori anche molto elevati come 10^8, per avere $\overline{N}=1$, l'energia minima dei fotoni che occorrerebbe osservare sarebbe pur sempre dell'ordine di 10^{-77} eV, quindi le considerazioni svolte non sono modificate anche in questo caso.

2) Escludendo ora la considerazione di fotoni di energia così bassa, supponiamo di poter rivelare solo i fotoni di energia superiore ad un valore prefissato k_m, per esempio 1 eV (10), ed esaminiamo se $\overline{N}$ può assumere valori dell'ordine dell'unità per energie p_0 sufficientemente grandi (nel sistema in cui $\boldsymbol{p}' = 0$) della particella, di massa m e sempre di carica elettronica. Utilizziamo l'approssimazione relativistica (6) di $\overline{N}$, e poniamo come limite superiore dell'energia dei fotoni quella massima per cui si può ritenere applicabile il metodo di Bloch e Nordsieck, dell'ordine di γm. Poichè, come si è notato, è

---

(9) Basti osservare che la loro lunghezza d'onda è di gran lunga maggiore del « raggio dell'Universo ».

(10) È di questo ordine di grandezza la minima energia dei fotoni che si possono rivelare singolarmente con un'efficienza ragionevole usando i mezzi attualmente a nostra disposizione (fotomoltiplicatori con catodo sensibile all'infrarosso).

molto improbabile che in fenomeni elettromagnetici γ possa avere valori elevati [11], poniamo qui come esempio per m la massa del nucleone. Si ottiene:

$$\bar{N} \cong \frac{e^2}{2\pi^2} \ln \frac{\gamma^m}{k_m} (\ln 2\gamma - 1) \cong \frac{1}{215} \ln 10^9 \gamma (\ln \gamma - 0{,}3) .$$

Si ha di qui $\bar{N} = 1$ per $\gamma \cong 2\,500$, da cui $p_0 \cong 2{,}5 \cdot 10^{12}$ eV [12]. Quindi nel caso di fenomeni nucleari di energia elevatissima dei raggi cosmici sono forse possibili casi in cui si abbia con notevole probabilità l'emissione di uno o più fotoni nel campo di energie considerato; tali fotoni sarebbero emessi entro un angolo dell'ordine di γ^{-1} (nel sistema in cui $\boldsymbol{p}' = 0$) e quindi si avrebbe con la direzione della particella che li emette una correlazione angolare molto più stretta di quella propria dei mesoni prodotti. Per uno studio completo del fenomeno sarebbe poi necessaria una apposita trattazione, essendo esso accompagnato dalla produzione multipla di particelle cariche [13].

---

[11] Il fatto che γ possa avere valori molto elevati nel caso di fenomeni elettromagnetici è, se pure improbabile, teoricamente non impossibile. Se il fenomeno avesse luogo, sarebbe accompagnato, per energie elevatissime, da emissione di più fotoni con notevole probabilità. Le formule ottenute si possono, per esempio, applicare allo studio dell'emissione di N ulteriori fotoni nel processo in cui un positrone di energia $p_0 = \gamma m$ si annichila con un elettrone fermo emettendo due fotoni. Per $\gamma \gg 1$ si ha: $\bar{N} \cong (2/\pi) \cdot (e^2/4\pi) \ln (p_0/k_m) \ln (2p_0/m)$. Dalla (7) si ha per la sezione d'urto σ_N del processo:

$$\sigma_N = \sigma_0 \frac{\bar{N}^N}{N!} e^{-\bar{N}} \cong \left(\frac{e^2}{4\pi}\right)^N \frac{1}{N!} \frac{2^N}{\pi^N} \sigma_0 \left(\ln \frac{2p_0}{m}\right)^N \left(\ln \frac{p_0}{k_m}\right)^N e^{-\frac{2}{\pi}\frac{e^2}{4\pi} \ln \frac{2p_0}{m} \ln \frac{p_0}{k_m}} ,$$

essendo σ_0 la sezione d'urto per l'annichilazione dell'elettrone col positrone con emissione di due fotoni. Avendosi per energie elevate: $\sigma_0 \cong \pi (e^2/4\pi)^2 1/m p_0 \ln (2p_0/m)$, è:

$$\sigma_N \cong \left(\frac{e^2}{4\pi}\right)^{N+2} \frac{1}{N!} \frac{2^N}{\pi^{N-1}} \frac{1}{m p_0} \left(\ln \frac{2p_0}{m}\right)^{N+1} \left(\ln \frac{p_0}{k_m}\right)^N e^{-\frac{2}{\pi}\frac{e^2}{4\pi} \ln \frac{2p_0}{m} \ln \frac{p_0}{k_m}} .$$

Questa formula coincide, eccetto per la presenza dell'ultimo fattore esponenziale, con quella recentemente ottenuta, con approssimazioni valide per energie elevate, da S. N. Gupta (comunicazione privata) con l'uso del metodo perturbativo. L'assenza nel risultato perturbativo dell'ultimo fattore, che nei casi che interessano non è molto diverso da 1, è probabilmente dovuta al fatto che nel suddetto calcolo perturbativo non sono considerate le correzioni radiative.

Per energie del positone dell'ordine di grandezza di 10^{14} o 10^{16} eV, e quando si considerano i fotoni che possono interessare esperienze fatte con emulsioni fotografiche, σ_N è dello stesso ordine di σ_0 quando N vale alcune unità, però il fenomeno è praticamente impossibile perchè σ_0 è dell'ordine di 10^{-8} o 10^{-10} volte la sezione d'urto per bremsstrahlung.

[12] Questi valori si riducono se si osserva il fenomeno da un sistema di riferimento in cui l'impulso finale abbia un valore molto elevato, e si richiede che i fotoni emessi abbiano un'energia almeno di 1 eV in tale sistema.

[13] Si osservi che per poter eseguire il calcolo nell'approssimazione di Bloch e Nord-

È interessante notare che ci si trova nel caso qui esaminato anche se una particella (carica), pur subendo una piccola variazione di impulso, cede la carica ad un'altra particella che si trovi in un sistema di riferimento nel quale la particella incidente abbia un'energia dell'ordine di quelle sopra ricavate ([14]).

3) Mentre, come si è visto, il campo di frequenza dei fotoni considerati e l'energia della particella influiscono debolmente su $\bar{N}$, la carica della particella stessa ha invece su $\bar{N}$ una forte influenza. Considerando una particella di carica Ze si ha, invece della (4) ([15]):

$$\bar{N} = \frac{Z^2e^2}{2\pi^2} \ln \frac{k_M}{k_m} \left[\frac{\sqrt{1+(\beta\gamma)^2}}{\beta\gamma} \ln \left(\beta\gamma + \sqrt{1+(\beta\gamma)^2}\right) - 1 \right]. \tag{8}$$

Vi è quindi innanzitutto da attendersi, nel caso di fenomeni energici a cui prendano parte nuclei, una maggior probabilità di emissione di fotoni. Il fattore $Z^2e^2/2\pi^2$, che vale $1/215$ per $Z=1$, diventa infatti maggiore di 1 per $Z \geqslant 15$. Le condizioni per una notevole probabilità di emissione multipla di fotoni nel campo che interessa sperimentalmente si possono trovare in particolare negli urti nucleari prodotti da nuclei primari dei raggi cosmici. Anche questo tipo di evento esige però una apposita trattazione, perchè è complicato dalla produzione di mesoni e generalmente dalla disintegrazione dei nuclei; inoltre le cariche non si possono considerare puntiformi.

Nel caso poi in cui Ze rappresenti una carica macroscopica sono sufficienti energie molto basse per una produzione multipla di fotoni. È questo un caso particolare dei fenomeni macroscopici che si utilizzano normalmente per la produzione del numero enorme di fotoni di radiofrequenza utilizzati, per esempio, nelle comunicazioni elettriche.

---

sieck è sufficiente ammettere la conoscenza sperimentale del fenomeno. Sull'argomento vedi R. Oehme: *Zeits. f. Phys.*, **129**, 573 (1951).

([14]) Questa possibilità è stata segnalata da S. Hayakawa e S. Tomonaga: *Progr. Theor. Phys.*, **2**, 161 (1947).

([15]) $\bar{N}$ risulta proporzionale al quadrato della carica Ze, in quanto legato linearmente alla densità di energia del campo elettromagnetico; questa a sua volta è proporzionale al quadrato dell'intensità del campo che, nell'approssimazione di Bloch e Nordsieck, è proporzionale alle cariche che lo producono.

SUMMARY

The author investigates the characteristic properties of the emission of an infinite number of photons which occurs according Bloch and Nordsieck treating in all the

processes in which a charged particle undergoes a transition from a definite momentum state to another definite momentum state. For electronic charges the probability for one of this photons to fall in the frequency range that interests in ordinary experiments is found to be no more than some hundredths, in agreement with the perturbation method. This probability, however, may approach unity at very high energies in nuclear events of cosmic rays. The results, moreover, depend strongly upon the value of the charge and the probability for nuclear charges to emit several photons is considerably increased. In the case of macroscopical charges multiple emission usually occurs.

Theory of Circularly Symmetric Standing TM Waves in Terminated Irisloaded Guides.

C. C. Grosjean (*)

Interuniversitair Instituut voor Kernwetenschappen
Centrum van de Rijksuniversiteit Gent - België

(ricevuto il 22 Aprile 1955)

Summary. — An exact treatment is given for the problem of describing the possible resonance modes of the circularly symmetric TM type in a terminated irisloaded guide with cylindrical symmetry, which is commonly used in experiments. The applied method based on matching the field components at the corrugations mouths, is very similar to the one used in a previous article on infinite wave guides. For the sake of generality, none of the usually accepted theorems about the field configurations have been introduced in the theory. On the contrary, they finally appear as consequences of the present calculations. After suitable combination the final equations can be grouped into systems which are directly comparable to the final system established for infinite guides. The possible resonance modes are deduced and the properties of the corresponding field configurations are discussed in detail. The obtained modes are also compared to those that can exist in another type of terminated guides, which can equally well be treated by the present method.

1. – Introduction.

In the design of the cavities of a linear electron accelerator, a practical way to determine the last unknown dimension with the desired accuracy consists in performing frequency measurements on circularly symmetric TM waves in terminated irisloaded wave guides. The obtained results are known to be applicable to the corresponding infinite guides. Indeed, using relatively

(*) Address: Natuurk. Laboratorium, Universiteit Gent, Rozier, 6, Gent, Belgium.

simple arguments, it has been shown that the frequencies of the possible resonance modes in a terminated system of identical cavities are the same as those at which traveling waves characterized by the same phase angles are generated in the corresponding infinite guide [1]. However, without doubting the correctness of these arguments and their consequences, some questions can be asked, e.g. if certain theorems whose proofs are based on essential properties of infinite guides are still entirely valid for terminated guides, or questions about the symmetry properties of the field configurations in terminated systems of cavities. An interesting discussion on this subject has been given by CHU [2].

In the present paper, the problem is reexamined using a modified field matching method similar to the one presented in a preceding article on infinite guides [3]. It starts with completely arbitrary functions for the representation of the component E_z at the corrugation mouths, without introducing Floquet's theorem or the important theorem proved by WALKINSHAW and BELL for infinite guides [4]. Our final equations can be brought into a form which makes them after suitable grouping directly comparable to the final system which we found for infinite guides [3]. This enables us to make a detailed discussion about the validity of certain theorems and the general properties of the resonance modes and their configurations. All this is worked out for a commonly used system of identical cavities closed by two half cavities. But the theory can easily be extended to other types of terminated guides. It can also be generalized to systems of cavities with slightly different dimensions.

Finally, let us mention that similar calculations have been made by VANHUYSE [5], who imposes some restrictions on the representation of E_z at the corrugation mouths (apart from an arbitrary constant factor, the *same* field configuration at each corrugation, and *even parity* with respect to the middle of each cavity). This theory served as a starting point for an approximate treatment of the case in which the cavities have slightly different diameters.

2. – Theoretical Development (*).

Returning to Fig. 1 of (G), showing part of the cross-section of an infinite corrugated wave guide with axial symmetry around the z axis, let us introduce

(1) J. C. SLATER: *Microwave Electronics* (New York, 1951), pp. 185-186.

(2) E. L. CHU: *The Theory of Linear Electron Accelerators*; M. L. Report n. 140, Microwave Laboratory, Stanford University (1951).

(3) C. C. GROSJEAN: *Nuovo Cimento*, **1**, 427 (1955). References to this paper will be preceded by the symbol G.

(4) W. WALKINSHAW and J. S. BELL: *Report T/R 864, A.E.R.E.* (Harwell, 1952).

(5) V. J. VANHUYSE: *Physica*, **21**, 269 (1955).

(*) To avoid repetition of lengthy definitions throughout the work, we keep as much as possible the same symbols as those used in our article (G).

metal walls at the planes $z = 0$ and $z = ND$ $(N = 1, 2, \ldots)$. This leads to the terminated guide represented on Fig. 1. Again we wish to obtain analytical solutions of the electromagnetic field equations satisfying the perpendicularity condition for the electric field on the perfectly conducting walls. Since the component $\mathcal{E}_r$ must vanish at $z=0$ and $z = ND$, its Fourier expansion with respect to z in the region $(0 \leqslant r \leqslant a)$ can only contain the following eigenfunctions:

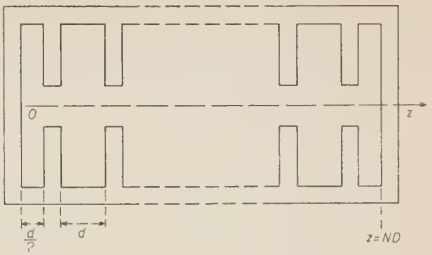

Fig. 1.

$$\sin \frac{m\pi z}{ND} \qquad (m = 1, 2, \ldots)\,. \tag{1}$$

Taking this into account and solving Maxwell's equations, the most general expressions for the desired circularly symmetric field components in $(0 \leqslant r \leqslant a)$ are:

$$\mathcal{E}_z(r, z, t) = E_z(r, z)e^{i\omega t}; \quad \mathcal{E}_r(r, z, t) = E_r(r, z)e^{i\omega t}; \quad \mathcal{H}_\theta(r, z, t)/H_\theta(r, z)e^{i\omega t}; \tag{2}$$

$$E_z(r, z) = \frac{A_0}{2} J_0(kr) + \sum_{m=1}^{\infty} A_m J_0(\gamma_m r) \cos \frac{m\pi z}{ND}\,, \tag{3}$$

$$E_r(r, z) = \sum_{m=1}^{\infty} \frac{A_m}{\gamma_m} \frac{m\pi}{ND} J_1(\gamma_m r) \sin \frac{m\pi z}{ND}\,, \tag{4}$$

$$Z_0 H_\theta(r, z) = i\left[\frac{A_0}{2} J_1(kr) + k \sum_{m=1}^{\infty} \frac{A_m}{\gamma_m} J_1(\gamma_m r) \cos \frac{m\pi z}{ND}\right], \tag{5}$$

in which

$$\gamma_m = \sqrt{k^2 - \frac{m^2\pi^2}{N^2D^2}}\,.$$

The coefficients A_m can again be expressed in terms of the electric field component $E_z(a, z)$ existing along the surface $r = a$. Without making any assumptions concerning the mathematical form of $E_z(a, z)$ its most general representation can be written as follows:

$$\begin{aligned} E_z(a, z) &= f_0\left(\frac{2z}{d}\right) && \left(0 \leqslant z \leqslant \frac{d}{2}\right) \\ &= f_n\left[\frac{2}{d}(z - nD)\right] && \left(nD - \frac{d}{2} \leqslant z \leqslant nD + \frac{d}{2}\right) \\ &= f_N\left[\frac{2}{d}(z - ND)\right] && \left(ND - \frac{d}{2} \leqslant z \leqslant ND\right) \\ &= 0 && \left(nD + \frac{d}{2} < z < (n+1)D - \frac{d}{2}\right) \end{aligned} \tag{6}$$

in which $f_0(x)$, $f_1(x)$, ..., $f_N(x)$ are arbitrary complex functions of x existing in the following intervals:

$$(7)\quad f_0 \text{ in } (0 \leqslant x \leqslant 1);\quad f_1,\ f_2, \ldots,\ f_{N-1} \text{ in } (-1 \leqslant x \leqslant 1);\quad f_N \text{ in } (-1 \leqslant x \leqslant 0).$$

Identifying (3) at $r = a$ with (6), we get

$$(8)\quad A_m J_0(\gamma_m a) = \frac{2}{ND}\left\{\int_0^{d/2} f_0\left(\frac{2z}{d}\right)\cos\frac{m\pi z}{ND}\,\mathrm{d}z + \right.$$

$$\left. + \sum_{n'=1}^{N-1}\int_{n'D-(d/2)}^{n'D+(d/2)} f_{n'}\left[\frac{2}{d}(z - n'D)\right]\cos\frac{m\pi z}{ND}\,\mathrm{d}z + \int_{ND-(d/2)}^{ND} f_N\left[\frac{2}{d}(z - ND)\right]\cos\frac{m\pi z}{ND}\,\mathrm{d}z\right\} =$$

$$= \frac{d}{ND}\left\{\int_0^1 f_0(y)\cos\frac{m\pi d}{2ND}\,y\,\mathrm{d}y + (-1)^m\int_0^1 f_N(-y)\cos\frac{m\pi d}{2ND}\,y\,\mathrm{d}y + \right.$$

$$+ \sum_{n'=1}^{N-1}\cos\frac{n'm\pi}{N}\int_0^1 [f_{n'}(y) + f_{n'}(-y)]\cos\frac{m\pi d}{2ND}\,y\,\mathrm{d}y$$

$$\left. - \sum_{n'=1}^{N-1}\sin\frac{n'm\pi}{N}\int_0^1 [f_{n'}(y) - f_{n'}(-y)]\sin\frac{m\pi d}{2ND}\,y\,\mathrm{d}y\right\}.$$

Let us now define the following functions and symbols:

$$(9)\quad \begin{cases} u_m(x) = f_0(x) + \sum_{n'=1}^{N-1}\cos\frac{n'm\pi}{N}[f_{n'}(x) + f_{n'}(-x)] + (-1)^m f_N(-x) \\ \qquad\qquad (0 \leqslant x \leqslant 1;\ m = 0, 1, \ldots, N), \\ v_m(x) = \sum_{n'=1}^{N-1}\sin\frac{n'm\pi}{N}[f_{n'}(x) - f_{n'}(-x)] \\ \qquad\qquad (0 \leqslant x \leqslant 1;\ m = 1, 2, \ldots, N-1), \end{cases}$$

$$(10)\quad U_m(x) \equiv \int_0^1 u_m(y)\cos xy\,\mathrm{d}y\,, \qquad V_m(x) \equiv \int_0^1 v_m(y)\sin xy\,\mathrm{d}y\,,$$

$$(11)\quad \Phi_0(r, \beta) \equiv \frac{J_0[(k^2 - \beta^2)^{\frac{1}{2}}r]}{J_0[(k^2 - \beta^2)^{\frac{1}{2}}a]}\,, \quad \Phi_1(r, \beta) \equiv \frac{k}{(k^2 - \beta^2)^{\frac{1}{2}}}\,\frac{J_1[(k^2 - \beta^2)^{\frac{1}{2}}r]}{J_0[(k^2 - \beta^2)^{\frac{1}{2}}a]}\,.$$

After some transformations, the components E_z and H_ϑ can be reduced to

$$(12)\quad E_z(r,z)=\frac{d}{2ND}\Bigg\{\sum_{m=-\infty}^{\infty}U_0\left(\frac{m\pi d}{D}\right)\Phi_0\left(r,\frac{2m\pi}{D}\right)\cos\frac{2m\pi z}{D}+$$

$$+\sum_{m=-\infty}^{\infty}U_N\left(\frac{(1+2m)\pi d}{2D}\right)\Phi_0\left(r,\frac{(1+2m)\pi}{D}\right)\cos\frac{(1+2m)\pi z}{D}+$$

$$+2\sum_{n'=1}^{N-1}\sum_{m=-\infty}^{\infty}\left[U_{n'}\left(\frac{(n'+2mN)\pi d}{2ND}\right)-V_{n'}\left(\frac{(n'+2mN)\pi d}{2ND}\right)\right]\cdot$$

$$\cdot\Phi_0\left(r,\frac{(n'+2mN)\pi}{ND}\right)\cos\frac{(n'+2mN)\pi z}{ND}\Bigg\},$$

$$(13)\quad Z_0H_\vartheta(r,z)=\frac{id}{2ND}\Bigg\{\sum_{m=-\infty}^{\infty}U_0\left(\frac{m\pi d}{D}\right)\Phi_1\left(r,\frac{2m\pi}{D}\right)\cos\frac{2m\pi z}{D}+$$

$$+\sum_{m=-\infty}^{\infty}U_N\left(\frac{(1+2m)\pi d}{2D}\right)\Phi_1\left(r,\frac{(1+2m)\pi}{D}\right)\cos\frac{(1+2m)\pi z}{D}+$$

$$+2\sum_{n'=1}^{N-1}\sum_{m=-\infty}^{\infty}\left[U_{n'}\left(\frac{(n'+2mN)\pi d}{2ND}\right)-V_{n'}\left(\frac{(n'+2mN)\pi d}{2ND}\right)\right]\cdot$$

$$\cdot\Phi_1\left(r,\frac{(n'+2mN)\pi}{ND}\right)\cos\frac{(n'+2mN)\pi z}{ND}\Bigg\}$$

$$(0\leqslant r\leqslant a;\ 0\leqslant z\leqslant ND).$$

Let us now consider the fields inside each corrugation. In the regions

$$nD-\frac{d}{2}\leqslant z\leqslant nD+\frac{d}{2},\qquad a\leqslant z\leqslant b\qquad (n=1,2,\ldots,N-1),$$

the components can be found using exactly the same procedure as in the preceding article. The functions f_1, f_2, ... f_{N-1} must first be represented by appropriate Fourier expansions containing the eigenfunctions

$$(14)\qquad \cos\frac{2p\pi x_n}{d},\qquad \sin\frac{(2q+1)\pi x_n}{d}\qquad (p,q=0,1,\ldots).$$

This leads to:

$$(15)\quad f_n\left[\frac{2}{d}(z-nD)\right]=\frac{B_0^{(n)}}{2}+\sum_{p=1}^{\infty}B_p^{(n)}\cos\frac{2p\pi x_n}{d}+\sum_{q=0}^{\infty}C_q^{(n)}\sin\frac{(2q+1)\pi x_n}{d}$$

$$(x_n\equiv z-nD)$$

in which

$$B_p^{(n)} = \int_{-1}^{1} f_n(y) \cos p\pi y \, dy , \qquad C_q^{(n)} = \int_{-1}^{1} f_n(y) \sin (q + \tfrac{1}{2})\pi y \, dy .$$

E_z and H_θ can be represented by the following series:

$$(16) \qquad E_z(r, z) = \frac{B_0^{(n)}}{2} \frac{F_0(k; r, b)}{F_0(k; a, b)} + \sum_{p=1}^{\infty} B_p^{(n)} \frac{F_0(\xi_p; r, b)}{F_0(\xi_p; a, b)} \cos \frac{2p\pi x_n}{d} + - \sum_{q=0}^{\infty} C_q^{(n)} \frac{F_0(\zeta_q; r, b)}{F_0(\zeta_q; a, b)} \sin \frac{(2q-1)\pi x_n}{d} .$$

$$(17) \qquad Z_0 H_\theta(r, z) \quad i \left[\frac{B_0^{(n)}}{2} \frac{F_1(k; r, b)}{F_0(k; a, b)} - \sum_{p=1}^{\infty} B_p^{(n)} \frac{k^2 F_1(\xi_p; r, b)}{\xi_p^2 F_0(\xi_p; a, b)} \cos \frac{2p\pi x_n}{d} - + \sum_{q=0}^{\infty} C_q^{(n)} \frac{k^2 F_1(\zeta_q; r, b)}{\zeta_q^2 F_0(\zeta_q; a, b)} \sin \frac{(2q+1)\pi x_n}{d} \right] .$$

In the remaining corrugations, the conditions that E_r should vanish on the iris walls and on the terminating walls requires that the expansions of E_z and H_θ should only contain the eigenfunctions

$$\cos \frac{2p\pi x_n}{d} \qquad (p = 0, 1, \ldots)$$

and we find

1) in $0 \leqslant z \leqslant \frac{d}{2}$, $a \leqslant r \leqslant b$:

$$(18) \qquad E_z(r, z) = B_0^{(0)} \frac{F_0(k; r, b)}{F_0(k; a, b)} + 2 \sum_{p=1}^{\infty} B_p^{(0)} \frac{F_0(\xi_p; r, b)}{F_0(\xi_p; a, b)} \cos \frac{2p\pi z}{d} .$$

$$(19) \qquad Z_0 H_\theta(r, z) = i \left[B_0^{(0)} \frac{F_1(k; r, b)}{F_0(k; a, b)} + 2 \sum_{p=1}^{\infty} B_p^{(0)} \frac{k^2 F_1(\xi_p; r, b)}{\xi_p^2 F_0(\xi_p; a, b)} \cos \frac{2p\pi z}{d} \right] ,$$

in which

$$B_p^{(0)} = \int_{0}^{1} f_0(y) \cos p\pi y \, dy ;$$

2) in $ND - \frac{d}{2} \leqslant z \leqslant ND$, $a \leqslant r \leqslant b$:

$$E_z(r, z) = B_0^{(N)} \frac{F_0(k; r, b)}{F_0(k; a, b)} + 2 \sum_{p=1}^{\infty} B_p^{(N)} \frac{F_0(\xi_p; r, b)}{F_0(\xi_p; a, b)} \cos \frac{2p\pi x_N}{d} , \tag{20}$$

$$Z_0 H_\theta(r, z) = i \left[B_0^{(N)} \frac{F_1(k; r, b)}{F_0(k; a, b)} + 2 \sum_{p=1}^{\infty} B_p^{(N)} \frac{k^2 F_1(\xi_p; r, b)}{\xi_p^2 F_0(\xi_p; a, b)} \cos \frac{2p\pi x_N}{d} \right] , \tag{21}$$

in which

$$B_p^{(N)} = \int_{-1}^{0} f_N(y) \cos p\pi y \, dy .$$

The final condition to be satisfied concerns the continuity of H_θ at $r = a$. Putting both expressions for $H_\theta(a, z)$ equal to each other at each corrugation mouth, one obtains $(N+1)$ equations. Making use of the orthogonality properties and extending the integrations over the proper intervals, it is found that each of the equations gives rise to an infinite set of relations. These sets can be written in a particularly simple form using the following abbreviations:

$$S_n^{(p)} = (-1)^p \frac{d}{D} \sum_{m=-\infty}^{\infty} \left[U_n\left(\frac{(n+2mN)\pi d}{2ND}\right) - V_n\left(\frac{(n+2mN)\pi d}{2ND}\right) \right] \cdot \Phi_1\left(a, \frac{(n+2mN)\pi}{ND}\right) \frac{\frac{(n+2mN)\pi d}{2ND} \sin \frac{(n+2mN)\pi d}{2ND}}{\left[\frac{(n+2mN)\pi d}{2ND}\right]^2 - p^2\pi^2} \tag{22}$$

$$(n = 0, 1, ..., N; \; p = 0, 1, ...);$$

$$T_n^{(q)} = (-1)^q \frac{d}{D} \sum_{m=-\infty}^{\infty} \left[U_n\left(\frac{(n+2mN)\pi d}{2ND}\right) - V_n\left(\frac{(n+2mN)\pi d}{2ND}\right) \right] \cdot \Phi_1\left(a, \frac{(n+2mN)\pi}{ND}\right) \frac{\frac{(n+2mN)\pi d}{2ND} \cos \frac{(n+2mN)\pi d}{2ND}}{\left[\frac{(n+2mN)\pi d}{2ND}\right]^2 - (q+\tfrac{1}{2})^2\pi^2} \tag{23}$$

$$(n = 1, 2, ..., N-1; \; q = 0, 1, ...).$$

In $S_n^{(p)}$, the factor V_n should be omitted for $n = 0$ and $n = N$. The infinite sets become:

$$B_p^{(0)} \frac{k^2 F_1(\xi_p; a, b)}{\xi_p^2 F_0(\xi_p; a, b)} = \frac{1}{2N} \left[S_0^{(p)} + 2 \sum_{n'=1}^{N-1} S_{n'}^{(p)} + S_N^{(p)} \right] , \tag{24}$$

$$B_p^{(n)} \frac{k^2 F_1(\xi_p; a, b)}{\xi_p^2 F_0(\xi_p; a, b)} = \frac{1}{N} \left[S_0^{(p)} + 2 \sum_{n'=1}^{N-1} S_{n'}^{(p)} \cos \frac{n' n \pi}{N} + (-1)^n S_N^{(p)} \right] \tag{25}$$

$$(n = 1, 2, ..., N-1).$$

$$B_p^{(N)} \frac{k^2 F_1(\xi_p;\, a,\, b)}{\xi_p^2 F_0(\xi_p;\, a,\, b)} = \frac{1}{2N}\left[S_0^{(p)} + 2\sum_{n'=1}^{N-1} (-1)^{n'} S_{n'}^{(p)} + (-1)^N S_N^{(p)} \right], \tag{26}$$

$$C_q^{(n)} \frac{k^2 F_1(\zeta_q;\, a,\, b)}{\zeta_q^2 F_0(\zeta_q;\, a,\, b)} = \frac{2}{N} \sum_{n'=1}^{N-1} T_{n'}^{(q)} \sin \frac{n' n \pi}{N} \qquad (n = 1, 2, \ldots N-1)\,. \tag{27}$$

These sets can be suitably combined. After having replaced n by n'' in (25) and (27), let us first multiply (24), (25) and (26) respectively by 1, $\cos n'' n\pi/N$ and $(-1)^n$, and let us sum the equations. Making use of the formula:

$$1 + 2\sum_{n''=1}^{N-1} \cos \frac{n' n'' \pi}{N} \cos \frac{n'' n \pi}{N} + (-1)^{n+n'} = \begin{cases} 0 & (n \neq n') \\ N & (n = n' = 1, \ldots, N-1) \\ 2N & (n = n' = 0 \text{ or } N) \end{cases} \tag{28}$$

$$(n,\, n' = 0,\, 1,.,\, N)\,,$$

we get

$$\left[B_p^{(0)} + \sum_{n''=1}^{N-1} B_p^{(n'')} \cos \frac{n'' n \pi}{N} + (-1)^n B_p^{(N)} \right] \frac{k^2 F_1(\xi_p;\, a,\, b)}{\xi_p^2 F_0(\xi_p;\, a,\, b)} = S_n^{(p)}\,, \tag{29}$$

and since

$$B_p^{(0)} + \sum_{n''=1}^{N-1} B_p^{(n'')} \cos \frac{n'' n \pi}{N} + (-1)^n B_p^{(N)} = \tag{30}$$

$$= \int_0^1 \left\{ f_0(y) + \sum_{n''=1}^{N-1} \cos \frac{n'' n \pi}{N} [f_{n''}(y) + f_{n''}(-y)] + (-1)^n f_N(-y) \right\} \cos p\pi y \, \mathrm{d}y =$$

$$= \int_0^1 u_n(y) \cos p\pi y \, \mathrm{d}y = U_n(p\pi)\,,$$

we see that the sets of equations (24), (25) and (26) are equivalent to

$$\frac{k^2 F_1(\xi_p;\, a,\, b)}{\xi_p^2 F_0(\xi_p;\, a,\, b)} U_n(p\pi) = S_n^{(p)} \qquad (n = 0, 1, \ldots, N)\,. \tag{31}$$

In the same way, let us multiply (27) $\sin n'' n\pi/N$ and add the equations together. Making use of

$$2\sum_{n''=1}^{N-1} \sin \frac{n' n'' \pi}{N} \sin \frac{n'' n \pi}{N} = \begin{cases} 0 & (n \neq n') \\ N & (n = n') \end{cases} \qquad (n,\, n' = 1, 2, \ldots, N-1), \tag{32}$$

we obtain finally:

$$\frac{k^2F_1(\zeta_q;\,a,\,b)}{\zeta_q^2F_0(\zeta_q;\,a,\,b)}\,V_n\left[\left(q+\frac{1}{2}\right)\pi\right]=T_n^{(q)} \qquad (n=1,2,\ldots,N-1). \tag{33}$$

The $2N$ sets of equations (31) and (33) should all be satisfied at once. Putting the simultaneous equations together, we find that the $2N$ sets can be divided into $(N+1)$ groups:

1)

$$\frac{k^2F_1(\xi_p;\,a,\,b)}{\xi_p^2F_0(\xi_p;\,a,\,b)}\,U_0(p\pi)=S_0^{(p)} \qquad (p=0,1,\ldots). \tag{34}$$

This set has exactly the same form as the first one in (G 21) written for a 0 mode.

2)

$$\begin{cases} \dfrac{k^2F_1(\xi_p;\,a,\,b)}{\xi_p^2F_0(\xi_p;\,a,\,b)}\,U_n(p\pi)=S_n^{(p)} & (p=0,1,\ldots) \\ \dfrac{k^2F_1(\zeta_q;\,a,\,b)}{\zeta_q^2F_0(\zeta_q;\,a,\,b)}\,V_n\left[\left(q+\dfrac{1}{2}\right)\pi\right]=T_n^{(q)} & (q=0,1,\ldots) \end{cases} \tag{35}$$

in which $n=1,2,\ldots,N-1$. These sets are identical to the entire system (G 21) in which we put respectively

$$\beta_m=\frac{(n+2mN)\pi}{ND}=\frac{n\pi}{ND}+\frac{2m\pi}{D}\,.$$

Therefore they seem to be associated with waves which are characterized by phase angles given by

$$\beta_0D=\frac{n\pi}{N} \qquad (n=1,2,\ldots,N-1). \tag{36}$$

3)

$$\frac{k^2F_1(\xi_p;\,a,\,b)}{\xi_p^2F_0(\xi_p;\,a,\,b)}\,U_N(p\pi)=S_N^{(p)} \qquad (p=0,1,\ldots), \tag{37}$$

having again the form of the first set in (G 21) written for a π mode.

Using the method that enabled us to transform the system (G 21) into (G 24), we find for the mentioned sets:

$$U_0(0)\left[\frac{k^2F_1(\xi_p;\,a,\,b)}{\xi_p^2F_0(\xi_p;\,a,\,b)}-\frac{J_1(ka)}{J_0(ka)}\right]\delta_{p0}+ \tag{38}$$

$$+2\sum_{m=1}^{\infty}U_0\left(\frac{m\pi d}{D}\right)\left[\frac{k^2F_1(\xi_p;\,a,\,b)}{\xi_p^2F_0(\xi_p;\,a,\,b)}-\Phi_1\left(a,\frac{2m\pi}{D}\right)\right]\frac{(m\pi d/D)\sin(m\pi d/D)}{(m\pi d/D)^2-p^2\pi^2}=0$$

$$
(39)\quad
\begin{cases}
\displaystyle\sum_{m=-\infty}^{\infty}\left[U_n\left(\frac{(n+2mN)\pi d}{2ND}\right)-V_n\left(\frac{(n+2mN)\pi d}{2ND}\right)\right]\cdot \\
\displaystyle\cdot\left[\frac{k^2F_1(\xi_p;\,a,\,b)}{\xi_p^2F_0(\xi_p;\,a,\,b)}-\Phi_1\left(a,\,\frac{(n+2mN)\pi}{ND}\right)\right]\frac{\dfrac{(n+2mN)\pi d}{2ND}\sin\dfrac{(n+2mN)\pi d}{2ND}}{\left[\dfrac{(n+2mN)\pi d}{2ND}\right]^2-p^2\pi^2}=0 \\
\displaystyle\sum_{m=-\infty}^{\infty}\left[U_n\left(\frac{(n+2mN)\pi d}{2ND}\right)-V_n\left(\frac{(n+2mN)\pi d}{2ND}\right)\right]\cdot \\
\displaystyle\cdot\left[\frac{k^2F_1(\zeta_q;\,a,\,b)}{\zeta_q^2F_0(\zeta_q;\,a,\,b)}-\Phi_1\left(a,\,\frac{(n+2mN)\pi}{ND}\right)\right]\frac{\dfrac{(n+2mN)\pi d}{2ND}\cos\dfrac{(n+2mN)\pi d}{2ND}}{\left[\dfrac{(n+2mN)\pi d}{2ND}\right]^2-\left(q+\dfrac{1}{2}\right)^2\pi^2}=0 \\
(n=1,\,2,\,\ldots,\,N-1)
\end{cases}
$$

$$
(40)\qquad \sum_{m=0}^{\infty}U_N\left(\frac{(1+2m)\pi d}{2D}\right)\cdot
\left[\frac{k^2F_1(\xi_p;\,a,\,b)}{\xi_p^2F_0(\xi_p;\,a,\,b)}-\Phi_1\left(a,\,\frac{(1+2m)\pi}{D}\right)\right]\frac{\dfrac{(1+2m)\pi d}{2D}\sin\dfrac{(1+2m)\pi d}{2D}}{\left[\dfrac{(1+2m)\pi d}{2D}\right]^2-p^2\pi^2}=0\,.
$$

The condition that these equations have a non-zero solution is that the determinant of their coefficients vanish. In the present case, this determinant splits into $(N+1)$ infinite determinants and at least one of them should vanish to satisfy the condition. This leads to $(N-1)$ separated frequency equations associated with the $(N+1)$ groups of equations mentioned above. Now, as we pointed out in our previous article, the frequency equation implicitly contained in (G 21) must give rise to an infinite number of pass bands in each $(\beta_0,\,k)$ diagram corresponding to a cut-off frequency of the unloaded guide. Although the system (G 21) does not lend itself to a direct check of this statement, VANHUYSE [6] showed that in the special case of infinitely thin irises $(d=D)$ and only considering 0 and π modes, some simplifications arise which permit him to fit the roots of the frequency equation in the well-known band structure of each $(\beta_0,\,k)$ diagram. Returning to our discussion about the $(N+1)$ groups of equations, all these considerations show that the following resonance modes are observable:

[6] V. J. VANHUYSE: *Nuovo Cimento*, **1**, 447 (1955).

1) those characterized by the angles

$$\frac{\pi}{N}, \frac{2\pi}{N}, \cdots, \frac{(N-1)\pi}{N} \tag{41}$$

in all the pass bands of each (β_0, k) diagram.

2) those characterized by the phase angles $\beta_0 D = 0$ and π, in each « cut-off » diagram, but *only in the pass bands with an odd number*. This can be proved as follows. For 0 or π modes, the equations in the system (G 21) can be grouped in two sets, one only containing the G_1 function and the other only containing G_2. Indeed, in the upper equations the function G_2 drops out, whereas in the lower equations G_1 vanishes, both for reasons of parity. Therefore, the frequency equation splits into two distinct frequency equations, each one being expected to provide a number of frequencies. The simplest way to find how they are distributed among the pass bands consists in going over to the limiting case $d = D$. It is quite reasonable to admit that by letting d approach D, the frequencies giving rise to 0 and π modes will only shift toward limit values, and that no discontinuities such as appearance of new frequencies or sudden interchanges will occur. Now, from the calculations made in ref. ([6]), it can be seen that both for 0 and π modes in the case of $d = D$, the upper equations in (G 21) give rise to frequencies marking the limits of the odd pass bands, whereas the lower equations provide frequencies marking the limits of the even bands. As the systems of equations (34) and (37) are exactly of the form of the mentioned upper equations, and as those corresponding to the lower equations do not appear in the theory, we may conclude that only the resonance frequencies for 0 and π modes in the odd bands are provided by (34) and (37). Hence, it is impossible to obtain the breadth of the even pass bands by direct measurement in terminated guides of the type represented by Fig. 1.

The theory also shows that in such a terminated guide the frequencies at which all the possible modes can be generated under the form of standing waves, are identical to those at which traveling waves with the same phase angle are generated in the corresponding infinite guide. Therefore, measurements, done in finite systems of cavities provide direct information about the band structure of the infinite corrugated wave guide. Moreover if it happens that a certain mode can appear in two or more terminated systems of identical cavities only differing by their number of corrugations, the measured frequencies must have one well-defined value independent of that number. This has been experimentally verified for the resonance modes in the lowest pass band of a closed system with a variable number of cavities. The guide consisted of two « half cavities » and an iris slice, surrounding respectively zero, one, two, ..., up to fifteen identical cavities (among which we omitted

the rather unimportant cases of 10 and 12 cavities, which lead to $n\pi/11$ and $n\pi/13$ modes). The observed modes appearing more than once were found at the same frequencies within an experimental error less than $\pm 0.015\%$. At the same time, the measured values provided the frequency curve of the lowest band in the fitst (β_0, k) diagram with a high accuracy and enabled us to establish a semi-empirical relation which is very well satisfied. All these results have been discussed in a previous paper ([7]).

Finally, let us turn our attention towards the field configurations in the terminated guide. Since the expressions for the fields are entirely determined by the knowledge of $E_z(a, z)$, it is sufficient to examine this component. We may suppose that the frequencies of all the possible modes are different from each other, as it is generally the case. This is not a restriction because if it happened that two entirely different modes in different cut-off diagrams could be generated at the same frequency, the discussion given below could equally well be made, but it would be slightly more complicated.

Let us now consider a frequency giving rise to a mode characterized by the particular phase angle $s\pi/N$, s being an integer satisfying $(0 < s < N)$. For this frequency, the determinant of the linear system of equations (39) for which $n = s$ will vanish, whereas the N other determinants in (38), (39) and (40) will not become equal to zero. Therefore, all the groups of equations will only be satisfied by the trivial zero solution, except the one with $n = s$. Taking this into account and making use of (12), $E_z(a, z)$ can be written as

$$(42) \qquad E_z(a, z) = \frac{d}{ND} \cdot \cdot \sum_{m=-\infty}^{\infty} \left[U_s\left(\frac{(s + 2mN)\pi d}{2ND}\right) - V_s\left(\frac{(s + 2mN)\pi d}{2ND}\right)\right] \cos \frac{(s + 2mN)\pi z}{ND},$$

in which the factors $U_s(...) - V_s(...)$ satisfy (39) where n is replaced by s. Comparing this with (G 24), it is clear that they must be, apart from an arbitrary proportionality factor, identical to the corresponding solution for the infinite guide, namely

$$\left[G_1\left(\frac{\beta_m d}{2}\right) - G_2\left(\frac{\beta_m d}{2}\right)\right],$$

in which $\beta_0 = s\pi / ND$. Now, from the expressions of $E_z(a, z)$ valid for the infi-

---

([7]) C. C. GROSJEAN and V. J. VANHUYSE: *Nuovo Cimento*, **1**, 193 (1955).

nite guide, we obtain

$$(43)\qquad \frac{d}{D}\sum_{m=-\infty}^{\infty}\left[G_1\left(\frac{\beta_m d}{2}\right)-G_2\left(\frac{\beta_m d}{2}\right)\right]\exp\left[-i\beta_m z\right]=$$

$$=\begin{cases}0 & \left(-\frac{D}{2}\leqslant x_n<-\frac{d}{2}\right)\\ \left[g_1\left(\frac{2x_n}{d}\right)+ig_2\left(\frac{2x_n}{d}\right)\right]\exp\left[-i\beta_0 nD\right] & \left(-\frac{d}{2}\leqslant x_n\leqslant\frac{d}{2}\right)\\ 0 & \left(\frac{d}{2}<x_n\leqslant\frac{D}{2}\right)\end{cases}$$

in which $x_n\equiv z-nD$. Putting $\beta_0=s\pi/ND$ and taking the real part on both sides, we get

$$(44)\qquad \frac{d}{D}\sum_{m=-\infty}^{\infty}\left[G_1\left(\frac{(s+2mN)\pi d}{2ND}\right)-G_2\left(\frac{(s+2mN)\pi d}{2ND}\right)\right]\cos\frac{(s+2mN)\pi z}{ND}=$$

$$=\begin{cases}0\\ g_1\left(\frac{2x_n}{d}\right)\cos\frac{ns\pi}{N}+g_2\left(\frac{2x_n}{d}\right)\sin\frac{ns\pi}{N}\\ 0\end{cases}$$

respectively in the same intervals. Since the functions $g_1(x)$ and $g_2(x)$ would still contain an arbitrary proportionality factor even if they were solved explicitly, we can write in the case of the considered terminated guide:

$$(45)\qquad E_z(a,z)=g_1\left(\frac{2z}{d}\right)\qquad\left(0\leqslant z\leqslant\frac{d}{2}\right)$$

$$=g_1\left(\frac{2x_n}{d}\right)\cos\frac{ns\pi}{N}+g_2\left(\frac{2x_n}{d}\right)\sin\frac{ns\pi}{N}\qquad\left(nD-\frac{d}{2}\leqslant z\leqslant nD+\frac{d}{2}\right)$$

$$=(-1)^s g_1\left(\frac{2x_N}{d}\right)\qquad\left(ND-\frac{d}{2}\leqslant z\leqslant ND\right)$$

$$=0\qquad\left(nD+\frac{d}{2}<z<(n+1)D-\frac{d}{2}\right)$$

in which $g_1(x)$ and $g_2(x)$ are the functions appearing in the description of the corresponding traveling wave, propagating through the infinite guide. They have the mathematical properties outlined in our previous article (G). It can easily be proved that (45) also holds for $s=0$ and $s=N$ in the odd pass bands. In these cases, the terms containing $g_2(x)$ vanish for a double reason.

In the different intervals corresponding to the $(N+1)$ corrugation mouths,

$E_z(a, z)$ can be brought into the following form

$$(46) \qquad \frac{1}{2}\left[g_1\left(\frac{2x_n}{d}\right)+ig_2\left(\frac{2x_n}{d}\right)\right]\exp\left[-i\frac{ns\pi}{N}\right]+\frac{1}{2}\left[g_1\left(\frac{2x_n}{d}\right)-ig_2\left(\frac{2x_n}{d}\right)\right]\exp\left[i\frac{ns\pi}{N}\right],$$

showing the well-known fact that the standing waves can be regarded as the result of a superposition of two waves identical to those traveling in both directions through the infinite guide. It is clear that:

1) Floquet's theorem applies to both traveling waves;

2) they have the same amplitude;

3) they are combined in such a way that the even function $g_1(x)$ is multiplied with a cosine factor as in (45).

A few other remarks can be made. Multiplying $E_z(a, z)$ given by (G 5) with $\exp[i\omega t]$ and separating the real and the imaginary parts, we get as possible (equivalent) formulae for the field at the corrugation mouths:

$$(47) \qquad g_1\left(\frac{2x_n}{d}\right)\cos(\omega t - n\beta_0 D) - g_2\left(\frac{2x_n}{d}\right)\sin(\omega t - n\beta_0 D)$$

and

$$(48) \qquad g_1\left(\frac{2x_n}{d}\right)\sin(\omega t - n\beta_0 D) + g_2\left(\frac{2x_n}{d}\right)\cos(\omega t - n\beta_0 D),$$

showing that in the infinite guide, there is always a 90° phase-shift between the symmetric and the antisymmetric parts of the traveling wave configuration. This is not the case in a terminated guide, in which we found the following formulae for the allowed modes:

$$(49) \qquad \left[g_1\left(\frac{2x_n}{d}\right)\cos n\beta_0 D + g_2\left(\frac{2x_n}{d}\right)\sin n\beta_0 D\right]\begin{matrix}\cos\omega t\\ \sin\omega t\end{matrix}.$$

A further comparison can be made writing (47) and (48) as follows:

$$(50) \qquad (g_1\cos n\beta_0 D + g_2\sin n\beta_0 D)\begin{matrix}\cos\omega t +\\ \sin\omega t -\end{matrix}(g_1\sin n\beta_0 D - g_2\cos n\beta_0 D)\begin{matrix}\sin\omega t\\ \cos\omega t\end{matrix}$$

which shows that in a terminated guide, one gets only the first part of these expressions, which is generally depending on both g_1 and g_2. Therefore in the considered terminated guide, these symmetric and antisymmetric parts of the field configuration are still admitted but combined as in (49), whereas the combination

$$(51) \qquad (g_1\sin n\beta_0 D - g_2\cos n\beta_0 D)$$

is annihilated. As we know from our previous calculations, this does not introduce any changes in the values of the frequencies at which the allowed modes are generated.

The discussion clearly proves that measurements (of frequencies, field distributions, etc.) carried out with finite systems of cavities provide direct information about the waves in the corresponding infinite guides.

It is evident that the remaining problem consists in finding the solutions of infinite systems as (G 21), (G 24) or (G 26) in a relatively simple mathematical form, either exact or in a useful approximation.

3. – Remarks.

As we have seen in the preceding paragraph, the terminated guide represented by Fig. 1 only permits the direct measurement of zero and π modes in odd numbered pass bands. Since the most interesting band for the design of a linear electron accelerator is just the lowest band in the first (β_0, k) diagram, a system of cavities closed by two half cavities is entirely suited for the measurement of its frequency curve. In fact, considering the region around those cavity dimensions which are interesting in accelerator design, one only needs to determine three points on the $k(\beta_0)$ curve to represent it entirely in a simple mathematical form. A precise measurement of the resonance frequencies of the 0, $\pi/2$ and π mode of the lowest band will be sufficient. The system in which this can be done, simply consists of a cavity, an iris slice and two half cavities. On the contrary, one would need a much larger guide to obtain a sufficiently large number of points on the frequency curve of an even pass band, and the 0 and π modes could only be obtained by calculation.

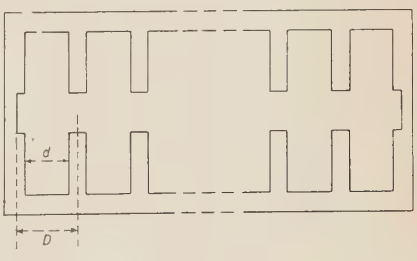

Fig. 2.

There is, however, another type of terminated guide which can be constructed, namely, one in which the short circuit planes are introduced in the middle of two iris walls (Fig. 2). It seems interesting to examine in how far such a guide permits the measurement of the missing frequencies of the previous case. Using exactly the same method as in § 2, one can easily find the resonance modes and the field configurations of the corresponding standing TM waves in the new guide. Let us simply state one result of the theory. It turns out that in the system with N corrugations (total length equal to ND), the following modes are observable

1) in every pass band: the modes characterized by the phase angles

$$\frac{\pi}{N}, \frac{2\pi}{N}, \cdots, \frac{(N-1)\pi}{N};$$

2) in every odd pass band: the 0-mode;
3) in every even pass band: the π-mode.

Therefore, in the present case, there is always one element missing for a direct measurement of the breadth of a pass band. The system is less suited for the determination of the frequency curve in an odd band, and it does not entirely compensate the other type of terminated guide for the even bands, since it provides only π-modes in these bands.

I am grateful to the Institut Interuniversitaire des Sciences Nucléaires, and to Prof. Dr. J. L. VERHAEGHE for his interest in this work.

— — —

RIASSUNTO (*)

Si dà un trattamento esatto del problema di descrivere i possibili modi di risonanza di tipo TM a simmetria circolare della guida finita con diaframmi a iride a simmetria cilindrica quale si usa normalmente negli esperimenti. Il metodo seguito, basato sull'adattamento delle componenti del campo alla bocca dei diaframmi, è molto simile a quello seguito in un precedente articolo dedicato alle guide d'onda indefinite. Per non perdere in generalità non si è introdotto nella teoria nessuno dei teoremi generalmente accettati riguardanti le configurazioni del campo. Al contrario, questi compaiono alla fine come conseguenze dei nostri calcoli. Dopo un'opportuna combinazione, le equazioni finali si possono raggruppare in sistemi direttamente confrontabili col sistema finale ottenuto per le guide indefinite. Si deducono i possibili modi di risonanza e si discutono dettagliatamente le corrispondenti configurazioni del campo. I modi ottenuti si confrontano anche con quelli possibili in un altro tipo di guide finite, che si può trattare altrettanto bene col metodo qui esposto.

IL NUOVO CIMENTO Vol. II, N. 1 1° Luglio 1955

Čerenkov and Isotropic Radiations from Single μ-Mesons in Air.

F. R. Barclay and J. V. Jelley

Atomic Energy Research Establishment - Harwell, Berks.

(ricevuto il 25 Aprile 1955)

Summary. — The Čerenkov effect has been used to detect single μ-mesons in 6 m of air at atmospheric pressure. The yield of light and rate of occurrence of events is consistent with the classical theory of the effect. A separate experiment revealed that, in the absence of Čerenkov radiation, the production of light associated with ionization is $< 10^{-2}$ of that of Čerenkov radiation, or $< 4 \cdot 10^{-6}$ of the rate of loss of energy by ionization for relativistic μ-mesons.

1. – Introduction.

The present investigation was prompted by the discovery of light pulses from the night-sky (Galbraith and Jelley, 1953) associated with large cosmic-ray air showers, believed to be due to the Čerenkov effect in the atmosphere (Čerenkov, 1934; Blackett, 1948 and Goldanskii and Zhidanov, 1954). The experiment, which was designed to be complementary to the work on the night-sky pulses, was initiated with two aims in view. First, to see if it was possible to make a gas Čerenkov counter for single particles, using a fairly short length of track, such a counter having an energy threshold depending on the choice of gas and its pressure. Secondly, to make a direct comparison between the light output in air by Čerenkov radiation on the one hand, and light associated with ionization, on the other.

The choice of μ-mesons ensured that any visible radiation from the Bremsstrahlung process (Heitler, 1949) would be quite negligible, as also would be that due to the acceleration of the particles in the horizontal component of the earth's field (Schwinger, 1949).

Since μ-mesons were selected throughout the experiment, it was known

with some certainty that most of the events would then be due to *single* particles.

Previous work on the Čerenkov effect in gases has been carried out by BALZANELLI and ASCOLI (1953) in which they obtained evidence for light produced by the passage of cosmic-ray particles through chloroform vapour. More recently, the same authors (1954) have identified the light with Čerenkov radiation and obtained effects in air in the absence of the chloroform. However, owing to the limited length of track and a relatively poor optical system, their counting rates and pulse amplitudes were small.

2. – Principle of the Experiment.

The experiment described here is in many ways similar to one carried out earlier (JELLEY, 1951) in establishing the Čerenkov effect for single μ-mesons in water; in both cases the directional features of the radiation have been used to identify it. From the well known relations between the refractive index, angle of emission of the light, particle velocity and output of light (see e.g. JELLEY, 1953), we find that in the case of air at N.T.P. (refractive index 1.00029, the threshold energy is 4.3 GeV for μ-mesons, the maximum angle of light emission 1.3°, and the light output for an ultra-relativistic particle is ~ 0.3 photons/cm (between wavelength limits $3\,500 \div 5\,500$ Å). It is seen that these figures differ considerably from those found when solid and liquid media are used. For example, in the case of water, the corresponding figures are 54 MeV, 41° and 250 photons/cm.

Even with the 6 m track length used in the present experiment, the light pulses are so weak that they correspond to the emission of only a few photoelectrons in the multiplier; hence it was essential to use a coincidence technique to eliminate the dark current pulses.

The μ-mesons were selected by a Geiger counter telescope which included a lead absorber to eliminate the soft component, and any electrons that might accompany the mesons.

The experiment was divided into two parts; in the first, the light receiver was placed at the foot of the air column so as to collect Čerenkov radiation which would be radiated in a downward direction, since the cosmic-rays themselves travel predominantly downwards. In the second experiment the apparatus was inverted, with the light receiver at the top of the air column, looking downwards. In this case the Čerenkov radiation would not be detected. Any atomic or molecular radiation caused by ionization would be emitted isotropically and hence would be detected with approximately the same efficiency in both cases.

3. – Arrangement of Apparatus.

The light receiver was contained in a light tight aluminium box X, approximately 6 metres high, and of section 1 metre × 1 metre, see figure 1(a); the inside was painted dull black.

A parabolic reflector M, of diameter 60 cm and focal length 25 cm was mounted in the base of the box. It was aluminised on the top surface to avoid collecting light formed by Čerenkov radiation produced by particles traversing the glass. The box was placed on a lead platform 20 cm thick, space being left under the lead for counter tray B. The other tray, A, on top of the box, completed the counter telescope.

A photomultiplier P (E.M.I. type 6260, with a 5 cm diameter photocathode), which was run at 2.53 kV, was mounted so that the photocathode was at the focus of the mirror. A stop, of diameter 4.1 cm, was always in position on the photocathode. A small metal shutter HH' could be interposed between the mirror and the phototube. The shutter, which was large enough to cut-off all the direct light from the mirror falling on the photocathode, was operated from outside the box. Immediately above the multiplier was a set of 7 short anticoincidence counters G, mounted vertically in a light tight container. These covered an area approximately equal to the cross-section of the multiplier.

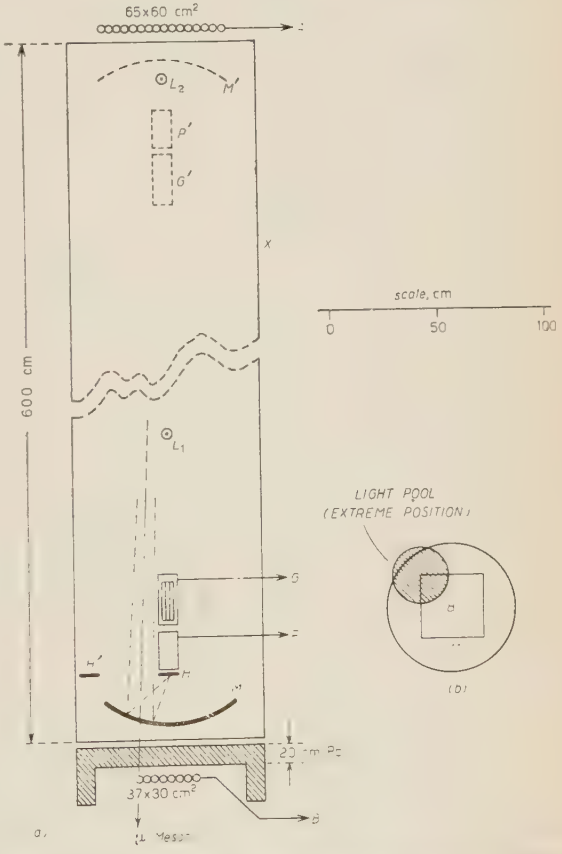

Fig. 1. – Diagram of the essential features of the apparatus.

To facilitate focusing, two small lamps L_1 and L_2 were supported on the vertical axis of the box, at a height of 236 cm and at the top respectively. When the box was inverted, the counter trays and the lead remained in their

same positions, while the mirror, phototube and anticoincidence counters were then situated at M', P' and G' respectively.

The output pulses from the phototube were taken to an amplifier having a maximum gain of 10^4, and a bandwidth of ~ 5 MHz. Integrating and differentiating time-constants of 0.032 μs were used throughout. The output of a discriminator following the amplifier, and the output of trays A and B, were fed into a three channel coincidence unit having a resolving time of ~ 1 μs. The light pulses were also displayed on a recording oscilloscope, using a 15 μs time-base, which was triggered by the output of the coincidence unit. This coincidence output was also fed into one channel of a second coincidence circuit, the other channel of which received pulses from the counters G. The output of this unit was used to illuminate a small lamp mounted in the oscilloscope, to indicate when a particle has traversed the counters G.

Optical Arrangements. – If we take 1.3° for the Čerenkov angle, the radiation produces a circular pool of light 28 cm in diameter at the bottom of the box. The size of counter tray B was chosen so that if a particle passed through any part of it, almost all of the light would fall on the mirror, see fig. 1(*b*). With a parabolic mirror it is not possible to focus the Čerenkov radiation from all parts of the track of the particle simultaneously, owing to the small depth of focus. It was therefore decided to set the position of the phototube so that a sharp image of L_1 was obtained on the photocathode; the diameter of the out-of-focus image of L_2 was then comparable to that of the stop.

The field of view of the instrument, set by the stop and the focal length of the mirror, was $\pm 4.5°$, more than sufficient to include all particles selected by the counter telescope which has a field of wiew of $\pm 3.6°$.

4. – Routine Checks and Calibration.

The single rates of the counter trays were measured daily, and the phototube dark-current pulse rate was monitored continuously on a recording ratemeter. A daily check on the overall gain of the system was carried out by placing a small ^{60}Co source outside the box, in a standard position near the phototube, and measuring the increased count rate at a definite bias setting on the discriminator.

The method used to correlate pulse height, as measured on the film, with the number of electrons liberated at the photocathode, was that used by HOFSTADTER and MCINTYRE (1950). Measurements were made on the fractional width of a pulse-height distribution curve obtained from a source of γ-radiation of known energy in a crystal of NaI(Tl). For this purpose we used the 60 keV γ-ray line from ^{241}Am. Scales calibrated in electron numbers are attached to

the histograms of results, Figs. 2 and 3. The operating conditions of the apparatus were of necessity considerably altered during the calibration.

First, it was found necessary to reduce the voltage on the phototube from its normal value of 2.53 kV, to 1.30 kV, to prevent saturation in the phototube during the pulses, these being ~ 45 times as large from the scintillator as from the light flashes in the air. Secondly, to allow for the relatively long decay times for the light from NaI, 0.24 μs, the amplifier differentiating time-constant was increased from the normal value of 0.032 μs to 1.6 μs. The overall gain of the system during the calibration was then brought to the same value as that used during the experiments. This was accomplished by adjusting the gain of the amplifier so that the rate from the

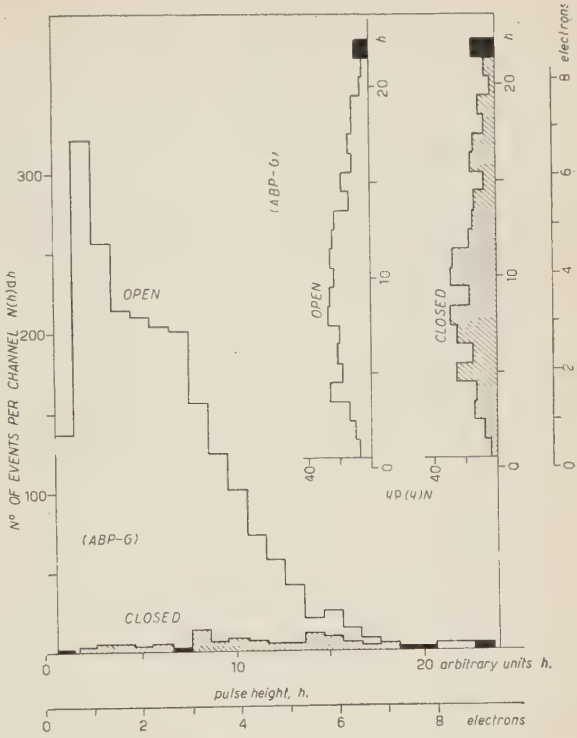

Fig. 2. – Histograms of the pulse-height distributions of the various types of event with the apparatus pointing upwards.

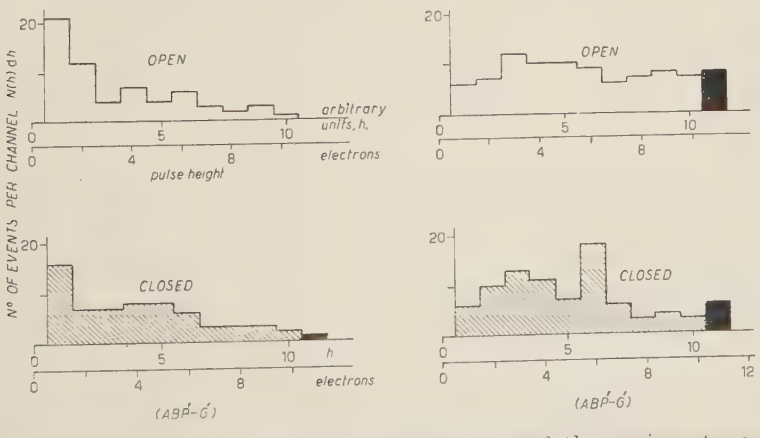

Fig. 3. – Histograms of the pulse-height distributions of the various types of event with the apparatus inverted.

^{60}Co source (without crystal) was the same, at the standard setting of the discriminator, as that throughout the experiments.

The validity of this procedure rests on the assumption that pulses in the phototube from the ^{60}Co source without the crystal, are fast compared with 0.032 μs. If these pulses arise from direct effects of γ-rays on the electrodes of the tube, or from Čerenkov radiation from secondary electrons in the glass window of the tube, this assumption may be justified.

About 600 pulses from the ^{241}Am were photographed, and the full-width at half-height, for the resultant pulse-height distribution, was found to be $(28 \pm 4)\%$ of the mean pulse height. Corrections were made for the statistical fluctuations in the stage gain of the phototube (Morton, 1949). From the relatively poor statistics of the ^{241}Am curve, the estimated error on the electron scales attached to Figs. 2 and 3 is $\sim \pm 30\%$ at any point.

5. – Results.

a) *With the light receiver at the bottom of the box.* – Some preliminary tests were carried out without the anticoincidence counters *G*. With this arrangement a ratio of only $(3.6 \pm 0.5)/1$ was obtained for the pulse rates with the shutter open and closed respectively. The tests revealed that a photomultiplier is remarkably efficient in detecting single particles passing through it even when screened from light; they showed also that the frequency of satellite pulses (Godfrey *et al.*, 1951) was higher for those pulses arising from the passage of particles through the phototube than from the normal dark-current pulses. Since the phototube pulses in all these experiments correspond to the liberation of only a few primary electrons from the photocathode, the satellite pulses are comparable in height to the main pulse. Of 246 pulses with the shutter open, 17% of these had associated satellites within 13 μs of the main pulse, while of 68 pulses with the shutter closed, the corresponding fraction was 41%. This difference might well be expected since, with the shutter closed, the particles giving rise to a phototube pulse will in general traverse the whole dynode structure of the tube.

In all the subsequent experiments the counters *G* were in use. The oscilloscope was triggered on triple coincidences of the type *ABP*, the discriminator following *P* being set at low bias. The recorded events were classified as $(ABP - G)$ or $(ABP + G)$ depending on whether the counters *G* had been fired or not. It was first verified, from the single rates and from independent checks of various types, that all contributions to chance coincidences were negligible.

The pulse height distributions obtained during runs with this arrangement are shown in Fig. 2. There were in all fourteen runs, seven runs with the shutter open interlaced with seven with the shutter closed. 2536 pulses were

recorded in 181.4 hours with the shutter open and 157 pulses were obtained in 186.3 hours with the shutter closed.

Of the events of most interest, those of type $(ABP - G)$, there were 2 183 with the shutter open and 106 when closed (normalised to 181.4 hours). Extrapolating to zero pulse height to allow for the deficiency in channel No. 1 of the histogram imposed by the discriminator bias level, the approximate corrected number with shutter open is 2 400. The true number of light pulses observed is then $(2\,400 - 106) \sim 2\,300$, and the ratio of the number of events with the shutter open to those with it closed is now $(2\,400/106) \sim (23/1)$.

Of the events of type $(ABP+G)$, there are 354 and 338 with the shutter open and closed respectively. The overall anticoincidence efficiency, taken from the « closed » runs, is given by $(ABP-G)/(\text{total } ABP)=[338/(338+106)]=76\,\%$.

It is seen from the histograms of the $(ABP-G)$ events that the average pulse height is rather higher than that for light pulses [type $(ABP - G)_{\text{open}}$] suggesting that the passage of the particles through the phototube releases in general bunches of several electrons at once.

It was expected that the pulse height distributions for the open and closed conditions, i.e. events of type $(ABP - G)$, might differ from one another, for in the « open » runs there would be a contribution to the pulse amplitude from the light, in addition to electrons produced by the passage of the particle itself; however the difference, if present, is insignificant in the histograms of Fig. 2.

The fraction of particles that traverse the system AB and at the same time give rise to a light pulse, is obtained as follows. The total number of light pulses was $\sim 2\,654$ in 181.4 hours $= (14.6 \pm 0.2)$/hour. The figure of 2 654 is obtained by adding the 354 events of type $(ABP+G)_{\text{open}}$ to the figure of 2 300. This assumes that particles which traverse the counters G in addition produce light. The rate of AB events, without the phototube in coincidence, and corrected for chance rate, was measured to be (97 ± 4)/hour. The fraction of particles selected by the counters that pass through the lead absorber, having associated light pulses, is thus $\sim (15 \pm 1)\,\%$.

b) *Experiment with the detector inverted.* – As described earlier, the Čerenkov radiation is not detected if the apparatus is inverted. During a series of runs in which the apparatus was inverted, as described in § **2** above, 153 pulses were observed with the shutter open, over a period of 209.88 hours, and 152 pulses with the shutter closed (normalised to the same time). Of the events $(ABP' - G')$, there were 63 and 64 pulses with the shutter open and closed respectively, and of the events $(ABP'+G')$ the corresponding numbers were 90 and 88. Histograms of the pulse-height distributions of these events are shown in Fig. 3; the scale of pulse heights was calibrated as before, see § **4**.

It is at once apparent within the limits of the statistics that there is no

measurable light from ionization by the μ-mesons traversing the air path. From the statistics on the $(ABP'-G')$ events, for both the open and closed runs, it is deduced that there were < 10 pulses in the 210 hours that could be attributed to light, i.e. the light-pulse rate was < 0.048/hour, to be compared with the rate of 14.6/hour found previously with the light receiver at the bottom of the air column.

6. – Discussion.

Light associated with ionization. – From the results obtained with the apparatus inverted, it is possible to set an upper limit to the amount of light emitted as a result of ionization processes. It will be assumed that light production from these processes does not depend on the energy of the μ-mesons, their energy being $> 2.8 \cdot 10^8$ eV in order to penetrate the lead. From § **5** it was found that the light pulse rate was < 0.048/hour. From the measured AB-rate (corrected for chance coincidences), (97 ± 4)/hour, the fraction of μ-meson tracks giving rise to the emission of at least one photoelectron was therefore $< 4.9 \cdot 10^{-4}$.

A value of 10% for the cathode conversion efficiency was deduced from the figure of 40 μA lumen (quoted by the makers of the phototube, E.M.I.) and the energy conversion factor of 685 lumen = 1 W at 5 560 Å (Leverenz, 1950).

With this value for the cathode efficiency, the above figure for the photoelectron emission will represent a collection of $< 4.9 \cdot 10^{-3}$ photons, on the average, for each μ-meson. If we assume that the light is emitted isotropically from each element of track, it is calculated that approximately 2.5% of the light produced is collected by the mirror. However, owing to the very poor depth of focus of the mirror, a much smaller fraction of the light is received at the photocathode. A subsidiary experiment was carried out to measure the overall efficiency of light collection of the system for isotropic radiation. In this experiment a point source of pulsed light was moved along the optic axis, and the variation of received light measured as the distance of the source from the mirror was varied from 0.5 m to 6.0 m. In this way it was found that the fraction of the total light emitted along the track which was collected by the mirror *and* received at the photocathode, amounted to only 0.27%. The discrepancy between this figure and the 2.5% quoted above arises owing to the greatly increased size of the image for those parts of the track nearest the mirror, just the region where the contribution to the total received light would be greatest if the instrument had an infinite depth of focus.

From our figure of $< 4.9 \cdot 10^{-3}$ photons obtained above, it is then deduced that the total amount of light along the track is < 2.0 photons. This, in turn,

corresponds to a light production of $< 3 \cdot 10^{-3}$ photons/cm (between 3 500-5 500 Å) which is $< 10^{-2}$ of the Čerenkov production rate, or $< 4 \cdot 10^{-6}$ of the rate of energy loss of a relativistic μ-meson due to ionization.

This upper limit assumes that any light formed by the ionization processes would be emitted in a time short compared with 0.03 μs, the differentiation time-constant in the amplifier.

Absolute light intensity for Čerenkov radiation and the pulse-height distribution. – From the rate of light production quoted in § 2, i.e. ~ 0.3 photons/cm, and the path length, we would expect ~ 180 photons to be produced by an ultrarelativistic μ-meson. Because of the steep power-law spectrum for μ-mesons (GLASER *et al.*, 1950), the number of photons liberated will in general be considerably less than the maximum. Fig. 4 illustrates the variation of Čerenkov light output, $\varphi(E)$, as a function of the kinetic energy E of the mesons.

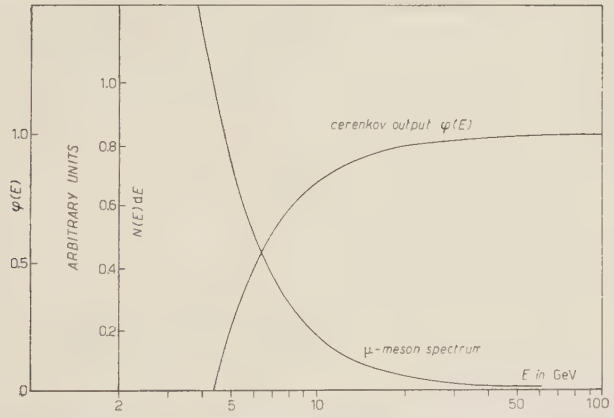

Fig. 4. – Calculated curve for the variation of Čerenkov radiation output as a function of the μ-meson kinetic energy; and the differential μ-meson energy spectrum.

The differential μ-meson energy spectrum, which is also shown, has the form $N(E)\,\mathrm{d}E \propto E^{-\gamma}\,\mathrm{d}E$, a value of 2.0 has been used for γ, an average figure from the data from several observers (see e.g. GLASER, loc. cit.).

The chance of obtaining exactly ν photons would thus be given by a formula of the type

$$f(\nu) = \int_{\text{threshold}}^{\infty} \left(\frac{\varphi^{\nu}}{\nu!} \exp\left[-\varphi \right] \right) E^{-2.0}\,\mathrm{d}E\,,$$

assuming a Poisson distribution for the number of photons emitted. One would expect that a similar law would hold in principle for the number of

electrons emitted at the photocathode (see MORTON, 1949), and hence for the pulse height distribution. The numbers involved would be much smaller, for if we take 10% as the conversion of the cathode, an ultra-relativistic meson would only produce 18 electrons even if the focusing arrangements were perfect. We cannot use the figure obtained in the previous paragraph for the amount of light actually collected, because the angular spread of the Čerenkov light is so narrow. Attempts to fit the formula to the pulse-height distribution of Fig. 2 have not been successful, but it is clear that the average number of electrons liberated by an ultra-relativistic μ-meson is very much less than 18, and may be more nearly equal to 2. It will be realized that the statistical spread in the pulse height will be dominated by the spread in the electron numbers at the photocathode. The small number of electrons emitted reduces the observed rate of reception of pulses below that originally expected, owing to the loss of pulses of amplitude lower than the discriminator bias level.

With the apparatus mounted to receive Čerenkov radiation, the observed value for the ratio of rates $(ABP)/AB$ was 15%, § 5 *a*) above, whereas, on the basis of a Čerenkov threshold of $4.3 \cdot 10^9$ eV, an energy cut-off in the lead absorber of $2.8 \cdot 10^8$ eV, and the accepted form of the μ-meson range spectrum (WILSON, 1940), the calculated ratio is 27%. It is probable that better agreement could have been obtained by operating at a lower bias.

7. – Conclusions.

It is confirmed that Čerenkov radiation exists for μ-mesons passing through air, with a production rate in agreement with the theory of Frank and Tamm, within the limits of error of the experiment. In addition it was found that the amount of isotropic radiation associated with the ionization by the μ-mesons was $< 10^{-2}$ of the intensity of the Čerenkov radiation. On the assumption that the intensity of light produced by ionization is the same for electrons as for μ-mesons, the result of this experiment adds weight to the evidence that the light pulses from the night sky are also due to the Čerenkov effect. The experiments have shown the feasibility of designing gaseous directional Čerenkov detectors for studies of single high-energy particles, such detectors having threshold energies considerably higher than those obtainable with solid and liquid media.

* * *

We wish to express our gratitude to Dr. E. BRETSCHER for his keen interest throughout the work, and to thank Mr. W. J. WHITEHOUSE for helpful discussions and criticism of this paper. We thank also Mr. R. B. OWEN for suggestions in connection with the calibration procedure.

REFERENCES

A. Ascoli Balzanelli and R. Ascoli: *Nuovo Cimento*, **10**, 1345 (1953).
A. Ascoli Balzanelli and R. Ascoli: *Nuovo Cimento*, **11**, 562 (1954).
P. M. S. Blackett: *Gassiot. Comm. Rep. Phys. Soc.* (1948), p. 34.
P. A. Čerenov: *Compt. Rend. Acad. Sci. U.R.S.S.*, **2**, 451 (1934).
S. C. Curran: *Luminescence and the scintillation couter* (London), p. 62.
I. Frank and Ig. Tamm: *Compt. Rend. Acad. Sci. U.R.S.S.*, **14**, 109 (1937).
W. Galbraith and J. V. Jelley: *Nature*, **171**, 349 (1953).
D. A. Glaser, B. Hammermesh and G. Safonov: *Phys. Rev.*, **80**, 625 (1950).
T. N. K. Godfrey, F. B. Harrison and J. W. Keuffel: *Phys. Rev.*, **84**, 1248 (1951).
V. I. Goldanskii and G. B. Zhdanov: *Žhur. Eksp. Teor. Fiz.*, **26**, 405 (1954).
W. Heitler: *The Quantum Theory of Radiation* (Oxford, 1949), p. 222.
R. Hofstadter and J. A. McIntyre: *Phys. Rev.*, **80**, 631 (1950).
J. V. Jelley: *Proc. Phys. Soc.*, A **64**, 82 (1951).
J. V. Jelley: *Progress in Nuclear Physics* (London), (1953), vol. 3, pp. 86, 94.
H. W. Leverenz: *An introduction to luminescence in solids* (New York, 1950), p. 481.
G. A. Morton: *R.C.A. Rev.*, **10**, 525 (1949).
J. Schwinger: *Phys. Rev.*, **75**, 1912 (1949).
J. G. Wilson: *Nature London*, **158**, 414 (1946).

RIASSUNTO (*)

Si è ricorso all'effetto Čerenkov per rivelare singoli mesoni μ in 6 m d'aria a pressione atmosferica. La quantità di luce emessa e la frequenza degli eventi sono in accordo con la teoria classica dell'effetto. Un esperimento apposito ha mostrato che, in assenza di radiazione Čerenkov, la produzione di luce associata a ionizzazione è $< 10^{-2}$ di quella della radiazione Čerenkov, o $< 4 \cdot 10^{-6}$ della perdita di energia per ionizzazione, per i mesoni μ relativistici.

(*) *Traduzione a cura della Redazione.*

Une analyse en déphasages de la diffusion et de la polarisation dans les collisions neutron-proton à grande energie.

C. A. Klein

Laboratoire de Physique de l'École Normale Supérieure - Paris

(ricevuto il 26 Aprile 1955)

Résumé. — L'analyse en déphasages de la diffusion et de la polarisation dans les collisions neutron-proton à grande énergie peut être effectuée conformément au principe de l'indépendance des forces nucléaires par rapport à la charge, si l'on attribue aux états antisymétriques précisément les déphasages $^1K_0$, δ_0; δ_1 et δ_2, qui avaient déjà retenu l'attention lors de l'analyse des interactions proton-proton (inversion des niveaux ^3P_J, potentiel répulsif ^1S). A l'aide des trois paramètres supplémentaires $^3K_0$, $^1K_1$ et $^3K_2$, on est alors en mesure d'obtenir les sections efficaces avec une précision remarquable, et d'approcher convenablement les polarisations. Les valeurs relevées pour les déphasages, en particulier pour $^1K_1$, soulignent l'intérêt que présente à l'heure actuelle le potentiel $V+\lambda V_4^{(a)}$ muni d'un cœur répulsif dans les seuls états S. La présence éventuelle de forces du type spin-orbite peut toutefois poser un délicat problème.

1. – Introduction.

Parmi les conclusions de l'étude des interactions nucléaires aux basses énergies, figure en premier lieu le principe de l'indépendance des forces nucléaires par rapport à la charge. D'autre part, les données expérimentales relatives aux propriétés des mésons π^+, π^- et π^0, organisées dans le cadre de la théorie dite « symétrique », font qu'on a de bonnes raisons d'admettre la validité de ce principe, quelle que soit l'énergie des nucléons.

Par contre, il est incontestable, qu'au-delà de 50 MeV, les caractéristiques générales de la diffusion et de la polarisation dans les collisions (p, p) et (n, p) sont loin de mettre l'indépendance par rapport à la charge en évidence. Toutes les tentatives, entreprises dans l'espoir de retrouver ces caractéristiques à partir de potentiels conçus ad hoc, ont échoué, entre autres le modèle de Jastrow, dont le « cœur répulsif » avait pourtant paru prometteur. Il semble

donc, qu'à l'heure actuelle, le seul procédé susceptible de mener l'étude phénoménologique des forces nucléaires à des conclusions concrètes, consiste à « analyser en déphasages » le résultat des expériences de diffusion et de polarisation. On obtiendra ainsi directement certains renseignements essentiels sur les interactions dans les différents états quantiques, en particulier les états S et P.

C'est dans cet esprit que nous avons récemment examiné le résultat des collisions proton-proton à 170, 260 et 330 MeV [1]. Ne tenant compte que des déphasages subis par les ondes dont le moment cinétique orbital L est $\leqslant 1$, nous avons pu montrer qu'il est possible d'en sélectionner trois séries capables de rendre compte de la situation physique. Parmi ces séries de déphasages, l'une avait d'ailleurs particulièrement retenu notre attention, car elle permet:

a) d'envisager dans l'état ^1S la présence d'un potentiel muni d'un cœur répulsif du type Lévy-Jastrow;

b) d'établir que dans les états ^3P_J ($J=0, 1, 2$) les interactions s'effectuent conformément aux prescriptions du modèle des couches de Mayer-Jensen.

Nous nous proposons maintenant de rechercher, si parmi les solutions fournies par l'analyse de la diffusion et de la polarisation (p, p), il en existe qui soient susceptibles de confirmer la validité du principe de l'indépendance des forces nucléaires par rapport à la charge. Le cas échéant, nous compléterons ces solutions de manière à réaliser une analyse en déphasages de la diffusion et de la polarisation dans les collisions neutron-proton, qui se déroulent aux énergies comprises entre 100 et 400 MeV.

2. – Le formalisme mis en oeuvre.

Dire que les forces nucléaires sont indépendantes de la charge, cela signifie que les interactions (p, p) et (n, p) sont identiques dans les états à caractère antisymétrique. Autrement dit, cela signifie que les forces qui s'exercent entre deux nucléons dérivent du même potentiel lorsque le spin isotopique $T=1$; elles ne diffèrent donc que par suite des contributions provenant des états $T=0$, contributions dont seul bénéficie le système neutron-proton.

Notre analyse de l'interaction (p, p) n'ayant fait appel qu'aux états ^1S et ^3P_J ($J=0, 1, 2$), les seuls états symétriques à envisager dans une analyse de l'interaction (n, p) conforme au principe de l'indépendance par rapport à la charge, sont les états ^3S, ^1P et éventuellement ^3D. Si l'on admet que de toute façon les trois déphasages triplets D sont confondus, et si l'on néglige le couplage $^3S_1$–$^3D_1$ qu'introduit une force non centrale, on obtient pour la section efficace différentielle de la diffusion neutron-proton,

---

[1] C. A. Klein: *Nuovo Cimento*, **1**, 581 (1955).

a) dans le cas d'un faisceau non polarisé (2):

$$(1)\quad \left[\frac{d\sigma(k,\theta)}{d\Omega}\right]_{np} = \frac{1}{4}\left[\frac{d\sigma(k\ \theta)}{d\Omega}\right]_{pp} + \frac{1}{4k^2}\left\{\left[3C(^3K_0, {}^3K_0)\right] P_0(\cos\theta) + \right.$$
$$+ \left[6C(^1K_0, {}^1K_1) + 2\sum_{J=0}^{2}(2J+1)C(^3K_0, \delta_J)\right] P_1(\cos\theta) +$$
$$+ \left[9C(^1K_1, {}^1K_1)\right] P_1^2(\cos\theta) + \left[30\,C(^3K_0, {}^3K_2)\right] P_2(\cos\theta) +$$
$$\left. + \left[10\sum_{J=0}^{2}(2J+1)C(^3K_2, \delta_J)\right] P_1(\cos\theta)P_2(\cos\theta) + \left[75C(^3K_2, {}^3K_2)\right] P_2^2(\cos\theta)\right\},$$

où $[d\sigma(k,\theta)/d\Omega]_{pp}$ désigne la section efficace différentielle de la diffusion proton-proton en l'absence de champ coulombien, soit

$$(2)\quad \left[\frac{d\sigma(k,\theta)}{d\Omega}\right]_{pp} = \frac{1}{k^2}\left\{\left[C(^1K_0, {}^1K_0) + \sum_{J=0}^{2}(2J+1)C(\delta_J, \delta_J)\right] P_0(\cos\theta) + \right.$$
$$\left. + \left[\frac{3}{2}C(\delta_1,\delta_1) + \frac{7}{2}C(\delta_2,\delta_2) + 4C(\delta_0,\delta_2) + 9C(\delta_1,\delta_2)\right] P_2(\cos\theta)\right\}.$$

Le symbole $C(x, y)$ représente le produit $\sin(x)\sin(y)\cos(x-y)$: $^1K_0$, $^3K_0$, $^1K_1$, $^3K_2$ désignent les déphasages respectifs des ondes ^1S, ^3S, ^1P, ^3D, et δ_0, δ_1, δ_2 ceux des ondes $^3P_0$, $^3P_1$, $^3P_2$; les autres notations sont standard.

b) dans le cas d'un faisceau complètement polarisé (3):

$$(3)\quad \left[\frac{d\Sigma(k,\theta,\varphi)}{d\Omega}\right]_{np} = \left[\frac{d\sigma(k,\theta)}{d\Omega}\right]_{np} + \frac{\sin\theta\cos\varphi}{4k^2}\left\{\left[5S(^3K_0,\delta_2) - 3S(^3K_0,\delta_1) - \right.\right.$$
$$- 2S(^3K_0,\delta_0)\left]P_0(\cos\theta) + \left[6S(\delta_0,\delta_2) + 9S(\delta_1,\delta_2)\right] P_1(\cos\theta) + \right.$$
$$\left.\left. + \left[25S(^3K_2,\delta_2) - 15S(^3K_2,\delta_1) - 10S(^3K_2,\delta_0)\right] P_2(\cos\theta)\right\},$$

où le symbole $S(x, y)$ désigne le produit $\sin(x)\sin(y)\sin(x-y)$.

Par définition, l'asymétrie observée dans la diffusion d'un faisceau polarisé est donnée par

$$(4)\quad 2\varepsilon(k,\theta) = \frac{\left[\frac{d\Sigma(k,\theta,0^\circ)}{d\Omega}\right]_{np} - \left[\frac{d\Sigma\ (k,\theta,180^\circ)}{d\Omega}\right]_{np}}{\left[\frac{d\sigma(k,\theta)}{d\Omega}\right]_{np}}.$$

(2) R. M. Thaler, J. Bengston et G. Breit: *Phys. Rev.*, **94**, 683 (1954).
(3) B. D. Fried: *Phys. Rev.*, **95**, 851 (1954).

Le faisceau incident étant complètement polarisé, l'asymétrie est égale à deux fois la polarisation $\mathcal{P}(\theta)$ engendrée par la collision. On en déduit:

$$(5) \qquad \mathcal{P}(\theta) = \frac{1}{4k^2}\left[\frac{\mathrm{d}\sigma(k,\theta)}{\mathrm{d}\Omega}\right]^{-1}_{np} \sin\theta \left\{\left[5S(^3K_0, \delta_2) - 3S(^3K_0, \delta_1) - \right.\right.$$
$$- 2S(^3K_0, \delta_0)\left.\right] P_0(\cos\theta) + \left[6S(\delta_0, \delta_2) + 9S(\delta_1, \delta_2)\right] P_1(\cos\theta) +$$
$$\left. + \left[25S(^3K_2, \delta_2) - 15S(^3K_2, \delta_1) - 10S(^3K_2, \delta_0)\right] P_2(\cos\theta)\right\}.$$

Disposant ainsi de la section efficace différentielle et de la polarisation en fonction de sept déphasages $^1K_0$, $^3K_0$, $^1K_1$, δ_0, δ_1, δ_2, et $^3K_2$, nous sommes en mesure d'aborder le problème de l'analyse des interactions neutron-proton. Procéder à cette analyse conformément au principe de l'indépendance des forces nucléaires par rapport à la charge (*), signifie qu'il faut attribuer aux quatre paramètres $^1K_0$, δ_0, δ_1, δ_2 des valeurs déduites de l'analyse des interactions $(p\text{-}p)$. Remarquons que dans ces conditions le terme en $P_2(\cos\theta)$ de (2) disparait, car les déphasages triplets P assurent précisément l'isotropie de la section efficace différentielle (p, p).

3. – La sélection des déphasages $(^1K_0, \delta_0, \delta_1, \delta_2)$ conformes au principe (I).

Cette sélection peut s'opérer en recherchant les ensembles $(^1K_0, \delta_0, \delta_1, \delta_2)$ qui donnent les meilleurs résultats du point de vue de la diffusion (n, p). On dispose en effet depuis quelques mois, à 150 et 400 MeV, d'indications précises sur le comportement de la section efficace différentielle dans la zone sensible des petits angles de diffusion ([4, 5]).

C'est ainsi, qu'opérant successivement à l'aide des trois solutions de l'interaction (p, p) à 330 MeV, nous avons pu obtenir les courbes de la fig. 1. Les valeurs correspondantes de la polarisation — à noter que dans le cadre de cette recherche préliminaire nous n'avons nullement cherché à reproduire les polarisations — sont représentées sur la fig. 2. Manifestement la solution $^1K_0 = 29°$ est à éliminer; seuls restent donc à envisager les potentiels à cœur répulsif. A 170 MeV l'ultime sélection a pu se faire. Car, cherchant à obtenir les sections efficaces mesurées par Griffith *et al.* ([4]) aux environs de 55° et par Randle *et al.* ([6]) aux environs de 125°, nous avons constaté que seule la solutions $^1K_0 = -37°$ permet d'aboutir.

(*) Par la suite nous désignerons ce principe par « principe (I) ».

([4]) H. S. Massey: *Proceedings of the* 1954 *Glasgow Conference on Nuclear and Meson Physics* (London, 1955), p. 7, où l'on trouvera le résultat des mesures de Griffith *et al.* à 145 MeV.

([5]) A. J. Hartzler, R. T. Siegel et W. Opitz: *Phys., Rev.*, **95**, 591 (1954).

([6]) T. C. Randle, A. E. Taylor et E. Wood: *Proc. Roy. Soc.*, A **213**, 392 (1952).

On en conclut que, parmi les solutions de l'analyse des collisions (p, p), ce sont précisément les plus intéressantes à d'autres points de vue qui se prêtent le mieux à une analyse de l'interaction (n, p) dans l'hypothèse du principe (I). On trouvera au tableau I les valeurs des déphasages utilisés pour construire les courbes représentées sur la fig. 1, 2, et en *B* sur les fig.3, 4. Soulignons que ces courbes ont été obtenues en « consacrant » à la diffusion les trois paramètres disponibles.

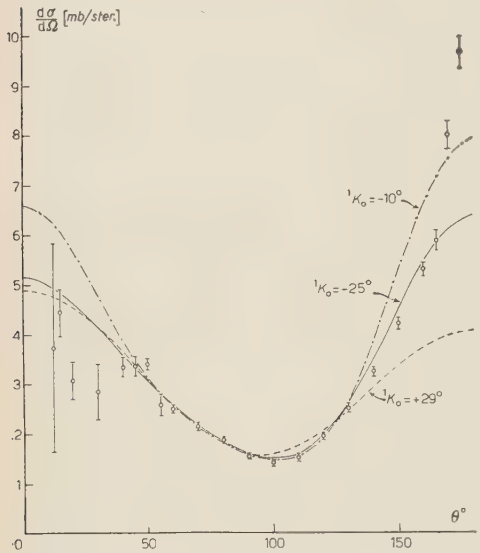

Fig. 1. – Diffusion (n, p) à 330 MeV. Les mesures sont celles de Hartzler *et al.* à 400 MeV. Les courbes ont été calculées à l'aide des déphasages qui figurent au tableau I.

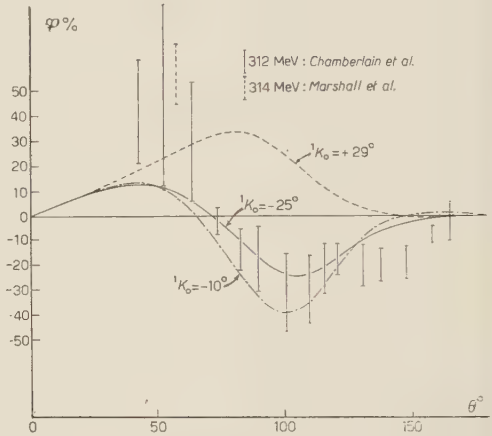

Fig. 2. – Polarisation (n, p) à 330 MeV. Les trois courbes illustrent le comportement du point de vue polarisation de solutions obtenues en ignorant à priori cette dernière.

Tableau I.

Déphasages en degrés, si la polarisation n'est pas prise en considération.

E (MeV)		$^1K_0$	$^3K_0$	$^1K_1$	δ_0	δ_1	δ_2	$^3K_2$
330	1	+ 29	33.8	— 48	9.5	— 26.5	20.4	— 1.2
330	2	— 10	6.4	- 66.9	- 4.5	— 16.5	28.8	— 11.6
330	3	— 25	15.5	62	— 21	— 6	28.2	— 8
170	3	— 37	— 40	31	— 24	— 2.5	12.5	— 5

4. – La détérmination des dephasages ($^3K_0$, $^1K_1$. et $^3K_2$) dans l'hypothèse du principe (I).

Utilisant systématiquement pour les états $T=1$ les déphasages sélectionnés au § 3, nous avons analysé l'ensemble des données expérimentales relatives aux interactions (n, p) entre 100 et 400 MeV. Malheureusement, si la situation paraît maintenant claire en ce qui concerne la diffusion, il n'en est guère de même pour la polarisation. En fait, toutes les mesures, sauf celles de Dickson et Salter (7), ont été effectuées selon le procédé dit de la « collision quasi-libre » d'un nucléon polarisé avec un nucléon dans un noyau léger. Or il n'est pas établi à l'heure actuelle, sauf peut-être dans le cas du deutéron, que la polarisation qu'engendre une telle collision n'est pas affectée par la présence des autres particules (8). D'autre part, les erreurs expérimentales sont encore notables.

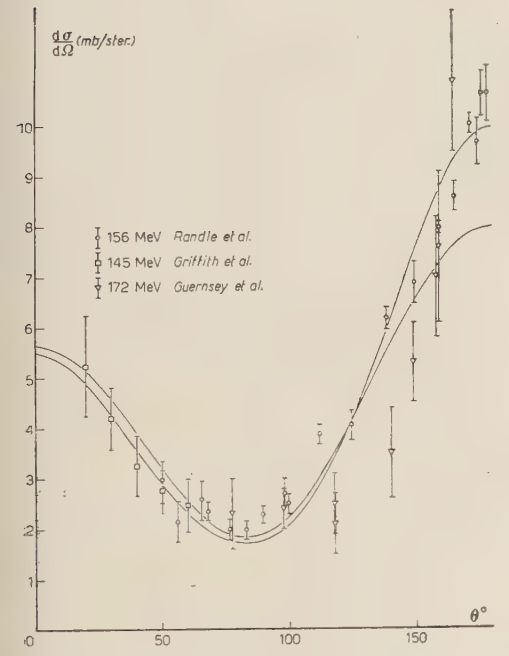

Fig. 3. – Diffusion (n, p) à 170 MeV. La courbe B, obtenue à l'aide des déphasages indiqués en I, représente la meilleure solution possible, lorsqu'on néglige la polarisation. La corbe A par contre, obtenue avec les déphasages indiqués en II, représente une solution également acceptable du point de vue polarisation.

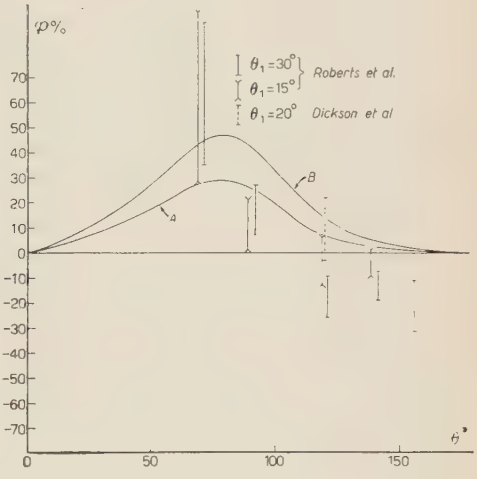

Fig. 4. – Polarisation (n, p) à 170 MeV. θ_1 désigne l'angle de première diffusion, c'est-à-dire pratiquement l'angle d'éjection des neutrons polarisés utilisés. La signification des courbes est claire: A représente l'aspect polarisation de la solution retenue, B l'aspect polarisation de la solution préliminaire.

(7) J. M. Dickson et D. C. Salter: *Proc. Phys. Soc.*, A **66**, 721 (1953).

(8) J. R. Oppenheimer: *Proceedings of the 4th. annual Rochester Conference on High Energy Nuclear Physics* (1954), p. 18.

Néanmoins, en ajustant successivement la section efficace à 90°, 55° et 125°, puis la polarisation à 90°, 60° et 120°, et enfin la section efficace à 30° et 150°, nous avons pu obtenir les résultats qu'illustrent les courbes des figs. 3, 4, 5, 6, 7 et 8. On trouvera au tableau II les déphasages utilisés pour calculer ces courbes.

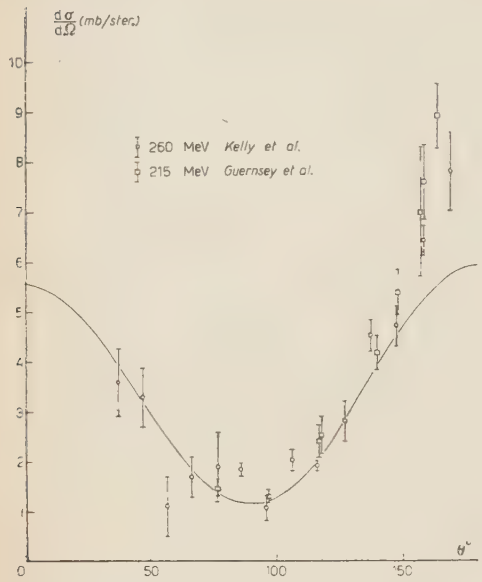

Fig. 5. – Diffusion (n, p) à 260 MeV. La courbe a été construite avec les déphasages qui figurent au tableau II.

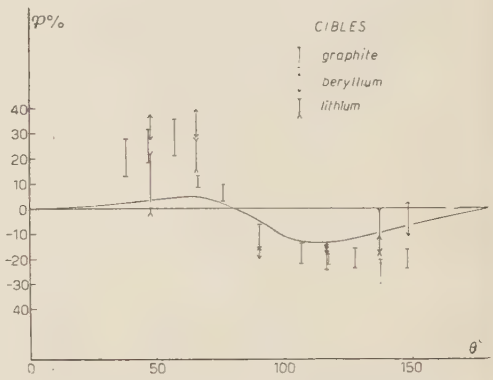

Fig. 6. – Polarisation (n, p) à 260 MeV. La courbe a été construite avec les déphasages qui figurent au tableau II.

TABLEAU II.

Déphasages en degrés, si la polarisation est prise en considération.

E (MeV)		$^1K_0$	$^3K_0$	$^1K_1$	δ_0	δ_1	δ_2	$^3K_2$
170		— 37	— 31	42	— 24	2.5	12.5	0
260		— 43	— 22	49	— 50	5	8.6	— 2
330	A	— 25	15	56	— 21	— 6	28.2	— 9
330	B	— 25	0	59	— 21	— 6	28.2	— 11

a) *100 à 200 MeV*: Sur la fig. 3 nous avons porté les mesures de GRIFFITH *et al.* [4] à 145 MeV raccordées à celles de RANDLE *et al.* [6] à 156 MeV, ainsi que les mesures de GUERNSEY *et al.* [9] à 172 MeV. Les valeurs expérimentales

[9] G. GUERNSEY, G. MOTT et B. K. NELSON: *Phys. Rev.*, **88**, 15 (1952).

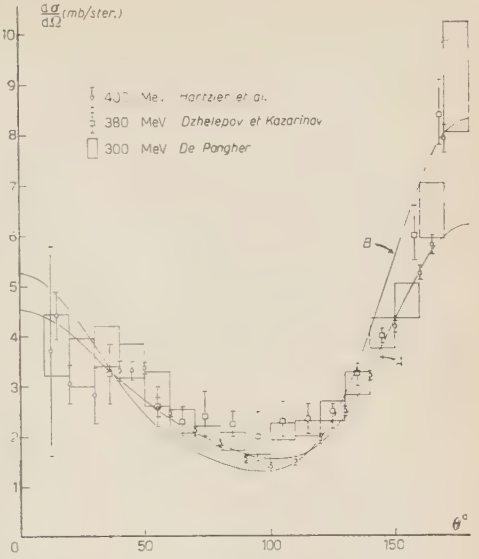

Fig. 7. – Diffusion (n, p) à 330 MeV. La courbe *A* est issue d'une tentative visant à reproduire aussi exactement que possible les résultats remarquablement précis de HARTZLER *et al.*, tout en tenant compte de la polarisation. La courbe *B*, par contre, a été obtenue en recherchant les solutions qui présenteraient le maximum de disymétrie compatible avec la polarisation. Les valeurs des déphasages correspondant sont indiqués au tableau II.

de la polarisation (fig. 4) ont été calculées à partir des mesures d'asymétrie de ROBERTS *et al.* ([10]) et de DICKSON-SALTER ([7]). A noter que ces auteurs ont réalisé des « scattering d'échange », c'est-à-dire qu'il faut poser $\theta = 180° - 2\theta_2$ si θ doit désigner comme d'habitude l'angle de diffusion du neutron dans le système du centre de gravité. Sauf en ce qui concerne la polarisation aux très grands angles, la situation est convenablement décrite avec

$$-35° < {}^3K_0 < 31°,$$

$$33° < {}^1K_1 < 45°,$$

$$-2° \leqslant {}^3K_2 \leqslant 2°,$$

étant entendu que les trois déphasages sont toujours étroitement solidaires.

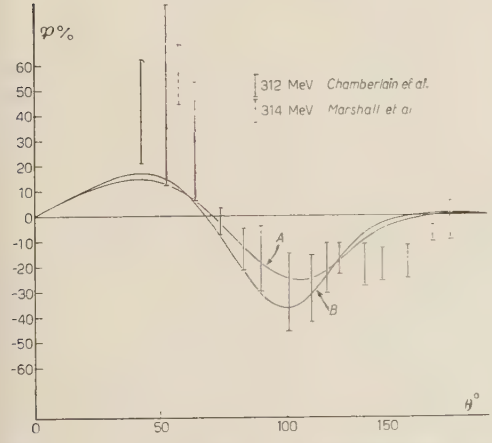

Fig. 8. – Polarisation (n, p) à 330 MeV. *A* et *B* correspondent aux courbes à même dénomination de la fig. 7.

b) 200 à 300 MeV : Fig. 6 on trouvera les valeurs relevées par KELLY *et al.* ([11]) à 260 MeV valeurs déjà anciennes, qui ont pendant plusieurs années laissé présager une symétrie par rapport à 90°, et devaient ainsi induire l'étude des interactions (n, p) en erreur — en compagnie de celles

([10]) A. ROBERTS, J. TINLOT et E. M. HAFNER: *Phys. Rev.*, **95**, 1099 (1954).
([11]) E. KELLY, C. LEITH, E. SEGRÈ et C. WIEGAND: *Phys. Rev.*, **79**, 96 (1950).

de GUERNSEY *et al.* (9) à 215 MeV. Fig. 7 on trouvera la polarisation d'après l'asymétrie observée par BRADNER-DONALDSON (12) lors de la production de neutrons par des protons de 285 MeV polarisés à 65 %. Les solutions valables sont obtenues avec

$$-30^\circ \leqslant {}^3K_0 \leqslant -16^\circ\,, \qquad 49^\circ \leqslant {}^1K_1 \leqslant 51^\circ\,, \qquad -2^\circ \leqslant {}^3K_2 \leqslant 0\,.$$

c) 300 à 400 MeV: On peut comparer sur la fig. 7 les mesures de HARTZLER *et al.* (5) effectées à 400 MeV à l'aide du synchrocyclotron du Carnegie Institute of Technology, avec celles de DZHELEPOV-KAZARINOV (13) menées à 380 MeV avec l'appareil de l'Académie des Sciences de l'URSS. Les résultats obtenus par DE PANGHER (14) à 300 MeV, par détection à la chambre de Wilson, y figurent également. Les valeurs de la polarisation à 310 MeV selon MARSHALL *et al.* (15) et d'après CHAMBERLAIN *et al.* (16) sont indiquées sur la fig. 8. Notons que l'analyse en série de Fourier que ces derniers auteurs croient pouvoir donner parait assez artificielle, étant donné qu'ils font appel aux mesures de KELLY *et al.* (11) pour la diffusion. Les résultats de notre analyse sont satisfaisants, sauf pour la polarisation aux angles extrêmes. Ils conduisent à admettre que

$$-2^\circ \leqslant {}^3K_0 \leqslant 22^\circ\,, \qquad 43^\circ \leqslant {}^1K_1 \leqslant 62^\circ\,, \qquad -14^\circ \leqslant {}^3K_2 \leqslant -5^\circ\,.$$

D'une façon générale, on constate que, si notre analyse reproduit presque parfaitement la diffusion de 0 à 160°, elle ne donne que l'allure générale et l'ordre de grandeur de la polarisation. Il apparait toutefois que, dans la mesure où les données actuelles sont valables, un progrès notable pourrait être réalisé en renforçant l'harmonique deux de $\mathcal{P}(\theta)$. Or on constate sur la formule (5) que l'intensité de cet harmonique dépend exclusivement des déphasages δ_J, c'est-à-dire est déterminée par la polarisation (p, p). Il y aurait donc lieu d'abandonner éventuellement l'hypothèse d'un état ${}^3D$ dégénéré, de sorte que les interférences entre ondes ${}^3S_1$ et ${}^3D_J$ ($J=1, 2, 3$), qui dépendent précisément de θ par l'intermédiaire des $\sin\theta\cdot\cos\theta$, puissent contribuer à la polarisation (3). Il suffirait peut-être même de considérer simplement le couplage ${}^3S_1$–${}^3D_1$ pour améliorer $\mathcal{P}(\theta)$.

(12) H. BRADNER et R. DONALDSON: *Phys. Rev.*, **95**, 1701 (1954).

(13) V. P. DZHELEPOV et Y. M. KAZARINOV: *Dokl. Akad. Nauk. SSSR*, **99**, 939 (1954).

(14) J. DE PANGHER: *Phys. Rev.*, **95**, 518 (1954).

(15) J. MARSHALL, L. MARSHALL, D. NAGLE et W. SKOLINK: *Phys. Rev.*, **95**, 1020 (1954).

(16) O. CHAMBERLAIN, R. DONALDSON, E. SEGRÈ, R. TRIPP, C. WIEGAND et T. YPSILANTIS: *Phys. Rev.*, **95**, 850 (1954).

Cette situation n'est d'ailleurs pas sans analogie avec ce qui résulte de l'étude de la polarisation (p, p), étude qui a mis en évidence l'intérêt que présenterait la prise en considération du couplage ${}^3P_2$–${}^3F_2$. Dans une deuxième phase de travail, on pourrait donc envisager de procéder aux analyses en déphasages sur la base $J \leqslant 2$ au lieu de $L \leqslant 2$.

Quoiqu'il en soit, la qualité des résultats que nous avons pu obtenir, tant pour la diffusion (p, p) que (n, p), avec simplement sept paramètres, paramètres dont les variations en fonction de l'énergie présentent une remarquable continuité, et qui sont conformes à la notion d'indépendance par rapport à la charge, nous autorise sans doute à leur attribuer une signification profonde.

5. – Quelques conclusions à partir des déphasages.

Les analyses auxquelles nous venons de procéder, analyses qui reposent exclusivement sur la notion de « déphasage », notion qu'on sait à l'abri de toute espèce d'objection, confirment que les forces nucléaires sont indépendantes de la charge. D'autre part, les déphasages qu'elles ont mis en évidence incitent dès maintenant à formuler un certain nombre de conclusions, dont l'intérêt ne saurait échapper.

a) *Etat S Singulet*: Nous avons déjà fait observer que les déphasages ${}^1K_0$ retenus ne peuvent provenir que d'un potentiel muni d'un cœur fortement répulsif. Un premier examen indique qu'il doit s'agir d'un cœur dont le rayon serait compris entre 0,6 et $0{,}7 \cdot 10^{-13}$ cm.

b) *Etat S Triplet*: Répulsif de 100 à 300 MeV, le potentiel correspondant donne l'impression de redevenir faiblement attractif au-delà. On pourrait peut-être essayer d'interpréter ce phénomène par la présence d'une force tenseur très singulière (en $1/r^3$ par exemple), qui compenserait en quelque sorte la répulsion aux très faibles distances. On sait en effet qu'une force tenseur présente un caractère attractif quel que soit l'allure de son terme radial ([17]).

c) *Etat P Singulet*: Parmi les résultats les plus interessants de notre analyse figure la forte interaction attractive dans l'état ${}^1P$. La nature de cette interaction fait en effet l'objet de controverses dans le cadre des théories mésiques pseudoscalaires. Notons que ${}^1K_1$ augmente encore au-delà de 300 MeV, ce qui signifie qu'il s'agit en fait d'un potentiel attractif extrèmement singulier.

d) *Etat P Triplet*: Un rapide examen des déphasages δ_0, δ_1 et δ_2 basé sur l'approximation de Born suggère que la force non centrale qui opère dans

---

([17]) M. Matsumoto et W. Watari: *Progr. Theor. Phys.*, **12**, 503 (1954).

les états ${}^3P_J$ est essentiellement du type spin-orbite. Signalons également que ce caractère s'accentue apparament avec l'énergie. D'autre part, le potentiel est attractif pour $J=2$ et nettement répulsif pour $J=0$. On peut en déduire que le signe du facteur radial de $\boldsymbol{L}\cdot\boldsymbol{S}$ est en accord avec ce que donne l'étude du modèle des couches: les niveaux à J élevé sont les plus bas.

c) *Etat D Triplet*: Les déphasages D se sont toujours révélés remarquablement faibles, et ceci tant pour satisfaire la polarisation que la diffusion. Ce résultat est des plus heureux, d'ailleurs aussi bien du point de vue de notre analyse, puisqu'elle ignore les déphasages d'ordre supérieur, que du point de vue de la théorie des champs, puisque les potentiels mésiques sont extrèmement faibles dans les zones extérieures ($\mu r > 1{,}2$). Dans la mesure où c'est l'état ${}^3D_1$ qui prédomine — vraisemblablement par suite de son couplage avec ${}^3S_1$ — on pourrait interprêter la répulsion observée à 330 MeV, en l'attribuant à la force spin-orbite mise en évidence plus haut, car elle devient fortement positive pour $J=1$ et $L=2$ ($\boldsymbol{L}\cdot\boldsymbol{S}=-6$).

Sans vouloir entrer dans les détails, il est frappant de constater à quel point les conclusions auxquelles nous venons de parvenir sont en accord avec les résultats de la théorie mésique pseudoscalaire des forces nucléaires, et plus particulièrement avec la version qu'en a donnée Lévy ([18,19]). En effet, le potentiel statique

$$V = V_2 + \lambda V_4^{(a)} \tag{6}$$

où

$$V_c = \frac{1}{3}\left(\frac{G^2}{4\pi}\right)\left(\frac{\mu}{2M}\right)^2 \boldsymbol{\tau}_1\cdot\boldsymbol{\tau}_2 \left\{\boldsymbol{\sigma}_1\cdot\boldsymbol{\sigma}_2 + S_{12}\left[1+\frac{3}{\mu r}+\frac{3}{(\mu r)^2}\right]\right\}\frac{\exp[-\mu r]}{r} - \tag{7a}$$

$$V_4^{(a)} = -\frac{6}{\pi}\left(\frac{G^2}{4\pi}\right)^2\left(\frac{\mu}{2M}\right)^2\cdot\frac{1}{\mu r^2}K_1(2\mu r)\,, \tag{7b}$$

muni d'un cœur répulsif dans les seuls états S, conformément à ce que donne la méthode de Tamm-Dancoff, présente, du moins dans les états ${}^1S$, ${}^3S$ et ${}^1P_1$ des caractéristiques identiques à celles que l'analyse en déphasages vient de mettre en évidence.

D'une part, l'examen du potentiel (6) aux basses énergies indique que le rayon de son cœur doit être égal à $0{,}38/\mu$, donc du même ordre que le « cœur phénoménologique » aux grandes énergies. D'autre part, la présence du facteur $(\boldsymbol{\tau}_1\cdot\boldsymbol{\tau}_2)$ fait que sa force tenseur est particulièrement active dans les états pairs

---

([18]) M. M. Lévy: *Phys. Rev.*, **88**, 725 (1952).

([19]) M. M. Lévy et R. E. Marshak: *Proceedings of the 1954 Glasgow Conference on Nuclear and Meson Physics* (London, 1955), p. 10.

($T=0$). En outre (6) s'impose par suite de son comportement dans l'état ${}^1P$. La force de Wigner attractive $V_4^{(a)}$ prédomine en effet aux courtes distances, et sa singularité em $1/r^3$ pourrait expliquer les énormes déphasages ${}^1K_1$ relevés à 330 MeV.

Par contre, il faut envisager d'avoir à adjoindre à (6) un terme spin-orbite tel que $-|V_{s0}|\boldsymbol{L}\cdot\boldsymbol{S}$, qui rendrait compte des déphasages P triplets. LÉVY et MARSHAK ([19]) ont déjà attiré l'attention sur cette éventualité en soulignant que la composante spin-orbite pourrait jouer un rôle important dans la polarisation aux grandes énergies. Cependant, le potentiel V_{s0} qu'ils considèrent, et qui est issu des termes du quatrième ordre de la théorie $PS(PS)$,

$$V_{s0}=\frac{12}{\pi}\left(\frac{G^2}{4\pi}\right)^2\left(\frac{\mu}{2M}\right)^4\frac{1}{\mu^2r^3}\cdot\left|\frac{3}{\mu r}K_1(2\mu r)+2K_0(2\mu r)\right|, \tag{8}$$

n'est pas muni du bon signe. Mais selon ARAKI ([20]), le terme spin-orbite se présenterait correctement, à la condition toutefois que l'interaction dans l'état en question présente une singularité répulsive centrale. Reste à savoir si ce point peut être élucidé à l'heure actuelle.

* * *

Cette étude nous a été proposée par Mr. le Professeur M. LÉVY. Elle a bénéficié de ses encouragements et de ses conseils. Nous lui en sommes profondément reconnaissant.

([20]) G. ARAKI: *Proceedings of the* 1954 *Glasgow Conference on Nuclear and Meson Physics* (London, 1955), p. 273.

RIASSUNTO (*)

L'analisi in termini di sfasamento della diffusione e della polarizzazione nelle collisioni neutrone-protone di grande energia può effettuarsi in conformità del principio dell'indipendenza delle forze nucleari rispetto alla carica se agli stati antisimmetrici si attribuiscono precisamente gli sfasamenti ${}^1K_0$, δ_0, δ_1 e δ_2; che già avevano fermato la nostra attenzione nell'analisi delle interazioni protone-protone (inversione dei livelli ${}^3P_J$, potenziale repulsivo ${}^1S$). Con l'ausilio dei tre parametri supplementari ${}^3K_0$, ${}^1K_1$, e ${}^3K_2$, si è allora in grado di ottenere le sezioni efficaci con precisione notevole e di approssimare convenientemente le polarizzazioni. I valori rilevati per gli sfasamenti, in particolare ${}^1K_1$, mettono in rilievo l'interesse che al momento attuale presenta il potenziale $V_2+\lambda V_4^{(a)}$ dotato di un « core » repulsivo nei soli stati S. L'eventuale predi forze del tipo spin-orbita può tuttavia porre un problema delicato.

(*) *Traduzione a cura della Redazione.*

Many-point Correlation-functions in Quantum Field Theory.

E. Freese (*)

California Institute for Technology - Pasadena, California

(ricevuto il 28 Aprile 1955)

Summary. — It is shown how one may calculate the correlation-functions (=Schwingers-Greens-functions) in quantum field-theory for coordinate values not lying too near to the relative light cones of the different coordinates. One may expect that these coordinate values give the most important contributions for the scattering of small energy or large enough angular momentum.

Whenever the probability-distribution of a field (velocity-, density, or particle-) has to be determined, one can describe the probability-functional in terms of an infinite set of correlation-functions, correlating the field-values at different space points with one another. For most experimental questions it is not necessary to know the whole probability-functional, resp. its Fourier-transform, but only some correlation-functions with small coordinate number occur in the calculation of measurable quantities. To determine these functions for the most important coordinate-values it is desirable to break off the infinite set of differential—or integral—equations connecting the different correlation-functions with one another, in order to get a finite set of equations which one may try to solve. In general it will not be a good approximation simply to neglect the higher correlation-functions, but it will be necessary to introduce a set of other functions; these new functions shall be properly chosen so that for some physical reason the neglect of functions with more than a certain coordinate-number gives a good approximation for the physical problem we have in mind. Instead of writing down the infinite set of equations and transforming it, it is in general considerations always easier to use the functional

---

(*) This research was supported by a grant from the Foreign-Operations-Administration.

formalism. In the following it will be shown how one may find suitable approximations in quantum field-theory if one asks for the scattering of particles with low energy.

Let us assume for definiteness a theory with two interacting fields, f.i. meson-theory, which is from beginning on renormalized. Then all transition-amplitudes, that is all S-matrix elements, for the scattering of free particles can easily be obtained by integrations over the incoming and outgoing wave-functions, if the following functions are known (see f.e. ([1,2]))

$$\tau(x_1 \dots | y_1 \dots | z_1 \dots) = (\Omega_{\text{out}} , T A(x_1) \dots \psi(y_1) \dots \psi(z_1) \dots \Omega_{\text{in}}) ;$$

$A(x)$ is the Boson field, $\psi(y)$ the Fermion field with $\bar{\psi} = \psi^+ \beta$;

Ω_{in} is the Heisenberg-vacuum for the incoming particles, defined by $O_{\text{in}}^{(+)}(x)\,\Omega_{\text{in}} = 0$ if $O_{\text{in}}(x)$ is any incoming field operator;

Ω_{out} is the Heisenberg-vacuum for the outgoing particles: $O_{\text{out}}^{(+)}\,\Omega_{\text{out}} = 0$.

If there are no time dependent external fields, Ω_{in} and Ω_{out} can differ only by an imaginary phase and we can assume $\Omega_{\text{in}} = \Omega_{\text{out}}$. For time dependent external fields $|(\Omega_{\text{out}}, \Omega_{\text{in}})| < 1$ because the external field can produce real particles ([3]).

It is very practical to write the general equations for the infinite set of τ-functions as a functional differential equation of the functional

$$\mathfrak{T}(J_1 \mu_1 \bar{\mu}) = (\Omega_{\text{out}}, T \exp\left[i \int_{-\infty}^{\infty} \{ J(x) A(x) + \bar{\mu}(x) \psi(x) + \bar{\psi}(x) \mu(x) \} \mathrm{d}^4 x \right] \Omega_{\text{in}}) .$$

Here J, μ, $\bar{\mu}$ are c-numbers in the continuum space and μ, $\bar{\mu}$ operators in spinor-space anticommuting with one-another and with all ψ and $\bar{\psi}$.

(Such functions μ can in reality not be constructed quite arbitrarily as here assumed, but this shall not concern us here, because we will use them only as a practical way of deriving equations for the τ and connections with other functions ϱ, which could have been derived also in another but more complicated way.)

The τ-functions are now easily obtained by expanding $\mathfrak{T}$ in powers of the functions J, μ and $\bar{\mu}$ ([4]).

([1]) E. Freese: *Zeits. f. Naturfor.*, 8a, 775 (1953); *Acta Phys. Austr.*, 8, 289 (1954).

([2]) H. Lehmann, K. Symanzik and W. Zimmermann: *Zur Formulierung quantisierter Feldtheorien*, preprint.

([3]) For the definition including bound particles see (1).

([4]) K. Symanzik: *Zeits. f. Naturfor.*, **10**, 809 (1954).

Whatever theory one uses, one gets an infinite set of differential or integral equations connecting all the τ-functions with one-another. In the functional space one gets functional-differential equations whose coefficients are either space-derivatives or space-integrals. As example may serve the equations of renormalized pseudoscalar charge-symmetric meson-theory. In functional form they are [4]

$$\{(\gamma_\nu p_\nu + m)\,\delta_y - \mu(y)\}\mathfrak{T} = -ig\gamma_5\tau_\alpha\delta_y^\alpha\delta_y\mathfrak{T} + \text{Ren.}$$

$$\{(\Box_x - \varkappa^2)\,\delta_x^\alpha + J^\alpha(x)\}\mathfrak{T} = -ig\bar{\delta}_x\gamma_5\tau_\alpha\delta_x\mathfrak{T} + \text{Ren.}$$

$$\delta_x^\alpha = \frac{1}{i}\frac{\delta}{\delta J^\alpha(x)}\,; \qquad \delta_y = \frac{1}{i}\frac{\delta}{\delta\mu(y)}\,; \qquad \bar{\delta}_y = \frac{1}{i}\frac{\delta}{\delta\bar{\mu}(y)}\,.$$

Here Ren. means additional terms which are formally written down to make the theory renormalized.

The equation for τ's have been written down by several authors [4], we need not repeat them here. The main feature is that the differential equation for each τ-function contains a δ-function, coming from the δ-function commutation-relations which is assumed for equal times.

The problem now is: How can we solve this infinite set in a reasonably good approximation if we wish to know the smallest τ-functions, which are only necessary for the calculation of scattering processes of some particles. Naturally we shall try to brake off the set, assuming that all functions with more then a certain coordinate number can be neglected. Then we will get a finite set of equations which we can try to solve either by some other approximation or integrating numerically. To neglect the higher τ-functions itself would be a very bad approximation, because we know that f.i. for *free fields* all τ-functions can be expressed as products of Δ_F, S_F functions; in functional form this looks again rather simple:

$$\mathfrak{T}_{\text{free}} = \exp\left[-\int_{-\infty}^{\infty}\{J(x)\Delta_F(x-y)J(y) + \bar{\mu}(x)S_F(x-y)\mu(y)\}\mathrm{d}^4x\,\mathrm{d}^4y\right].$$

Generally we do not want to refer anyhow to the free fields, because these considerations here are mainly of interest when the coupling is intermediate, and accordingly an approximation by free fields is a bad one. Therefore we must find some property of the τ-functions which we know to be right from physical considerations. (Quite generally also in the theory of fluids or in that of isotropic turbulence etc., we shall try to find as many physical properties of the functions in question as we can predict a priori, and in this way we can find the reasonable approach for braking off the infinite system

of equations.) This property is quite clear here: if in a τ-function with a certain number of coordinates some group of coordinates lie space like or time like very far apart from another ($x_\nu^2 \gg (\hbar/mc)^2$ or $\ll (\hbar/mc)^2$ where m is the mass of the free particle) but not the coordinates of one group near the light cone of the other then the τ-function decays into a product of two τ-functions each one belonging to one group,

$$\tau(x_i \ldots y_k \ldots) = \tau(x_i \ldots)\, \tau(y_k \ldots) .$$

The reason for this separation is that the space points of one group can only have a negligible interaction with the space-points of the other group.

We now introduce new functions ϱ having the property to vanish always if any coordinates are far separated in the said way. That is we set:

$$\tau(x_1\|) = \varrho(x_1\|)$$

$$\tau(x_1x_2\|) = \varrho(x_1\|)\,\varrho(x_2\|) + \varrho(x_1x_2\|)$$

$$\tau(|y|z) = \varrho(|y|z)$$

$$\tau(x|y|z) = \varrho(x\|)\,\varrho(|y|z) + \varrho(x|y|z)$$

$$\tau(x_1x_2|y|z) = \varrho(x_1\|)\,\varrho(x_2\|)\,\varrho(|y|z) + \varrho(x_1\|)\,\varrho(x_2|y|x) + \varrho(x_2\|)\,\varrho(x_1|y|z) + \varrho(x_1x_2\|)\,\varrho(|y|z) + \varrho(x_1x_2|y|z)$$

and so on.

If we have a closed system, that is a system without any external field, the function $\tau(x\|) = \varrho(x\|)$ is zero. The functions $\tau(|y|) = \langle\psi(y)\rangle_0$ and $\tau(|z|) = \langle\bar{\psi}(z)\rangle_0$ are always zero because of the conservation of the « fermion-number » (= number of fermions minus number of antifermions).

One can find a general rule for the correspondence between τ and ϱ-functions. If we define a functional $\mathfrak{R}$ whose expansion-coefficients are the ϱ-functions instead of the τ, the connection between the functional $\mathfrak{T}$ and $\mathfrak{R}$ is extremely simple:

$$\mathfrak{T} = e^{\mathfrak{R}} \qquad \text{or} \qquad \mathfrak{R} = \ln \mathfrak{T} .$$

If we expand these equations on both sides in powers of J, μ and $\bar{\mu}$ we get a fairly simple relation between the ϱ and the τ-functions:

$$\tau(\ldots) = \varrho(\ldots) + \frac{1}{2!}\,\varrho(\ldots)_2 + \frac{1}{3!}\,\varrho(\ldots)_3 + \frac{1}{4!}\cdots$$

$$\varrho(\ldots) = \tau(\ldots) - \frac{1}{2}\,\tau(\ldots)_2 + \frac{1}{3}\,\varrho(\ldots)_3 - \frac{1}{4}\cdots$$

Here $\tau(\ldots)_\nu$ f.i. means, one has to take the sum over all possible ways of decomposing this τ-function into a produt of ν smaller τ-functions. One has to take all possible permutations of the coordinates leaving out only the permutations within one τ-function. One easily checks that the first simple functions really give the right result. The general derivation is given in the Appendix.

Now we can understand in a different way, why the ϱ-functions are more reasonable than the τ: in statistical mechanics it is more reasonable to develop not the functions themselves but their logarithm in powers of some parameters because we have an extremely high number of particles. Here the same principle is better, because we have a very large number of interacting space-points (namely the continuum).

In the usual graph-formalism these ϱ-functions have again a simple meaning. If we develop the τ-functions as graphs in powers of the coupling-constant, f.e. using the interaction-representation ([5]), we see immediately that the ϱ-functions are just the parts of the τ which cannot be decomposed into groups of independent graphs. For instance $\tau(x_1 x_2 x_3 | y | z)$ contains graphs of the form

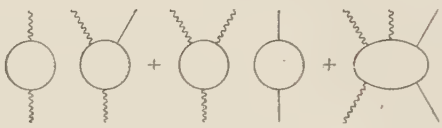

while $\varrho(x_1 x_2 x_3 | y | z)$ contains only the inseparable graphs:

If we insert this Ansatz for $\mathfrak{T}$ in the functional-differential equation we get new equations for $\mathfrak{R}$:

$$(\gamma_\nu p_\nu + m)\,\delta_y \mathfrak{R} - \mu(y) = -ig\gamma_5\tau_\alpha \{ \delta_y^\alpha \delta_y \mathfrak{R} + \delta_y^\alpha \mathfrak{R}\, \delta_y \mathfrak{R} \} + \text{Ren.}$$

$$(\Box - \varkappa^2)\,\delta_x \mathfrak{R} + J^\alpha(x) = -ig \left\{ \bar{\delta}_x \gamma_5 \tau_\alpha \delta_x \mathfrak{R} + (\bar{\delta}_x \mathfrak{R}) \gamma_5 \tau_\alpha (\delta_x \mathfrak{R}) \right\} + \text{Ren.}$$

If we again expand in powers of J, μ and $\bar{\mu}$ we get the differential equations

---

([5]) W. Zimmermann: *Nuovo Cimento*, **11**, 416 (1954).

for the ϱ-functions:

$$\begin{cases} (\gamma p_y + m)\, \varrho(|y|z) + i\,\delta(y-z) = -ig\gamma_5\tau_\alpha\, \varrho(y_y^{(\alpha)}|y|z) + \text{Ren.} \\ (\Box_{x_1} - \varkappa^2)\, \varrho(x_1^{(\alpha)} x_2^{(\beta)}\|) - i\delta_{\alpha\beta}\delta(x_1 - x_2) = -ig\gamma_5\tau_\alpha\, \varrho(x_2^{(\beta)}|x_1|x_1) + \text{Ren.} \end{cases}$$

$$(l+m+n>2) \quad \begin{cases} (\gamma p_y + m)\, \varrho(x_1 \dots x_l | y y_1 \dots y_m | z_1 \dots z_n) = \\ \quad = -ig\gamma_5\tau_\alpha \{ \varrho(x_1 \dots x_l\, y^{(\alpha)} | y y_1 \dots y_m | z_1 \dots z_n) + \\ \quad + \varrho(x_1 \dots x_l\, y^{(\alpha)} | y y_1 \dots y_m | z_1 \dots z_n)_2 \} + \text{Ren.} \\ (\Box_x - \varkappa^2)\, \varrho(x^{(\alpha)} x_1 \dots x_l | y_1 \dots y_m | z_1 - z_n) = \\ \quad = -ig\gamma_5\tau_\alpha \{ \varrho(x_1 \dots x_l | y_1 \dots y_m\, x | x z_1 \dots z_n) + \\ \quad + \varrho(x_1 \dots x_l | y_1 - y_n\, x | x z_1 \dots z_n)_2 \} + \text{Ren.} \end{cases}$$

$\varrho(\dots|\dots x|x\dots)_2$ has a similar meaning as before: Take the sum over all possible products of 2 ϱ-functions in which each of them contains just once the coordinate x.

These differential equations of the ϱ have two properties different from the equations of the τ: Only the differential equation of the ϱ-function with two coordinates contains a δ-function, while the equations for the higher ϱ-functions do not. The equations do not only connect one function with the others, but they do this in a non linear way.

If we want to calculate a simple ϱ-function, f.i. $\varrho(x_1 x_2|y|z)$, and we are only interested in its « outside behaviour » (all coordinate differences $|x_\mu^2| \gtrsim M^2$) but not the behaviour on the light-cone, we may expect to get a good approximation, neglecting all ϱ-functions with more than 4 coordinates and solving the resulting set of differential equations. The reason is roughly the following: The ϱ-functions have the property to be concentrated to smaller and smaller regions, the higher their coordinate number is. The integral equations, following from the differential equations of the ϱ-functions have as integral kernel the Δ_F and S_F functions, which essentially are Bessel-functions giving their main contribution in the region $|x_\mu^2| \lesssim m^2$ about the light-cone. The higher now the coordinate number in the ϱ-function, the smaller is the space region for which the integral gives any contribution and we can neglect this ϱ-function compared with the product of smaller ϱ, if it is not just very large for small coordinate-differences. How good such an approximation is, naturally depends on the special nature of the interaction and cannot be argued without a real calculation. In quantum elctrodynamics, where the coupling is rather weak, the solution is a very good one, but then we even can develop every integral equation in powers of the coupling constant and do not need the ϱ-functions. In meson theory the situation is very involved, because it has not been possible to give equations which avoid any renormalization but still

are easy to handle (compare [2]), nor to find wave functions for dressed particles (those including the meson cloud about the nucleon) and a way to describe their scattering.

As the only example for the usefulness of the functional $\mathfrak{R}$ I shall give here, therefore, the simple (linear) case of an electromagnetic field interacting with an external source, where the exact solution can be given, as well known. We obtain this here very simply, writing down the equation for $\mathfrak{R}(J) = \ln(\Omega_{\text{out}} \exp[i \int J_\nu A_\nu \, \mathrm{d}^4x] \Omega_{\text{in}})$

$$\frac{1}{i} \Box_x \frac{\delta}{\delta J^\nu(x)} \mathfrak{R} = j^\nu(x) - J^\nu(x) , \qquad (j^\nu(x) = \text{external current})$$

and integrating this:

$$\mathfrak{R} = -\int \left\{ J_\nu(x) \, \Delta_F(x - x') \, j_\nu(x') - \frac{1}{2} J_\nu(x) i \Delta_F(x - x') J_\nu(x') \right\} \mathrm{d}x \, \mathrm{d}x' + \text{const} ,$$

$$\mathfrak{T}(J) = e^{\mathfrak{R}} .$$

Expanding $\mathfrak{T}$ in powers of J we get all possible τ-functions for the emission and absorption of light quanta by means of the external field. The constant in $\mathfrak{R}$ is determined by the conservation of probability: the transition probability for getting any final state from a certain initial state must be 1 [1].

Appendix

Connection between ρ- and τ-functions.

Expanding the functional $\mathfrak{T}$ in powers of J, $\bar{\mu}$, μ we get:

$$\mathfrak{T} = \sum_{l,m,n=0}^{\infty} \frac{i^{l+m+n}}{l! \, m! \, n!} \int J(x_1) \dots J(x_l) \bar{\mu}(y_1) \dots \bar{\mu}(y_m) \, \tau(x_1 \dots x_l \,|\, y_1 \dots y_m \,|\, z_1 \dots z_n) \cdot \\ \cdot \mu(z_1) \dots \mu(z_n) \, \mathrm{d}x_1 \dots \mathrm{d}y_1 \dots \mathrm{d}z_n .$$

Let us write this as $\mathfrak{T} = 1 + G$
Then we get for G^2

$$G^2 = \sum_{l,m,n} \frac{i^{l+m+n}}{l! \, m! \, n!} \sum_{l_1, m_1, n_1} \frac{l!}{l_1! \, (l - l_1)!} \cdot \frac{m!}{m_1! (m - m_1)!} \cdot \frac{n!}{n_1! \, (n - n_1)!} \int J(x_1) \dots J(x_l) \cdot \\ \cdot \bar{\mu}(y_1) \dots \bar{\mu}(y_m) \, \tau(x_1 \dots x_{l_1} \,|\, y_1 \dots y_{m_1} \,|\, z_1 \dots z_{n_1}) \, \tau(x_{l_1+1} \dots x_l \,|\, y_{m_1+1} \dots y_m \,|\, z_{n_1+1} \dots z_n) \cdot \\ \cdot \mu(z_1) \dots \mu(z_n) \, \mathrm{d}x_1 \dots \mathrm{d}z_n .$$

Here each of the two τ-functions must at least contain one coordinate (but cannot be 1). Introducing a new symbol for the second sum we can write this simpler:

$$G^2 = \sum_{l,m,n} \frac{i^{l+m+n}}{l!\,m!\,n!} \int J \dots \bar{\mu} \dots \tau(x_1 \dots x_l \,|\, y_1 \dots y_m \,|\, z_1 \dots z_n)_2 \, \mu \dots \mathrm{d}x_1 \dots \mathrm{d}z_n \,.$$

In a straightforward manner we can write for the higher powers of G

$$G^\nu = \sum_{l,m,n} \frac{i^{l+m+n}}{l!\,m!\,n!} \int y \dots \bar{\mu} \dots \tau(x_1 \dots x_l \,|\, y_1 \dots y_m \,|\, z_1 \dots z_n)_\nu \, \mu \dots \mathrm{d}x_1 \dots \mathrm{d}z_n \,,$$

where now $\tau(\dots)_\nu$ represents the sum over all products of ν τ-functions with the total number of coordinates l, m, n. Again each of the τ-functions must at least contain one coordinate.

The connection between ϱ and τ is now easily established if we expand

$$\mathfrak{R} = \ln(1 + G) = G - \frac{1}{2} G^2 + \frac{1}{3} G^3 - + \dots$$

resp.

$$\mathfrak{T} = e^{\mathfrak{R}} = 1 + \mathfrak{R} + \frac{1}{2!} \mathfrak{R}^2 + \frac{1}{3!} \mathfrak{R}^3 + \dots$$

and write both sides as power-series in J, $\bar{\mu}$, μ. In this way we obtain the relation between ϱ and τ as given in the text. (The ϱ functions with index are in the same way composed of products of smaller ϱ functions as the τ.)

RIASSUNTO (*)

Si mostra come si possano calcolare le funzioni di correlazione (funzioni di Schwinger-Green) nella teoria quantistica dei campi per valori delle coordinate non troppo prossimi ai coni di luce relativi delle differenti coordinate. Si può ritenere che tali valori delle coordinate diano i più importanti contributi per lo scattering di bassa energia o di momento angolare sufficientemente grande.

(*) *Traduzione a cura della Redazione.*

Numerical Calculations on the Fluctuation Problem in Cascade Theory.

J. W. Gardner, H. Gellman (*) and H. Messel

The F.B.S. Falkiner Nuclear Research and Adolph Basser Computing Laboratories, School of Physics (+), The University of Sydney - Sydney, N.S.W.

(ricevuto il 28 Aprile 1955)

Summary. — The problem of obtaining numerical results for the fluctuation problem in cascade theory is discussed. Results, using the electronic computer, Ferut and desk calculating machines are presented for a « model-test-run » on the nucleon cascade in homogeneous nuclear matter. These are discussed in relation to an extensive program of computations for the physically important case of electron-photon cascades.

1. – Introduction.

An analytical solution of the fluctuation problem in cosmic ray shower theory has been presented in a series of recent publications [1-6]. These cover nucleon cascades in homogeneous nuclear matter [2], and a finite absorber [3,5]; and the electron-photon cascade [4,5]; ionization loss being taken into account where appropriate [5]. The formal solution is effected when we have obtained an expression, however complicated, for the function Φ which satisfies the diffusion equations describing the multiplication of particles in the cascade.

(*) Adalia Ltd., 20 Carlton St., E. Toronto, Canada.

(+) Also supported by the Nuclear Research Foundation within the University of Sydney.

(1) H. Messel and J. W. Gardner: *Phys. Rev.*, **84**, 1256 (1951).

(2) H. Messel: *Proc. Phys. Soc.* (London), A **65**, 465 (1952).

(3) H. Messel and R. B. Potts: *Proc. Phys. Soc.* (London), A **65**, 473 (1952).

(4) H. Messel and R. B. Potts: *Phys. Rev.*, **86**, 847 (1952).

(5) H. Messel and R. B. Potts: *Phys. Rev.*, **87**, 759 (1952).

(6) H. Messel and R. B. Potts: *Proc. Phys. Soc.* (London), A **65**, 854 (1952).

Physically Φ represents the probability of finding a given number of particles, of a particular kind and above a given energy, at a certain depth below the cascade origin.

The lack of reasonable numerical tables of such a probability function has made the quantitative interpretation of many cosmic ray and machine experiments next to impossible; and in many other cases has led to results of dubious value.

Unfortunately, we have found the problem of obtaining numerical values for Φ by carrying out the integrals in the formal solutions most forbidding indeed, even with the aid of an electronic computer.

We have therefore examined at length an alternative method of obtaining numerical results. References ([2-6]), in addition to the solutions for Φ, also give the general analytical solutions for the k-th moment $\Phi_{(k)}$ of Φ and these, for small values of k, are more amenable to numerical computation.

The first few moments give useful information about the probability distribution: average numbers, spread, asymmetry, etc.. Furthermore, one can sometimes construct a good approximation to Φ from an expansion in terms of its first few moments and the moments of a suitably chosen weight function ([7]). This method is discussed, in regard to the present problem in Section 3.

Though the method of constructing the distribution function from its first few moments is sometimes more amenable to numerical work than carrying out the complex integrations in the formal solution for Φ, the amount of work involved is still forbidding. Before proceeding with the numerical evaluation of the complex moment expressions arising in the case of an electron-photon cascade we therefore decided to test our method on the much simpler but similar case of a nucleon cascade developing in homogeneous nuclear matter.

As pointed out by JÁNOSSY and MESSEL ([8]), the moment curves for nucleon cascades and electron-photon cascades are similar in shape and differ only in magnitude. Though the present results are not completely without interest in themselves, we prefer to look upon the work as a « model-pilot-run » for future computations on the mathematically more complicated but physically more interesting cascade of electrons and photons.

This paper presents the results of computation of the first three moments of Φ for the nucleon cascade in homogeneous nuclear matter. The function $\Phi(\varepsilon, n; x)$, whose moments are computed, expresses the probability of finding n nucleons with energies above εE_0 at depth x as a result of a single incident primary nucleon of energy E_0 at zero depth. We have taken $\varepsilon = 10^{-1}$, 10^{-2}, 10^{-3}, 10^{-4} and x from 0 to about 30 collision units.

In Section 3 we have constructed a number of sample probability distri-

---

([7]) H. S. GREEN and H. MESSEL: *Quarterly of Applied Maths.*, **11**, 403 (1954).

([8]) L. JÁNOSSY and H. MESSEL: *Proc. Roy. Irish Ac.*, **54**, A 16, 245 (1951).

butions for $\varepsilon = 10^{-2}$ and various depths using the expansion method of reference (7). Besides acting as a pilot-run our results might have applicability to the cascades occurring for example in nuclei of photographic emulsions and may help predictions to be made about the probable number of star particles ejected in a given energy range. One should note, however, that the present state of nucleon cascade theory is not one which allows any high degree of confidence to be placed in the quantitative results derived from it.

2. – Evaluation of Moments.

The general formula for the k-th factorial moment of $\Phi(\varepsilon, n; x)$ — formula (37) of reference (2) — becomes for $k = 1$. with a slight and obvious change in notation:

$$\Phi_1(\varepsilon, x) = \frac{1}{2\pi i} \int_{\lambda - i\infty}^{\lambda + i\infty} \varepsilon^{-s} \exp[-x\alpha_s] \frac{\mathrm{d}s}{s} . \tag{2.1}$$

The quantity α_s depends on the nucleon-nucleon collision cross-section; the general analysis is valid for any cross-section which is a homogeneous function of the primary and secondary energies, but to obtain numerical results one must choose some specific function. We have taken:

$$w(\varepsilon_1, \varepsilon_2) = 120\varepsilon_1\varepsilon_2(1 - \varepsilon_1 - \varepsilon_2) . \tag{2.2}$$

Here $w(\varepsilon_1, \varepsilon_2)$ is the cross-section for the production of secondary and recoil nucleons of energies $\varepsilon_1 E_0$, $\varepsilon_2 E_0$ by a primary of energy E_0, the balance of energy going into meson production.

The approximate validity of (2.2) for primary energies above 1 GeV — and the present work applies only to such energies — has been discussed elsewhere (9) in the light of experimental results available at the time. We are not aware of any conclusive results which would justify using a greatly different cross-section at the present time; recent experimental results by POMERANTZ (10), surprisingly enough, are consistent with (2.2). At any rate, the general pattern of the present computations would be unaltered by the substitution of another cross-section, provided it were still a homogeneous function of the primary and secondary energies, as are the full screening cross-sections for the pair production and bremsstrahlung.

---

(9) H. MESSEL: *Progress in Cosmic Ray Physics* (Amsterdam, 1954), vol. 2, ch. 4.
(10) M. A. POMERANTZ: *Phys. Rev.*, **95**, 531 (1954).

Using (2.2), α_s takes the form:

$$\alpha_s = 1 - 240\{(s+2)(s+3)(s+4)(s+5)\}^{-1}. \tag{2.3}$$

The first moment was evaluated by two different methods. The first was a direct numerical integration using FERUT (Ferranti Electronic Computer at the University of Toronto). For this purpose (2.1) was rewritten by the aid of a familiar theorem ([11]), in the form:

$$\Phi_1(\varepsilon, x) = -\frac{\exp[-\lambda \ln \varepsilon]}{\pi} \int_0^\infty \frac{\exp[-xA]}{\lambda^2 + r^2} [\lambda \cos(xB + r \ln \varepsilon) - \\ - r \sin(xB + r \ln \varepsilon)] \cdot \mathrm{d}r \tag{2.4}$$

with

$$s = \lambda + ir \tag{2.5}$$

$$A = 1 - 40(P_2 - 3P_3 + 3P_4 - P_5) \tag{2.6a}$$

$$P_j = (\lambda + j)\{(\lambda + j)^2 + r^2\}^{-1} \tag{2.6b}$$

$$B = -40(Q_2 - 3Q_3 + 3Q_4 - Q_5) \tag{2.7a}$$

$$Q_j = -r\{(\lambda + j)^2 + r^2\}^{-1}. \tag{2.7b}$$

Simpson's rule with various intervals was used for the numerical integration. For values of the depth parameter x greater than 10 cascade units, the oscillatory part of the integral is negligible. For $x < 10$ the integral was done only for the range $0 \leqslant r < 10$, and for the range $r = 10$ to $r = \infty$ the following formula was used ([12]):

$$\int_{10}^\infty f(\lambda, x, r)\,\mathrm{d}r = e^{-x}\left\{-\varepsilon \int_{r \ln \varepsilon}^\infty \sin z \frac{\mathrm{d}z}{z} + \frac{(\varepsilon - 1)\cos(r \ln \varepsilon)}{r} + \right. \\ + \frac{(\varepsilon - 1 - \ln \varepsilon)\sin(r \ln \varepsilon)}{(r \ln \varepsilon)^2} - (2!)\left[\varepsilon - 1 - \frac{\ln \varepsilon}{1!} - \frac{(\ln \varepsilon)^2}{2!}\right] \cdot \\ \cdot \cos(r \ln \varepsilon) \cdot (r \ln \varepsilon)^{-3} - (3!)\left[\varepsilon - 1 - \frac{\ln \varepsilon}{1!} - \frac{(\ln \varepsilon)^2}{2!} - \frac{(\ln \varepsilon)^3}{3!}\right] \cdot \\ \left. \cdot \sin(r \ln \varepsilon) \cdot (r \ln \varepsilon)^{-4} + \ldots\right\} \tag{2.8}$$

([11]) See for example R. V. Churchill: *Modern Operational Mathematics in Engineering* (New York, 1944).

([12]) See Appendix A.

TABLES *of* $\Phi_1(\varepsilon, x)$. – *The First Moment of the Number Distribution Function for a Nucleon Cascade in Homogeneous Nuclear Matter.*

TABLE I-*A*. – Results of Direct Numerical Integration.

x	$\varepsilon = 10^{-1}$	$\varepsilon = 10^{-2}$	$\varepsilon = 10^{-3}$	$\varepsilon = 10^{-4}$
1	1.40	2.30	—	—
2	1.22	3.51	—	—
3	$8.590 \cdot 10^{-1}$	3.995	9.015	15.40
5	$3.100 \cdot 10^{-1}$	3.079	12.96	33.43
7	$8.853 \cdot 10^{-2}$	1.582	11.06	44.42
10	$1.063 \cdot 10^{-2}$	$3.807 \cdot 10^{-1}$	4.909	34.34
15	$2.18578 \cdot 10^{-4}$	$1.88450 \cdot 10^{-2}$	$5.3045 \cdot 10^{-1}$	7.63274
20	$3.507 \cdot 10^{-6}$	$5.9739 \cdot 10^{-4}$	$3.09307 \cdot 10^{-2}$	$7.81595 \cdot 10^{-1}$
30	$6.05 \cdot 10^{-10}$	$2.924 \cdot 10^{-7}$	$3.8524 \cdot 10^{-5}$	$2.31956 \cdot 10^{-3}$

TABLE I-*B*. – Selected Results of Saddle Point Calculation of $\Phi_1(\varepsilon, x)$.

x	$\varepsilon = 10^{-1}$	x	$\varepsilon = 10^{-2}$	x	$\varepsilon = 10^{-3}$	x	$\varepsilon = 10^{-4}$
0.947	1.452	0.791	1.995	1.021	2.664	—	—
2.057	1.254	2.157	3.652	2.223	6.172	2.253	7.941
2.934	$9.234 \cdot 10^{-1}$	2.798	4.009	3.170	9.481	3.655	19.52
5.184	$2.904 \cdot 10^{-1}$	4.883	3.238	4.975	13.08	4.826	31.43
6.621	$1.184 \cdot 10^{-1}$	6.573	1.911	6.976	11.27	7.161	44.94
10.276	$8.996 \cdot 10^{-2}$	9.714	$4.525 \cdot 10^{-1}$	10.667	3.898	9.815	35.91
15.206	$1.915 \cdot 10^{-4}$	15.346	$1.531 \cdot 10^{-1}$	15.463	$4.225 \cdot 10^{-1}$	14.762	8.469
19.928	$3.725 \cdot 10^{-6}$	20.920	$3.122 \cdot 10^{-4}$	19.42	$4.472 \cdot 10^{-2}$	21.212	$4.204 \cdot 10^{-1}$
23.643	$9.3 \cdot 10^{-8}$	30.585	$1.86 \cdot 10^{-7}$	29.53	$5.458 \cdot 10^{-5}$	29.538	$3.144 \cdot 10^{-3}$

where $f(\lambda, x, r)$ is the integrand on the right side of (2.4). The results of these calculations are given in Fig. 1.

At this stage a recalculation of the first moment was carried out on FERUT, using the saddle point method described elsewhere [13]. A number of the results using direct numerical integration are given in Table I-*A*, results using the saddle point method in Table I-*B*. It can be seen that the agreement between the results obtained by the different methods is usually well within 5 per cent. This point is not without interest, since a good deal of discussion has gone on in the past as to the accuracy of the saddle point method in relation to cascade calculations.

Because of the difficulty involved in evaluating on FERUT, the second and third moments by direct numerical integration, and in view of the accu-

[13] See for example H. MESSEL: *Proc. Roy. Irish Ac.*, **54**, 125 (1951).

racy obtained using the saddle point method for the first moment, it was decided to try the saddle point method for the second and third moments. We do not claim that because of the 5 per cent accuracy obtained using the saddle point method for the first moment, the same accuracy holds for the second and third moments. It is, however, the best one could do in a rather difficult situation.

Numerical integration for the second and third moments is difficult for two reasons. First, the oscillatory nature of the integrands necessitates the use of very small intervals, and second, if n is the number of points for which the integrand must be evaluated for the first moment, then n^2 points are needed for the second, and n^3 points for the third. The integrands involve complicated combinations of transcendental functions, and the amount of work required for direct numerical integration is very great even with the help of an electronic computer. Moreover, because of the complexity of the integrands in the second and third moments, we cannot here use an approximate formula corresponding to (2.8). The vast number of points required for the double and triple integrations of oscillating functions would have taken up too much machine time on FERUT, even if the project could have been coded, which was doubtful with the existing facilities. With the Sydney University digital computer (SILLIAC) such a project should be more feasible, a point to which we shall return when discussing future programs in Section **4**.

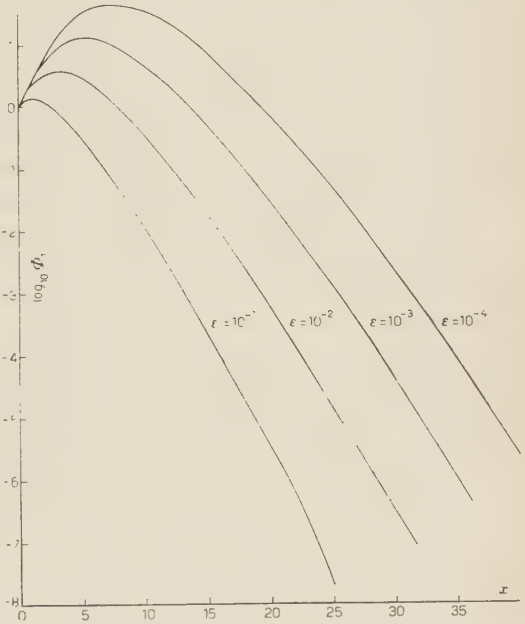

Fig. 1. – First moment of the number distribution function $\Phi(n, \varepsilon; x)$ for nucleon cascade in homogeneous nuclear matter. $\mathrm{Log}_{10}\, \Phi_1$ plotted against depth x (in cascade units) for various energy parameters ε. (Note: for primary energy $\varepsilon = 1$.)

For the second moments FERUT was used to map out the regions containing values of x which satisfied the saddle point relation expressing $\ln \varepsilon$ in terms of λ and x. With these values of x as a first approximation, Newton's iterative method ([14]) was used to find accurate values of x for given values

([14]) See for example, W. E. Milne: *Numerical Calculus* (Princeton, 1949).

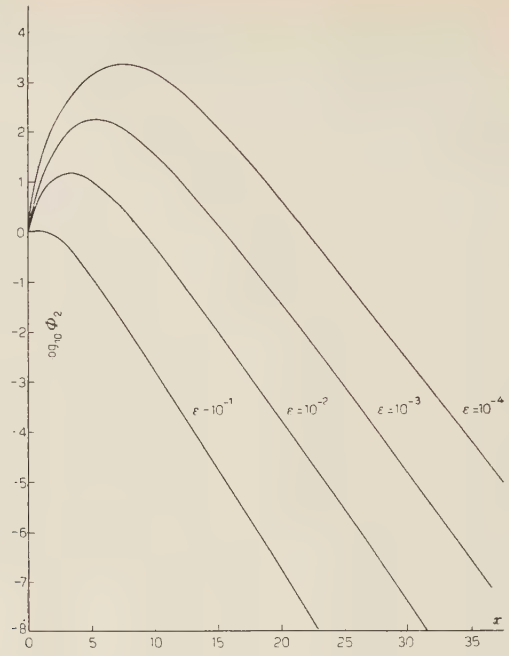

Fig. 2. – Second factorial moment of $\Phi(n, \varepsilon; x)$. $\mathrm{Log}_{10}\ \Phi_2$ plotted against depth x for various energy parameters ε.

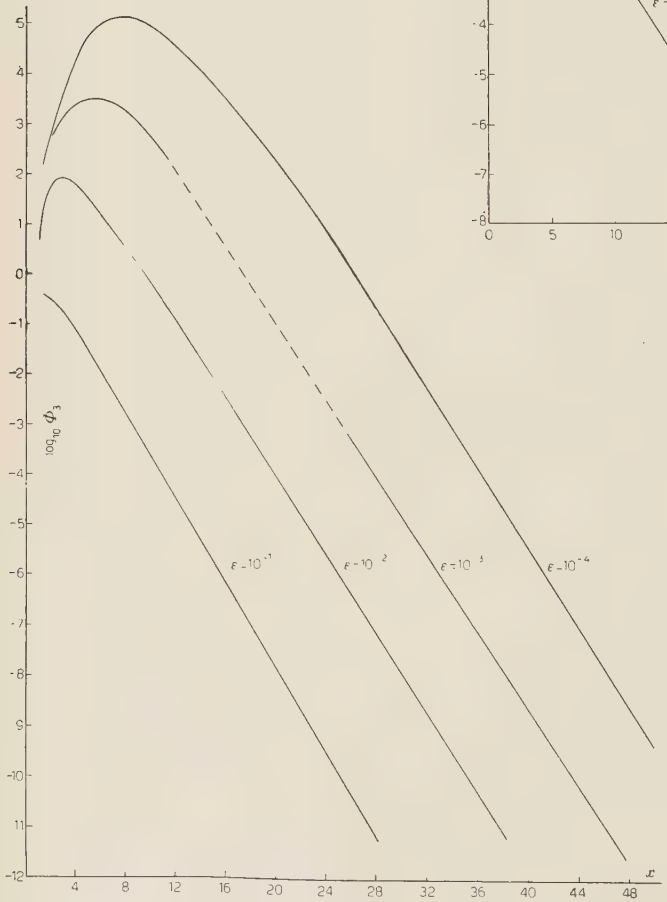

Fig. 3. – Third factorial moment of $\Phi(n, \varepsilon; x)$. $\mathrm{Log}_{10}\ \Phi_3$ plotted against depth x for various energy parameters.

of λ and $\ln \varepsilon$. Desk machines were used for this and the rest of the calculations. FERUT could have been used, but with no great advantage, since scaling difficulties would have made coding extremely tedious in the absence

of a floating point routine ([15]). Results for the second factorial moments are presented in Fig. 2.

In the third moment calculation, inverse interpolation ([14]) was used to find values of x at the saddle point corresponding to given values of λ and $\ln \varepsilon$. The function $2\alpha_1 - \alpha_2 = \{2\alpha(\lambda) \quad \alpha(2\lambda)\}$ occurring in the denominator of the expression for the third moment has a root in the neighbourhood of $\lambda = 1.06$. Because of this, the saddle point method is uncertain in the region $0.9 \leqslant \leqslant \lambda \leqslant 1.1$. For $\varepsilon = 10^{-1}$, 10^{-2} and 10^{-4} this did not prove a serious restriction, since the useful range of x for these values of ε is covered by values of λ outside the range 0.9 to 1.1, and enough points could be obtained to plot the full curves in Fig. 3. However, for $\varepsilon = 10^{-3}$, the range $0.9 \leqslant \lambda \leqslant 1.1$ corresponds to $9.57 \leqslant x \leqslant 25.25$ so that no reliable points could be obtained for this part of the curve, which has therefore been sketched in and is shown dotted.

The function $2\alpha_1 - \alpha_2$ also occurs in the denominator of the second moment formula, but in this case its root occurs together with that of the expression $\{\exp[-2\alpha_1 x] - \exp[-\alpha_2 x]\}$ in the numerator.

3. – Construction of Distribution Functions.

In this section we shall use our calculated moments to construct a number of sample distributions $\Phi(\varepsilon, n; x)$. The method is that of reference ([7]). Briefly, it runs as follows: we consider an expansion of the type,

$$\Phi(n) = W(n) \sum_{r=0}^{\infty} \varphi_r S_r(n) , \tag{3.1}$$

where

$$S_r(n) = \begin{vmatrix} W_{(0)} & W_{(1)} & \dots & W_{(r)} \\ \dots & \dots & \dots & \dots \\ W_{(r-1)} & W_{(r)} & \dots & W_{(2r-1)} \\ 1 & n & \dots & n^r \end{vmatrix} \qquad \text{for} \quad r \geqslant 1 , \tag{3.2}$$

$$S_0(n) = 1 ,$$

and

$$W_{(r)} = \sum_{n=0}^{\infty} W(n) n^r . \tag{3.3}$$

([15]) Digital computers can operate only on quantities whose numerical values fall within a certain limited range, e.g. from -1 to $+1$. In general it is necessary to scale a calculation so that all numbers fall within the operative range. A floating point routine performs this scaling automatically at each step in the calculation - but only at the expense of a considerable increase in the running time required.

$S_r(n)$ are orthogonal polynomials and $W(n)$ is a weight function which decreases at least exponentially for large values of n.
The $S_r(n)$ satisfy the orthogonality relations

$$\sum_{n=0}^{\infty} W(n)\, S_q(n)\, S_r(n) = N_q\, \delta_{qr}\,, \tag{3.4}$$

thus

$$N_q = \Delta_n \Delta_{n-1}\,,$$

$$\Delta_n = \begin{vmatrix} W_{(0)} & W_{(1)} & \dots & W_{(n)} \\ W_{(1)} & W_{(2)} & \dots & W_{(n+1)} \\ \dots & \dots & \dots & \dots \\ W_{(n)} & W_{(n+1)} & \dots & W_{(2n)} \end{vmatrix} \qquad \text{for} \quad n \geqslant 0\,, \tag{3.5}$$

$\Delta_{-1} = 1$.

The coefficients φ_r in (3.1) are determined by the relation

$$\sum_{n=0}^{\infty} S_q(n)\, \Phi(n) = N_q \varphi_q\,, \tag{3.6}$$

which yields on using (3.2) and the definition of the moments of the distribution $\Phi(n)$,

$$\Phi_{(q)} = \sum_{n=0}^{\infty} \Phi(n) n^q\,, \tag{3.7}$$

$$N_q \varphi_q = \begin{vmatrix} W_{(0)} & \dots & W_{(q)} \\ W_{q-1} & \dots & W_{(2q-1)} \\ \Phi_{(0)} & \dots & \Phi_{(q)} \end{vmatrix} \qquad \text{for} \quad q \geqslant 1\,. \tag{3.8}$$

$$N_0 \varphi_0 = \Phi_{(0)}\,.$$

Thus

$$\Phi(n) = W(n) \sum_{r=0}^{\infty} \frac{S_r(n)}{N_r} \begin{vmatrix} W_{(0)} & \dots & W_r \\ W_{(r-1)} & \dots & W_{(2r-1)} \\ \Phi_{(0)} & \dots & \Phi_{(r)} \end{vmatrix} \tag{3.9}$$

This gives us $\Phi(n)$ as an expansion in terms of its ordinary moments $\Phi_{(n)}$, weight function $W(n)$, and its moments $W_{(n)}$. To insure that (3.9) converges, it is necessary to impose rather severe conditions on $W(n)$ depending on the nature of $\Phi(n)$. In actual practice if the weight function $W(n)$ is chosen to approximate fairly closely to $\Phi(n)$, the series is either convergent, or else asymptotic.

In principle the weight function can be obtained from the asymptotic behaviour of the k-th moment of Φ. This method has been used to construct a lateral distribution of particles in a cascade ([16]); however, the method suffered from the fact that it was unable to establish the nature of the singularity near the shower axis; that is for very small values of the argument « r » the displacement from the axis.

The above difficulty does not exist in the present instance; however, for the longitudinal distribution it is by no means easy to see the asymptotic behaviour from the general expression for the k-th moment. Rather than follow this approach, therefore, we choose directly the Pólya distribution as our weight function.

The Pólya distribution has two parameters and embraces both Poisson and Furry distributions as special cases; it has already proved most useful in the theory of the longitudinal development of the electron-photon cascade, where in general the Poisson and Furry distributions give too small a value for the second moment of Φ, if fitted to the first moments ([17,18]). Since fluctuations in the numbers of particles above a given energy at a given depth are expected to behave very similarly for all cascade processes with a multiplication ratio of two ([8]) and with a homogeneous type of cross-section, it is reasonable to take the Pólya distribution as a good first approximation, that is as the weight function $W(n)$ in the present instance.

Arley in his work on the electron-photon distribution ([17]) *assumed* that it was Pólya, used the calculated first moment of the distribution and a « guessed » value of the second moment to fit the two Pólya parameters.

Messel ([18]) likewise *assumed* that the distribution was Pólya, but rather than using a « guessed » value for the second moments, actually used the calculated values obtained by Jánossy and Messel ([19]). These methods were equivalent to placing $\Phi_{(0)}=W_{(0)}$; $\Phi_{(1)}=W_{(1)}$; and $\Phi_{(2)}=W_{(2)}$ in the second and third terms of the expansion (3.9), and neglecting all other higher terms.

It should be noted that the present work does NOT assume a Pólya distribution, but merely chooses it as the weight function. The calculation of the third moments allows us to use an additional term in (3.9). This fact could be helpful as it might permit one to estimate roughly the deviation of the true distribution from a Pólya.

The Pólya distribution, in terms of its parameters a and b, is given by:

$$W(n)=\frac{1\cdot(1+b)\ldots[1+(n-1)b]}{n!}\left\{\frac{a}{1+ab}\right\}^{n}(1+ab)^{-1/b}, \tag{3.10}$$

([16]) H. Messel and H. S. Green: *Phys. Rev.*, **87**, 738 (1952).
([17]) N. Arley: *On the Theory of Stochastic Processes* (New York, 1943).
([18]) H. Messel: *Proc. Phys. Soc.* (London), A **64**, 807 (1951).
([19]) L. Jánossy and H. Messel: *Proc. Phys. Soc.* (London), A **63**, 1101 (1950).

a is the first moment of $W(n)$ and b is related to the second (ordinary) moment by:

$$W_{(2)} = \sum_{n=0}^{\infty} n^2 W(n) = a + a^2(1 + b) . \tag{3.11}$$

The higher ordinary moments of $W(n)$ may be obtained more easily from the factorial moments W_n of $W(n)$, thus

$$W_n = \sum_{c=0}^{\infty} \frac{(n + c)!}{c!} W(n + c) = 1(1 + b) \ldots [1 + (n - 1) b]a^n = \sum_{s=1}^{\infty} B_{n,s} W_{(s)} \tag{3.12}$$

with

$$B_{n,s} = B_{n-1,s-1} - (n - 1)B_{n-1,s} . \tag{3.13}$$

In the choice of a and b, we have a certain amount of freedom; actually in the present work there are three obvious choices, we may set:

(*1*) $\quad W_{(1)} = a = \Phi_{(1)} , \quad W_{(2)} = a + a^2(1 + b) = \Phi_{(2)} ;$

(*2*) $\quad W_{(1)} = \Phi_{(1)} , \quad W_{(3)} = a^3(2b^2 + 3b + 1) + 3a^2(1 + b) + a = \Phi_{(3)} ;$

(*3*) $\quad W_{(2)} = \Phi_{(2)} , \quad W_{(3)} = \Phi_{(3)} .$

In each case it will be observed that we equate two moments of the weight function to the corresponding two moments of our true function Φ. One might expect that for large n best results would be obtained by equating higher moments and for small n, lower moments. If $W_{(i)}$ denote the moment (first, second or third as the case may be) which is not equated to the corresponding $\Phi_{(i)}$ then clearly $\Phi_{(i)} - W_{(i)}$ is a partial measure of how closely $W(n)$ represents $\Phi(n)$. In fact, it may be shown without actually multiplying out the determinants of (3.9) that this expansion can be put in the form:

$$\Phi(n) = W(n)[1 + (\Phi_{(i)} - W_{(i)}) \text{ (polynominal in } n)] . \tag{3.13}$$

This result can be extended beyond $i=1, 2, 3$, of course: in general it simply states that if we konw j moments of $\Phi(n)$ and use $j - 1$ of them to fix our weight function, and $\Phi_{(i)}$ is the one known moment which is not used in constructing $W(n)$, then $W(n) \to \Phi(n)$ as $W_{(i)} \to \Phi_{(i)}$, within the limit of the expansion.

In Table II are presented the results of calculation of the Pólya parameters a and b for the three cases listed above, and in the last column in each case we have given $\Phi_{(i)} - W_{(i)}$ as a percentage of $\Phi_{(i)}$. It will be noted that not all the values of the depth parameter x in Table I-A appear in all the

TABLE II. – *Parameters for the Polya Weight Function.*

Case *1*: $W_{(1)} = \Phi_1$, $W_{(2)} = \Phi_{(2)}$.

x	a	b	$100\,(\Phi_{(3)} - W_{(3)})/\Phi_{(3)}$
1	2.30	$3.97 \cdot 10^{-2}$	— 42.5
2	3.51	$2.19 \cdot 10^{-2}$	16.3
5	3.08	$1.17 \cdot 10^{-1}$	13.0
15	$1.88 \cdot 10^{-2}$	$2.41 \cdot 10^{+1}$	5.21
20	$5.97 \cdot 10^{-4}$	$4.43 \cdot 10^{+2}$	3.49
30	$2.92 \cdot 10^{-7}$	$4.15 \cdot 10^{+5}$	0.556

Case *2*: $W_{(1)} = \Phi_{(1)}$, $W_{(3)} = \Phi_{(3)}$.

x	a	b	$100\,(\Phi_{(2)} - W_{(2)})/\Phi_{(2)}$
2	3.51	$1.17 \cdot 10^{-1}$	— 7.26
3	4.00	$9.43 \cdot 10^{-2}$	— 10.6
5	3.08	$4.86 \cdot 10^{-2}$	4.77
7	1.58	$2.83 \cdot 10^{-1}$	10.2
15	$1.88 \cdot 10^{-2}$	$2.58 \cdot 10^{+1}$	— 2.16
20	$5.97 \cdot 10^{-4}$	$4.65 \cdot 10^{+2}$	— 1.04
30	$2.92 \cdot 10^{-7}$	$4.23 \cdot 10^{+5}$	— 0.199

Case *3*: $W_{(2)} = \Phi_{(2)}$, $W_{(3)} = \Phi_{(3)}$.

x	a	b	$100\,(\Phi_{(1)} - W_{(1)})/\Phi_{(1)}$
7	1.84	$3.03 \cdot 10^{-2}$	— 16.5
15	$1.82 \cdot 10^{-2}$	$2.79 \cdot 10^{+1}$	+ 3.50
20	$5.85 \cdot 10^{-4}$	$5.00 \cdot 10^{+2}$	+ 2.14
30	$2.92 \cdot 10^{-7}$	$4.28 \cdot 10^{+5}$	+ 0.308

cases (1), (2) and (3) of Table II; those omitted were found to give values of a and b which violated one or the other of the conditions for validity of the expansion (3.9). For example, in case (1) the values of a and b corresponding to depths $x = 7$ and 10 give Pólya distributions which decrease too slowly for large n.

For computing a and b values of the ordinary moments $\Phi_{(1)}$, $\Phi_{(2)}$, $\Phi_{(3)}$ were obtained via the factorial moments Φ_1, Φ_2, Φ_3, from the graphs of these

quantities in Figs. 1-3. The error involved in reading the graphs of $\log \Phi_i$ and looking up the antilogarithms was not greater than that (probably around five or ten percent) involved by using the saddle point method instead of direct numerical integration to compute the Φ_i. Had we been more confident of the accuracy of our calculated Φ_i, we might have used an interpolation formula instead of graphs to obtain the $\Phi_{(i)}$ at intermediate values of x.

Inspection of the last column of Table II discloses that in most instances $W_{(i)}$ is within about 10 percent of $\Phi_{(i)}$, that is to say $W_{(i)} = \Phi_{(i)}$ to the accuracy with which we know either quantity, and hence, from (3.13), $\Phi(n) = W(n)$. This result simply means that the weight function obtained by using two of the moments of $\Phi(n)$ is sufficiently close to our true function that no improvement can result from using the other moment $\Phi_{(i)}$ to compute a correction factor like that in (3.13). Where $\Phi_{(i)} - W_{(i)}$ significantly exceeds 10 percent of $\Phi_{(i)}$ one might at first sight expect to obtain a closer approximation to $\Phi(n)$ by using the correction factor, and to this end the coefficients in the polynomial of (3.14):

$$\Phi(n) = W(n)\{\gamma_0 + \gamma_1 n + \gamma_2 n^2 + \gamma_3 n^3\} \tag{3.14}$$

were computed for a number of cases and are presented in Table III. These coefficients are not so small that, *a*) the correction factor is very close to unity even for low n; nor *b*), that one feels justified in terminating the polynomial

TABLE III. – *Parameters occurring in the expansion of* $\Phi(\varepsilon, n; x)$ *for* $\varepsilon = 10^{-2}$.

i	$100\,(\Phi_{(i)} - W_{(i)})/\Phi_{(i)}$	Depth x in Collision Units	Coefficient γ_r of n^r in polynomial multiplying the weight function $W(n)$			
			γ_0	γ_1	γ_2	γ_3
3	— 42.5	1	2.23	— 2.46	0.944	— 0.0904
3	16.3	2	— 1.27	2.57	— 0.687	0.0491
3	13.0	5	1.57	— 0.747	0.205	— 0.0142
1	— 16.5	7	2.51	— 2.85	1.07	— 0.103

at the n^3 term. Thus, it appears that *unless* one chooses the weight function so well that $W_{(i)}$ is within 10 percent of $\Phi_{(i)}$ the expansion (3.9) does not converge rapidly enough to be useful for numerical computation. On the other hand, if one *does* choose the weight function so well that $W_{(i)}$ is within 10 per cent of $\Phi_{(i)}$ one cannot improve on this by using the expansion (3.14) unless the moments of $\Phi(n)$ are known with appreciably better accuracy than 10 percent (say 1 or 2 percent).

Fig. 4 shows the effect of variations of ± 5 percent and ± 10 percent in $\Phi_{(1)}$ and $\Phi_{(2)}$ ([20]), on one of the Pólya weight functions constructed by setting $W_{(1)} = \Phi_{(1)}$, $W_{(2)} = \Phi_{(2)}$ and neglecting the correction factor. It is apparent that a 5 or 10 percent uncertainty in the values of the calculated moments of $\Phi(n)$ limits the usefulness of the weight function to relatively small values of n in this case ([21]). For example, a 5 percent uncertainty in the calculated moments means a factor of more than 10 in the value of $W(n)$ at $n = 20$; a 10 percent uncertainty means a factor of 1000! This, of course, again emphasizes the need for a more accurate calculation of the moments in future work, a point to which we shall return in the next section.

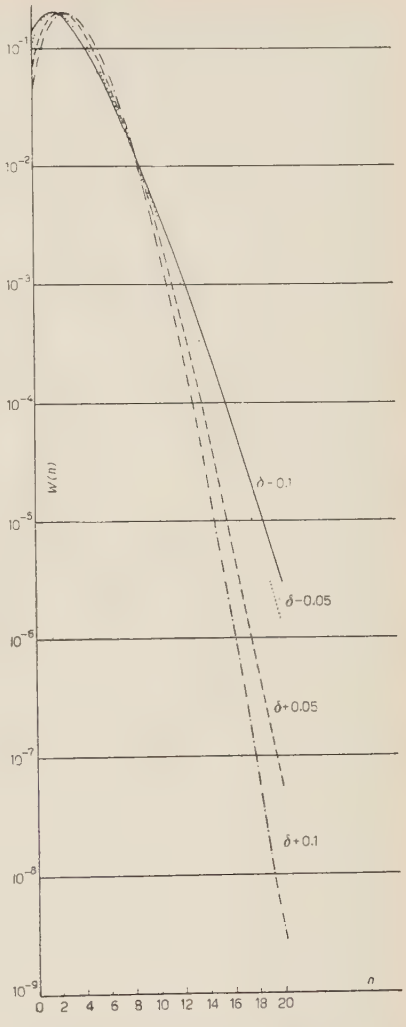

Fig. 4. - Pólya probabilities $W(n)$, calculated by setting $W_{(1)} = (1 + \delta)\Phi_{(1)}$ and $W_{(2)} = (1 + \delta)\Phi_{(2)}$ with $\delta = 0.1$, 0.05, -0.05, -0.1, and using values of the moments $\Phi_{(1)}$, $\Phi_{(2)}$ corresponding to depth $x = 5$ cascade units.

4. – Summary and Conclusion.

The first three moments of the number distribution function $\Phi(\varepsilon, n; x)$ for the nucleon cascade in homogeneous nuclear matter have been computed for $\varepsilon = 10^{-1}$, 10^{-2}, 10^{-3}, 10^{-4}, and for x ranging from zero to about 30 collision units. The first moments were computed both by direct numerical integration on FERUT and by a saddle point method using desk machines, and the results agreed within five percent. It proved impracticable to use FERUT for evaluation of the second and third moments by direct numerical

([20]) The percentage error in $\Phi_{(2)}$, calculated from $\Phi_{(2)} = \Phi_1 + \Phi_2$; cannot exceed the percentage error in Φ_1 or Φ_2; whichever is greater.

([21]) The example given is for depth $x = 5$ and is one of the worst cases. At great depths (20-30 collision units) the Pólya parameters are such that the percentage uncertainty in $W(n)$ is about the same as that in $\Phi_{(1)}$ and $\Phi_{(2)}$, regardless of n.

integration, and these were therefore evaluated by the saddle point method only, using desk machines. Thus we cannot assume that the accuracy of our second and third moments is better than five percent, and it may in fact be worse. However, such accuracy was considered reasonable for the purpose of the present work which was largely exploratory and preliminary to future computations on the physically more interesting but mathematically more complicated case of the electron-photon cascade.

One result which emerges from the present work is the following: it is in general possible to construct a Pólya distribution $W(n)$ whose first three moments are respectively equal (within our present accuracy) to the first three moments of our true function $\Phi(n)$. However, it is also clear that the accuracy of the present work is insufficient unless one is interested only in relatively low values of n. For example in Fig. 4, a ± 5 percent uncertainty in the first three moments means that $W(n=20)$ is uncertain to within a factor of 10 or more.

Further extensive computations on both the longitudinal and lateral development of electron-photon cascades are being planned in this laboratory. This work will be carried out on SILLIAC which, with its greater speed and extensive library of subroutines should prove equal to the task of evaluating the first three moments of $\Phi(\varepsilon, n; x)$ by direct numerical integration, resulting in higher accuracy than with the saddle point method. In the present work it was the limited accuracy of our calculated moments $\Phi_{(i)}$ rather than the difficulty of choosing a weight function $W(n)$ that handicapped the construction of $\Phi(n)$ by the expansion method. However, when the moments are known to higher accuracy it may still turn out that a better weight function than the Pólya is desirable in order to profit from this increased accuracy in the moments, and give a rapidly convergent expansion for all useful values of n. In this event it may be worth while to try to program SILLIAC for a large Monte Carlo calculation of $\Phi(n)$ and use the (approximate) distribution so obtained as our weight function for the expansion method. If this does not prove feasible then it will be essential to resort to the Pólya distribution using very accurate values of the moments.

* * *

The calculation of the moments was performed while two of the authors (J.W.G. and H.G.) were with Atomic Energy of Canada, Ltd., to whom we are grateful for the computational facilities afforded. Thanks are due to Mr. J. Moyal for a critical reading of this paper in manuscript, and to all those, both at Toronto and at Sydney, who assisted in the computations. We are particularly indebted to Mr. V. Weston who wrote the FERUT program for

direct numerical integration of the first momenta formula, and to Miss JEAN TUCKER (AECL) and Miss WENDELL SIMMONS (University of Sydney) for most of the tedious desk machine work.

APPENDIX A

Derivation of Formula (2.8).

The integral to be evaluated is:

$$(A.1) \qquad I = \int_y^\infty \frac{\exp[-xA]}{\lambda^2 + r^2} [\lambda \cos(xB + r \ln \varepsilon) - r \sin(xB + r \ln \varepsilon)] \, dr .$$

I is independent of the parameter λ which can have any value consistent with the condition that the integration in (2.1) is to be performed along a line parallel to the imaginary axis and to the right of all singularities in the integrand. Taking $\lambda = 1$, then, and calculating a table of values for A and B we find that for $r = 10$, $B = -0.016279$, $A = 1.001719$, and that as r increases $B \to 0.0000...$ very rapidly and $A \to 1.0000....$ very rapidly. Also since the minimum value of $|\ln \varepsilon|$ to be considered is 2.30259, we see that for $x < 10 < r$ we have $|r \ln \varepsilon| \gg |xB|$, so $\cos(xB + r \ln \varepsilon) \approx \cos(r \ln \varepsilon)$. Thus, for $y \geqslant 10$, equation (A.1) may to sufficient accuracy be written:

$$(A.2) \qquad I = \int_y^\infty \frac{\exp[-x]}{\lambda^2 + r^2} [\lambda \cos(r \ln \varepsilon) - r \sin(r \ln \varepsilon)] dr .$$

Now if we expand $(\lambda^2 + r^2)^{-1}$ in powers of $(\lambda/r)^2$ and set $\lambda = 1$, equation (A.2) becomes:

$$(A.3) \qquad I = \exp[-x] \left[\int_y^\infty \frac{\cos(r \ln \varepsilon)}{r^2} \, dr - \int_y^\infty \frac{\cos(r \ln \varepsilon)}{r^4} \, dr + \ldots - \right.$$

$$\left. - \int_y^\infty \frac{\sin(r \ln \varepsilon)}{r} \, dr + \int_y^\infty \frac{\sin(r \ln \varepsilon)}{r^3} \, dr + \ldots \right] .$$

Introducing the notation:

$$S^2_{2n+2} = \int_y^\infty \frac{\cos(r \ln \varepsilon)}{r^{2n+2}} \, dr ; \qquad S'_{2n+1} = \int_y^\infty \frac{\sin(r \ln \varepsilon)}{r^{2n+1}} \, dr ,$$

we have the recursion relations:

$$S^2_{2n+2} = -\frac{\ln \varepsilon}{2n+1} S'_{2n+1} + \frac{\cos (y \ln \varepsilon)}{(2n+1) y^{2n+1}}, \tag{A.4}$$

$$S^2_{2n+1} = \frac{\sin (y \ln \varepsilon)}{2n y^{2n}} + \frac{\ln \varepsilon}{2n} S^2_{2n}. \tag{A.5}$$

Equation (2.8) then follows immediately from substituting (A.4) and (A.5) in (A.3), and rearranging terms.

RIASSUNTO (*)

Si discute il problema di ottenere risultati numerici per il problema della fluttuazione nella teoria della cascata. Si presentano risultati per un « calcolo d'assaggio campione » della cascata nucleonica in materia nucleare omogenea ottenuti servendosi della calcolatrice elettronica Ferut e di ordinarie calcolatrici da tavolo. I risultati si discutono in relazione ad un vasto programma di calcoli per il caso fisicamente importante delle cascate elettron-fotoniche.

(*) *Traduzione a cura della Redazione.*

IL NUOVO CIMENTO Vol. II, N. 1 1° Luglio 1955

A Theoretical Investigation of Nuclear Reactions with Neutrons.

M. Cini ed S. Fubini

Istituto di Fisica dell'Università - Torino
Istituto Nazionale di Fisica Nucleare - Sezione di Torino

(ricevuto il 29 Aprile 1955)

Summary. — A theory of the interaction of neutrons with complex nuclei is developed with the aim of obtaining a cross-section averaged over the resonances, to be compared with the results of the phenomenological model proposed by Feshbach, Porter and Weisskopf (2). It is shown what kind of assumptions have to be introduced in order that the compound nucleus formation give rise to an absorption of the incident beam, irrespective of what happens after the compound nucleus decay. The problem is reduced to the determination of the complex index of refraction of an indefinite nuclear matter, taking properly into account the effect of the Pauli principle. Subsequently this index of refraction has to be introduced into a one-body Schrödinger equation with the correct boundary conditions at the nuclear wall. By assuming nuclear forces which fit the low energy two-body data, and an average binding energy of 8 MeV per nucleon, an expression is derived for the absorption coefficient which is compared with the imaginary part of the FPW potential. At zero energy the absorption coefficient is just in the right range 0.03-0.05. For higher energies it becomes so large that already for 6-8 MeV the absorption is almost complete for medium sized nuclei. This agrees quite satisfactorily with experimental evidence.

1. – Introduction.

The study of the interaction of neutrons with complex nuclei has been for a long time based on the Bohr assumption of the compound nucleus (1). The neutron was supposed to be completely absorbed immediately after entering the nucleus. In this « strong coupling » picture the incoming particle pe-

(1) See e.g. J. M. Blatt and V. F. Weisskopf: *Theoretical Nuclear Physics* (New York, 1952) (to be denoted in the following as BW), p. 340 and ff.

netrates inside the nucleus only in the immediate vicinity of the resonances while for all the other values of the incident energy the nucleus behaves like an impenetrable sphere.

A different, weak coupling, picture of the interior of the nucleus has been recently proposed ([2]) in order to account for many experimental data on the scattering of neutrons in the energy range from 0 to 3 MeV, which could not be understood on the basis of the strong coupling model. The effect of the nucleus upon the incident particle is described as the effect of a potential well with small absorption. Such a description reproduces the main features of nuclear reactions, after averaging over the resonances of the compound nucleus. In this model the compound nucleus formation is considered as an absorption of the incident beam irrespective of what happens afterwards (either reemission in the entrance channel or anelastic processes). In contrast with the strong coupling assumption the nucleus behaves like an almost transparent sphere far away from the resonances. The weak coupling picture is most probably no longer valid already for energies of the order of ten MeV at which energy the experimental data indicate an almost complete absorption of the incident neutron ([2bis]).

It seems therefore interesting to investigate the problem of neutron scattering by nuclei from a more fundamental point of view, with the aim of understanding, on the basis of our knowledge of two body nuclear forces and other known properties of nuclei the behavior predicated by these different models.

From a general point of view the scattering of a neutron by a nucleus is an exceedingly complicated many body problem. At low energy the corresponding scattering matrix is expected to be a rapidly varying function of energy with numerous sharp resonances.

In this paper we shall study which assumptions have to be introduced in the many body problem in order to obtain a cross-section averaged over such resonances. This allows a comparison with the predictions of the Weisskopf model.

The physical meaning of these assumptions can be understood in the following way. Two possibilities arise when the neutron hits the nucleus. Either the neutron does not share its energy with the nucleus and escapes immediately through the entrance channel, or its energy is shared among all the other nucleons with compound nucleus formation. In the first case boundary effects will give rise to broad resonances in the cross-section. In the second case the

---

([2]) H. FESHBACH, C. E. PORTER and V. F. WEISSKOPF: *Phys. Rev.*, **96**, 448 (1954) (to be denoted in the following as FPW).

([2bis]) H. L. TAYLOR, O. LÖUSJÖ, and T. W. BONNER: *Phys. Rev.* **94**, 807 (1954).

particle can be re-emitted either in the entrance channel or in the other open channels. In any case because of multiple reflections at the nuclear wall a long time will elapse before the re-emission. Such a phenomenon gives rise to numerous and sharp resonances in the cross-section. Therefore if these boundary effects are eliminated for the states of the compound nucleus by considering an indefinite nuclear matter one obtains a cross-section averaged over the sharp resonances. The absence of reflections at the nuclear wall entails as a consequence that, as postulated in F.P.W., the compound nucleus formation always leads to an absorption of the incident beam, because the particle can no longer escape through the entrance channel .

By using these boundary conditions the degrees of freedom of the compound nucleus can be eliminated from the many body equations. In this way a Schrödinger equation with a complex potential is obtained for the amplitude corresponding to the entrance channel. The only assumption on the states of the compound nucleus, needed to obtain this potential, is the orthogonality between these states and the ground state of the target nucleus. Our calculations are performed by assuming the ground state of the target nucleus to be given by an independent particle model.

It is important to notice that no detailed knowledge of the compound nucleus states is required, as long as we are interested only in connecting the FPW parameters with the many body problem. This would not be the case if one wanted to study not only the compound nucleus formation, but also its decay.

A first investigation (section 2) will be performed by using the method of distorted waves developed in the theory of atomic collisions ([3]). In this method the incoming neutron and the particles in the target nucleus are treated on an essentially different footing. This does not allow to take easily into account the effects of the Pauli principle.

However in this way one has the advantage that the different behavior of the incident particle outside and inside the nucleus can be easily analyzed: this approach is necessary if one wants to discuss the difference between the boundary conditions responsible for the actual and the averaged-over-resonances cross-sections respectively.

This preliminary investigation provides a physical justification for a more formal procedure developed in section 3. In this approach the propagation of a neutron in an indefinite nuclear matter is studied, taking properly into account the effects of the Pauli principle, and a complex refraction index (to be introduced in a one body Schrödinger equation) is formally derived. A

([3]) V. F. Mott and H. S.W. Massey: *Theory of Atomic Collisions* (Oxford, 1950), p. 140 and ff.

further advantage of this second approach consists in the possibility of testing the consistency of the results by means of a perturbation calculation.

Since the validity of the FPW model relies heavily on the smallness of the absorption coefficient, the first task of our investigation is to actually compute and discuss the behaviour of the imaginary part of the potential.

A detailed investigation of the real part of the potential is deferred to future work. A paper on this and other related subjects has been published by BRÜCKNER *et al.* [4]. Their method, starting from a point of view quite different from ours, connects, only the real part of the FPW potential with the low energy two body scattering amplitudes.

2. – The Method of Distorted Wawes for Nuclear Scattering.

We start from the Schödinger equation for the system of A nucleons in the target nucleus and the incoming neutron,

$$H\Psi = E\Psi \,, \tag{1}$$

where

$$H = H_N + H_n + H' \,, \tag{2}$$

$$H_N = \sum_{i=1}^{A} -\frac{1}{2M}\nabla_{x_i}^2 + \frac{1}{2}\sum_{i,j=1}^{A} V(\boldsymbol{x}_i - \boldsymbol{x}_j) \,, \tag{3}$$

$$H_n = -\frac{1}{2M}\nabla_x^2 \,, \tag{4}$$

$$H' = \sum_{i=1}^{A} V(\boldsymbol{x}_i - \boldsymbol{x}) \,.$$

In these expressions $\boldsymbol{x}_i$ stands for the space as well as for the spin and isotopic spin variables of the i-th nucleon in the nucleus and $\boldsymbol{x}$ has the same meaning for the incident neutron $V(\boldsymbol{x}_i - \boldsymbol{x}_j)$ is the two body potential between nuclear particles.

We choose a complete orthogonal set Φ_n of eigenfunctions of the target nucleus Hamiltonian. Thus

$$H_N\Phi_n = E_n\Phi_n \qquad 0 \leqslant n < \infty \tag{6}$$

---

[4] K. A. BRUECKNER, C. A. LEVINSON, and H. M. MAHMOUD: *Phys. Rev.*, **95** 219 (1954).

in which E_0, Φ_0 refer to the ground state. The method of distorted waves consists in expanding the total wave function Ψ as follows:

$$\Psi(\boldsymbol{x}, \boldsymbol{x}_1, \ldots \boldsymbol{x}_A) = \sum_{n=0}^{\infty} \varphi_n(\boldsymbol{x})\, \Phi_n(\boldsymbol{x}_1 \ldots \boldsymbol{x}_A)\,. \tag{7}$$

As pointed out in the introduction we disregard with such an expansion, for the time being, the effects of the Pauli principle between the incoming neutron and the nuclear particles. By introducing the definitions (2)–(7) in eq. (1) we get:

$$\left(\frac{1}{2M}\nabla_x^2 + \varepsilon - \varepsilon_n\right)\varphi_n(\boldsymbol{x}) = \sum_m V_{nm}(\boldsymbol{x})\varphi_m(\boldsymbol{x})\,, \tag{8}$$

where:

$$V_{nm}(\boldsymbol{x}) = (\Phi_n, H'\Phi_m) \tag{8'}$$

and $\varepsilon = E - E_0$ is the kinetic energy of the neutron, and $\varepsilon_n = E_n - E_0$ are the excitations of the states Φ_n.

To obtain a one body Schrödinger equation we must separate from the set of eqs. (8) the equation referring to $\varphi_0(\boldsymbol{x})$, probability amplitude for the neutron to remain in the entrance channel. Thus we write (5):

$$\left[\frac{1}{2M}\nabla_x^2 + \varepsilon - V_{00}(\boldsymbol{x})\right]\varphi_0(\boldsymbol{x}) = \sum_\beta V_{0\beta}(\boldsymbol{x})\varphi_\beta(\boldsymbol{x})\,, \tag{9}$$

$$\left[\frac{1}{2M}\nabla_x^2 + \varepsilon - \varepsilon_\alpha - V_{\alpha\alpha}(\boldsymbol{x})\right]\varphi_\alpha(\boldsymbol{x}) = V_{\alpha 0}(\boldsymbol{x})\varphi_0(\boldsymbol{x}) + \sum_{\beta\neq\alpha} V_{\alpha\beta}(\boldsymbol{x})\varphi_\beta(\boldsymbol{x})\,. \tag{9'}$$

Equations (9') have to be solved for the amplitudes φ_α as functions of φ_0. Since the matrix elements V_{nm} are different from zero only in the interior of the nucleus, outside of this region the different amplitudes φ_α propagate freely with wave number (real or imaginary) $k_\alpha = \sqrt{2M(\varepsilon - \varepsilon_\alpha)}$.

By matching the internal solution with free outgoing waves in the external region one obtains expressions for the φ_α which have to be introduced in the right hand side of eq. (9). With such a procedure eq. (9) would reduce to a one body equation containing a complex potential (6) whose real and ima-

---

(5) We shall use latin indexes n, m to denote the whole set of states including the ground state, while greek indexes α, β refer only to excited states.

(6) More precisely this potential would be the kernel of an integro-differential equation. In this case the words « real » and « imaginary » have to be understood as « hermitian » and « antihermitian ».

ginary part would give rise to the total elastic and reaction cross-sections respectively. This potential is a wildly fluctuating function of energy and furthermore we know that the imaginary part must vanish below threshold for inelastic reactions.

Our purpose is, on the contrary, to obtain a potential whose imaginary part is related to the probability for compound nucleus formation (i.e. to the probability that the incident neutron leaves the entrance channel and goes into one of the excited channels φ_β, without asking which is the probability that due to multiple reflections at the nuclear wall, the neutron goes back from the state φ_β to the initial state φ_0).

Let us consider eqs. (9′) in more detail. We notice that in the assumption of constant density for nuclear matter, the quantities $V_{nn}(\boldsymbol{x})$ are the same for all states and do not depend on $\boldsymbol{x}$ at least sufficiently far from the nuclear surface (7); we will denote their common values by $-V$.

Furthermore we also expect the off diagonal terms to be small in comparison with V (8). In this case the amplitudes φ_α will propagate inside the nucleus with wave number $K_\alpha = \sqrt{(\varepsilon - \varepsilon_\alpha + V)2M}$. The essential step to obtain a complex potential such to give rise to a cross-section averaged over the resonances is to impose that the amplitudes φ_λ propagate outside the nucleus with the internal wave number K_α rather than with the external k_λ. This avoids the multiple reflections at the nuclear wall and allows the excited channels to propagate undisturbed to infinity.

Such a procedure is most conveniently carried out by introducing a Fourier transform of eqs. (9′). We have:

$$(10)\qquad (p^2 - K_\alpha^2)\varphi_\alpha(\boldsymbol{p}) = \frac{1}{(2\pi)^{\frac{3}{2}}}\int \mathrm{d}^3\boldsymbol{q}\, V_{\alpha 0}(\boldsymbol{q})\varphi_0(\boldsymbol{p}+\boldsymbol{q}) + \sum_{\beta\neq\alpha}\frac{1}{(2\pi)^{\frac{3}{2}}}\int \mathrm{d}^3\boldsymbol{q}\, V_{\alpha\beta}(\boldsymbol{q})\varphi_\beta(\boldsymbol{p}+\boldsymbol{q})\,.$$

Where $\varphi_\alpha(\boldsymbol{p})$, $V_{\alpha 0}(\boldsymbol{q})$ are the Fourier transforms of $\varphi_\alpha(\boldsymbol{x})$ and $V_{\alpha 0}(\boldsymbol{x})$.

The solution of these equations can be performed by a perturbation method because the amplitudes φ_β are small in comparison with φ_0. The first approx-

(7) This is due to the range of the nuclear forces being small compared with the nuclear size.

(8) These conditions, which are just the conditions for the reliability of the method of distorted waves, are very well satisfied if the matrix elements V_{mn} are computed with an independent particle model for the states Φ_n. In the next section a consistent perturbation method will be developed in order to test such an assumption. The potential V represents an approximation for the real part of the FPW potential when all the correlations between nuclear particles are neglected.

ximation gives:

$$\varphi_\alpha(\boldsymbol{p}) = \frac{1}{(2\pi)^{\frac{3}{2}}} \int \mathrm{d}^3\boldsymbol{q} \, \frac{V_{\alpha 0}(\boldsymbol{q})}{p^2 + K_\alpha^2 - i\eta} \, \varphi_0(\boldsymbol{p} + \boldsymbol{q}) \,, \tag{11}$$

where the infinitesimal imaginary term $i\eta$ in the denominator insures the absence of incoming waves in the excited channels (9). It is interesting to discuss in more detail the form of the quantities $V_{\alpha n}(\boldsymbol{q})$. By using eq. (8′) we have:

$$V_{\alpha n}(\boldsymbol{q}) = v(\boldsymbol{q}) \, C_{\alpha n}(\boldsymbol{q}) \tag{12}$$

$$v(\boldsymbol{q}) = \int \mathrm{d}^3x \, \exp\left[i\boldsymbol{q}\boldsymbol{x}\right] V(\boldsymbol{x}) \,, \tag{12′}$$

where $v(\boldsymbol{q})$ is the Fourier transform of the two-body potential and the quantities

$$C_{\alpha n}(\boldsymbol{q}) = (\Phi_\alpha \sum_{i=1}^{A} \exp\left[-i\boldsymbol{q}\boldsymbol{x}_i\right] \Phi_n) \frac{1}{V_N^{\frac{1}{2}}} \,, \tag{13}$$

depend only on the nuclear wave functions and the nuclear volume V_N. Clearly the use of the expression (13) for the derivation of $\varphi_\alpha(\boldsymbol{q})$ would give a complex potential in eq. (9) dependent on the size of the different nuclei, namely on A. However in the present paper our aim is mainly to obtain a common potential for all nuclei by neglecting all effects which tend to zero as A goes to infinity. This amounts to let the nuclear volume and the number of particles go to infinity with constant nuclear density.

The preceding discussion shows that the two different requirements of averaging the cross-section over resonances and looking for an absorption coefficient independent of A amount to derive the complex refraction index of a plane neutron wave propagating through an indefinite nuclear matter. Subsequently this refraction index has to be used in a one body Schrödinger equation with the correct boundary conditions at the nuclear wall following the procedure of FPW.

A suitable formalism for the study of such a problem will be developed in the next section.

3. – The Refraction Index of Nuclear Matter.

We assume a wave function for the system of a neutron propagating in the nucleus A:

$$\Psi = \Psi_{se} + \Psi_c \tag{14}$$

(9) As is well known in the integration $1/(x+i\eta) = 1/x - i\pi\,\delta(x)$.

where:

$$\Psi_{se} = \varphi_0(\boldsymbol{x})\, \Phi_0(\boldsymbol{x}_1, ..., \boldsymbol{x}_A) + \text{antisymmetric terms} \tag{15}$$

represents the amplitude for neutron propagation without energy loss and $\Psi_c(\boldsymbol{x}, \boldsymbol{x}_1, ..., \boldsymbol{x}_A)$ is the amplitude for compound nucleus formation.

Two fundamental assumptions underlie our treatment:

a) The ground state wave function Φ_0 is given by a Slater determinant of A free particle states.

b) The compound nucleus probability amplitude Ψ_0 is orthogonal to Φ_0 [10].

The assumptions *a*) and *b*) suggest the introduction of a suitable representation for the wave function Ψ. We choose as a basis the antisymmetrized wave functions of $A+1$ free particles, for which we introduce the following notation. Let us denote with $|\,\rangle$ the state in which the $A+1$ nucleons fill all levels up to the top (k_F) of the Fermi sphere. The other states will be denoted by:

$$|n\rangle = |\boldsymbol{k}_1, \boldsymbol{k}_2, ..., \boldsymbol{k}_n; \boldsymbol{j}_1, \boldsymbol{j}_2, ..., \boldsymbol{j}_n\rangle \tag{16}$$

where $\boldsymbol{k}_1, \boldsymbol{k}_2, ..., \boldsymbol{k}_n$ ($|\boldsymbol{k}_i| < k_F$) refer to the momenta and spin coordinates of the particles outside the Fermi sphere and $\boldsymbol{j}_1, \boldsymbol{j}_2, ..., \boldsymbol{j}_n$ ($|\boldsymbol{j}_i| < k_F$) are the momenta and spin of the corresponding « holes ».

Instead of the form (2), the total Hamiltonian is written now as a sum of the kinetic term T and the interaction term U:

$$H = T + U\,. \tag{17}$$

We notice that the state $|\,\rangle$ is an eigenstate of T the eigenvalue which we denote as T_0^{A+1}. The physical state corresponding to the ground state of the nucleus $A+1$ is an eigenstate of $T+U$ with an eigenvalue E_0^{A+1} obviously different from T_0^{A+1}.

The propagation of a neutron of momentum $\boldsymbol{k}$ in the nuclear matter has to be studied by means of an interaction Hamiltonian which must not alter the energy of the ground state E_0^{A+1}.

It is therefore necessary to separate the total Hamiltonian in two terms:

$$T' = T + E_0^{A+1} - T_0^{A+1}\,, \tag{18}$$

and

$$U' = U - E_0^{A+1} + T_0^{A+1} \tag{19}$$

[10] See e.g. A. BOHR and B. R. MOTTELSON: *Kgl. Danske Vidnskab.*, **27**, No. 16 (1953), Appendix V.

Of course T' is still diagonal in the representation (16)

$$T'|n\rangle = (\varepsilon_n + E_0^{A+1})|n\rangle, \tag{20}$$

where:

$$\varepsilon_n = \sum_{i=1}^{n}\left(\frac{k_i^2}{2M} - \frac{j_i^2}{2M}\right). \tag{21}$$

In terms of the set (16) we can write

$$\Psi_{se} = \sum a(\boldsymbol{k})|\boldsymbol{k};\boldsymbol{k}_F\rangle \tag{22}$$

and

$$\Psi_c = \sum_r b_r|r\rangle\,. \tag{23}$$

Where $|r\rangle$ are all the states of the type (16) orthogonal to Ψ_{se}:

The Schrödinger equation (1) becomes in this representation [11]:

$$\left(\varepsilon - \frac{k^2}{2M} + \frac{k_F^2}{2M} + w_A\right)a(\boldsymbol{k}) = \langle\boldsymbol{k}|U'|\boldsymbol{k}\rangle a(\boldsymbol{k}) + \sum_r \langle\boldsymbol{k}|U'|r\rangle b_r\,, \tag{24}$$

$$(\varepsilon + w_A - \varepsilon_r)b_r = \sum_{k'}\langle r|U'|\boldsymbol{k}'\rangle a(\boldsymbol{k}') + \sum_s \langle r|U'|s\rangle b_s \tag{25}$$

where, as in section 2:

$$E = \varepsilon + E_0^A \tag{26}$$

and

$$w_A = E_0^A - E_0^{A+1} \tag{27}$$

is the binding energy of the last neutron. Since we are interested in the average properties of nuclei we will assume for w_A the standard value $q = 8$ MeV.

For an indefinite nuclear matter the sums on the momenta become integrals. We deduce from eq. (25) the coefficients b_r in terms of $a(\boldsymbol{k})$ by means of a perturbation expansion, and introduce them in eq. (24). This gives:

$$(k_0^2 - k^2)a(\boldsymbol{k}) = u(k)a(\boldsymbol{k})\,, \tag{28}$$

where:

$$k_0^2 = 2M(\varepsilon + q) + k_F^2.$$

Because of our definitions (26), (27) $\varepsilon = -q$ for $k = k_F$; therefore from (28)

---

[11] For simplicity we write: $|\boldsymbol{k};\boldsymbol{k}_F\rangle = |\boldsymbol{k}\rangle$.

$u(k_F) = 0$. From this it follows that the real part of the complex quantity $u(k)$ gives the difference between the effective potential

$$W = q + \frac{k_F^2}{2M}, \tag{29}$$

for the ground state, and the real part of the FPW potential. The problem of studying this correction, and the comparison with the related work of KIND and VILLI ([12]), will be considered in a future investigation. A first rough estimate confirms the expectation, already anticipated by WEISSKOPF, that this correction is small; it will therefore be neglected in this work, by postulating in a phenomenological way $W = 42$ MeV.

Our main interest is to study the absorption coefficient, given by the imaginary part of $u(k)$. From the lowest order perturbation approximation $u_0(k_0)$, we have ([13]):

$$\mathrm{Im}[u_0(k_0)] = g_0 \frac{4}{\pi} \frac{(2M)^2}{(2\pi)^6} \int\int\int \mathrm{d}^3\boldsymbol{k}_1 \, \mathrm{d}^3\boldsymbol{k}_2 \, \mathrm{d}^3\boldsymbol{j} \; v^2(\boldsymbol{j} - \boldsymbol{k}_1) \cdot \cdot \delta(k_2^2 - k_1^2 + j^2 + k_0^2) \, \delta(\boldsymbol{k}_2 - \boldsymbol{k}_0 - \boldsymbol{j} + \boldsymbol{k}_1) \, . \tag{30}$$

The integrations on $\boldsymbol{j}$, $\boldsymbol{k}_1$, $\boldsymbol{k}_2$ have of course to be performed inside and outside of the Fermi sphere respectively: $v(\boldsymbol{j} - \boldsymbol{k}_1)$ is the Fourier transform of the two body potential already introduced in eq. (12); g_0 is a numerical factor due to the presence of exchange forces, to be discussed in detail in the next section.

([12]) A. KIND and C. VILLI: *Nuovo Cimento*, **1**, 799 (1955).

([13]) The whole procedure of obtaining the complex part starting from eqs. (18), (19) is an oversimplification of the problem. LIPPMAN and SCHWINGER (*Phys. Rev.*, **79**, 469 (1950)) have shown that the reduction in intensity of a plane wave passing through a scattering medium can be obtained from an S matrix theory by the rate of transition out of the initial state as:

$$\text{(LS 1.75)} \qquad \sum_b w_{ba} = -\frac{2}{\hbar} \mathrm{Im}(T_{aa}) \, .$$

In the theory of the S-matrix the interaction Hamiltonian must not alter *any* eigenvalue of the free Hamiltonian. Therefore the proper counter term to add in eqs. (18) and (19) should take into account the dependence of the well on k (see J. PIRENNE: *Helv. Phys. Acta*, **21**, 226 (1948); M. GELL-MANN and M. L. GOLDBERGER: *Phys. Rev.*, **91**, 398 (1953)).

The first perturbation approximation of (LS 1.75) coincides with the imaginary part of $u_0(k_0)$ given by (30).

4. – Numerical Results and Discussion.

We assume for the two body potential the following expression

$$V(\boldsymbol{x}) = -Jw(\beta x)\frac{1+aP_{12}}{1+a}. \tag{31}$$

P_{12} is the Majorana exchange operator. Calculations will be performed with two types of radial dependence:

(32) Yukawa:
$$\begin{cases} w_{\mathrm{Y}}(\beta x) = \dfrac{\exp[-\beta x]}{\beta x}, \quad J = 39\ \mathrm{MeV}, \quad \beta = 0.614\cdot 10^{13}\ \mathrm{cm}^{-1}, \\ v_{\mathrm{Y}}(p) = 4\pi\dfrac{J}{\beta}\dfrac{1}{\beta^2+p^2}\ ; \end{cases}$$

(33) Exponential:
$$\begin{cases} w_{\mathrm{E}}(\beta x) = \exp[-2\beta x], \quad J = 175\ \mathrm{MeV}, \quad \beta = 0.717\cdot 10^{13}\ \mathrm{cm}^{-1}, \\ v_{\mathrm{E}}(p) = 4\pi J\dfrac{4\beta}{(4\beta^2+p^2)^2}. \end{cases}$$

The value of the two parameters J and β are those which fit the low energy two-body experimental data ([14]). Obviously these data do not give any indication about a. The a dependence of eq. (30) for the absorption coefficient is given by the factor

$$g_0 = \frac{1+a^2-a/2}{(1+a)^2}. \tag{34}$$

The value of a is not clearly determined from experiment, but most probably lies in the range between 1 and 3. Correspondingly g_0 varies between 0.37 and 0.53. Therefore, our results are rather insensitive to the choice of a, and, since we have used, in a phenomenological way, the experimental value $q = 8$ MeV, the study of the connection between a and q goes beyond the purposes of the present work.

As we have seen, the real part of the FPW potential is, apart from small k-dependent corrections, equal to $q + k_F^2/2M$.

The value of $k_F = 1.22\cdot 10^{13}\ \mathrm{cm}^{-1}$ is fixed from the phenomenological value $W = 42$ MeV. of FPW. We notice that this value is not far from the value $1.07\cdot 10^{13}\ \mathrm{cm}^{-1}$ given by the well known expression

$$k_F = \left(\frac{9\pi}{8}\right)^{\frac{1}{3}}\frac{1}{r_0},$$

with $r_0 = 1.45\cdot 10^{-13}$ cm as in FPW ([15]).

([14]) See J. F. Marshall and E. Guth: *Phys. Rev.*, **78**, 738 (1949).

([15]) This discrepancy can be understood if one considers the various corrections which should be applied to the theoretical value $1.07\cdot 10^{-13}\ \mathrm{cm}^{-1}$. For example the effect of the difference in number of neutrons and protons is in the right direction.

The integrations indicated in eq. (30) are performed in the Appendix, where it is shown that, for our values of k_F and q, the absorption coefficient.

$$\zeta = \frac{1}{2MW} \operatorname{Im}[u_0(k_0)], \tag{35}$$

can be written as:

$$\zeta = \zeta_0 \frac{(\varepsilon + q)^2}{q^2}, \tag{36}$$

where ζ_0 is practically independent from the incident energy, its value being:

$$\zeta_0 = g_0 \frac{M^3}{W} q^2 \frac{1}{(2\pi)^3} \frac{1}{k_0} \int_{k_0 - k}^{k_0 + k_F} v^2(p)\, \mathrm{d}p. \tag{37}$$

With our numerical values we have:

$$\text{Yukawa potential:} \qquad \zeta_0 = 0.045$$

$$\text{Exponential potential:} \qquad \zeta_0 = 0.024$$

where for sake of definiteness we have chosen $g_0 = 0.5$.

We notice that these values for $\varepsilon = 0$ are just in the range $0.03 \div 0.05$ used in FPW. We point out also that formula (36) predicts a strong dependence of ζ_0 on the incident energy ε. Already for $\varepsilon = 3$ MeV it is increased by a factor $(11/8)^2 = 1.9$. This suggests that even in this energy range the assumption of a unique value for ζ may be an oversimplification.

For higher energies ζ becomes so large that already for $6 \div 8$ MeV the absorption is almost complete for medium sized nuclei. This agrees quite satisfactorily with experimental evidence ([16]).

The present paper shows that, starting from our knowledge of two body nuclear forces and of nuclear binding energies, it is possible to understand the transparency of nuclear matter at low energy together with the rapid increase of absorption with energy. This general behaviour is practically independent on the type of two body potential and is due mostly to the effect of the Pauli principle between the incoming neutron and the particles in the target nucleus, as qualitatively discussed in BW.

The approximations introduced in taking the limit for indefinite nuclear matter, and the assumption of a constant value of q for all nuclei are necessary

([16]) See reference ([44]) in FPW.

if one wants to derive a unique absorption coefficient for all nuclei. Therefore, since these approximations are certainly rough, one might expect an appreciable variation of ζ with A. On the other hand the comparison of the results of the FPW model with experiment, does not exclude the possibility of such a variation ([17]).

* * *

In the early stage of the present work one of us (M.C.) was member of the CERN Theoretical Study Group in Copenhagen, where he has beneficed of the kind hospitality of Professor NIELS BOHR in his Institute, and of a very illuminating discussion with Dr. B. MOTTELSON.

The authors are grateful to Prof. G. WATAGHIN for his kind interest and to Prof. R. MALVANO and A. GAMBA for very useful discussions and criticism.

APPENDIX

For the evaluation of the integral in eq. (30) with the conditions $|k_1|$, $|k_2|>k_F$ and $|j|<k_F$ it is useful to introduce the step function:

$$I(x-a)\begin{cases}=1 & x<a\,,\\ =0 & x>a\,.\end{cases} \tag{A.1}$$

The following relations will prove to be useful:

$$I(x^2-a^2)=I(x-|a|)I(x+|a|)\,, \tag{A.2}$$

$$I(a^2-x^2)=1-I(x^2-a^2)=I(|a|-x)+I(x+|a|)\,, \tag{A.3}$$

$$I(x-a)I(b-a)=I(x-a)I(a-b)+I(x-b)I(b-a)\,, \tag{A.4}$$

$$I(a-x)I(x-b)=I(a-b)[I(a-x)-I(b-x)]\,. \tag{A.5}$$

Eq. (30) together with the definition (35) gives:

$$\zeta=g_0\frac{2M}{W}\frac{4}{\pi}\frac{1}{(2\pi)^6}\iint \mathrm{d}^3\boldsymbol{j}\,\mathrm{d}^3\boldsymbol{p}\;v^2(p)\,\delta(p^2-2\boldsymbol{p}\cdot\boldsymbol{k}_0+(\boldsymbol{p}-\boldsymbol{j})^2-j^2)\cdot \tag{A.6}$$

$$\cdot I(j^2-k_F^2)I[k_F^2-(\boldsymbol{p}-\boldsymbol{j})^2]I(k_F^2-p^2-2\boldsymbol{p}\cdot\boldsymbol{k}_0)\,,$$

the integrations on $\boldsymbol{j}$ and $\boldsymbol{p}$ are now performed over all space.

Since ζ obviously does not depend on the direction of $\boldsymbol{k}_0$ it is useful to

---

([17]) See e.g. FPW, Fig. 8.

perform a preliminary integration by averaging over all directions of $\boldsymbol{k}_0$, i.e. over the angle α between $\boldsymbol{k}_0$ and $\boldsymbol{p}$.

We will use the identity:

$$\frac{1}{2}\int_{-1}^{+1}\zeta(\cos\alpha)\,\mathrm{d}(\cos\alpha)=\frac{1}{2}\int_{-\infty}^{+\infty}\zeta(\cos\alpha)\,I(\cos^2\alpha-1)\,\mathrm{d}(\cos\alpha)\,,$$

in order to obtain in the integrand, after the δ function has been eliminated, a new limitation $I\{[p^2-j^2+(\boldsymbol{p}-\boldsymbol{j})^2]^2-4k_0^2p^2\}$.

After having combined this step function with the other ones be means of the rules (A.2), (A.5), we obtain, dropping a negligible term:

$$\text{(A.7)}\qquad \zeta=\frac{M}{Wk_0}\frac{1}{(2\pi)^5}\iint \mathrm{d}^3\boldsymbol{j}\,\mathrm{d}^3\boldsymbol{p}\,\frac{v^2(p)}{p}\,I(j^2-k_F^2)\,I[k_F^2-(\boldsymbol{p}-\boldsymbol{j})^2]\cdot$$
$$\cdot I[(\boldsymbol{p}-\boldsymbol{j})^2-j^2-\xi]I[(p-k_0)^2-k_F^2]\,.$$

where $\xi=k_0^2-k_F^2$. Let us study the behaviour of ζ as a function of ξ. We notice that $\zeta(\xi)=0$ for $\xi=0$. Moreover:

$$\text{(A.8)}\qquad \frac{\mathrm{d}\zeta}{\mathrm{d}\xi}=\frac{M}{Wk_0}\frac{1}{(2\pi)^5}\int \mathrm{d}^3p\,I[(p-k_0)^2-k_F^2]\frac{v^2(p)}{p}\,F(p,\xi),$$

where

$$\text{(A.9)}\qquad F(p,\xi)=\int \mathrm{d}^3\boldsymbol{j}\,I(j^2-k_F^2)\,I[k_F^2-(\boldsymbol{p}-\boldsymbol{j})^2]\,\delta(p^2-2\boldsymbol{pj}-\xi)\,,$$

by performing the integrations in (A.9) we get

$$\text{(A.10)}\qquad F(p,\xi)=\frac{\pi}{2p}\left\{\xi+\left[k_F^2-\frac{(p^2+\xi)^2}{4p^2}\right]I(2pk_F-p^2-\xi)\right\}.$$

By integrating over p as indicated in (A.9) it is possible to check that the second term in the r.h.s. of (A.10) gives a negligible contribution do $\mathrm{d}\zeta/\mathrm{d}\xi$ at least for $0<\xi<k_0^2-k_F^2$.

From (A.8) and (A.10) recalling that $\zeta(0)=0$ it is easy to obtain eq. (36) and (37).

RIASSUNTO

Si presenta una teoria dell'interazione dei neutroni con i nuclei complessi, che ha per scopo di ottenere una sezione d'urto mediata sulle risonanze, che possa essere paragonata con i risultati del modello fenomenologico di Feshbach, Porter e Weisskopf (2).

Si discutono le approssimazioni che devono essere introdotte affinchè la formazione del nucleo composto dia sempre luogo a un assorbimento del fascio incidente, indipendentemente da quello che accade dopo il decadimento del nucleo composto. Il problema è ridotto alla determinazione dell'indice di rifrazione complesso di una materia nucleare indefinita, tenendo conto del principio di Pauli. Successivamente questo indice di rifrazione deve essere introdotto in una equazione di Schrödinger per una particella, con le corrette condizioni al contorno sulla superficie del nucleo. Prendendo forze nucleari che spiegano i fenomeni di due corpi a bassa energia, e un valore di 8 MeV per nucleone dell'energia di legame media dei nuclei, si ottiene un'espressione per il coefficiente di assorbimento che deve essere confrontata con la parte immaginaria del potenziale di FPW. Per energia zero il coefficiente di assorbimento è proprio compreso nell'intervallo $0{,}03 \div 0{,}05$ in accordo con i valori assunti in FPW. Per energie più elevate esso aumenta in modo tale che già a $6 \div 8$ MeV l'assorbimento diviene quasi completo per nuclei intermedi, in soddisfacente accordo con l'esperienza.

Some Aspects of the Nuclear Capture of Hyperons and K-Mesons.

M. W. Friedlander, Y. Fujimoto (*), D. Keefe (+) and M. G. K. Menon

H. H. Wills Physical Laboratory, University of Bristol

(ricevuto il 30 Aprile 1955)

Summary. — Some predictions are made concerning the characteristics of the interactions produced by the nuclear capture of K^-- and Y^--particles. It is assumed that the capture reaction is the inverse of the « associated production mechanism ». A comparison is made between these predictions and the experimental data. The significant conclusions are: (i) the capture process sometimes involves two or more nucleons rather than a single nucleon; (ii) in view of the possible existence of Σ^0-particles and their rapid transformation to Λ^0-particles, the observation of Λ^0-particles as end products of a capture process does not necessarily indicate that they were produced in the initial reaction; (iii) there appears to be an absence of μ-mesons of ~ 120 MeV; this might indicate the production of a Σ^0-particle instead of a Λ^0-particle in the initial reaction or that the capture involves two or more nucleons; (iv) the available observations on capture stars are consistent with the general features of the theory of Gell-Mann and Pais.

1. – Introduction.

The production of a hyperon (Y-particle) and a K-meson in association, in π-meson/nucleon and nucleon/nucleon collisions is now well established. From experiments carried out by the Brookhaven group, the cross-sections for these reactions appear to be quite appreciable. If the reactions

$$\pi + \mathcal{N} \rightarrow Y + K \tag{1a}$$

$$\mathcal{N} + \mathcal{N} \rightarrow \mathcal{N} + Y + K \qquad (\mathcal{N} = \text{nucleon}) \tag{1b}$$

(*) On leave of absence from the University of Kyoto, Japan.

(+) On leave of absence from University College, Dublin.

are fairly common modes for the production of certain types of hyperons and K-mesons, then it is possible to make some predictions about the characteristics of the interactions produced by the nuclear capture of the negative K- and Y-particles of these types. A comparison of these predictions with the experimental data on capture stars would provide information on questions concerning the « associated production mechanism », which would be complementary to that obtained from a direct study of the production processes.

1·1. *Nomenclature.* – At the moment there is good evidence that two distinct types of negative hyperons exist, one assumed to decay according to the mode,

$$Y_I^- \to n + \pi^- + \sim 110 \text{ MeV} \tag{2}$$

and the other, the « cascade decay »,

$$Y_{II}^- \to \Lambda^0 + \pi^- + \sim 60 \text{ MeV} . \tag{3}$$

What little evidence there is at present from direct mass measurements on negative interacting hyperons in emulsions and other experimental observations suggests that it is Y_I which has most commonly been observed to produce capture stars. Also, thus far, only the Y_I-particle has been observed to be produced in association with a single K-particle (cf. eq. (1)).

In the nomenclature of Gell-Mann and Pais (1954), $Y_I = \Sigma$ and $Y_{II} = \Xi$. It is also useful to add at this stage, that according to the isotopic spin assignments of these authors the Σ-particle exists as a triplet i.e. in three charge states, positive, negative and neutral, whilst the Ξ-particle is a doublet state, negative and neutral.

The term K-meson is used throughout in the sense of Powell (1954), with no reference to the phenomenological classification, (τ, $\varkappa$, χ, etc.), according to their various well-established modes of decay.

2. – The Capture of Negative Hyperons.

If it can be established that the negative interacting hyperon is produced copiously according to reaction (1) in association with a K-meson and that the same K-mesons are produced similarly in association with the Λ^0-particles, then it is clear that, unless artificial assumptions are made concerning the reversibility of reactions, the following strong reaction must occur:

$$Y^- + p \to \Lambda^0 + n + Q . \tag{4}$$

Weaker processes arising from decay interactions and single production processes such as

$$Y^- \rightarrow \pi^- + n \qquad \text{(decay, weak)}$$

$$Y^- + p \rightarrow n + n \qquad \text{(single production: presumed weak)}$$

can hardly be expected to compete with reaction (4).

2·1. *The capture of the* Σ^-*-particle.* – In reaction (4) if $Y = \Sigma$, then $Q = 70$ MeV. Now the τ-meson has been seen to be produced in association with a Λ^0-particle (bound in an ejected nuclear fragment) on the one hand (Debenedetti *et al.*, 1954) and with a charged hyperon ($\Sigma^{\pm}$) on the other (Lal *et al.*, 1953; Gottstein, 1955).

Thus reaction (4) may be assumed to take place in the case of the capture of Σ -particles and the resulting star will occur in one of the following ways:

a) The Λ^0-particle can escape from the nucleus directly upon recoiling in reaction (4). Such a capture star will then, on the average, appear much smaller than a typical π^--meson induced σ-star, since the excitation energy is only $\lesssim 35$ MeV. Alternatively, the Λ^0-particle may remain within the nucleus for a time period of $\sim 10^{-20}$ s and escape during the « evaporation stage »; the total excitation energy in this case will be $\lesssim 70$ MeV.

b) The Λ^0-particle from reaction (4) is trapped within the nucleus and does not escape during the evaporation process. In a fairly heavy nucleus the Λ^0-particle may well be quite tightly bound since for this single particle the Pauli exclusion principle need not be invoked. In a time $\sim 10^{-10}$ s (as compared with the 10^{-20} s required for the evaporation process), a second disruption will occur, corresponding to non-mesonic or mesonic breakup of the excited nucleus; (this is identical to the disintegration of an excited fragment). In the first case the hyperon capture star will present the appearance of a typical π^--meson induced σ-star and in the other the track of a π-meson of about 30 MeV energy should be seen emerging from an otherwise very small star. The disintegration resulting from the mesonic or non-mesonic break-up is superimposed on the evaporation star produced 10^{-10} s earlier.

c) A third, though less likely possibility, is the emission during the evaporation stage of a fragment containing the bound Λ^0-particle; this fragment will break up later in the characteristic manner. The event will then consist of two interconnected stars, one of which has the track of the incoming negative hyperon (*).

(*) *Note added in proof.* – An event of this type has in fact been recently observed (G. Stack: *Collaboration Experiment* (1954), mimeographed report, date 18-th May 1955).

2·2. *The* Σ^0*-particle.* – Recently, some experimental evidence has been brought forward (WALKER, 1955; SHUTT, 1955) for the existence of the Σ^0-particle, postulated earlier by GELL-MANN and PAIS (1954); it is suggested that the Σ^0-particle transforms rapidly into a Λ^0-particle. In view of this, it is useful to emphasize that the observation of a Λ^0-particle as the end product of the capture process does not necessarily indicate that it was produced in the initial reaction.

The masses of the charged and neutral Σ-particles do not appear to be very different; at least not sufficiently for an experimental distinction to be made between them at the moment. If it is not forbidden by energy considerations, it is possible that the Σ^0-particle takes the place of the Λ^0-particle in the fast reaction (4) viz.

$$\Sigma^- + \mathrm{p} \rightarrow \Sigma^0 + \mathrm{n} + Q\,. \tag{5}$$

It is obviously important to determine the relative frequencies of occurrence of reactions (4) and (5). This will be governed by a variety of causes such as the conservation laws of angular momentum, parity, etc., and by isotopic spin considerations. Also, the ratio of (4) to (5) in the case of capture by a nucleon in a nucleus, may be different from that of capture by a free nucleon. If process (5) occurs with a reasonable frequency then one has the following possibilities:

a) The Σ^0-particle can escape from the nucleus and the final nuclear disintegration will be a very small one in view of the low excitation energy, probably smaller than that of 2.1*a*.

b) The Σ^0-particle is trapped within the nucleus. It can then give rise to a Λ^0-particle in a fast reaction

$$\Sigma^0 + \mathcal{N} \rightarrow \mathcal{N} + \Lambda^0, \tag{6}$$

the position then being analogous to that resulting from reaction (4). It would thus appear that the conclusions derived from a consideration of equation (4) are an adequate representation for a comparison with the experimental data. This unfortunately means that it is difficult to distinguish between (4) and (5) from observations on hyperon capture stars.

2·3. *Experimental Observations.* – The experimental observations are rather meagre but are substantially in agreement with the above scheme. The two clear-cut examples reported by JOHNSTON and O'CEALLAIGH (1954, 1955) both show the characteristics of small evaporation or σ-stars in which the visible energy releases are 20 MeV and 40 MeV respectively, (2.1*a*). In the example

of FRIEDLANDER (1954) a single fast proton of ~ 100 MeV energy is emitted, an event which has been observed when a negative π-meson suffers nuclear capture, (2.1*b*). There are also two examples (LAL *et al.*, 1953; FRIEDLANDER *et al.*, 1954) of negative interacting particles which may be hyperons since they are both produced in association with K-mesons which later decay at rest; from each of these capture disintegrations there emerges a negative π-meson of 28.1 MeV. The energies of these π-mesons are remarkably similar to that commonly observed in the breakup of excited fragments, (2.1*b*).

2·4. *The capture of the Ξ^--particle.* – According to GELL-MANN and PAIS (1954), the Ξ-particle cannot be produced in a simple « associated production » process such as reaction (2). Instead, considering only known and established particles for the moment, it has to be produced in association with two K-mesons, $K^+ + K^+$, $K^+ + K^0$, $K^0 + K^0$, (but not two anti-K-mesons). If so, the arguments which lead to eq. (4) are not relevant to it. Instead, the capture processes would be of the following fast types:

$$(7) \qquad \begin{cases} (a) \quad \Xi^- + p \to \Lambda^0 + \Lambda^0 \\ (b) \quad \Xi^- + p \to \Xi^0 + n \\ \text{with} \quad \Xi^0 + n \to \Lambda^0 + \Lambda^0 . \end{cases}$$

The production of Σ^0-particles in place of the Λ^0-particles in the above reactions is possible from isotopic spin considerations but extremely unlikely from energy considerations; in any case, as has been shown before, (eqs. (6)), the end products of the fast capture reactions will in general be Λ^0-particles.

The Λ^0-particles arising from reaction (7) have, each, energies of ~ 24 MeV. The resultant nuclear disintegration can therefore occur in one of the following ways:

A) Both the Λ^0-particles escape from the nucleus either immediately on creation, or during the succeeding evaporation. The appearance of the star will be similar to that already discussed in 2.1*a* with a nuclear excitation energy ranging up to a maximum of ~ 50 MeV.

B) One of the Λ^0-particles escapes whilst the other is trapped inside the nucleus. This is analogous to 2.1*b*.

With Λ^0-particles of energies ~ 24 MeV, the above two are the most likely processes and the capture star cannot be distinguished by its appearance from that caused by a Σ^--particle.

C) Both the Λ^0-particles may be trapped inside the nucleus. An initial evaporation process will occur with a nuclear excitation of ~ 50 MeV. Either of the Λ^0-particles may then cause a mesonic or non-mesonic nuclear explosion.

None, one, or two charged π-mesons (with energy ~ 30 MeV each) will be seen emerging from the star. The remaining part of the disintegration will in these three cases correspond to energies of $\lesssim 354$ MeV, $\lesssim 184$ MeV and $\lesssim 14$ MeV respectively. No events of this nature have yet been reported.

3. – Capture of K^--Mesons.

In the case of the capture of negative K-mesons there is good evidence from cloud chamber work (BARKER, 1953; DESTAEBLER, 1954) and from emulsion work (NAUGLE *et al.*, 1954) that a Λ^0-particle is produced in the interaction

$$K^- + \text{nucleus} \to \Lambda^0 + ?$$

There are also a few examples (the first of which was reported by DI CORATO *et al.*, 1954) of a K^--meson induced star from which emerges a charged hyperon

$$K^- + \text{nucleus} \to \Sigma^{\pm} + ?$$

In view of this evidence it would seem reasonable to suppose that the K^--meson can undergo capture by a single nucleon in a nucleus by a process closely similar to (1*a*) i.e. in the reactions

$$(8) \qquad \begin{cases} (a) & K^- + p \to \Lambda^0 + \pi^0 \\ (b) & K^- + p \to \Sigma^- + \pi^+ \\ (c) & K^- + p \to \Sigma^+ + \pi^- \\ (d) & K^- + n \to \Lambda^0 + \pi^- \\ (e) & K^- + n \to \Sigma^- + \pi^0 . \end{cases}$$

It is useful to emphasize that one can have the Σ^0-particle in place of the Λ^0-particle in these equations, as pointed out earlier while considering this question in relation to reaction (4).

When more than one nucleon takes part in the initial capture process, the reaction will be similar to 1(*b*) and the emission of a real π-meson is not necessary to conserve momentum, (cf. eq. (8)).

If a Λ^0-particle is produced (cfr. eqn. (8 *a*, and *d*)), it will carry away about 27 MeV and the π-meson ~ 150 MeV. In addition, a 150 MeV π-meson can also be seen as a result of the charge exchange scattering of a π^0-meson created in (8*a*). On the other hand, if a Σ-particle is produced, the π-meson and hyperon energies will be ~ 90 MeV and ~ 15 MeV respectively. These energies correspond to capture by a nucleon at rest and need modification before a

comparison can be made with the experimental energy spectra of hyperons and π-mesons emerging from K^--induced stars, since one is then dealing with a capture process inside a nucleus. Firstly, the energy available for the process $K^- + p \rightarrow \Sigma + \pi$ is somewhat less than the rest mass energy of the K-meson, since there is a small, but irreversible, loss of energy in the form of X-rays during the initial cascading down of the meson through the various orbits and a loss of energy to the nucleus as a whole, through interaction during the transformation $\mathcal{N} \rightarrow \Sigma$. Secondly, there is a Doppler smearing arising from the motion of the capturing nucleon inside the nucleus. A further modification is that the spectrum of the positive particles (Σ^+) has a low energy cut-off as a result of the Coulomb barrier of the nucleus, whilst the energies of the negative particles (Σ^- and π^-) can extend from zero upwards since they are attracted to the nucleus; the neutral particles of course remain unaffected. It must also be remarked that the hyperons are moving inside a potential well within the nucleus and must have a certain minimum energy before they can escape. A rough estimate of these effects suggests that in the capture process $K^- + \mathcal{N} \rightarrow \Sigma + \pi^-$ the π-meson will emerge with an energy between about 50 to 100 MeV and the hyperon with energies up to about 30 MeV. Probably about half the hyperons will not be sufficiently energetic to escape and will remain behind in the nucleus. Both these spectra however, are expected to be degraded as a result of the interfering effects of the other nucleons during the initial capture process and because of collision loss before escape. These latter effects will further increase the number of hyperons which remain trapped within the nucleus.

If the hyperon does not escape from the nucleus when it recoils, the situation reduces to that discussed previously for hyperon capture, with some difference of course in the nuclear excitation energy. Under these circumstances the three essential characteristic modes of behaviour 2·1 (*a*), (*b*), and (*c*) can occur. On a time scale the train of events is threefold: i) a fast interaction with the production of a recoil hyperon and π-meson with the possibility of escape of both, one, or neither of these particles in $\sim 10^{-22}$ s; ii) resultant excitation of the nucleus with evaporation of nucleons and perhaps the hyperon, if it has remained behind, in a time $\sim 10^{-20}$ s; iii) if the hyperon is still within the residual nucleus, the subsequent mesonic or non-mesonic decay of this nucleus in a time $\sim 10^{-10}$ s. The importance of such a separation on a time scale lies in the fact that the various stages which contribute to the finally observed event occur at widely separated time periods, and as a result, the conservation laws must be applied to each stage separately. In particular, the energy available in each stage is severely limited.

3·1. *Experimental Observations.* – In the event observed by BARKER (loc. cit.) the energy of the emitted Λ^0-particle was ~ 28 MeV. In those of DE

STAEBLER the energies were 31 ± 3 MeV, 30 ± 8 MeV and 59 ± 15 MeV, and associated with the first of these was a π-meson of energy $(81 \div 106) \pm 3.5$ MeV. These events are presumably examples of stage i). The Minnesota event (NAUGLE *et al.*, loc. cit), of an emergent excited fragment appears likely to be a result of stage ii). Several events due to K^--capture have been observed with the production of π-mesons; the majority of these emitted π-mesons lies between 25 MeV and 75 MeV. As a combined result of i) and iii), three groups of π-mesons centred at about 120 MeV, ~ 70 MeV and ~ 30 MeV would be expected to occur.

There are two points concerning the observed hyperon and π-meson energies in K^--capture which are worth mentioning.

i) The Genoa-Milan event (DI CORATO *et al.*, loc. cit.) in which a 60 MeV charged hyperon emerges is not easily compatible with a capture process involving a single nucleon (eqn. (8)). It is explicable in terms of a reaction of the type:

$$K^- + \mathcal{N} + \mathcal{N} \to \mathcal{N} + Y^{\pm}$$

which is analogous to (1*b*). Hyperon and π-meson energies resulting from this type of reaction will be different from those discussed in previous sections.

ii) No clear example of a π-meson of energy ~ 120 MeV (i.e. the first group), has yet been seen to emerge from a K^--capture star; π-mesons of this energy are expected, (cf. eqn. (8)), from K^--capture reactions involving the production of a Λ^0-particle. It if could be established from further experiments that π-mesons of this energy are rare, than this might be an indication that either the hyperon produced in the initial capture process is a Σ^0-particle, which subsequently gives rise to a Λ^0-particle (either through a nuclear interaction or by decay) i.e. the Λ^0-particle is not created in the first interaction; or that the initial capture involves in general more than a single nucleon.

In some cases of K^--capture two π-mesons, one in the intermediate or high energy group, and the other in the low energy group should be observed; the first, corresponding to « prompt emission » in the capture reaction and the second to « delayed emission » from the decay of the residual nucleus.

If in the capture process neutral π-mesons are produced, these would escape detection in emulsions and thus a large amount of the energy apparently available would not appear in visible form. In particular, the production of a Λ^0 (or Σ^0) and a π^0-particle and the escape of both would explain well the observed examples of K^--capture stars in which no charged paticles or only a few tiny prongs are seen. In general, the surprisingly small fraction of the available energy (~ 500 MeV) which appears in the form of visible prongs argues for the escape of neutral particles other than simple evaporation neutrons.

4. – Conclusions.

Some of the conclusions arrived at in the previous sections may be summarized in the following manner:

a) There is one case of K^--capture (Di Corato *et al.*, 1954) which suggests that the capture process sometimes involves two or more nucleons, rather than a single nucleon.

b) In view of the possible existence of Σ^0-particles and their rapid transformation to Λ^0-particles, the observation of Λ^0-particles as the end products of a capture process does not necessarily indicate that they were produced in the initial reaction.

c) The absence of high energy (~ 120 MeV) π-mesons from K^--capture stars, if confirmed, might be taken as an indication that it is the Σ^0-particle rather than the Λ^0-particle which is produced in the initial capture mechanism and that the observed Λ^0-particles arise from the subsequent decay of Σ^0-particles; or that the initial capture process involves more than one nucleon .

d) From the general characteristics of negative hyperon induced stars, it is not possible to say whether the captured hyperon is a Σ^- or a Ξ^--particle, except in the case described in 2.4*c*.

e) In the case of Σ^--capture it is difficult to decide from the experimental observations whether the Λ^0-particle or the Σ^0-particle is produced in the initial capture mechanism.

f) The observations so far available on capture stars are consistent with the general features of the theory of Gell-Mann and Pais.

* * *

We are grateful to Professor C. F. Powell for the hospitality of his laboratory. Some of us wish to thank the following bodies: The British Council for a Scholarship (YF); The National University of Ireland for a Travelling Studentship (DK); The Royal Commission for the Exhibition of 1851 for a Senior Studentship (MGKM).

REFERENCES

K. H. Barker, *Report of the Proceedings of the Duke Conference* (1953).

A. Debenedetti, C. M. Garelli, L. Tallone and M. Vigone: *Nuovo Cimento*, **12**, 466 (1954).

H. DeStaebler: *Phys. Rev.*, **95**, 1110 (1954).
M. Di Corato, B. Locatelli, G. Mignone and G. Tomasini: *Suppl. Nuovo Cimento*, **12**, 270 (1954).
M. W. Friedlander: *Phil. Mag.*, **45**, 418 (1954).
M. W. Friedlander, D. Keefe and M. G. K. Menon: *Nuovo Cimento*, **1**, 482 (1955).
M. Gell-Mann and A. Pais: *Proc. Int. Nucl. Phys. Conf.* (*Glasgow*), 1954, and *Proc. Rochester Conf. on High Energy Physics*, 1955. Also, work on similar lines carried out independently by K. Nishijima: *Prog. Theor. Phys.*, **12**, 107 (1954) and T. Nakano and K. Nishijima: *Prog. Theor. Phys.*, **10**, 581 (1953).
K. Gottstein: *Nuovo Cimento*, **1**, 277 (1955).
R. H. W. Johnston and C. O'Ceallaigh: *Phil. Mag.*, **45**, 424 (1954) and *Nuovo Cimento*, **1**, 468 (1955).
D. Lal, Y. Pal and B. Peters: *Proc. Ind. Acad. Sci.*, **38**, 398 (1953).
J. E. Naugle, E. P. Ney, P. S. Freier and W. B. Cheston: *Phys. Rev.*, **96**, 1383 (1954).
C. F. Powell: *Proc. Roy. Soc.*, A **221**, 278 (1954).
R. P. Shutt: *Proc. Rochester Conference on High Energy Physics*, 1955.
W. D. Walker: *Proc. Rochester Conference on High Energy Physics*, 1955.

RIASSUNTO (*)

Si fanno alcune previsioni riguardanti le caratteristiche delle interazioni prodotte dalla cattura nucleare di particelle K^- e Y^-. Si assume che la reazione di cattura sia l'inversa del « meccanismo delle produzioni associate ». Si istituisce un confronto tra queste previsioni e i dati sperimentali. Le conclusioni di rilievo sono: (i) il processo di cattura coinvolge a volte due o più nucleoni anzichè uno solo; (ii) in vista della possibile esistenza di particelle Σ^0 e della loro rapida trasformazione in particelle Λ^0, l'osservazione di particelle Λ^0 quali prodotti finali di un processo di cattura non è necessariamente un indice che esse sono state prodotte nella reazione iniziale; (iii) si constata l'assenza di mesoni μ di ~ 120 MeV; questo potrebbe essere un indice della produzione nella reazione iniziale di una particella Σ^0 invece di una Λ^0, o che la cattura coinvolge due o più nucleoni; (iv) le osservazioni di stelle di cattura note sono in accordo con le linee generali della teoria di Gell-Mann e Pais.

(*) *Traduzione a cura della Redazione.*

Remarks on Pion Nucleon Scattering.

U. Haber-Schaim (*) and W. Thirring

Physikalisches Institut der Universität - Bern, Switzerland

(ricevuto il 3 Maggio 1955)

Summary. — The scattering of pions on nucleons is considered under the assumption of pv-coupling with cut-off. A model due to T. D. Lee is extended in two directions: *a*) to include recoil effects and *b*) to admit two mesons in the meson cloud of the nucleon. The model permits a rigorous renormalization prescription without the use of perturbation theory. The phase shifts for the $\frac{1}{2}\,\frac{1}{2}$ and $\frac{3}{2}\,\frac{3}{2}$ scattering can be calculated to any desired accuracy, in this paper about 10%.

1. – Introduction.

An attempt to explain the low energy p-wave scattering of pions on nucleons has been made by Chew [1]. He used the static approximation for the nucleon and symmetrical pv-coupling with cut-off. He calculated the phase shifts by selecting some terms of the perturbation expansion which seemed to be the dominant ones and found quite a good agreement with the experimental values. However it has not yet been demonstrated how close his approximation comes to the exact solution.

Recently Lee [2] suggested a model of coupled « nucleon » and « meson » fields which can be solved exactly. There ar two kinds of nucleons, V and N, and an interaction that allows the following elementary processes: $V \leftrightarrow \mathrm{N}+\pi$. In one nucleon problems the number of mesons in an eigenstate of the Hamil-

(*) Now at the Department of Physics, University of Illinois, Urbana, Illinois/USA.

(1) G. F. Chew: *Phys. Rev.*, **95**, 1669 (1954); see also S. Fubini: *Nuovo Cimento*, **10**, 546 (1953).

(2) T. D. Lee: *Phys. Rev.*, **95**, 1329 (1954).

tonian is also limited to one (O.M.M.) and the Damm-Dancoff approximation is, therefore, the exact solution. This model has several attractive features:

a) As one is dealing with exact solutions only, one is always sure that the results have something to do with the equations.

b) There is no adiabatic switching on of the interaction and one has the correct boundary conditions at $t = \pm \infty$ e.g. for scattering a free meson plus a « dressed » nucleon.

c) It permits a well defined renormalization procedure which can be carried out without the aid of perturbation theory.

There is, however, one qualification. The model looses its physical consistency if the renormalized coupling constant is greater than a certain critical value which depends on the cut-off. In this case there appear negative probabilities and the S-matrix ceases to be unitary. In this paper we apply the Lee-model to the scattering of ps mesons and try to make it more realistic in the following way:

a) We generalize the Lee-model to include three kinds of nucleons P, P′, P″ which are connected by the elementary processes $P \leftrightarrow P' + \pi$, $P' \leftrightarrow P'' + \pi$. The solution to this problem is essentially a second Tamm-Dancoff approximation, just as the first T.D. approximation solves the original Lee-model.

b) We use symmetrical pv-coupling and include the recoil and $(\boldsymbol{\sigma v})$ (« Galileian ») term. In previous publications a sharp cut-off was used. We find that this gives rise to a stable excited state just above the cut-off energy. This state exists even in the limit of the coupling constant going to zero and is certainly an unphysical feature of the theory. We therefore apply a smooth cut-off which suppresses the interaction at energies when the effects of recoil and the $(\boldsymbol{\sigma v})$ term become large. It turns out that the original Lee-model contains all the contributions which have been taken into account by CHEW in his latest [1] calculation.

This raises the following questions:

a) Is the effect noted by CHEW, namely the suppression of the $\frac{1}{2}\,\frac{1}{2}$ and the enhancement of the $\frac{3}{2}\,\frac{3}{2}$ phase shift also present in the model containing one more meson?

b) Is this model still physically consistent with values for the coupling constants which reproduce the scattering data?

The answer to both questions is in the affirmative, again with some qualifications. The Chew-effect is indeed much more pronounced in the two meson model (T.M.M.). Furthermore the ground state of the nucleon has quite dif-

ferent percentages of one meson amplitude in the O.M.M. and the T.M.M. It does not seem therefore, that successive Tamm-Dancoff approximations will give a rapidly convergent series. As to *b*) we can choose in the T.M.M. a coupling constant for which the state with the negative probability is not yet present but the enhancement is just due to a « resonance » with this almost present state. This means mathematically that the pathological state appears when a certain denominator vanishes and the enhancement of the $\frac{3}{2}\,\frac{3}{2}$ phase is due to the smallness of this very denominator. In the O.M.M. the situation is rather critical and whether *b*) can be answered in the affirmative depends on the cut-off.

In order to be able to compare the O.M.M. and the T.M.M. the coupling constants have to be renormalized. The renormalization prescription used is in close analogy to renormalization in quantum electrodynamics where the observable charge is conveniently defined by the one electron expectation value of the total charge. In our theory the quantity corresponding to the charge is the source denstity of the meson field and we define the renormalized coupling constant by matrix elements of this operator between physical one-nucleon states. To test the success of this renormalization prescription we have calculated a model with n kinds of nucleons coupled to scalar mesons which corresponds to the n-th T.D. approximation. In this case all integral equations can be solved exactly and with our renormalization prescription all quantities become finite without cut-off, although in every approximation states with negative probabilities occur. In the limit $n \to \infty$ the theory agrees with the fully renormalized neutral scalar theory, where the exact solution is known (in the static limit). With pv-coupling one has to use a cut-off even after renormalization but our procedure renders all integrals only linearily divergent. It further implies that the two processes $\mathrm{P} \longleftrightarrow \mathrm{P}' + \pi$ and $\mathrm{P}' \longleftrightarrow \mathrm{P}'' + \pi$ must be given two different unrenormalized coupling constants. Taking them equal, for instance, in the scalar case would prevent the elimination of all infinities. It seems, therefore, erroneous to make a second T.D. approximation with the same coupling constants for the first and the second meson. The second meson has to be coupled more weakly than the first meson. Its coupling is sort of between that of the first meson and the uncoupled third meson.

In the next section we shall discuss the O.M.M. including recoil and the $(\boldsymbol{\sigma v})$ term. Some results other than the phase shifts are indicated as this model admits exact the evaluation of some quantities which are usually only found by perturbation theory. The T.M.M. is presented in section **3**, for shortness in the limit nucleon mass $\to \infty$ only. Section **4** contains the numerical evaluation of the integral equations for the phase shifts. In view of the present status of the experimental data the numerical calculations have an accuracy of 10 %. Some mathematical tools are compiled in the appendix.

2. – The One-Meson Model.

Expressing everything by the renormalized fields, we have for the Hamiltonian of the free fields,

$$H_0 = N^2 \sum_p \psi_V^+(p)\{E_p + \delta E_p\}\psi_V(p) + \sum_p \psi_N^+(p) E_p \psi_N(p) + \sum_{k,i} \alpha_i^+(k)\alpha_i(k)\omega_k \,, \tag{2.1}$$

with

$$E_p = \sqrt{M^2 + p^2} \,, \qquad \omega_k = \sqrt{k^2 + 1} \,.$$

We use the usual Fourier-decomposition of the fields in a volume Ω

$$\varphi_i(x) = \sum_k \left(\exp\left[i(kx - \omega t)\right] \frac{\alpha_i(k)}{\sqrt{2\Omega\omega}} + \exp\left[-i(kx - \omega t)\right] \frac{\alpha_i^+(k)}{\sqrt{2\Omega\omega}} \right) \tag{2.2}$$

and similarly for ψ_V and ψ_N where the α and ψ obey the commutation-relations

$$\{\psi_N^{+i}(p),\, \psi_N^j(p')\} = N^2\{\psi_V^{+i}(p),\, \psi_V^j(p')\} = [\alpha_i^+(p),\, \alpha_j(p')] = \delta_{ij}\,\delta_{pp'} \,; \tag{2.3}$$

N is a constant to be determined below.

In this notation the interaction term becomes

$$H' = -i \sum_{k,k'} \frac{g(k')\tau_j}{\sqrt{2\Omega\omega'}} \cdot \\ \cdot \{\psi_N^+(k-k')(\boldsymbol{\sigma}\cdot\boldsymbol{q}_k(k))\psi_V(k)\alpha_j^+(k') - \psi_V^+(k)(\boldsymbol{\sigma}\cdot\boldsymbol{q}_k(k'))\psi_N(k-k')\alpha_j(k')\} \,. \tag{2.4}$$

For compactness we combine the cut-off factor with the coupling-constant, writing $g^2(k')$ for $g^2/(1+\omega_{k'}^4/L^4)$.

In the numerical calcuation $L = 5$ will be used.

$\boldsymbol{q}_k(k')$ is the momentum of the meson, corrected for the effects of the nucleon velocity:

$$\boldsymbol{q}_k(k') = \boldsymbol{k}' - \frac{\omega_{k'}}{2}\left(\frac{\boldsymbol{k}}{E_k} + \frac{\boldsymbol{k}-\boldsymbol{k}'}{E_{k-k'}}\right) . \tag{2.5}$$

We shall write $|k, 0\rangle$ resp. $|0, k\rangle$ for a state with a bare V- respectively N-particle with momentum k:

$$H_0|k, 0\rangle = E_k|k, 0\rangle \,. \tag{2.6}$$

The physical states are indicated by capitals $|V\rangle$, $|N\rangle$

$$\begin{cases} H|V_k\rangle = E_k|V_k\rangle \\ H|N_k\rangle = E_k|N_k\rangle \,. \end{cases} \tag{2.7}$$

The constant N, which renormalizes the ψ_V field, is determined by the conditions

$$\langle 0|\psi_V|V\rangle = \langle 00|\psi_V|10\rangle\, N = 1 \tag{2.8}$$

for the nucleon at rest ([3]).

The renormalized coupling constant g is defined by the source strength of the physical nucleons.

$$\langle N|Q_{ij}|V\rangle = g\langle 10|\sigma_i\tau_j|01\rangle\,; \qquad Q_{ij} = g\psi_N^+(0)\sigma_i\tau_j\psi_V(0)\,. \tag{2.9}$$

The g thus defined agrees with the g in (2.4).

The physical N-particle is identical with the bare N-particle

$$|N\rangle = |01\rangle\,. \tag{2.10}$$

Whereas the physical V-particle is a combination of a bare V-particle plus a N^+ meson state. The latter state has to be a $\frac{1}{2}\,\frac{1}{2}$ state (see appendix). By solving (2.7) we find after normalizing the state properly:

$$|V_k\rangle = \frac{n_0^k}{N}\left\{ N|k0\rangle + \sum_{k'} \frac{ig(k')}{\sqrt{2\Omega\omega'}}\,\frac{(\sigma q_k(k'))}{\varepsilon_0^k(k')}\,\tau_j\alpha_j^+(k')|0,\, k-k'\rangle \right\}, \tag{2.11}$$

where

$$\varepsilon_{\omega_0}^k(k') = E_{k-k'} + \omega_{k'} - E_k - \omega_0\,;$$

N is given in accordance with (2.8) by

$$|N|^2 = |n_0^0|^2 = 1 - 3\sum_{k'} \frac{g^2(u')\,q_0^2(k')}{2\Omega\omega'\,\varepsilon_0^0(k')^2} \tag{2.12}$$

([3]) One might think of N to depend on k. This would, however, spoil the anti-commutativity of the renormalized ψ_V for different space points.

and

$$\left\{\begin{array}{l} n_0^k = N\left\{1 - 3\sum \dfrac{g^2(k')q_k^2(k')}{2\Omega\omega'}\left(\dfrac{1}{\varepsilon_0^0(k')^2} - \dfrac{1}{\varepsilon_0^k(k')^2}\right)\right\}, \\ \delta E_k = \dfrac{3}{N^2}\sum \dfrac{g^2(k')q_k^2(k')}{2\Omega\omega'\varepsilon_0^k(k')}. \end{array}\right. \tag{2.13}$$

There are other eigenstates of H than the groundstates which are of the general form

$$|N+\pi\rangle = n_{\omega_0}^k |k0\rangle + \sum_{k'} f_{\omega_0}^k(k')(\sigma q_k(k'))\tau_j \alpha_j^+(k')|0,\ k-k'\rangle \tag{2.14}$$

and belong to an eigen-value $E_k + \omega_0$. They are denoted by $N+\pi$, because they describe the scattering of a meson by an N-particle. In order to find the wave function $\chi_{\omega_0}^k(k')$ of the meson we have to express (2.14) in terms of the physical states:

$$|N+\pi\rangle = \sum_{k'} \chi^k(k')(\sigma q_k(k'))\tau_j \alpha_j^+(k')|N\rangle + n_{\omega_0}^k |V\rangle . \tag{2.14'}$$

This means

$$f_{\omega_0}^k = \frac{n_{\omega_0}^k}{N} f_0^k + \chi_{\omega_0}^k . \tag{2.15}$$

Writing the Schrödinger-equation for $N-\pi$ we obtain two equations, one of which gives:

$$\chi_{\omega_0}^k(k') = b\delta_{k'p} + \frac{n_{\omega_0}^k}{N}\frac{ig(k')}{\sqrt{2\Omega\omega'}}\left(\frac{1}{\varepsilon_{\omega_0}^k(k')} - \frac{1}{\varepsilon_0^k(k')}\right), \tag{2.16}$$

where b is a constant yet to be determined and $\varepsilon_{\omega_0}^k(p) = 0$. From the other equation one obtains after combining certain terms with the renormalization costants given by (2.12) and (2.13):

$$\frac{n_{\omega_0}^k}{N} = \frac{3ig(p)q_k^2(p)6}{\sqrt{2\Omega\omega_0}h_k(\omega_0)}, \tag{2.17}$$

where

$$\frac{h_k(z)}{z} = 1 - 3\sum_{k'} \frac{g^2(k')}{2\Omega\omega'}\left(\frac{q_0^2(k')}{\varepsilon_0^0(k')^2} - \frac{q_k^2(k')}{\varepsilon_0^k(k')\varepsilon_z^k(k')}\right). \tag{2.18}$$

If $h(z)$ vanishes for a certain value of z there exists a solution for χ with $b = 0$. For our cut-off function this happens only for $g > g_{\text{crit}}$ where $N(g_{\text{crit}}) = 0$.

For $g > g_{\text{crit}}$ $h(z)$ vanishes for a positive and a negative energy giving a resonance in the scattering and a bound state respectively. There is nothing peculiar with the resonance and it will not be discussed any further. The bound state arises with an energy $-\infty$ (4). Its energy increases with g. Expressed in terms of bare particle states the bound state of the meson with energy λ, $h(\lambda) = 0$, is worked out to be given by

$$|V_\lambda\rangle = \frac{n_\lambda^k}{N}\left\{N|k0\rangle + \sum_{k'}\frac{ig(k')}{\sqrt{2\Omega\omega'}}\frac{\sigma q_k(k')}{\varepsilon_\lambda^k(k')}\tau_j\alpha_j^+|0, k-k'\rangle\right\}, \tag{2.19}$$

with

$$\left(\frac{N}{n_\lambda^k}\right)^2 = h'(\lambda) < 0\,. \tag{2.20}$$

For $g > g_{\text{crit}}$ $|N^2 < 0$ and the theory can only be formulated in a mathematically consistent way by introducing an indefinite metric (5). The probability balance is then always formally satisfied but it contains some negative terms, which render the theory physically inacceptable. We shall, therefore, restrict ourselves to the region $g < g_{\text{crit}}$.

Determining the normalization constant b we obtain for the scattering state in the limit $\Omega \to \infty$

$$\chi_\omega^k(k') = \left\{\delta_{kp} - \frac{3g(p)g(k')\omega_0}{2\Omega\sqrt{\omega_p\omega'}\,\varepsilon_{\omega_0}^k(k')\,\varepsilon_0^k(k')h_k(\omega_0)}\right\}\frac{1}{|q_k(p)|}\sqrt{\frac{\Omega}{3(2\pi)^3}}\,. \tag{2.21}$$

One can check by use of the various quantities and (2.19) that the states (2.11), (2.14) and (2.19) are properly normalized and orthogonal to each other. To prove the completness it is instructive to calculate the propagator of the V-particle (6).

$$S_F(x) = P\langle 0|\psi_V(x+y)\psi_V^+(y)|0\rangle \sum_{k,\omega}\exp\left[i(kx - (\omega + E_k)t)\right]\cdot \tag{2.22}$$

$$\cdot\int_{-\infty}^{\infty}\frac{d\omega'}{\omega' - \omega + i\varepsilon}\left|\frac{n_{\omega'}^k}{N}\right|^2\,.$$

(4) Note that $\lim_{z\to\infty} h(z)/z = N^2$.

(5) W. PAULI and G. KÄLLEN, to be published. We are indebted to Prof. PAULI for communicating these results prior to publication.

(6) Here S_F is identical with S_{ret} because there are no antinucleons in this model.

The integral over ω' can be evaluated by complex integration (7) and gives

$$S_F(x) = \sum_k \exp[i(kx - E_k t)] \sum_\omega \frac{\exp[-i\omega t]}{h_k(\omega)} . \tag{2.23}$$

The completness of the eigenstates is identical with the statement

$$\langle 0 | \{\psi_V(x+y)\, \psi_V^+(y)\}_{x_0=0} | 0 \rangle = \sum \exp[ikx] \lim_{\omega\to\infty} \frac{\omega}{h^k(\omega)} = \frac{1}{N^2}\delta(x) . \tag{2.24}$$

The phase-shift for the $\frac{1}{2}\,\frac{1}{2}$ scattering is easily obtained from (2.21) by specializing to the center of mass system ($k = 0$):

$$\operatorname{tg}\delta_{11}(p) = -\frac{3p\,q_0^2(p)g^2(p)}{4\pi(\omega_p - M + E_p)[1 + (\omega_p/E_p)]} \cdot \left[1 + \frac{3}{4\pi^2}\int_0^\infty \frac{\mathrm{d}k'k'^2\, q_0^2(k')g^2(k')(\omega_p - M + E_p)}{\omega'(\omega' - M + E_{k'})^2(\omega' + E_{k'} - \omega_p - E_p)}\right]^{-1} . \tag{2.25}$$

The effects of the recoil and the (σv) term cancel approximately in $[\,]^{-1}$ so that the net effect of the finite nucleon mass is the factor $(1 + \omega_p/E_p)^{-1}$. This gives a reduction of 30 % in the cross-section in the energy region of interest.

To simplify the calculation we investigate the $\frac{3}{2}\,\frac{3}{2}$ scattering only in the limit $M\to\infty$. This scattering state cannot be described by an $|N+\pi\rangle$ state since here the absorption of the meson must precede the emission. It is, therefore, appropriate to describe the $\frac{3}{2}\,\frac{3}{2}$ scattering by $|V+\pi\rangle$ where the meson emission precedes the absorption. Using the U-operators discussed in the appendix we write:

$$\begin{aligned} |V+\pi\rangle_{33} &= \sum_1 U_3^+(1) r_1(1) |10\rangle + \sum_{1,2} U_{13}^+(12) r_2(12) |01\rangle = \\ &= \sum_1 U_3^+(1)\varrho_1(1)|V\rangle + \sum_{1.2} U_{13}^+(12)\varrho_2(12)|N\rangle , \end{aligned} \tag{2.26}$$

where $r(1)$ is $r(k_1)$, etc.. The Schrödinger-equation $(H - m - \omega_0)|V+\pi\rangle_{33} = 0$ yields the two equations:

$$\begin{cases} r_1(1)(\delta M + \omega_1 - \omega_0) + \dfrac{g}{N}\sum_2 \dfrac{1}{\sqrt{2\Omega\omega'}}\left[3r_2(21) + \dfrac{4}{3}\, r_2(12)\right] = 0 , \\ (\omega_1 + \omega_2 - \omega^0) r_2(12) + \dfrac{g}{N}\dfrac{r_1(2)}{\sqrt{2\Omega\omega_1}} = 0 , \end{cases} \tag{2.27}$$

(7) This is due to W. Pauli (private communication); c.p. G. Wentzel: *Helv. Phys. Acta*, **15**, 115 (1942).

which give the following equation for the physical one meson amplitude:

$$(2.28)\qquad \varrho_1(1)(\omega_1-\omega_0)G(\omega_1-\omega_0)=\frac{4}{3}\sum_{\frac{1}{2}}\frac{g^2(2)\varrho_1(2)}{2\Omega\sqrt{\omega_1\omega_2}(\omega_1+\omega_2-\omega_0)}$$

$$\text{where } G(-z)=\frac{h(z)}{z}\,,$$

h is (2.18) in the limit $M\to\infty$. This equation cannot be solved in a closed form as in the $\frac{1}{2}\,\frac{1}{2}$ case. It is found, however, that the Fredholm series converges quite rapidly ([8]). The numerical work for solving (2.28) and similar equations will be discussed in Section **4**.

It may finally be mentioned that another renormalization prescription e.g. defining g by $\operatorname{tg}\delta_{11}=3p^3g^2/4\pi$ can also be used. The only difference between the two procedures is that the latter changes $h(z)$ from (2.18) to

$$(2.29)\qquad h(z)=z\left(1-3\sum_k\frac{g^2(z+1)}{2\Omega(\omega-1)\omega^2(\omega+z)}\right).$$

This method has advantage of giving a closer connection between the $\frac{1}{2}\,\frac{1}{2}$ and $\frac{3}{2}\,\frac{3}{2}$ phase shifts. The function (2.29) is however not so easy to evaluate and in discussing the results we will use (2.18). Both methods coincide in the limit of vanishing meson mass.

3. – The Two Meson Model.

We proceed to the model with three kinds of nucleons, P, P′, P″. The interaction allows for the following elementary processes:

$$(3.1)\qquad \begin{cases} \mathrm{P}\longleftrightarrow \mathrm{P}'+\pi \\ \mathrm{P}'\longleftrightarrow \mathrm{P}''+\pi\,. \end{cases}$$

For simplicity we take $M\to\infty$. The renormalization needs some care and we therefore express H' by the unrenormalized fields ψ; $\psi_{,}$; $\psi_{,,}$ for the particles P, P′, P″:

$$(3.2)\qquad H'=-i\sum_k\frac{1}{\sqrt{2\,\Omega\omega}}\{g_1(\psi_{,,}^{+}U_1^{+}(k)\psi,-\text{ c. c.})+g_2(\psi_{,}^{+}U_1^{+}(k)\psi-\text{ c. c.})\}\,.$$

As discussed in the introduction we renormalize to equal source strength for

([8]) J. L. Gammel: *Phys. Rev.*, **95**, 209 (1954).

the two processes (3.1) for the physical particles. The two unrenormalized constants g_1 and g_2 which determine the strength for these processes for the bare particles, will in general be different. To put this in formulae, we define

$$Q_{ij} = g_1 \psi^+_{,,} \sigma_i \tau_j \psi, + g_2 \psi^+_{,} \sigma_i \tau_j \psi \tag{3.3}$$

and normalize the interaction strength according to

$$\langle P'' | Q_{ij} | P' \rangle = P' | Q_{ij} | P \rangle = g \langle 010 | \sigma_i \tau_j | 010 \rangle . \tag{3.4}$$

Here we use the same notation for the bare particles as in Section 2, e.g. $|010\rangle$ meaning a bare P'-particle. For the ground-states of the physical particles we make the general « Ansatz »

$$\left\{ \begin{array}{l} |P\rangle = N|100\rangle + \sum_1 f(1)\, U_1^+(1)|010\rangle + \sum_{12} h(12)\, U_{11}^+(12)|001\rangle \\ |P'\rangle = N'|010\rangle + \sum_1 f'(1)\, U_1^+(1)|001\rangle \\ |P''\rangle = |001\rangle . \end{array} \right. \tag{3.5}$$

The constants N and N' are expressed with the aid of (A.2)

$$N'^2 = 1 - 3 \sum_k k^2 |f'(\omega)|^2$$

$$N^2 = 1 - 3 \sum_k k^2 |f(\omega)|^2 - \sum_{k,k'} k^2 k'^2 h^*(\omega\omega')(9h(\omega\omega') + h(\omega'\omega)) .$$

Using the expressions for the physical states the connections (3.4) between the renormalized and unrenormalized coupling constants become:

$$g = N' g_1 = N N' g_2 + \frac{g_1}{3} \sum k^2 f^*(\omega) f'(\omega) . \tag{3.6}$$

The quantities occurring in (3.5) can be calculated exactly by solving the Schrödinger-equation for the physical states with the exception of an integral equation for f:

$$\left\{ \begin{array}{l} f'(\omega) = \dfrac{ig}{\sqrt{2\Omega\omega^3}}; \quad \delta M' = 3 \dfrac{g^2}{N'^2} \sum \dfrac{k^2}{2\Omega\omega^2}; \quad N'^2 = 1 - 3 \sum \dfrac{g^2 k^2}{2\Omega\omega^3} , \\ \delta M = -\dfrac{3ig_2}{N} \sum \dfrac{f(\omega) k^2}{\sqrt{2\Omega\omega}} , \quad h(\omega\omega') = \dfrac{ig_1}{\omega + \omega'} \dfrac{f(\omega')}{\sqrt{2\Omega\omega}} , \\ f(\omega) = i \dfrac{F(\omega) g N'}{\sqrt{2\Omega\omega^3}} , \end{array} \right. \tag{3.7}$$

where F obeys the equation

$$F(\omega) = \frac{1}{G(\omega)}\left[1 - \frac{g^2}{3}\sum \frac{F(\omega')}{2\Omega\omega'^3}\,\frac{k^2\omega}{\omega+\omega'}\right], \tag{3.8}$$

where

$$G(z) = 1 - 3\sum \frac{k^2 g^2 z}{2\Omega\omega^3(\omega+z)}\,.$$

This equation has been solved numerically. A plot of $F(\omega)$ is presented in Fig. 1. $F(\omega)$ is the ratio between f and its perturbation theoretical expression and Fig. 1 shows that even for the ground state perturbation theory is insuf-

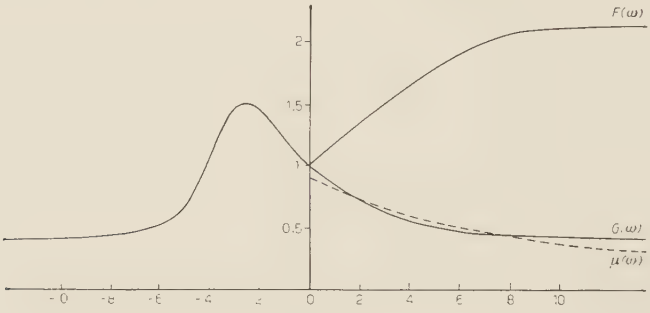

Fig. 1.

ficient. The numerical solution with $\beta^2 = g^2/4\pi = 0.037$ gives a probability for 0, 1 and 2 mesons in the ground state of 12, 80 and 8% respectively. In the O.M.M. we obtain for the probabilities of 0 and 1 meson 60 and 40% respectively.

The scattering in the $\frac{1}{2}\,\frac{1}{2}$ state will be represented by $|P'+\pi\rangle$. Thus the absorption of the meson can either precede or follow the emission. By applying the total Hamiltonian to the state

$$|P'+\pi\rangle = c|100\rangle + \sum_1 c_1(1)\,U_1^+(1)|010\rangle + \sum_{12} c_2(12)\,U_{11}^+(12)|011\rangle =$$

$$= \gamma|P\rangle + \sum_1 \gamma_1(1)\,U_1^+(1)|P'\rangle + \sum_{12} U_{11}^+(12)\gamma_2(12)|P''\rangle.$$

Combining the proper terms with the expression (3.7) for $\delta M'$ we arrive at the equation

$$-i\,\frac{cg^2N'^2}{\sqrt{2\Omega\omega}} + (\omega-\omega_0)\,G(\omega-\omega^0)c_1(\omega) = \frac{g^2}{\sqrt{2\Omega\omega}}\sum_{k'}\frac{k'^2 c_1(\omega')}{3\sqrt{2\Omega\omega'}(\omega+\omega'-\omega_0)}\,.$$

We now express the c's by the physical quantities γ

$$(3.9)\qquad (\omega-\omega_0)G(\omega-\omega_0)\gamma_1(\omega)=\frac{g^2}{\sqrt{2\Omega\omega}}\sum_{k'}\frac{k'^2\gamma_1(\omega')}{3\sqrt{2\Omega\omega'}(\omega+\omega'-\omega_0)}-$$

$$-\frac{g\gamma}{\sqrt{2\Omega\omega}}\sigma_1(\omega)\,,$$

with

$$\sigma_1(\omega)=1-\frac{\omega-\omega_0}{\omega}F(\omega)G(\omega-\omega_0)-\frac{g^2}{3}\sum\frac{(\omega-\omega_0)F(\omega')k'^2}{2\Omega\omega'^3(\omega+\omega'-\omega_0)}\,,$$

γ is conveniently determined by the orthogonality requirement $P'P'+\pi\quad 0$ which yields

$$cN+3\sum_1 f^*(1)c_1(1)k_1^2+\sum_{12}h^*(12)(9c_2(12)+c_2(21))k_1^2k_2^2$$

or by extensive rearrangement using (3.5), (3.7) and (3.8)

$$(3.10)\qquad \gamma=g\sum\frac{\gamma_1(1)k_1^2}{\sqrt{2\Omega\omega_1^3}}\,\frac{\sigma_1(1)}{\nu(\omega_0)}\,,$$

where

$$(3.11)\qquad \begin{cases} \nu(\omega_0)=1+g^4\sum_{kk'}\dfrac{\omega_0k^2k'^2[9\omega F^2(\omega')+\omega'F(\omega)F(\omega')]}{(2\Omega)^2(\omega+\omega')^2\omega^2\omega'^3(\omega+\omega'-\omega_0)}\,, \\ \sigma_2(\omega)=3F(\omega)-9g^2\sum_{k'}\dfrac{F(\omega)k'^2[(\omega-\omega_0)(\omega+\omega')-\omega\omega']}{2\Omega(\omega+\omega')\omega'^3(\omega+\omega'-\omega_0)}+ \\ \qquad\qquad +g^2\sum_{k'}\dfrac{\omega k'^2F(\omega')}{\omega'^2(\omega+\omega')(\omega+\omega'-\omega_0)}\,. \end{cases}$$

The integral equation for the meson wave function is obtained by inserting (3.10) into (3.9)

$$(3.12)\qquad (\omega-\omega_0)G(\omega-\omega_0)\gamma_1(\omega)=g^2\sum\frac{k'^2\gamma_1(\omega')}{2\Omega\sqrt{\omega\omega'}}\cdot$$

$$\cdot\left[\frac{1}{3(\omega+\omega'-\omega_0)}-\frac{\sigma_1(\omega)\sigma_2(\omega')}{\omega'\nu(\omega_0)}\right].$$

The solution of this equation and the comparison between (3.12) and (2.12) will be given in Section **4**.

In analogy to the previous section the $\frac{3}{2}\,\frac{3}{2}$ scattering will be calculated for $P+\pi$. In this case we have to take into account 1, 2 and 3 meson states. This causes some complication and we find that a consistent « Ansatz » for

the state has to contain some compensating terms:

$$(3.13)\quad P+\pi\rangle_{\frac{3}{2}\frac{3}{2}} = \sum \{r_1(1)U_3^+(1)|100\rangle + [r_2(12)U_{13}^+(12) + \hat{r}_2(12)U_{13}^+(\hat{12})]|010\rangle +$$
$$+ [r_3(123)U_{113}^+(123) + \hat{r}_3(123)U_{113}^+(\hat{123})]|001\rangle\} =$$
$$= \sum \{\varrho_1(1)U_3^+(1)|P\rangle + [\varrho_2(12)U_{13}^+(12) + \hat{\varrho}_2(12)U_{13}^+(\hat{12})]|P'\rangle +$$
$$+ [\varrho_3(123)U_{113}^+(123) + \hat{\varrho}_3(123)U_{113}^+(\hat{123})]|P''\rangle +$$
$$+ \frac{1}{N'}\varrho_1(1)f(2)[U_{13}^+(21) - U_{31}^+(12)]|P'\rangle + [\varrho_1(1)h(23)(U_{113}^+(123) - U_{311}^+(123)) -$$
$$- \varrho_2(12)f'(3)(U_{131}^+(123) - U_{113}^+(123)) - \frac{1}{N'}\varrho_1(1)f(2)f'(3)(U_{311}^+(123) - U_{113}^+(123)) -$$
$$- \hat{\varrho}_2(12)f'(3)(U_{131}(\hat{123}) - U_{113}(\hat{123}))]|P''\rangle\}.$$

The operators $U_{113}(123)$ and their properties are explained in the appendix. The physical wave-function of the mesons ϱ are expressed as before by

$$(3.14)\quad \varrho_1 N = r_1\,; \quad \hat{\varrho}_2(12)N' = \hat{r}_2(12)\,; \qquad \varrho_2(12)N' + f(1)\varrho_1(2) = r_2(12)\,.$$

The Schrödinger-equation gives five relations between the r's. Eliminating r_3 and expressing everything by the ϱ's we obtain [9]:

$$(3.15)\quad gG_{\frac{1}{3}}(\omega_1+\omega_2-\omega_0)\frac{\varrho_1(2)}{\sqrt{2\Omega\omega_1}} - g(\omega_1+\omega_2-\omega_0)G(\omega_1+\omega_2-\omega_0)\frac{\varrho_1(2)F(1)}{\sqrt{2\Omega\omega_1^3}} +$$
$$+ (\omega_1+\omega_2-\omega_0)G(\omega_1+\omega_2-\omega_0)\varrho_2(12) =$$
$$= \frac{g^2}{3}\sum_3 \frac{k_2^3}{2\Omega\sqrt{\omega_2}(\omega_1+\omega_2+\omega_3-(\omega_0)}\left[\frac{\varrho_2(23)+\varrho_2(32)}{\sqrt{\omega_1}} + \frac{\varrho_2(13)}{\sqrt{\omega_2}} + \right.$$
$$\left. + \frac{\hat{\varrho}_2(23)+\hat{\varrho}_2(32)}{\sqrt{\omega_1}}\right] - \frac{g^2}{3}\sum \frac{k_3^2\varrho_1(3)}{(2\Omega)^{\frac{3}{2}}\sqrt{\omega_2}(\omega_1+\omega_2+\omega_3-\omega_0)}\cdot$$
$$\cdot\left[\frac{F(2)}{\sqrt{\omega_1\omega_2^3}} + \frac{F(1)}{\sqrt{\omega_1^3\omega_2}}\right],$$

$$(3.16)\quad (\omega_1+\omega_2+\omega_0)G(\omega_1+\omega_2-\omega_0)\hat{\varrho}_2(12) =$$
$$- \frac{g^2}{3\cdot 2\Omega}\sum_3\left(\frac{\hat{\varrho}_2(13)}{\sqrt{\omega_2\omega_3}} + \frac{\hat{\varrho}_2(32)}{\sqrt{\omega\omega_3}}\right)\frac{k_2^2}{\omega_1+\omega_2+\omega_3-\omega_0} -$$
$$- \frac{g^2}{6\cdot\Omega}\sum_3\left(\frac{\varrho_2(23)}{\sqrt{\omega_1\omega_3}} + \frac{\varrho_2(13)}{\sqrt{\omega_2\omega_3}}\right)\frac{k_3^2}{\omega_1+\omega_2+\omega_3-\omega_0} +$$
$$+ \frac{g^3}{3(2\Omega)^{\frac{3}{2}}}\left(\frac{F(2)}{\sqrt{\omega_1\omega_2^3}} + \frac{F(1)}{\sqrt{\omega_1^3\omega_2}}\right)\sum_3 \frac{k_3^2\varrho_1(3)}{\sqrt{\omega_3}(\omega_1+\omega_2+\omega_3-\omega_0)},$$

$$(3.17)\quad (\delta M + \omega_1 - \omega_0)r_1(1) = g_2^2 N'^2 \sum_2 \frac{3r_2(21) + (4/3)r_2(12) + \hat{r}_2(12) + 2\hat{r}_2(21)}{2\Omega\omega_2 h(\omega_1+\omega_2-\omega_0)}.$$

[9] $G_{\frac{1}{3}}(z)$ is $G(z)$ as defined in (3.8) but with g replaced by $g/3$.

In (3.17) there are still renormalization constants and the sums without cut-off are still quadratically divergent. It is possible to obtain another equation which does not contain N or N' but only linearly divergent sums by computing the commutator between H and $U_3(q)$. Taking the matrix element of this commutator between the P and $P+\pi$ state and remembering that they are eigenstates of H we obtain an equation which is analogous to the orthogonality relation (3.10). This equation has the desired properties but is so complicated that it has no practical use. It would take too much space to quote this formula. It is, however, of theoretical interest to be able to verify that with our renormalization prescription one can obtain equations containing observable quantities only with the degree of divergence correspondingly reduced. This is, for instance, not possible if we were to put $g_1 = g_2$. In the practical calculations we use a sufficiently strong cut-off so that we shall use (3.15) to (3.17).

4. – Calculation of the Phase Shifts.

Adding (3.15) and (3.16) we find (the arguments of all functions will be written explicitly):

$$(4.1)\quad \frac{gG_{\frac{1}{3}}(\omega_1+\omega_2-\omega_0)}{\sqrt{2\Omega\omega_1}}\varrho_1(2)-(\omega_1+\omega_2-\omega_0)G(\omega_1+\omega_2-\omega_0)\frac{gF(\omega_1)\varrho_1(2)}{\sqrt{2\Omega\omega_1^3}}+$$

$$+(\omega_1+\omega_2-\omega_0)G(\omega_1+\omega_2-\omega_0)\varrho_2(12)+(\omega_1+\omega_2-\omega_0)G(\omega_1+\omega_2-\omega_0)\hat{\varrho}_2(1,2)=$$

$$=\sum_3\frac{g^2k_2^2}{6\Omega\sqrt{\omega_3}(\omega_1+\omega_2+\omega_3-\omega_0)}\left[\frac{\varrho_2(32)}{\sqrt{\omega_1}}+\frac{\hat{\varrho}_2(23)}{\sqrt{\omega_1}}-\frac{\hat{\varrho}_2(13)}{\sqrt{\omega_2}}\right].$$

We notice that (3.16) is consistent with the requirement that $\hat{\varrho}_2(12)=\hat{\varrho}_2(21)$. In any case, $\hat{\varrho}_2(12)$ cannot be different from $\hat{\varrho}_2(21)$ since the leading terms in (3.16) are symmetrical with respect to the interchange of the two variables. In (4.1) appears an antisymmetrical combination of ω_1 and ω_2. This suggests the « Ansatz »

$$(4.2)\qquad \hat{\varrho}_2(\omega_1\omega_2)=0\,.$$

Defining a new function $\varphi(12)$ by

$$(4.3)\qquad \varrho_2(12)=\frac{g}{\sqrt{2\Omega\omega_1}}\varphi(12)$$

we then obtain the following equation for $\varphi(12)$ in the limit $\Omega \to \infty$:

$$(4.4)\qquad \varphi(\omega_1\omega_2) = \left(\frac{F(\omega_1)}{\omega_1} - \frac{G_{\frac{1}{3}}(w_1 + w_2 - \omega_0)}{(\omega_1 + \omega_2 - \omega_0)\, G(\omega_1 + \omega_2 - \omega_0)}\right) \varrho_1(\omega_2) + \\ + \frac{g^2/4\pi}{3\pi(\omega_1 + \omega_2 - \omega_0)\, G(\omega_1 + \omega_2 - \omega_0)} \int \frac{\mathrm{d}\omega_3 k_3^3 \varphi(\omega_3\omega_1)}{(\omega_1 + \omega_2 + \omega_3 - \omega_0)(1 + \omega_3^4/5^4)} .$$

A simple expansion in powers of $g^2/4\pi$ shows that already the zeroth term gives a satisfactory approximation.

Hence we shall use

$$(4.5)\qquad \varphi(\omega_1\omega_2) = \left[\frac{F(\omega_1)}{\omega_1} - \frac{G_{\frac{1}{3}}(\omega_1 + \omega_2 - \omega_0)}{(\omega_1 + \omega_2 - \omega_0)\, G(\omega_1 + \omega_2 - \omega_0)}\right] \varrho_1(\omega_2) .$$

Feeding (4.2) and (4.5) into the sums in (3.16) and (3.15) we indeed find that the resulting corrections for ϱ_2 and $\hat{\varrho}_2$ are small and can be neglected. Inserting (4.2), (4.3) and (4.5) into (3.17) we obtain after combining the proper terms:

$$(4.6)\qquad (\omega_1 - \omega_0)\mu(\omega_1 - \omega_0)\, \varrho_1(\omega_1) = \frac{4}{3} \sum_{\omega_2} \frac{g^2 k_2^2 \varrho_1(\omega_2)}{2\Omega\sqrt{\omega_1\omega_2}\,(\omega_1 + \omega_2 - \omega_0)\, G(\omega_1 + \omega_2 - \omega_0)} - .$$

The function $\mu(x)$ is essentially the unrenormalized form of $G(x)$ and is defined by:

$$(4.7)\qquad \mu(x) = \frac{N^2 g}{g_2 G_{\frac{1}{3}}} + \frac{3g^2}{4\pi^2 x} \int \frac{\mu'^3(\omega')}{\omega'(\omega' + x)(1 - \omega'^4/5^4)} \left[\frac{\omega' + x}{G(\omega')} - \frac{\omega'}{G(\omega' + x)}\right] ;$$

$G(x)$ is close to one and therefore has been taken out of the integral and substituted by an average value $G = 0.9$. Also use has been made of the approximate relationship:

$$\frac{F(x)}{G_{\frac{1}{3}}(x)} \approx \frac{1}{G(x)} .$$

In the limit $\Omega \to \infty$ and with the proper boundary condition (3.12) and (4.6) become integral equations of the form:

$$(4.8)\qquad y(\omega_1) = \delta(\omega_1 - \omega_0) + \int k(\omega_1\omega_2) y(\omega_1)\, \mathrm{d}\omega_2 .$$

A good approximation to the exact solution (within 10 %) is given by the first term of the Fredholm expansion

$$(4.9)\qquad y(\omega_1) = \delta(\omega_1 - \omega_0) + (1 + \Lambda)^{-1} k(\omega_1, \omega_0)$$

where

$$\Delta = \int \mathrm{d}\omega\, k(\omega, \omega)\,.$$

Inserting (4.9) into the integral in (4.7) we have

$$y(\omega_1) = \delta(\omega_1 - \omega_0) + k(\omega_1\omega_0) + (1-\Delta)^{-1}\int \mathrm{d}\omega_2\, k(\omega_1\omega_2)\, k(\omega_2\omega_0)\,. \tag{4.10}$$

If the principal value of the integral is taken, the phase shift is given by

$$\mathrm{tg}\,\delta = \pi(\omega_1 - \omega_0)\left[k(\omega_1\omega_0) + (1-\Delta)^{-1}\int k(\omega_1\omega_2)\, k(\omega_2\omega_0)\,\mathrm{d}\omega_2\right]_{\omega_1=\omega_0}\,. \tag{4.11}$$

The first gives the contribution of the Born approximation including Heitler's radiation damping (the resistive part) whereas the second term accounts for the reactive part.

For the scattering in the $\frac{1}{2}\,\frac{1}{2}$ state (3.12) we have

$$k_{11}(\omega_1\omega_2) = \frac{g^2}{4\pi^2}\,\frac{k_2^3}{(\omega_1-\omega_0)\,G(\omega_1-\omega_0)}\cdot \left[\frac{1}{3}\,\frac{\sqrt{\omega_2/\omega_1}}{\omega_1+\omega_2-\omega_0} - \frac{\sigma(\omega_1)\,\sigma_2(\omega_2)}{\nu(\omega_0)\sqrt{\omega_1\omega_2}}\right]\frac{1}{1+\omega_2^4/5^4}\,. \tag{4.12}$$

From their definitions in (3.9) and (3.11) it can easily be verified that $\nu(\omega_0)\simeq 1$, $\sigma_1(\omega_0)=1$; $\sigma_2(\omega_0)\simeq 3$. This makes the Born term in the phase shift the be $-\frac{5}{3}\,(g^2/4\pi)(k_0^3/\omega_0)(1+\omega_0^4/5^4)^{-1}$. The second term has been calculated numerically for $\omega_0=2$, where it causes a decrease of tg δ by 22%. This correction, however, does not change appreciably with energy since $|\Delta_1|<1$. Our result for the $\frac{1}{2}\,\frac{1}{2}$ phase shift can therefore be expressed by

$$\mathrm{tg}\,\delta_{11} = -\,2\,\frac{g^2}{4\pi}\,\frac{k_0^3}{\omega_0(1+\omega_0^4/5^4)}\,. \tag{4.13}$$

Comparing this result with the O.M.M. we see that the factor 3 in (2.25) has been reduced to 2 by the inclusion of the states with two mesons. In both models the results of the exact calculation are not very different from the Born approximation. It may also be added, that in the O.M.M. (for the $\frac{1}{2}\,\frac{1}{2}$ state only) the first term of the Fredholm expansion gives the exact solution since the kernel K is degenerate.

For the scattering in the $\frac{1}{2}\,\frac{1}{2}$ state we have from (4.6)

$$(4.14)\qquad k_{33}(\omega_1\omega_2) = \frac{4g^2}{3\cdot 4\pi^2}\,\frac{k_2^3\sqrt{\omega_2/\omega_1}}{(\omega_1-\omega_0)\mu(\omega_1-\omega_0)(\omega_1+\omega_2-\omega_0)G(\omega_1+\omega_2-\omega_0)}\cdot\frac{1}{1+\omega^4/5^4}\,.$$

Comparing $\Delta_3 = \int \mathrm{d}\omega\, k_{33}(\omega,\omega)$ with Δ_1, we notice that $\Delta_3 > 0$ and moreover $\Delta_3 > |\Delta_1|$ since it has a factor μ in the denominator and does not have the factor $\sigma_1(\omega)$ which obeys the inequality $\sigma_1(\omega) \leqslant \omega_0/\omega$. For $g^2/4\pi = .037$ we find $\Delta_3 = 1$ at $\omega_0 = 2$. The energy dependence of the second term of the phase shift in (4.11) is essentially given by $(1-\Delta)^{-1}$. Therefore we shall neglect the energy dependence of the integral in the numerator at the vicinity of the resonance and express the phase shift in the following form:

$$(4.15)\qquad \operatorname{tg}\delta_{33} = \frac{g^2}{3\pi}\,\frac{k_0^3}{\omega_1(1+\omega_0^4/5^4)\mu(0)}\left(1+\frac{0.6\omega_0}{1-\Delta_3(\omega_0)}\right).$$

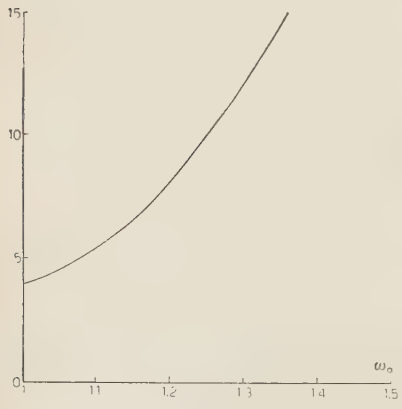

Fig. 2.

Since already for $\omega = 1.3$, $1-\Delta_3 = 0.1$ it is evident that the Born approximation yields exceedingly poor results for the $\frac{3}{2}\,\frac{3}{2}$ scattering, even at low energy (*). The dependence of ( ) in equs. (4.15) on ω_0 is shown in Fig. 2. The main difference between this result and that obtained in the one particle model is the occurrence of the function μ in the denominator which is equivalent to an additional G. Hence if one wishes to obtain a resonance at the same energy in the two models it is necessary to decrease the value of the coupling constant. Whether by generalizing this model to n-particles the coupling constant will tend to a finite limit is yet unknown.

* * *

It is a pleasure to express our gratitude to Prof. W. PAULI for stimulating discussions.

(*) It should be noted, however, that in the limit of vanishing meson mass the Born approximation gives the exact result for low energy. It is not clear whether this observation can serve as a severe test of the theory since this limit can not be realized experimentally and an extrapolation may well be unreliable.

Appendix I

We shall summarize here some properties of the operators U which were used in sections 2 and 3. They are defined by two auxiliary operators:

$$\text{(A1)} \qquad \begin{cases} Q_1(k) = Q_1^+(k) = (\sigma k)\,; \quad O_1(k) = (\tau\alpha_k)\,, \quad O_1^+(k) = (\tau\alpha_k^+) \\ U_1(k) = Q_1(k)\,O_1(k)\,, \qquad U_1^+(k) = Q_1(k)\,O_1^+(k)\,. \end{cases}$$

For more than one meson the following shorthand is used:

$$U_{12}(12) = U_1(1)\,U_1(2)\,, \qquad U_{11}^+(12) = U_1^+(1)\,U_1^+(2)\,;$$
$$U_{11}(\hat{12}) = Q_1(1)Q_1(2)\,O_1(2)O_1(1)\,.$$

Note that $U^+(12)$ is *not* the Hermitian conjugate of $U(12)$. $U^+(1 \ldots n)$ operating on a bare nucleon state produces a nucleon and n mesons in a $\frac{1}{2}\,\frac{1}{2}$ state. When summed over all variables and applied to a one-nucleon state they have the following properties:

$$\text{(A2)} \qquad \begin{cases} U_1(1)\,U_1^+(2) = 3k_1^2\,\delta(12) \\ U_1(1)\,U_{11}^+(23) = k_1^2\big[3\,\delta(12)\,U_1^+(3) + \tfrac{1}{3}\,\delta(13)\,U_1^+(1)\big] \\ U_1(1)\,U_{111}^+(23) = k_1^2\big[3\,\delta(12)\,U_{21}^+(3) + \tfrac{1}{3}\,\delta(13)\,U_{11}^+(24) + \\ \qquad + \delta(14)\big(\tfrac{1}{3}\,U_{11}^-(32) + \tfrac{1}{3}\,U_{11}^+(23) + \tfrac{2}{3}\,U_{11}^+(23) + \tfrac{2}{3}\,U_{11}^+(\hat{32})\big)\big] \\ U_1(1)\,U_{11}^+(\hat{23}) = -\,k_1^2\big[\delta(12)\,U_1^+(3) + \delta(13)\,U_1^+(2)\big] \\ U_1(1)\,U_{111}^+(\hat{234}) = k_1^2\big[3\,\delta(12)\,U_{11}^+(\hat{34}) - \delta(13)\big(U_{11}^+(24) + 2\,U_{11}^+(\hat{24})\big) - \\ \qquad - \delta(14)\big(U_{11}^+(23) + 2\,U_{11}^+(\hat{32})\big)\big] \\ U_{11}(01)\,U_{111}^+(234) = k_0^2k_1^2\big[\delta(12)\big(9\delta(13)\,U_1^+(4) + \delta(04)\,U_1^+(3)\big) + \\ \qquad + \delta(13)\big(\delta(02)\,U_1^+(4) + \tfrac{1}{9}\,\delta(04)\,U_1^+(2)\big) + \delta(14)\,\big(\tfrac{25}{9}\,\delta(03)\,U_1^+(2) + \\ \qquad + \tfrac{1}{9}\,\delta(02)\,U_1^+(33)\big] \\ U_{11}(01)\,U_{111}^+(\hat{234}) = -\,k_0^2k_1^2\,\big[3\,\delta(12)\,\big(\delta(03)\,U_1^+(4) + \delta(04)\,U_1^+(3)\big) + \\ \qquad + \delta(13)\,\big(\delta(02)\,U_1^+(4) - \tfrac{5}{3}\,\delta(04)\,U_1^+(2)\big) + \\ \qquad + \delta(14)\,\big(\delta(02)\,U_1^+(3) - \tfrac{5}{3}\,\delta(03)\,U_1^+(2)\big)\big]\,. \end{cases}$$

We further define

$$\text{(A3)} \qquad \begin{cases} Q_3(k) = k^3 + (\sigma k)\sigma^3\,, \qquad O_3(k) = \alpha_k^3 + (\tau\alpha_k)\tau^3 \\ U_3(k) = Q_3(k)\,O_3(k)\,. \end{cases}$$

Finally $U^+_{13}(12) = U^+_1(1)\,U^+_3(2)$, etc., as for the $\frac{1}{2}\,\frac{1}{2}$ case. These operators have the property that they produce a $\frac{3}{2}$ state when applied to a bare nucleon. As in the previous case when summed over all variables applied to a bare nucleon the following equations hold:

$$
\text{(A4)}\quad
\begin{cases}
U_1(1)\,U^+_3(2) = 0 \\
U_1(1)\,U^+_{13}(23) = k_1^2\left[3\,\delta(12)\,U^+_3(3) + \frac{4}{3}\delta(13)\,U^+_3(2)\right] \\
U_1(1)\,U^+_{113}(234) = k_1^2\left[3\,\delta(12)\,U^+_{13}(34) + \frac{1}{3}\,\delta(13)\,U^+_{13}(24) + \right. \\
\qquad \left. + \frac{1}{3}\,\delta(14)\left(U_{13}(23) + U_{13}(32) - \hat{U}_{13}(23) - \hat{U}_{13}(32)\right)\right] \\
U_1(1)\,U^+_{13}(\hat{23}) = 2k_1^2\left[\delta(12)\,U^+_3(2) + \delta(13)\,U^+_3(2)\right] \\
U_1(1)\,U^+_{113}(2\hat{34}) = k_1^2\left[3\delta(12)\,U^+_{13}(\hat{34}) + \frac{1}{3}\,\delta(13)\left(U^+_{13}(24) - \hat{U}(24)\right) + \right. \\
\qquad \left. + \frac{1}{3}\delta(14)\left(U^+_{13}(23) - U^+_{13}(\hat{32})\right)\right] \\
U_{11}(01)\,U^+_{113}(234) = k_0^2k_1^2\left[\delta(12)\left(9\delta(03)\,U^+_3(4) + 4\delta(04)\,U^+_3(3)\right) + \right. \\
\qquad + \delta(13)\left(\delta(02)\,U^+_3(4) + \frac{4}{9}\,\delta(04)\,U^+_3(2)\right) + \\
\qquad \left. + \frac{1}{9}\,\delta(04)\left(\delta(02)\,U^+_3(3) + \delta(03)\,U^+_3(2)\right)\right] \\
U_{11}(01)\,U^+_{113}(2\hat{34}) = k_0^2k_1^2\left[6\,\delta(12)\left(\delta(03)\,U^+_3(4) + \delta(04)\,U_3(3)\right) + \right. \\
\qquad + \delta(13)\left(\frac{1}{3}\delta(02)\,U^+_3(4) - \frac{2}{9}\,\delta(14)\,U^+_3(2)\right) + \\
\qquad \left. + \delta(14)\left(\frac{1}{3}\delta(02)\,U^+_3(3) - \frac{2}{9}\,\delta(03)\,U^+_3(2)\right)\right].
\end{cases}
$$

Appendix II

We shall briefly indicate a way of calculating the integral used in (3.8)

$$I(z) = P\int_0^\infty \frac{k^4\,\mathrm{d}k}{\omega^3(\omega - z)(1 + \omega^4/L^4)}\,.$$

By multiplying the numerator and denominator by $\omega + z$ the integral is split up in two parts, one even and one odd. For the even part the integral is extended to $-\infty$ and is solved by complex integration yielding

$$I_e(z) = \frac{\pi}{2}\left[\frac{(1 + L^4)^{\frac{3}{2}}}{z^4 + L^4}\left(L^2 \sin\left\{\frac{3}{2}\,\mathrm{arctg}\,L^2\right\} + z^2\cos\left\{\frac{3}{2}\,\mathrm{arctg}\,L^2\right\}\right) - \frac{1}{z^2}\right].$$

This takes a simpler form for $L^2 \gg 1$, namely

$$I_e(z) \simeq \frac{\pi}{2}\left[\frac{L^3}{L^4 + z^4}\,\frac{L^2 - z^2}{\sqrt{2}} - \frac{1}{z^2}\right].$$

The odd part is transformed by the substitution $\beta = k/\sqrt{1+k^2}$ to an integral of a rational function which can be expressed by elementary functions. The result is rather complex. For $L^2 \gg 1$ it goes over into

$$I_0 = \frac{L^4}{L^4 + z^4}\left[\left(z^2 + \frac{z^4}{L^2}\right)\ln 2L - \left(\frac{\pi}{4} - \frac{1}{2L}\ln 2L\right)\frac{z^2}{L}(z^2-1) - \right.$$
$$\left. - \frac{(z^2-1)^{\frac{3}{2}}}{z}\ln\frac{z+\sqrt{z^2-1}}{z+\sqrt{z^2-1}} - 1 - \frac{z^4}{L^2}\right].$$

Hence for $L^2 \gg 1$

$$\text{(B1)}\quad I(z) = I_0(z) + I_e(z) = \frac{1}{1+z^4/L^4}\left[\frac{\pi}{\sqrt{8}}Lz + z^2\left(\ln\frac{L}{z} - \frac{\pi}{\sqrt{8}}\frac{z}{L} - \frac{\pi}{4}\frac{z^2-1}{L^2}\right) + \right.$$
$$\left. + \left(\frac{z}{L}\right)^2\left(\frac{3}{2}\ln 2L - 1\right) - 1 - \frac{\pi}{2z}\left(1 + \frac{z^4}{L^4}\right)\right].$$

RIASSUNTO (*)

Lo scattering di pioni su nucleoni si considera nell'ipotesi di accoppiamento pv con cut-off. Un modello dovuto a T. D. Lee si estende in due direzioni: *a*) includendo gli effetti di rinculo e *b*) ammettendo la presenza di due mesoni nella nube mesonica del nucleone. Il modello consente l'adozione di rigorose regole di rinormalizzazione senza ricorso alla teoria di perturbazione. Gli spostamenti di fase per gli scattering $\frac{1}{2}\,\frac{1}{2}$ e $\frac{3}{2}\,\frac{3}{2}$ si possono calcolare con qualsiasi esattezza si desideri (nel presente lavoro circa il 10%).

(*) *Traduzione a cura della Redazione.*

Propagators of Quantized Field.

P. T. Matthews

Department of Mathematical Physics, The University - Birmingham, England

A. Salam

St. John's College - Cambridge, England

(ricevuto il 10 Maggio 1955)

Summary. — Feynman's formulation of quantum mechanics—the sum over histories—is discussed in its field theoretic form. It expresses the propagators of the interacting fields as functional integrals over the fields. The integrals over the anti-commuting Fermi fields are carried out. The complete propagators, including all radiative corrections, are thus expressed as functional integrals, over the meson field, of integrands involving the single nucleon propagator and the vacuum to vacuum transition amplitude in an external field. The latter factor is the Fredholm determinant of the external field problem for « nucleons » satisfying Fermi statistics, but its inverse if Bose statistics are assumed. These expressions for the propagators display some interesting distinctions between « renormalizable » and « unrenormalizable » interactions which are quite independent of an expansion in the coupling constant.

1. – Introduction.

A formulation of Quantum particle mechanics has been given by Feynman [1], which expresses the propagator, $\langle x'', t''\ x', t' \rangle$, for any system as a « sum over histories » or, in mathematical terminology, as a functional integral over the path $x(t)$. The direct application of this principle to interacting quantized fields leads to expressions for propagators which are functional integrals over the fields, $\varphi(x)$ and $\psi(x)$ say. In the case of Fermi fields the functions, $\psi(x)$, have to be assumed to anticommute with each other. In view of the

[1] R. P. Feynman: *Rev. Mod. Phys.*, **20**, 367 (1948).

apparant difficulty of functional integrals over anti-commuting functions, this direct approach has always been avoided in the past. It is the purpose of this paper ([2]) to show that such integrals can be defined and evaluated, and lead in a simple and unified way to compact expressions for the many particle propagators, from which scattering cross-sections and energy levels may, in principle, be deduced.

This paper describes a much more direct application of Feynman's principle to interacting field than has been made previously. The emphasis is on the formulation and the method. The result, namely a general expression for the propagator, (4.6), is to be found, at least by implication, in Feynman's original works ([3]).

In the first section the « sum over histories » postulate is stated in its field theoretic form and its relation to the dynamical principle proposed by SCHWINGER is exhibited ([4]). It is shown that the former is, in fact, the (functional) integral of the latter ([5]). Thus, whereas the dynamical principle leads to functional differential equations for propagators, the « sum over histories » states directly the solutions to these equations. Essentially, this paper consists in exploiting, as far as possible, the above remark.

The general expression for the many particle propagator, for interaction field, is derived by first considering the non-interacting Bose field, and then the n-nucleon propagator for a quantized nucleon field in a given external meson field. The exclusion principle, which was inserted explicitly in Feynman's original formulation ([6]), appears here as a consequence of the anti-commutation of the fields. It is also shown that the functional integral expression for the one-particle propagator is just the Fredholm solution of the appropriate integral equation. This result is modified in a rather surprising way if the « nucleon » is assumed to obey Bose statistics—the Fredholm determinant being then replaced by its inverse.

Once the propagators for nucleons in an external field have been found, the expressions for interacting quantized fields follow very simply, and lead very directly, in the case of weak coupling, to the well known graphical rules ([6,7]).

([2]) This is an amplification of results reported previously. P. T. MATTHEWS and A. SALAM: *Nuovo Cimento*, **12**, 563 (1954).

([3]) R. P. FEYNMAN: *Phys. Rev.*, **80**, 440 (1950).

([4]) J. SCHWINGER: *Phys. Rev.*, **82**, 914 (1951); **91**, 713 (1953); **91**, 728 (1953); **92**, 1283 (1953); **93**, 615 (1954); **94**, 1362 (1954).

([5]) This was pointed out by F. J. DYSON: *Advanced Quantum Mechanics*, Cornell University Lectures (1951). Unpublished.

([6]) R. P. FEYNMAN: *Phys. Rev.*, **75**, 749, 769 (1949).

([7]) F. J. DYSON: *Phys. Rev.*, **75**, 486 (1949).

The functional integrals for the propagators show up some interesting distinctions between renormalizable and unrenormalizable theories, which are discussed in the final section.

1. – The Feynman Postulate.

The « sum over histories » postulate, for the interaction of a nucleon (Fermi) field ψ, with a neutral meson (Bose) field φ, specified by some Lagrangian density $L(\varphi, \bar{\psi}, \psi)$ is that

$$\text{(I)} \qquad (\xi', \sigma_1 \,|\, T^*(A(1), ..., B(n)) \,|\, \xi'', \sigma_2) = \\ = \frac{1}{N} \int_{\xi''}^{\xi'} A(1), ..., B(n) \exp\left[i \int_{\sigma_2}^{\sigma_1} L(\varphi, \bar{\psi}, \psi) \, \mathrm{d}^4 x \right] \delta\varphi \, \delta\bar{\psi} \, \delta\psi \, .$$

Here $A(1), ..., B(n)$ are any set of field operators, or their derivatives, at points lying between the two space-like surfaces σ_1 and σ_2. The operator T^* is the chronological ordering operator, as defined by NISHIJIMA [8], with the additional sign changes for Fermi operators introduced by WICK [9]. ξ', ξ'' are the eigenvalues of a complete commuting set of operators, which specify the state of the system on the two surfaces. All functions in the integrand [10] on the right hand side are treated as c-numbers except that Fermi fields anti-commute [11]. The space integral in the exponent is performed between the two surfaces, and the functional integral is made over all fields which take on the values indicated by ξ' and ξ'' on the end surfaces. N is a normalizing costant which is defined so that the vacuum-to-vacuum transition amplitude, for an infinite time interval, is unity when no external sources are operating.

If one makes an infinitesimal variation of (I) for the unit operator—this may be a variation of the end surfaces, a variation of the field variables, or a variation of the Lagrangian—then

$$\text{(II)} \qquad \delta(\xi', \sigma_1 \,|\, \xi'', \sigma_2) = \frac{1}{N} \int \delta \left[\int i L \, \mathrm{d}^4 x \right] \exp\left[i \int L \, \mathrm{d}^4 x \right] \delta\psi \, \delta\bar{\psi} \, \delta\varphi \, , \\ = i \left(\xi', \sigma_1 \,\middle|\, \delta \int L \, \delta^4 x \,\middle|\, \xi'', \sigma_2 \right),$$

[8] K. NISHIJIMA: *Progr. Theor. Phys.* (Japan), **5**, 405 (1950).

[9] G. C. WICK: *Phys. Rev.*, **80**, 268 (1950).

[10] For the functional integrals we use the notation of S. F. EDWARDS and R. E. PEIERLS: *Proc. Phys. Soc.*, A **224**, 24 (1954).

[11] Alternatively and equivalently, all functions are operators, but an operator T^* is implied, which operates on the whole integrand. Bose fields commute and Fermi Fields anti-commute in a T^* product.

which is the dynamical principle proposed by SCHWINGER. To obtain the final equality we have used (I).

The vacuum expectation values of chronological products determined by (I) are the « propagators », which determine the scattering amplitudes. Since the rest of the paper will be concerned only with true vacuum expectation values, we introduce the notation

$$(A(1), ..., B(n)) = (0, \sigma_1 | T^*(A(1), ..., B(n)) | 0, \sigma_2) . \tag{1.1}$$

2. – The Bose Field.

Consider first a (pseudo-)scalar neutral meson field, $\varphi(x)$, without interaction. Define the action

$$I_m = -\tfrac{1}{2} \int \varphi(x) \mathcal{K}(x, y) \varphi(y) \, \mathrm{d}x \, \mathrm{d}y , \tag{2.1}$$

where

$$\mathcal{K}(x, y) = \delta(x - y)(-\Box_y + \mu^2 - i\varepsilon) . \tag{2.2}$$

The $i\varepsilon$ is introduced to make the functional integral over the action converge. The one meson propagator is

$$\begin{aligned} \Delta^{(1)}(1, 2) &\equiv (\varphi(1), \varphi(2)) , \\ &= \frac{1}{M} \int \varphi(1) \varphi(2) \exp [-iI_m] \, \delta\varphi , \end{aligned} \tag{2.3}$$

where

$$M = \int \exp [-iI_m] \, \delta\varphi . \tag{2.4}$$

Since only those fields $\varphi(x)$ will contribute to the integral (2.3) for which I_m is finite, we may introduce [12] a complete set of functions $\varphi_n(x)$, normalized so that

$$\tfrac{1}{2} \int \varphi_n(x) \mathcal{K}(x, y) \varphi_m(y) \, \mathrm{d}x \, \mathrm{d}y = \delta_{nm} , \tag{2.5}$$

---

[12] S. F. EDWARDS: *Phil. Mag.*, **47**, 758 (1954).

and expand $\varphi(x)$ in terms of them:

$$\varphi(x) = \sum a_n \varphi_n(x) . \tag{2.6}$$

Substituting in (2.3) gives

$$\Delta^{(1)}(1, 2) = \frac{\sum_{i,j} \varphi_i(1)\varphi_j(2) \int a_i a_j \exp\left[-i \sum_s a_s^2\right] \prod_t \mathrm{d}a_t}{\prod_r N(a_r)} , \tag{2.7}$$

where

$$N(a) = \int \exp[-ia^2]\,\mathrm{d}a . \tag{2.8}$$

This is now an infinitely multiple integral.

The integral for $\Delta^{(1)}$ vanishes unless the a's are equal, thus

$$\Delta^{(1)}(1, 2) = \sum_{ij} \varphi_i(1)\varphi_j(2)\,\delta_{ij} \int \frac{a^2 \exp[-ia^2]\,\mathrm{d}a}{N(a)} \tag{2.9}$$

$$= \sum_i \varphi_i(1)\varphi_i(2)(-i/2) . \tag{2.10}$$

But from (2.5)

$$\sum_i \varphi_i(1)\varphi_i(2) = 2\mathcal{K}^{-1}(1, 2) . \tag{2.11}$$

Therefore

$$\Delta^{(1)}(1, 2) = -i\mathcal{K}^{-1}(1, 2) . \tag{2.12}$$

In momentum space, if

$$\varphi(x) = \int \varphi(p) \exp[ipx]\,\mathrm{d}\varrho , \tag{2.13}$$

$$\Delta(p_1, p_2) = \int \Delta(x_1, x_2) \exp[i(p_1x_1 - p_2x_2)]\,\mathrm{d}p_1\,\mathrm{d}p_2 , \tag{2.14}$$

then

$$\Delta^{(1)}(p_1, p_2) = -i\,\frac{\delta(p_1 - p_2)}{(p_1^2 + \mu^2 - i\varepsilon)} , \tag{2.15}$$

which is the well known Feynman function ([6]).

To obtain the n-meson propagator, we first consider the integral

$$I = \int \frac{a^{2n} \exp[-ia^2]\,da}{N(a)} = c^{(n)} I , \tag{2.16}$$

where

$$I = I^{(0)} = (-i/2) , \tag{2.17}$$

and

$$c^{(n)} = \frac{2n!}{(n!\,2^n)} . \tag{2.18}$$

$c^{(n)}$ is the number of ways $2n$ particles can be arranged in pairs, regardless of the ordering, of the pairs, or within the pairs.

Now consider the two-meson propagator

$$\Delta^{(2)}(1,2,3,4) = \tag{2.19}$$
$$= \sum \varphi_i(1)\varphi_j(2)\varphi_k(3)\varphi_l(4) \int a_i a_j a_k a_l \exp[-i\sum a^2] \prod da \prod / N(a) .$$

This vanishes unless the a's are equal in pairs, or when all four a's are equal. These give rise to integrals $I^{(2)}$ and, in fact,

$$\Delta(1,2,3,4) = \sum_P \sum_{i \neq k} \varphi_i(r)\varphi_j(s)\varphi_h(t)\varphi_l(u)\,\delta_{ij}\delta_{kl} I^2 + \tag{2.20}$$
$$+ \sum_{i=k} \varphi_i(1)\varphi_j(2)\varphi_k(3)\varphi_l(4)\,\delta_{ij}\delta_{kl} C^{(2)} I^2 ,$$

where the summation $\sum_P$ is over all distinguishable permutations of the points r, s, t, u $(=1, 2, 3, 4)$. From the remark following (2.18), the number of terms in this summation is $c^{(2)}$. Thus the final term just adds the terms which are excluded by the condition $i \neq k$ in the first term, giving the result

$$\Delta(1,2,3,4) = \sum_P \sum_{ijkl} \varphi_i(r)\varphi_j(s)\varphi_k(t)\varphi_l(u)\,\delta_{ij}\delta_{kl} I^2 = \sum_P \Delta(r,s)\,\Delta(t,u) . \tag{2.21}$$

The final equality follows from a comparison with (2.6).

Similarly, for three mesons,

$$\Delta^{(3)}(1,2,3,4,5,6) = \sum_P \Delta(r,r)\,\Delta(t,u)\,\Delta(v,\omega) . \tag{2.22}$$

This result clearly generalizes to the $2n$-meson propagator [13].

---

[13] J. SCHWINGER: *Phys. Rev.*, **92**, 1283 (1953); E. R. CAIANIELLO: *Nuovo Cimento*, **11**, 492 (1954).

3. – Dirac Field.

We now consider a quantized Dirac field, ψ, in interaction with a given external Bose field φ^{ex}. Then the action is [14]

$$I_n(\varphi^{ex}) = -\int \bar{\psi}(x)\mathcal{D}(x, y, \varphi^{ex})\,\psi(y)\,dx\,dy\,, \tag{3.1}$$

where

$$\mathcal{D}(x, y, \varphi^{ex}) = \delta(x-y)(\gamma^\mu(\partial/\partial y_\mu) + \varkappa + g\varphi^{ex}(y))\,. \tag{3.2}$$

Then, by I,

$$K^{(1)}(1, 1'; \varphi^{ex}) \equiv (\psi(1), \bar{\psi}(1')) = \int \psi(1)\bar{\psi}(1')\exp[-iI_n(\varphi^{ex})]\,\delta\psi\,\delta\bar{\psi}/N(0)\,, \tag{3.3}$$

where

$$N(\varphi^{ex}) = \int \exp[-iI_n(\varphi^{ex})]\,\delta\psi\,\delta\bar{\psi}\,. \tag{3.4}$$

Rather than discuss $K^{(1)}$, it is more convenient for the next section, and more conventional, to define the propagator from which vacuum effects have been factored out [15],

$$S(1, 1'; \varphi^{ex}) \equiv \langle\psi(1), \bar{\psi}(1')\rangle_0 = \int \psi(1)\bar{\psi}(1')\exp[-iI_n(\varphi^{ex})]\,\delta\psi\,\delta\bar{\psi}/N(\varphi^{ex})\,. \tag{3.5}$$

We thus have

$$K(\varphi^{ex})\,N(0) = S(\varphi^{ex})\,N(\varphi^{ex})\,. \tag{3.6}$$

From I, $N(\varphi^{ex})/N(0)$ is the vacuum to vacuum transition amplitude in the presence of the external field.

---

[14] The Lagrangian should be completely anti-symmetrized (see for example SCHWINGER, reference [4]). We use (3.1) implying the full form in any context in which the two expressions are not precisely equivalent.

[15] $\langle\ldots\rangle_0$ is the notation of J. SCHWINGER: *Proc. Nat. Acad. Sci.*, **37**, 452 (1951).

To evaluate $S(\varphi^{ex})$, we choose a Majorana representation of the γ-matrices [16] so that $\mathcal{D}$ is a real operator, and the Lorentz transformations of the spinors are also real. It is then possible to make an invariant split of any complex field into two *real* fields ψ_a and ψ_b,

$$\psi = \psi_a + i\psi_b \,. \tag{3.7}$$

The action is then

$$I_n(\varphi^{ex}) = -\int \bar{\psi}_a \mathcal{D}(\varphi^{ex})\psi_a \,\mathrm{d}x - \int \bar{\psi}_b \mathcal{D}(\varphi^{ex})\psi_b \,\mathrm{d}x \,. \tag{3.8}$$

We now introduce a complete set of anticommuting functions $\psi_n(x)$, normalized so that

$$\int \bar{\psi}(x)\mathcal{D}(x, y, \varphi^{ex})\,\psi_m(y)\,\mathrm{d}x\,\mathrm{d}y = \delta_{nm} \,, \tag{3.9}$$

and expand

$$\left| \begin{array}{l} \psi_a(x) = \sum a_n \psi_n(x) \,, \\ \psi_b(x) = \sum b_n \psi_n(x) \,. \end{array} \right. \tag{3.10}$$

Then

$$\left| \begin{array}{l} S(1, 1', \varphi^{ex}) = \sum \psi_i(1)\bar{\psi}_i(1') \int (a^2 - b^2) \exp[-i(a^2 - b^2)]\,\mathrm{d}a\,\mathrm{d}b / N(a)\,N(b) \,, \\ \qquad\qquad = \sum \psi_i(1)\bar{\psi}_i(1')(-i) \,, \end{array} \right. \tag{3.11}$$

$$= -i\mathcal{D}^{-1}(1, 1', \varphi^{ex}) \,. \tag{3.12}$$

Again the integrals [5,6], and consequently the inverse operator, are defined by the replacement of $\varkappa$ by $\varkappa - i\varepsilon$.

For this special case of an unquantized external field, this result could have been obtained much more easily. Using a theorem proved by MATTHEWS and SALAM [17], it follows directly that

$$\int \mathcal{D}(y, x, \varphi^{ex})\, S(x, z, \varphi^{ex})\,\mathrm{d}x = -i\,\delta(y - z) \,, \tag{3.13}$$

[16] If γ_μ is the usual Hermitian representation, then define $\gamma^1 = \gamma_4$; $\gamma^2 = \gamma_2$; $\gamma^3 = \gamma_5$; $\gamma^4 = \gamma_1$ and $\gamma^5 = \gamma_3$. (Note that $x_4 = it$, so γ^4 is pure imaginary). To go over from scalar to pseudoscalar mesons, g must be replaced by $ig\gamma^5$ throughout. Since γ^5 is pure imaginary, $\mathcal{D}$ defined by (3.2) is again a real operator. We are indebted to Mr. J. S. BELL for information in this point.

[17] P. T. MATTHEWS and A. SALAM: *Proc. Roy. Soc.*, A **221**, 128 (1953), Theorem II.

which is just (3.12). The integral equation following from this is

$$S(x, y, \varphi^{ex}) = S(x, y) + ig \int S(x, z) \varphi^{ex}(z) S(z, y, \varphi^{ex}) \, dz \,, \tag{3.14}$$

where

$$S(x, y) = S(x, y, 0) = S_F(x - y) \,.$$

The purpose of the evaluation given above is to relate (3.5) to the Fredholm solution of this integral equation. We return to this below. This work also serves to define more precisely, what is meant by a functional integral over non-commuting functions.

For the n-nucleon propagator, we require the integral

$$J^n = \int (a^2 + b^2)^n \exp[-i(a^2 + b^2)] \, da \, db / N(a) \, N(b) \,, \tag{3.15}$$

$$= D^{(n)}(J) \,,$$

where

$$J = J^{(0)} = -i \,. \tag{3.16}$$

and

$$D^{(n)} = n! \tag{3.17}$$

$D^{(n)}$ is the number of ways of pairing n objects of type a with n objects of type b.

Consider the two-nucleon propagator,

$$S(1, 2, 1', 2'; \varphi^{ex}) = - \sum \psi_{i_1}(1) \bar{\psi}_k(1') \psi_{i_2}(2) \bar{\psi}_m(2') \cdot \tag{3.20}$$

$$\cdot \int (a_{i_1} + ib_{i_1})(a_k - ib_k)(a_{i_2} + ib_{i_2})(a_m - ib_m) \exp\left[-i \sum_i (a_i^2 + b_i^2)\right] \prod da \prod db \cdot$$

$$\cdot \left[\prod_s N(a_s) \prod_t N(b_t)\right]^{-1}$$

the minus sign coming from the rearrangement of the factors $\bar{\psi}$. The integral vanishes unless the a's are at least equal in pairs. Thus,

$$S(1, 2, 1', 2'; \varphi^{ex}) = - \sum_A \sum_{k \neq m} \psi_{i_1}(1) \bar{\psi}_k(r) \psi_{i_2}(2) \bar{\psi}_m(s) \, \delta(i_1, k) \, \delta(i_2, m) \, [D^{(1)}]^2 J^2 \tag{3.21}$$

$$- \sum_{k = m} \psi_{i_1}(1) \bar{\psi}_k(1') \psi_{i_2}(2) \, \bar{\psi}_m(2') \, \delta(i_1, k) \, \delta(i_2, m) \, D^{(2)} J^2 \,,$$

where $\sum_A$ is the sum over all permutations of the points r, s $(=, 1, 2)$ among

the ψ's (in this case just two terms), multiplied by the signature of the permutation. The proof then follows as for the Bose case, the final term being just that required to remove the restriction from the sum in the first term giving

$$S(1, 2, 1', 2'; \varphi^{ex}) = -\sum_A S(1, r; \varphi^{ex}) S(2, s; \varphi^{ex}) , \tag{3.22}$$

$$= -\operatorname{Det}[S(x, x'; \varphi^{ex})]^{(2)} .$$

This result can also be generalized to [13]

$$S(1, 2, ..., n, 1', 2', .., n'; \varphi^{ex}) = (-1)^{n(n-1)/2} \operatorname{Det}[S(x, x'; \varphi^{ex})]^{(n)} , \tag{3.23}$$

the suffix n denoting an $n \times n$ determinant, the initial sign factor coming from the first rearrangement of the $\overline{\psi}$'s to their alternating positions between the ψ's.

In the light of this result, it is of interest to re-examine the original functional integral (3.5) for $S(x, y; \varphi^{ex})$. Expanding (3.4) in powers of g gives

$$\frac{N(\varphi^{ex})}{N(0)} = \int \sum_n \frac{1}{n!} \left[-ig \int \overline{\psi}(x) \psi(x) \varphi^{ex}(x) \, dx \right]^n \exp[-iI_n(0)] \, \delta\psi \, \delta\overline{\psi}/N(0), \tag{3.26}$$

$$= \sum_n (-1)^n \frac{(ig)^n}{n!} \int \operatorname{Det}[S(x_i, x_j) \varphi(x_j)]^n (dx_i)^n . \tag{3.27}$$

This is just the Fredholm determinant [18], $d(g, \varphi^{ex})$, of the integral equation (3.14), and a similar analysis of (3.5) [dividing numerator and denominator by $N(0)$] shows that this is in fact the Fredholm solution. This is not a new result [19], but the interesting feature which we wish to stress is that postulate I, without more ado, automatically writes down the complete solution to the external field problem.

Notice that if the interaction were as in (3.2), but ψ was a charged Bose field, a similar analysis would apply, with $\mathcal{D}(0)$ replaced by $\mathcal{K}$ and determinants replaced by « permanents » [13]. In this case (3.27) is not the Fredholm determinant but its *inverse* [20].

---

[18] See for example E. T. WHITTAKER and G. N. WATSON: *Modern Analysis* (Cambridge, 1902).

[19] M. NEUMANN: *Phys. Rev.*, **83**, 1258 (1951); **85**, 129 (1952); A. SALAM and P. T. MATTHEWS: *Phys. Rev.*, **90**, 690 (1953); J. SCHWINGER: *Phys. Rev.*, **93**, 616 (1954).

[20] See for example MATTHEWS and SALAM, reference [19]. By (2.12) the inverse of $d(g)$ is obtained by replacing σ_n by $-\sigma_n$. Making this change in (1.6) converts determinants to permanents. We are particularly indebted to Dr. EDWARDS and Dr. FELDMAN for discussions on this point. See S. E. EDWARDS: *Nucleon Green Function in pseudo-scalar meson theory*, I; to be published.

4. – Interacting Quantized Fields.

We now consider the case of two interacting quantized fields with action

$$I = I_n(\varphi) + I_m \,, \tag{4.1}$$

where the φ appearing in $I_n(\varphi)$ is now the quantized field. The complete one-nucleon propagator (in the absence of external fields there is no difference between S' and K') is,

$$S'(1, 1') = (\psi(1), \overline{\psi}(1')) \,, \tag{4.2}$$

$$= N^{-1} \int \psi(1)\overline{\psi}(1') \exp[-i(I_n(\varphi) + I_m)](\delta\psi\, \delta\overline{\psi}\, \delta\varphi \,,$$

where

$$N = \int \exp[-i(I_n(\varphi) + I_m)]\, \delta\psi\delta\overline{\psi}\delta\varphi \,. \tag{4.3}$$

The functional integrals over ψ and $\overline{\psi}$ are just those which have been performed in the previous section ([21]). Using (3.3) and (3.6), we obtain

$$S'(1, 1') = \frac{\int S(1, 1'; \varphi)\, N(\varphi) \exp[-I_m]\, \delta\varphi}{\int N(\varphi) \exp[-iI_m]\, \delta\varphi} \,. \tag{4.4}$$

The n-nucleon propagator is, by (2.7),

$$S'^{(n)}(1, \ldots, n, 1', 2', \ldots, n') = (\psi(1), \ldots, \psi(n), \overline{\psi}(1') \ldots, \overline{\psi}(n')) = \tag{4.5}$$

$$= \frac{\int (-1)^{\frac{n(n-1)}{2}} \operatorname{Det}[S(i, j'; \varphi) \int^{(n)} N(\varphi) \exp[-iI_m]\, \delta\varphi}{\int N(\varphi) \exp[-iI_m]\, \delta\varphi} \,.$$

Similarly the n-nucleon, m-meson propagator is, symbolically,

$$S'^{(n,m)} = \frac{\int \varphi^m S^{(n)}(\varphi)\, N(\varphi) \exp[-iI_m]\, \delta\varphi}{\int N(\varphi) \exp[-iI_m]\, \delta\varphi} \,. \tag{4.6}$$

([21]) Great stress has been laid by R. P. FEYNMAN: *Phys. Rev.* **80**, 440 (1950); **84**, 108 (1951) on the alternative expression obtained by doing the φ integration first:

$$K^1(1, 1') = \frac{1}{N(0)} \int \psi(1)\, \overline{\psi}(1') \exp\left[-i\left(\overline{\psi}\mathcal{D}\psi - \frac{ig^2}{2}\, \overline{\psi}\psi\Delta\overline{\psi}\psi\right)\right] \delta\psi\, \delta\overline{\psi} \,.$$

This has certain advantages, but if one's object is to complete the functional integral, this is probably not the best way to proceed, since the integrations over Fermi fields are clearly more complicated and should be done first.

These are our main results, and they are discussed below. If these integrals can be evaluated they determine directly the scattering amplitudes.

It is of interest to note that the functional integration can be completed quite simply if the expressions are expanded in powers of the coupling constant, and leads directly to the Feynman graphs ([6,7]). Consider (4.2), which can be written formally as

$$S(1,1') = i \int \frac{\delta}{\delta \mathcal{D}_{1,1'}(0)} N(\varphi) \exp[-iI_m]\,\delta\varphi \Big/ \int N(\varphi) \exp[-iI_m]\,\delta\varphi \,. \tag{4.7}$$

Divide the numerator and denominator by $N(0)$, which is independent of φ. It follows from the discussion at the end of the previous section that the expansion of $N(\varphi)/N(0)$ gives all vacuum graphs in the « external field » φ, (including products of disconnected vacuum graphs). The result of § 2 shows that the effect of the φ integration is to connect the « external field » points in pairs in all possible ways and insert a factor $\Delta^{(1)}$ between each. This is just the Feynman-Dyson prescription for the vacuum graphs of two coupled quantized fields.

Now

$$\mathcal{D}_{12}(0) = -iS^{-1}(1,2) \,. \tag{4.8}$$

Hence

$$i \frac{\delta}{\delta \mathcal{D}_{12}(0)} = S(1,i) \frac{\delta}{\delta S(i,j)} S(j,2) \,; \tag{4.9}$$

graphically this operator replaces each internal line $S(i,j)$ by two external lines $S(1,i)$ and $S(j,2)$. Thus the differential operator in the numerator has the effect of splitting the internal lines in the vacuum graphs, one at a time, to create open nucleon lines running from 2 to 1. It is easily seen that this prescription produces all the graphs of the one-nucleon propagator. The result generalizes to the other propagators, and this approach could, of course, be used as the theoretical basis of the graphical formalism.

5. – Discussion.

The main result of this paper is the expression (4.4) for the one-particle propagator. This has been obtained by a partial evaluation of the functional integral for the propagator, which is given directly by (I). An approximate form of this expression was obtained previously by Edwards and Peierls ([22]), who started from the functional differential equations for the propagator which

can be deduced from (II). These authors have also carried out the final integration over $\delta\varphi$, for simple cases, and these results have been extended by EDWARDS ([23]).

In the above-mentioned work ([22]) the approximation of replacing $N(\varphi)$ by unity has always been used. Apart from renormalization, which can be done quite simply ([23]), the whole problem then reduces to the one of evaluating the functional integral, other than as an expansion in the coupling constant.

If the approximation of dropping $N(\varphi)$ is not made, more fundamental problems present themselves of the existence of non-existence of the integral and the, probably related, question of the distinction between renormalizable and unrenormalizable interactions, independent of expansions in the coupling constant. If the denominator of (4.4) is evaluated as an expansion in the coupling constant a series is obtained, each term of which is a vacuum graph. These have quartic « true » divergences, for renormalizable theories, which are not removed by renormalization. This suggests that something more than renormalization (as defined by DYSON ([24])) may be required to give (4.4) a meaning.

On the other hand, the integrand in the denominator of (4.4) is formally the Fredholm determinant of (3.14) (the external field propagator equation), and in the numerator, it is the Fredholm resolvent of the same equation. It has been shown that for renormalizable interactions these integrands are well defined finite expressions ([19]) for all fields φ, which, for large momenta, fall off faster than p^{-3}. It was pointed out in the discussion leading to (2.4) that fields which fall off slower than p^{-3} are excluded from the integral, anyway, by the infinite oscillations of the factor $\exp[-iI_m]$. Quantization of φ brings in the integration over φ, or (see (2.12)) the sum over base fields. It is this step which introduces the term by term divergences.

The situation for unrenormalizable interactions is quite different. For them the integrand is well defined only for fields which fall off faster than p^{-4}. Thus for unrenormalizable interactions, fields have to be included in the φ-integration, for which no Fredholm solution exists to the external field problem, which clearly introduces a more serious type of divergence. This, is a distinction between the two types of interaction, which does not depend on the expansion in the coupling constant.

One other way in which renormalizable and unrenormalizable theories stand

([22]) S. F. EDWARDS and R. E. PEIERLS: *Proc. Roy. Soc.*, A **224**, 24 (1954). A derivation of the complete formula from II has recently been given by E. C. FRADKIN: *Dokl. Akad. Nauk SSSR*, **98**, 47 (1954).

([23]) S. F. EDWARDS: *Proc. Roy. Soc.*, A **228**, 411 (1955) and *Nucleon Green Function in pseudo-scalar Meson Theory I and II*, to be published.

([24]) F. J. DYSON: *Phys. Rev.* **75**, 1736 (1949).

distinguished is seen as follows. Consider $\Delta'(1, 2)$, the Boson propagator in the fully interacting case

$$\Delta'(1, 2) = \frac{\int \varphi(1)\varphi(2) \exp[-iI_m(\varphi)] N(\varphi)\, \delta\varphi}{\int \exp[-iI_m(\varphi)] N(\varphi)\, \delta\varphi} .$$

$N(\varphi)$ can be written as an exponential, for certain classes of fields, (the Plemelj form). Writing $N(\varphi) = \exp[-L(\varphi)]$, we notice that $I_m(\varphi)+iL(\varphi)$ can be considered as an effective (non-local) action for the φ field ([25]). For renormalizable theories this action does not contain any derivatives besides those already present in $I_m(\varphi)$. For most unrenormalizable theories (e.g. pseudoscalar theory with pseudovector coupling) $L(\varphi)$ contains space and time derivatives of φ of all orders. It is impossible in this case to consider $L(\varphi)$ as defining an « effective » action. At the present stage of our knowledge of the theory this can not be considered as an objection. It is however, pointed out as a distinction between renormalizable and unrenormalizable theories which appears only in the present formalism.

The integrands in (4.4), both in the numerator and the denominator, in so far as they are the Fredholm resolvant and the Fredholm determinant define series which converge for all values of the coupling constant. Our results up to this stage (before the final Bose functional integration) thus do not suffer from any objections raised against series expansions. At this stage $N(\varphi)$ contains but one divergence, the divergence of the second order (vacuum polarization) loop. It is interesting that only this final term by term Bose functional integration introduces all the well known divergences as well as, possibly, leading to the non convergence of the series. It can be shown formally that if one restricts one's self to a finite base set in the Bose functional integral (restrict to a finite number of a's in (2.6)), and a term by term integration in (4.4) is performed, the resulting series has a finite radius of convergence. Restricting the base set is equivalent to a high energy cut-off. In this sense it would seem that the problem of the convergence of the series is closely linked with the problem of the term by term divergences.

* * *

This work is the direct result of numerous stimulating conversations with Professor R. E. Peierls, Dr. G. Feldman, and most particularly, Dr. S. F. Edwards, to whom we express our thanks. Each author also gratefully acknowledges hospitality extended to him by the University of the other.

([25]) It should be noted that the zeros of $N(\varphi)$, which are quite harmless, will appear as logarithmic infinities in $L(\varphi)$. This remark may be of significance in connection with recent work of R. P. Feynman in the *Proceedings of the Fifth Rochester Conference* (January 1955).

RIASSUNTO (*)

Si discute l'estensione alla teoria dei campi della formulazione di Feynman della meccanica quantistica — la somma rispetto alle « storie ». Si sviluppano gli integrali sui campi di Fermi anticommutativi. I propagatori completi, comprese tutte le correzioni radiative, si esprimono così come integrali funzionali sul campo mesonico di integrandi comprendenti il propagatore del nucleone isolato e l'ampiezza di transizione vuoto-vuoto in un campo esterno. Quest'ultimo fattore è il determinante di Fredholm del problema del campo esterno per « nucleone » che soddisfano la statistica di Fermi, ma è il suo inverso se le particelle obbediscono alla statistica di Bose. Queste espressioni pei propagatori mettono in risalto alcune interessanti distinzioni tra interazioni « rinormalizzabili » e « non rinormalizzabili » del tutto indipendenti dallo sviluppo in serie della costante di accoppiamento.

(*) *Traduzione a cura della Redazione.*

Zur Massenbestimmung an geladenen Teilchen in kernphotographischen Emulsionen mittels der Methode der variablen Zellen.

B. Roederer (*)

Max-Planck-Institut für Physik - Göttingen

(ricevuto il 16 Maggio 1955)

Summary. — The method of constant sagitta using the cell-size tables calculated by Fay, Gottstein and Hain (1) was applied for scattering measurements on 10 identified flat protons and 12 π-mesons in the region of short ranges (0 ÷ 5000 μm). Applying usual noise elimination methods, a systematic deviation from the theoretically expected values of D_0 was observed in the case of protons. Diverse sources for noise or systematic errors were investigated. Distortion was found to be insignificant. The falsifications of the results yielded by: i) the error in reading the cell length, ii) the wrong alignment of the track parallel to the stage movement, although significant, are not sufficient to explain fully the systematic deviation. It is found, however, that the usual way of working out second differences for the double cell size from those measured in the basic cells is not unrestrictedly applicable for the constant sagitta method because adjoining cells are frequently not of equal size. It is suggested, that noise elimination on short tracks (up to ~ 5 mm) should either be done between two different cell schemes, i.e. by measuring each particle twice, e.g. once in the $\pi_{0.5}$ scheme and once in the $P_{0.5}$ scheme; or by applying appropriate corrections in the conventional noise-elimination method. The magnitude of these corrections will then depend on the alignment and length of the track, the mass of the particle and the scheme used. By measuring each particle in two different schemes, we obtain a very good accordance with the values expected by the formula

$$D_0 = 0.5\,(M_{\text{scheme}}/M_{\text{particle}})^{0.43}$$

without any correction to the scattering constant assumed by Fay *et al.*. The calculated noise-level is shown to increase rapidly for double and quadruple cell-size.

(*) Comisión Nacional de la Energía Atómica, Buenos Aires.

(1) H. Fay, K. Gottstein and K. Hain: *Suppl. Nuovo Cimento*, **11**, 234 (1954).

1. – Einleitung.

Verschiedene Autoren haben sich in letzter Zeit bemüht, die sogenannte Streumeßmethode zur Energie- und Massenbestimmung von geladenen Teilchen in kernphotographischen Emulsionen zu vervollkomnen. Bei den Messungen an den Spuren von in der Schicht zur Ruhe gekommenen Teilchen ist neuerdings häufig die Methode der variablen Zellengröße angewandt worden. Dabei wurden meist die von [2,3] anhand halbempirischer Beziehungen zwischen Energie, Reichweite und Streuwinkel berechneten « Zellenschemata » verwendet. In diesen Schemata wurde jedoch die Abhängigkeit der Streukonstante von Zellengröße und Energie nicht berücksichtigt; die unechte Streuung wurde als konstant vorausgesetzt.

FAY *et al.* [1] haben eine Reihe von Schemata berechnet, bei denen die vorhergenannte Abhängigkeit mit in Betracht gezogen wurde. Diese Schemata wurden für drei verschiedene Massen (π und τ Mesonen und Protonen) aufgestellt und sollen für das zugehörige Teilchen einen Mittelwert für die Beträge der 2. Differenzen $D=0{,}5$ μm ergeben. Auf ein Teilchen angewandt, dessen Masse M_j nicht mit der des Schemas übereinstimmt, wird die Beziehung

$$\overline{D}_j(\mu) = 0.5 \left(\frac{M_j}{M_{\pi,\tau,\mathrm{P}}} \right)^{-0.43} \tag{1}$$

vorgeschlagen, die allerdings nur soweit strenge Gültigkeit hat, wie für die beiden Teilchen mit den Massen M_j und $M_{\pi,\tau,\mathrm{P}}$ gleiche Werte für die Streukonstante und den Exponenten in der Energie-Reichweite-Beziehung gelten.

Wie stellten uns die Aufgabe, die von FAY *et al.* ausgerechneten Schemata und die Gültigkeit der Beziehung (1) anhand von Teilchen bekannter Massen experimentell zu prüfen. Außerdem sollte bestimmt werden, welches der drei Schemata das jeweils vorteilhafteste ist, um ein möglichst großes Verhältnis von gemessener zu unechter Streuung und einen möglichst kleinen statistischen Fehler zu erhalten.

Zu diesem Zweck wurde eine Anzahl von Spuren ausgewählt, an denen die Eichmessungen durchgeführt wurden. Besondere Aufmerksamkeit wurde darauf geworfen, daß erstens die Spuren möglichst horizontal verliefen; zweitens sie sich möglichst entfernt vom Emulsionsrand befanden und drittens ihre Länge mindestens 5000 μm betrug. Diese Bedingungen erfüllten 12 π-Mesonen und 10 Protonen, erstere durch ihre Zerfallsprodukte und letztere anhand der

[2] C. DILWORTH, S. J. GOLDSACK und L. HIRSCHBERG: *Nuovo Cimento*, **11**, 113 (1954).

[3] D. LAL, YASH PAL and B. PETERS: *Proc. Ind. Acad. Sci.*, **38**, 277 (1953).

durchgeführten Streumessungen identifizierbar. Die Ilford G5 Emulsionen stammen aus einem in der Sardinienexpedition 1953 exponierten Block. Die Messungen wurden am Leitz-Koordinatenkomparator durchgeführt, unter Verwendung der Objektiv-Okular-Kombination 100×15. Die Zellen wurden direkt an der Präzisionsskala des Tisches abgelesen; die Koordinaten der Spur wurden durch eine Okularskala (1 Teilstrich=1,085 μm) bestimmt, dazu wurde visuell über mehrere Körner gemittelt. (Die Messungen wurden ausschließlich von der Verfasserin durchgeführt.)

2. – Meßergebnisse.

Abb. 1 zeigt die Verteilung der D_1 von Protonen und π-Mesonen für jedes der drei Schemata. Die einzelnen D_1 sind die Mittelwerte der Beträge der gemessenen 2. Differenzen D_i für jede Spur; dabei wurden alle Werte D_i eliminiert, die größer als $4D_1$ ausfielen. Jeder D_1 Wert wurde mit einer relativen

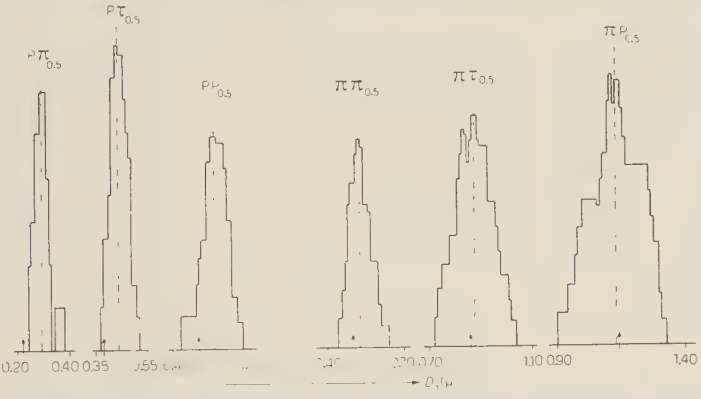

Abb. 1. – Verteilung der Mittelwerte der 2. Differenzen aus einfacher Zellengröße für 10 Protonen und 12 π-Mesonen, mit $P_{0.5}$, $\tau_{0.5}$ und $\pi_{0.5}$ Schemata vermessen. Jedem Meßwert entspricht eine Fläche gleicher Größe, deren Breite jeweils proportional zur statistischen Schwankung gewählt wurde. Die Mittelwerte der Verteilungen sind punktiert eingezeichnet; die nach Formel (1) zu erwartenden Werte der echten Streuung durch einen Pfeil gekennzeichnet.

statistischen Schwankung von $0.76/\sqrt{N}$ behaftet, wo N die Anzahl der unabhängigen Zellen bedeutet, die zur Bestimmung von D_1 verwendet wurden. Es zeigt sich eine Verschiebung der Verteilung gegen höhere Werte, wofür zunächst der Einfluß einer unechten Streuung verantwortlich zu machen ist. Setzt man voraus, daß diese unechte Streuung ausschließlich von der Tischbewegung, der Körnerverteilung und dem Ablesefehler herrührt, so kann sie nach der üblichen Methode eliminiert werden, indem man außer dem D_1 auch

den entsprechenden Wert $\bar{D}_2$ für die doppelte Zellengröße bestimmt und für die echte Streuung D_0 den Ausdruck ansetzt:

$$\bar{D}_0^2 = \frac{\bar{D}_1^2 \quad D_2^2(s_1/s_2)^a}{s_1^3 - s_2^3(s_1/s_2)^a} \,. \tag{2}$$

Dabei wurde vorausgesetzt, daß die Abhängigkeit der unechten Streuung n von der Zellengröße s folgendermaßen lautet:

$$n^2 = n_0^2 s^a \,, \tag{3}$$

wobei $a \approx 2/3$ für den Koordinatenkomparator [4].

Ferner wurde der Einfachheit halber zunächst der Umstand vernachlässigt, daß benachbarte Zellen in den Schemata i.a. nicht gleich groß sind. D.h., die D_2 wurden aus den Meßwerten berechnet, indem zwei aufeinanderfolgende 1. Differenzen addiert und daraus die 2. Differenzen gebildet wurden. In Tabelle I sind die D_0 Werte angegeben, gemittelt über alle Spuren einer Teilchensorte. Für die relative statistische Schwankung des D_0 einer jeden Spur wurde der Wert $1.35/\sqrt{N_1}$ angenommen, wobei N_1 die Zahl der Zellen ist. Der Faktor 1.35 ergibt sich aus (2), wenn man für $\bar{D}_1$ und D_2 unabhängige, relative Schwankungen von $0.76/\sqrt{N_1}$ und $0.76/\sqrt{N_2}$ zugrunde legt. Für die relative Schwankung des Mittelwertes der $\bar{D}_0$ von allen Spuren ergibt sich $1.35/\sqrt{N_{\text{ges}}}$ (N_{ges}=Gesamtzahl der Zellen aller Spuren.) Bei einem Vergleich mit den mittleren Fehlerquadraten $\varepsilon^2 = \sum_{i=1}^{n} (\bar{D}_0 - D_{0i})^2/n(n-1)$ (n: Zahl der Spuren), zeigt sich, daß

Tabelle I.

	P-$P_{0.5}$	P-$\tau_{0.5}$	P-$\pi_{0.5}$	π-$P_{0.5}$	π-$\tau_{0.5}$	π-$\pi_{0.5}$
Theor. Wert	0.500	0.379	0.220	1.138	0.860	0.500
$\bar{D}_0$ (μm)	0.550 $\pm$ 0.025	0.402 $\pm$ 0.017	0.248 $\pm$ 0.009	1.107 $\pm$ 0.047	0.812 $\pm$ 0.032	0.502 $\pm$ 0.016
$\bar{\delta}_0/\sqrt{2}$ (μm)	0.584 $\pm$ 0.027	0.448 $\pm$ 0.019	0.271 $\pm$ 0.010	1.153 $\pm$ 0.050	0.851 $\pm$ 0.034	0.526 $\pm$ 0.018

Mittelwerte der echten Streuung eliminiert zwischen einfacher und doppelter Zellengröße. Zweite Differenzen: $\bar{D}_0$; dritte Differenzen: $\bar{\delta}_0$.
P-$P_{0.5}$ bedeutet Protonenspur mit $P_{0.5}$ Schema vermessen
P-$\tau_{0.5}$ bedeutet Protonenspur mit $\tau_{0.5}$ Schema vermessen, usw.

[4] K. Gottstein: *Nuovo Cimento*, **12**, 619 (1954).

die relativen Schwankungen im Mittel um $10 \div 25\,\%$ überschätzt sind. Dieser Effekt kann daher rühren, daß bei der Berechnung des Faktors 1.35 die Korrelation zwischen $\bar{D}_1$ und $\bar{D}_2$ nicht berücksichtigt wurde.

Zum Vergleich sind in Tab. I die theoretischen Werte angegeben, die nach Formel (1) zu erwarten sind.

In Tab. I*a* ist die unechte Streuung $n = \sqrt{\bar{D}_1^2 - D_0^2}$ mit der relativen statistischen Schwankung $\varepsilon = (\bar{D}_1^2/n^2)\cdot(1.55/\sqrt{N_{ges}})$ angegeben.

TABELLE I*a*.

P-$P_{0.5}$	P-$\tau_{0.5}$	P-$\pi_{0.5}$	π-$P_{0.5}$	π-$\tau_{0.5}$	π-$\pi_{0.5}$
0.12 ± 0.14	0.18 ± 0.05	0.16 ± 0.02	0.23 ± 0.30	0.33 ± 0.10	0.17 ± 0.06

Unechte Streuung der Protonen und π-Mesonen, jeweils mit $P_{0.5}$, $\tau_{0.5}$ und $\pi_{0.5}$ Schema vermessen.

Es zeigt sich zunächst bei den π-Mesonen eine Übereinstimmung mit den theoretischen Werten für alle Schemata. Bei den Protonen jedoch tritt eine systematische Abweichung von $6 \div 13\,\%$ auf, die außerhalb der Fehlergrenzen liegt. In Abb. 2 sind die Verteilungen der $\bar{D}_0$ für Protonen wiedergegeben. Die drei als Deuteronen oder Tritonen hierdurch identifizierbaren Spuren sind schraffiert eingezeichnet.

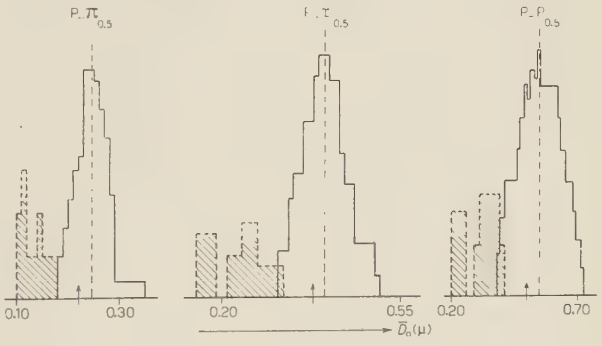

Abb. 2. – Verteilung der Werte D_0 der echten Streuung für Protonen mit $\pi_{0.5}$, $\tau_{0.5}$ und $P_{0.5}$ Schemata gemessen. Die Pfeile stellen die nach Gl. (1) zu erwartenden Werte dar. Drei Deuteronen oder Tritonen sind schraffiert eingezeichnet.

3. – Diskussion möglicher Fehlerquellen.

3·1. – *Verzerrung.* – Es besteht nun die Aufgabe, diese systematischen Abweichungen zu deuten. Es ist unwahrscheinlich, daß der bei der Berechnung der Schemata verwendete Wert der Streukonstante, der sich aus der Molière-

schen Theorie ergibt, für Protonen um $5 \div 10\,\%$ zu niedrig ist, zumal die gleichen Schemata, auf π-Mesonen angewendet, keine merklichen Abweichungen liefern. Vielmehr könnte man eine zusätzliche unechte Streuung vermuten, die durch das übliche Verfahren nicht miteliminiert wird, und u.a. von Schema und «Signal» (echte Streuung) abhängt.

Als erstes wurde untersucht, wie groß die Beiträge der Emulsionsverzerrung zur unechten Streuung waren. Dazu wurden die dritten Differenzen δ_0 gebildet, wodurch bekanntlich die C-förmigen Verzerrungen eliminiert werden können. Die aus einfacher und doppelter Zellengröße gewonnenen Mittelwerte voneinander unabhängiger dritter Differenzen wurde durch $\sqrt{2}$ geteilt, um einen Vergleich mit $\overline{D}_0$ zu ermöglichen. Die Resultate sind ebenfalls in Tab. I angegeben. Man erkennt, daß die C-förmigen Verzerrungen keine wesentliche Rolle spielen. Die aus dritten Differenzen errechneten Werte von D_0 sind systematisch größer als die der zweiten. Dieser Effekt, wenn auch innerhalb der statistischen Schwankungen, wurde gelegentlich auch von anderen Autoren [5] beobachtet, und ist auf das Abschneideverfahren zurückzuführen.

3·2. – *Der Größenunterschied benachbarter Zellen.* – Es wurde versucht, die Ursache der Abweichungen zunächst in der Art und Weise zu finden, wie die Messungen durchgeführt und ausgewertet wurden. Zwei Möglichkeiten bieten sich unmittelbar:

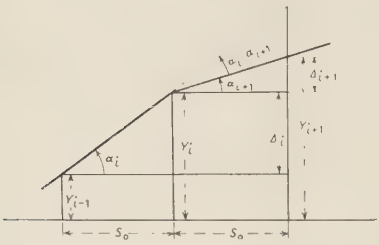

Abb. 3.

Erstens kann eine unechte Streuung dadurch entstehen, daß die tatsächlich benutzten Zellengrößen nicht mit den vorgeschriebenen identisch sind, sondern wegen der Einstellungenauigkeit um diese Werte streuen; zweitens muß bei der Berechnung der zweiten Differenzen die Tatsache berücksichtigt werden, daß zwei aufeinanderfolgende Zellen meistens verschiedene Länge haben, besonders bei kleinen Reichweiten.

Der Einfluß des Einstellfehlers kann folgendermaßen abgeschätzt werden: Zunächst betrachten wir eine konstante Zellengröße s_0. Unter der Voraussetzung, daß die wirklich am Mikroskoptisch eingestellte Zellenlänge mit einer quadratischen Abweichung σ um s_0 streut, geht aus Abb. 3 hervor, daß dadurch die ersten Differenzen Δ_i mit einer Streuung $\sigma(\Delta_i) \cong \sigma \cdot \alpha_i$ behaftet sind. In den zweiten Differenzen D_i wirkt sich also die Einstellungenauigkeit mit einer quadratischen Abweichung $\sigma(D_i) = \sigma \cdot \sqrt{\alpha_i^2 + \overline{\alpha_{i+1}^2}} = \sigma \cdot \sqrt{2\bar{\alpha}_i^2 + D_i^2/2s_0^2}$ ($\bar{\alpha}_i = (\alpha_i + \alpha_{i+1})/2$ mittlere Neigung der Spur bei den Zellen i und $i+1$) aus.

[5] M. Di Corato, D. Hirschberg and B. Locatelli: *Suppl. Nuovo Cimento*, 12, 381 (1954).

Nimmt man an, daß die Neigung der Spur über hinreichend viele Zellen nahezu konstant ist, und nähert man die Verteilung der 2. Differenzen durch eine Gaußverteilung der Breite $\sigma = \overline{D}\sqrt{\pi/2}$ an, erhält man für den Beitrag des Einstellfehlers zur unechten Streuung:

$$u_E^2 = \frac{4}{\pi}\sigma^2\overline{\alpha^2} + \frac{\sigma^2 D^2}{2s_0^2}$$

wobei $\overline{\alpha^2}$ die mittlere quadratische Neigung der Spur ist. Für eine variable Zellenlänge steht in 2. Summand $\overline{1/s^2}$.

Der erste Summand verbindet den Einstellfehler mit dem Ausrichtefehler ($\alpha = 0$ bedeutet, daß die Spur der Tischbewegung parallel ausgerichtet ist), der 2. Summand beschreibt den Einfluß des Einstellfehlers auf die Verteilung der 2. Differenzen. σ wurde experimentell bestimmt und ist von der Größenordnung 1 μm. Die Größenordnung der beiden Summanden ist für Protonen etwa $(0.05\ \mu m)^2$ und $(0.02\ \mu m)^2$. Der zweite Summand ist deshalb zu vernachlässigen. Der erste Summand wächst bei der rechnerischen Verdopplung der Zellengröße, fällt deshalb bei der Eliminierung der unechten Streuung nach (2) nicht heraus. Zu σ können aber außer dem experimentellen Einstellfehler auch systematische Fehler beitragen, die von dem Schema abhängen, wie z.B. die Aufrundung der Zellengrößen auf ganzzahlige Werte. Die Größenordnung dieser Beiträge zur unechten Streuung dürfte aber auch kaum den Wert 0.05 μm überschreiten, sodaß der Einstell- und Ausrichtefehler höchstens mit insgesamt $u = 0.07 \div 0.08$ μm beisteuern kann.

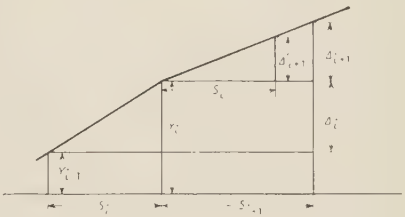

Abb. 4.

Zur Berücksichtigung der Unterschiedlichkeit zweier benachbarter Zellen, sei anhand von Abb. 4 gezeigt, daß die 2. Differenzen in besserer Näherung durch $D_i' = \Delta_{i+1}' \cdot \Delta_i = \Delta_i(s_i/s_{i+1}) - \Delta_i$ gegeben sind. Die in üblicher Weise errechneten 2. Differenzen D_i wären also zu korrigieren: $D_i' = D_i - \Delta_{i+1} \cdot ((s_{i+1} - s_i)/s_{i+1})$. Hieraus erkennt man sofort, daß diese Korrektur erstens relativ umso mehr ins Gewicht fällt, je kleiner D ist; zweitens umso größer ist, je schlechter ausgerichtet die Spur ist (große Δ_{i+1}); drittens für jedes Schema mit zunehmender Reichweite abnimmt; und viertens für das $P_{0.5}$ Schema größer als für das $\tau_{0.5}$ Schema und für dieses wiederum größer als für das $\pi_{0.5}$ Schema ist. Außerdem fällt sie für doppelte Zellengröße wesentlich größer aus, als für einfache. Ihre Vernachlässigung kann also zu einer unechten Streuung führen, die nicht nach (2) eliminiert wird. Die Einführung dieser Korrektur ist mit langwierigen Rechnungen verbunden. Sie wurde deshalb nur

angewendet für die ersten 1000 μm von Protonenspuren, die mit dem Protonen-Schema vermessen worden waren. Es ergaben sich folgende Mittelwerte:

	$\overline{D}_1(\mu m)$	$\overline{D}_2/\sqrt{8}(\mu m)$
ohne Korrektur	0.651 ± 0.030	0.558 ± 0.038
mit Korrektur	0.628 ± 0.029	0.540 ± 0.037

Wenn diese Korrektur auch ziemlich wesentlich im Fall einer größeren Statistik sein dürfte, so reicht sie hier nicht aus, um den Effekt quantitativ zu erklären. Außerdem sollte diese umständliche Korrektur auf jeden Fall umgangen werden, weil sie die Methode erheblich komplizieren würde.

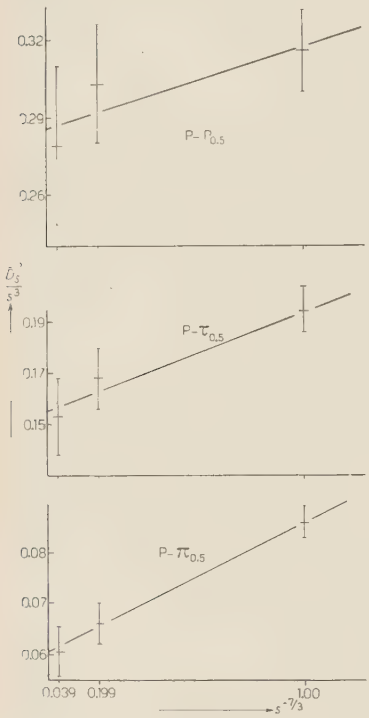

Abb. 5. – Zur graphischen Bestimmung der echten (D_0) und unechten (n_0) Streuung für Protonen aus einfacher ($s^{-7/3}=1$), doppelter ($s^{-7/3}=0{,}199$) und vierfacher ($s^{-7/3}=0{,}039$) Zellengröße, unter Annahme der Gültigkeit der Relation $\overline{D}_s^2/s^3 = D_0^2 + n_0^2 s^{-7/3}$.

3·3. – *Das Verfahren zur Eliminierung von unechter Streuung.* – Es sollen nun im Folgenden die möglichen Quellen eines systematischen Fehlers in der Eliminierung der unechten Streuung nach (2) untersucht werden. Zu diesem Zweck wurden zunächst für die Protonenspuren die 2. Differenzen bei vierfacher Zellengröße D_4 bestimmt und aus den Mittelwerten der D_1, D_2 und D_4 über alle Spuren die unechte Streuung graphisch eliminiert. Trägt man $\overline{D}_s^2/s^3$ als Funktion von $s^{-(7/3)}$ auf (Abb. 5), so sollen die Werte wegen $\overline{D}_s^2/s^3 = \overline{D}_0^2 + n_0^2 s^{-(7/3)}$ auf einer Geraden liegen. Die in Abb. 5 angegebenen Schwankungen ($0.76/\sqrt{N}$, wobei N die Gesamtzahl der unabhängigen Zellen ist) stellen obere Grenzen dar, da die Korrelation zwischen D_1, D_2 und D_4 nicht berücksichtigt wurde. Man erhält für D_0 und n_0 die Werte der Tab. II.

Eine systematische Abweichung bleibt also weiterhin erhalten. Anhand der Abb. 5 ist es auch nicht möglich zu entscheiden, ob der Ausdruck (3) mit $a = 2/3$ die Abhängigkeit der unechten Streuung von der Zellengröße annähernd richtig darstellt. (Dann müßten die 3 Punkte jeweils auf einer Geraden liegen.) Im Falle des π-Schemas trifft dies sicher zu; im τ- und P-Schema könnte man für a Werte von 1.5 bzw. $2 \div 2.5$ ansetzen, um die expe-

rimentellen D_0 näher an die theoretischen Werte zu rücken. Diese Werte für a sind jedoch überraschend groß, zumal sich der Einfluß, jedenfalls der C-förmigen Verzerrungen (die im Quadrat der unechten Streuung mit $\sim s^4$ eingehen) bereits als unwesentlich herausgestellt hat.

Tabelle II.

	P-$P_{0.5}$	P-$\tau_{0.5}$	P-$\pi_{0.5}$
D_0 (μm)	0.534 ± 0.015	0.396 ± 0.010	0.246 ± 0.008
n_0 (μm)	0.18 ± 0.04	0.20 ± 0.02	0.16 ± 0.01

Werte der echten (D_0) und unechten (n_0) Streuung für Protonen, graphisch aus Abb. 5 ermittelt.

Auf eine weitere Ursache für die systematischen Abweichungen deutet das häufige Auftreten von Spuren, bei denen $\bar{D}_0 > D_1$. Dieser Effekt tritt je nach Schema in bis zu 50% aller Spuren auf, sowohl bei Protonen als auch bei π-Mesonen. Für diese Spuren ist $\bar{D}_1^2 - (\bar{D}_2^2/8) = n_0^2(1 - 2^{a-3}) < 0$; $a \approx 2/3$. Berechnung der unechten Streuung n_0 ergibt also imaginäre Werte. In den Fällen, in denen das Quadrat der unechten Streuung klein ist gegenüber $\bar{D}_1^2$ sind Spuren mit «imaginärer unechter Streuung» auch theoretisch zu erwarten, wenn man die Schwankungen der $\bar{D}_1$ und $\bar{D}_2$ berücksichtigt. Für den Prozentsatz der Spuren mit imaginärem n_0 (bei denen also $D_1 - \bar{D}_2/\sqrt{8} < 0$ ist) gilt:

$$W_{\text{imag}}(\%) = 100\left[1 - \Phi\left(\frac{\bar{D}_1 - \bar{D}_2/\sqrt{8}}{\sqrt{2(\sigma_1^2 + \sigma_2^2)}}\right)\right]. \tag{4}$$

σ_1 und σ_2 sind die statistischen Schwankungen von $\bar{D}_1$ und $\bar{D}_2/\sqrt{8}$. Φ ist das Gaußsche Fehlerintegral. Tab. III zeigt trotz des großen Fehlers in der Bestimmung von W (> 100%), daß das Experiment erheblich mehr Spuren mit imaginärer unechter Streuung zu liefern scheint, als allein durch statistische Schwankungen zu erwarten ist. Es sieht also aus, als ob bei jenen Spuren tatsächlich $\bar{D}_1 < (\bar{D}_2/\sqrt{8})$ ist. Dies deutet auf eine zusätzliche unechte Streuung in der doppelten Zellengröße, die nicht durch (2) eliminiert wird.

Tabelle III.

	P-$P_{0.5}$	P-$\tau_{0.5}$	P-$\pi_{0.5}$	π-$P_{0.5}$	π-$\tau_{0.5}$	π-$\pi_{0.5}$
W berechnet (%)	33	4	0	34	6	8
W experimentell (%)	40	20	10	58	25	42

Prozentsatz der Spuren mit imaginärer unechter Streuung. «W berechnet» bedeuten die unter Anwendung der Formel (4) berechneten Prozentsätze, «W experimentell» die tatsächlich gefundenen.

Das Vorhergehende läßt vermuten, daß die Ursache für die systematischen Abweichungen der gemessenen Werte von D_0 von den theoretischen in der vereinfachten « Verdoppelung » der Zellengröße zu suchen ist. Diese « Verdoppelung », die lediglich aus dem Zusammenfügen je zweier benachbarter Zellen s_i und s_{i+1} zu einer neuen « doppelten » Zelle besteht, führt im Falle variabler Zellengrößen nicht zu $2s_i$, sondern zu einer größeren Zelle $2s_i(1+\varepsilon_i)$, wobei $\varepsilon_i = (s_{i+1} - s_i)/2s_i$. Schon allein dies bewirkt, daß der Anteil der echten Streuung in $\bar{D}_2$ um einen Faktor $1+(3/2)\bar{\varepsilon}_i$ zu groß ausfällt. Diese Korrektur ist zwar gering ($2 \div 5\,\%$ je nach Schema und Reichweite), größer ist aber eine damit verbundene, geometrische Korrektur für die zweiten Differenzen für doppelte Zellengröße $D_{2i} = (\Delta_{i+3} + \Delta_{i+2}) - (\Delta_{i+1} + \Delta_i)$. Deren Ausdruck sollte demnach lauten:

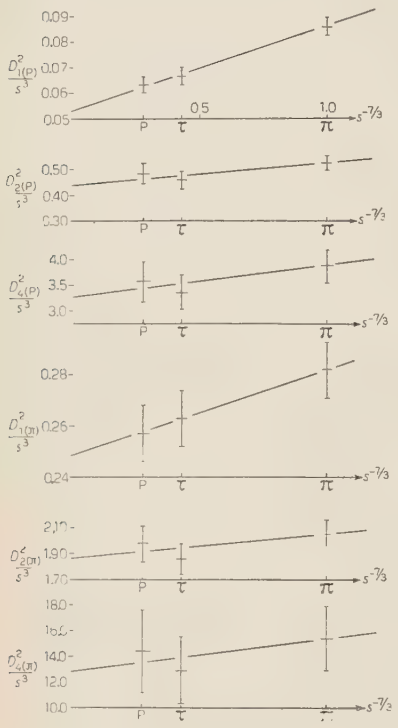

Abb. 6. – Zur graphischen Bestimmung der echten Streuung für das $\pi_{0,5}$-Schema und der unechten Streuung für einfache doppelte und vierfache Zellengröße bei Protonen und π-Mesonen. $\left[s_{\pi 0.5}^{-7/3} = 1;\ s_{\tau 0.5}^{-7/3} = 0.435;\ s_{\mathrm{p}0.5}^{-7/3} = 0.286\right]$.

$$(5) \qquad D'_{2i} = \left(\Delta_{i+3}\frac{s_{i+2}}{s_{i+3}} + \Delta_{i+2}\right)\frac{s_i}{s_{i+2}} - \left(\Delta_{i+1}\frac{s_i}{s_{i+1}} + \Delta_i\right).$$

(Die Ableitung verläuft ähnlich wie in § 3.2).

Durch eine Verdoppelung der Zellengröße im üblichen Sinn tritt eine zusätzliche unechte Streuung auf, die nicht durch Gl. (2) zu eliminieren ist. Die in § 2 angenommene Abhängigkeit der unechten Streuung $n^2 = n_0^2 s^{\frac{2}{3}}$ ist bei Zellenverdoppelung und Vervierfachung nicht mehr gültig.

Auf Grund der Tatsache, daß die Zellengrößen verschiedener Schemata bei gleicher Reichweite in einem bis auf $2 \div 3\,\%$ genau konstantem Verhältnis stehen ($s_\tau/s_\pi = 1.43$, $s_\mathrm{p}/s_\pi = 1.71$), wurde nun versucht, die unechte Streuung zwischen den verschiedenen Schemata zu eliminieren. Es soll nämlich für alle Schemata gelten:

$$D_1^2 = D_{01}^2 s^3 + n_1^2 s^{\frac{2}{3}}$$

$$D_2^2 = D_{02}^2 s^3 + n_2^2 s^{\frac{2}{3}}$$

$$D_4^2 = D_{04}^2 s^3 + n_4^2 s^{\frac{2}{3}}$$

s ist hier jeweils das Verhältnis s_τ/s_π, s_P/s_π (also $s=1$ für das π-Schema). Außerdem soll $D_{01}=D_{02}/\sqrt{8}=D_{04}/\sqrt{64}$ die echte Streuung im π-Mesonen Schema darstellen. n_1, n_2, n_4 sind die unechten Streuungen bei einfacher, doppelter und vierfacher Zellengröße, für die aber nach dem vorher Gesagten: $n_1^2 \neq n_2^2/2^{\frac{2}{3}} \neq n_4^2/4^{\frac{2}{3}}$ zu erwarten ist. In Abb. 6 wurde für Protonen und π-Mesonen D_1^2/s^3, D_2^2/s^3 und D_4^2/s^3 als Funktion von $s^{-(7/3)}$ aufgetragen. Man erhält daraus graphisch die Werte der Tab. IV.

TABELLE IV.

	D_{01}	D_{02}	$D_{02}/\sqrt{8}$	D_{04}	$D_{01}/\sqrt{64}$
Protonen	0.230 ± 0.008	0.662 ± 0.030	0.234 ± 0.010	1.81 ± 0.08	0.227 ± 0.012
π-Mesonen	0.498 ± 0.011	1.367 ± 0.043	0.484 ± 0.015	3.58 ± 0.04	0.45 ± 0.06

FORSETZUNG TABELLE IV.

	n_1	n_2	$n_2/2^{\frac{2}{3}}$	n_4	$n_4/4^{\frac{2}{3}}$
Protonen	0.18 ± 0.02	0.30 ± 0.06	0.24 ± 0.05	0.77 ± 0.15	0.49 ± 0.09
π-Mesonen	0.18 ± 0.01	0.44 ± 0.13	0.35 ± 0.10	$1.6\ \pm1.2$	$1.0\ \pm0.8$

Echte (D_0) und unechte Streuung (n) der Protonen und π-Mesonen für einfache, doppelte und vierfache Zellengröße, auf $\pi_{0.5}$-Schema reduziert, wie man sie graphisch aus Abb. 6 ermittelt.

Es ist zu erkennen, daß eine gute Übereinstimmung der Werte der echten Streuung bei einfacher, doppelter und vierfacher Zellengröße vorhanden ist. Bei der unechten Streuung hingegen sieht man sofort, daß sie bei Verdoppelung und Vervierfachung nicht nach dem Gesetz $n_0^2/s^{\frac{2}{3}}$ geht, sondern bei jedem Fall verschiedenen Werte für n_0 aufweist. Der Prozentsatz der Spuren mit «imaginärer» unechter Streuung ist jetzt geringer. Es handelt sich in diesem Fall um Spuren, bei denen $D_\pi - D_P/\sqrt{5.0} < 0$ ist. Bei der Elimination der unechten Streuung zwischen Protonen- und π-Mesonen Schema erhält man:

$$W_{\exp} = \begin{cases} 10\,\% \text{ für Protonenspuren} \\ 25\,\% \text{ für } \pi\text{-Mesonen}\,. \end{cases}$$

Bei den Protonen ist die Abweichung vom Sollwert geringfügig größer als der statistische Fehler: (0.230 ± 0.008 μm anstatt 0.220 μm). Infolge der ver-

schiedenen, in § 3·2 besprochenen Beiträge zur unechten Streuung, ist dies aber nicht unerwartet.

Die Werte der unechten Streuung in einfacher, doppelter und vierfacher Zellengröße für π-Mesonen stimmen innerhalb der großen Fehlergrenzen mit den genauer bestimmbaren Werten für Protonen überein.

Zum Schluß sei noch das aus den oben beschriebenen Messungen bestimmte Verhältnis D_1/n_1 (gemessene Streuung zu unechter Streuung) für die drei Schemata und für Protonen und π-Mesonen gegeben. (Tab. V).

Tabelle V.

	P-$P_{0.5}$	P-$\tau_{0.5}$	P-$\pi_{0.5}$	π-$P_{0.5}$	π-$\tau_{0.5}$	π-$\pi_{0.5}$
D_1/n_1	2.6	2.2	1.6	5.2	4.3	2.9

Verhältnis der D für einfache Zellen (Signal) zu unechter Streuung für Protonen und π-Mesonen für die Schemata $P_{0.5}$, $\tau_{0.5}$ und $\pi_{0.5}$.

4. – Schlußfolgerungen.

Aus dem Vorhergehenden ergeben sich einige Schlußfolgerungen für die zweckmäßige und korrekte Anwendung der Streumeßmethode mit variabler Zellengröße, für nicht sehr lange Spuren (bis etwa 5 mm) von Teilchen mit Massen oberhalb der π-Mesonenmasse.

a) Wenn man darauf Wert legt, daß die Größenordnung der systematischen Fehler 5% nicht übersteigt, ist es ratsam, in dem Verfahren zur Eliminierung der unechten Streuung die Unterschiede in der Länge benachbarter Zellen zu berücksichtigen.

b) In diesem Falle empfiehlt es sich, die unechte Streuung aus den Werten der D für zwei verschiedene Schemata zu eliminieren. Das setzt allerdings voraus, daß man eine Spur zweimal unabhängig vermessen muß, z.B. im π-Mesonen, und im Protonenschema (Tabelle IX und VI bei Fay *et al.* (loc. cit)). Die echte Streuung D_0 ergibt sich für diesen Fall aus der Formel

$$\bar{D}_0 = \sqrt{\frac{\bar{D}_P^2 - \bar{D}_\pi^2 (1{,}71)^a}{5{,}0 - (1{,}71)^a}}$$

Man kann das doppelte Vermessen jeder Spur auch vermeiden, indem man nach wie vor nach dem bisher üblichen Verfahren die Eliminierung der unechten Streuung aus einfacher und durch Zusammenfügen je zweier benach-

barter Zellen entstandener « doppelter » Zellengröße durchführt, und den bei dieser « Verdoppelung » gemachten Fehler durch eine Korrektur nach Formel (5) ausgleicht. Die Größe dieser Korrektur wird von der Ausrichtung der Spur, ihrer Länge, vom verwendeten Schema und der Masse des Teilches abhängen.

c) Wenn es nicht auf allzu große Genauigkeit ankommt, — z.B. bei kurzen Spuren —, genügt es, die Spur mit dem $P_{0.5}$ Schema zu vermessen und die unechte Streuung n_1 ($= 0.181 \pm 0.020$ μm) direkt von dem gemessenen D_1 quadratisch abzuziehen. Der Wert 0.18 scheint ziemlich unabhängig von dem Beobachter zu sein, und daher vom Instrument und von der Emulsion abzuhängen.

* * *

Den Herren Dr. K. Gottstein, H. M. Mayer und Dr. J. Roederer bin ich für wertvolle Diskussion und Hinweise zu aufrichtigem Dank verpflichtet. Ebenso möchte ich den Herren Prof. W. Heisenberg und K. Wirtz für die freundliche Aufnahme im Max-Planck-Institut für Physik Dank sagen. Die vorstehende Arbeit wurde im Rahmen eines Stipendiums der Comisión Nacional de la Energía Atómica gemacht; auch ihr möchte ich auf diesem Wege meinen herzlichsten Dank aussprechen.

RIASSUNTO (*)

Il metodo della saetta costante con l'impiego delle tabelle per le dimensioni della cella calcolate da Fay, Gottstein e Hain [1] è stato applicato a misure di scattering di 10 protoni con tracce piane identificati e 12 mesoni π nella regione dei percorsi brevi ($0 \div 5000$ μm). Applicando metodi usuali per l'eliminazione del disturbo, una deviazione sistematica dai valori teoricamente aspettati è stata osservata nel caso dei protoni. Sono state esaminate diverse cause di disturbo o di errori sistematici. La distorsione è risultata insignificante. Le alterazioni dei risultati causate da: 1) l'errore nella lettura della lunghezza della cella, 2) il difettoso allineamento della traccia rispetto alla direzione del moto del tavolino del microscopio, per quanto significanti non bastano a spiegare completamente la differenza sistematica. Si trova, tuttavia, che il metodo usuale seguito per calcolare le differenze seconde per la dimensione della cella doppia da quelle misurate nella cella standard non è applicabile senza restrizioni al metodo della saetta costante, perchè celle adiacenti spesso non sono uguali. Si propone di eliminare il disturbo sui percorsi brevi (fino a ~ 5 mm)

(*) *Traduzione a cura della Redazione.*

o con differenti schemi di celle, cioè misurando ogni particella due volte, o apportando opportune correzioni al metodo convenzionale per l'eliminazione del disturbo. La grandezza di tali correzioni dipenderà dall'allineamento e la lunghezza della traccia, dalla massa della particella e dallo schema seguìto. Misurando ogni particella in due schemi differenti, si ottiene un ottimo accordo coi valori forniti dalla formula

$$D_0 = 0{,}5(M_{\text{schema}}/M_{\text{particella}})^{0.4}{}_3$$

senza apportare alcuna correzione alla costante di scattering assunta da Fay *et al.*. Si dimostra che il livello di disturbo calcolato cresce rapidamente raddoppiando e quadruplicando la grandezza della cella.

LETTERE ALLA REDAZIONE

(La responsabilità scientifica degli scritti inseriti in questa rubrica è completamente lasciata dalla Direzione del periodico ai singoli autori)

On the Cosmological Implication of Galactic Magnetic Fields II (*).

R. L. BRAHMACHARY

Khaira Laboratory of Physics, Science College - Calcutta

(ricevuto il 16 Aprile 1955)

In the first part of our note (1) we obtained the equation

$$e^{-\lambda} = e^{\nu} = (1 + A/r + B/r^2)\,. \tag{1}$$

Assuming the conditions $t_1^1 = -t_2^2 = t_4^4$, $T_1^1 = -p = 0$; $T_4^4 = e = 0$, we find that the method of deducting the line-element as given by TOLMAN (2) is inapplicable in this case. We restrict ourselves to a discussion on the exterior and interior solutions of the line-element.

1. – For the «Exterior Solution» we have the condition

$$T_1^1 = T_2^2 = T_3^3 = -p = 0\,; \qquad t_\mu^\nu \neq 0$$

which enables us to set up a line-element of the form

$$\mathrm{d}s^2 = -e^{\lambda}\,\mathrm{d}r^2 - \ldots + e^{\nu}\,\mathrm{d}t^2 \tag{2}$$

together with the relation (1).

We have $A = -2m$, where m is the mass of the nebula. It is easy to compare our space-time with the De-Sitter universe.

We have (3)

(i) for De-Sitter universe

$$\mathrm{d}r/\mathrm{d}s = \pm\,(K^2 - 1 + r^2/R^2 - h^2/r^2 + h^2/R^2)$$
$$\mathrm{d}\varphi/\mathrm{d}s = h/r^2\,; \qquad \mathrm{d}t/\mathrm{d}s = K/(1 - r^2/R^2)$$

(*) DE SITTER: *in Memoriam.*
(1) R. L. BRAHMACHARY: *Nuovo Cimento* **1**, 953 (1955)
(2) R. C. TOLMAN: *Relativity, Thermodynamics and Cosmology* (1934), p. 243.
(3) R. C. TOLMAN: *ibid.*, p. 351.

and (ii) for the case treated here

$$\mathrm{d}r/\mathrm{d}s = \pm [K^2 - 1 - h^2/r^2 - (h^2/r^3)(A + B) - A/r - B/r^2]^{\frac{1}{2}}$$
$$\mathrm{d}\varphi/\mathrm{d}s = h/r^2 ; \qquad \mathrm{d}t/\mathrm{d}s = K/(1 + A/r + B/r^2)$$

we further find the relations

$$\mathrm{d}\varphi/\mathrm{d}t = h/Kr^2(1 + A/r + B/r^2)$$
$$\mathrm{d}r/\mathrm{d}t = \pm (\mathrm{d}r/\mathrm{d}s)(1 + A/r + B/r^2)(1/K) .$$

The singular surface at $r = m \pm \sqrt{m^2 - B}$ (as found from the equation $A/r + B/r^2 = -1$) is not encountered in outer space. There exists no « horizon » or « barrier » like that of the De-Sitter universe.
For a particle at rest,

$$\mathrm{d}r/\mathrm{d}s = 0 , \qquad \mathrm{d}\varphi/\mathrm{d}s = 0 , \qquad (\mathrm{d}t/\mathrm{d}s)^2 = (1 + A/r + B/r^2)^{-1} .$$

Hence we have

$$\mathrm{d}^2r/\mathrm{d}s^2 = \tfrac{1}{2}[A/r^2 + B/r^3] . \tag{3}$$

In De-Sitter universe we have

$$\mathrm{d}^2r/\mathrm{d}s^2 = \tfrac{1}{3}r/R^2 . \tag{3a}$$

For the displacement of spectral lines, we have the relation

$$t \propto 1/(1 + A/r^2 + B/r^3) .$$

For the case of purely radial motion we find the velocity of light to be

$$\mathrm{d}r/\mathrm{d}t = \pm (1 + A/r + B/r^2) . \tag{4}$$

While in the De-Sitter universe it is

$$\mathrm{d}r/\mathrm{d}t = \pm (1 - r^2/R^2) . \tag{4a}$$

2. – Interior Solution.

The region of space considered is filled with galactic matter or extragalactic dust. Thus $T_1^1 \neq 0$, $t_1^1 \neq 0$.

We then have

$$\begin{aligned} 8\pi\mathcal{T}_1^1 &= 8\pi T_1^1 + 8\pi t_1^1 \\ &= -8\pi p + C/r^4 \\ &= -e^{-\lambda}e^{-E}(-E'/r + 1/r^2) + 1/r^2 . \end{aligned} \tag{5}$$

Assuming $e^{-\lambda} = (1 - r^2/R^2)$ as in Einstein universe, we have from (5)

$$(e^{-E} r)' = 8\pi p r^2/(1 - r^2/R^2) - \frac{C}{(1 - r^2/R^2)} + \frac{1}{1 - r^2/R^2} .$$

Integrating, we obtain

$$e^{-E} = -8\pi p R^2 + C/r^2 + \left\{ \log \left| \frac{1 + r/R}{1 - r/R} \right| (K_1) \right\} \Big/ r + K_2/p , \tag{6}$$

where $K_2 = 4\pi p\alpha - C\beta/2 + \gamma$ and α, β, γ are constants of integration.

Here, for the displacement of spectral lines we have the equation

$$t = K_3 e^E \qquad \text{or} \qquad t \propto e^E .$$

3. – The relation (5) developed in the first part of our note [1] shows that in the non-static flat model of Einstein and De-Sitter [4], $g_{44} = f(t)$. While the general conditions of spherical symmetry allow the possibility

$$g_{11} = f(r, t) ; \qquad g_{44} = f(r, t)$$

the cosmological models treated up till now do not exhibit the property $g_{44} = f(t)$. Also all cosmological solutions (except that of De-Sitter) have the common property that in a sense space and time can be split up, thereby yielding an absolute time coordinate. This splitting up is no longer possible when $g_{\mu\nu} = f(r, t)$ $(\mu = 1, 2, 3)$ and $g_{44} = f(r, t)$

According to Godel [5] we may interpret this result (which follows from the existence of a magnetic pole) as a rotation.

---

[4] R. C. Tolman: *Relativity, Thermodynamics and Cosmology* (1934) p. 451.

[5] K Godel: *Rev. Mod. Phys.*, **21**, 447 (1949).

Remarks on Low-Energy Gamma-Radiation at Great Depths.

M. Mięsowicz, L. Jurkiewicz and J. M. Massalski

Laboratory of Nuclear Physics - Cracow
Institute of Physics, Polish Academy of Sciences

(ricevuto il 19 Maggio 1955)

M. Ageno, G. Cortellessa and R. Querzoli [1] describe, in the issue of this journal for 1st March, measurements with a scintillation counter performed in a laboratory at sea level, concerning some photon radiation of rather high intensity and of very low energies, with the energy spectrum having a distinct peak at about 100 keV. They consider this radiation as being due to cosmic radiation, and suggest the possibility that the low-energy γ-radiation observed by us in our measurements at great depths might also be of the same type. The purpose of this letter is to discuss the problem of the low-energy photon-radiation at great depths in connection with the suggestion of Ageno *et al.* [1].

The phenomenon which we have investigated at great depths underground was discovered by Barnóthy and Forró [2-4]. They found that at a depth 1000 m w.e. more double coincidences than threefold ones (in the same solid angle) were registered in the G.M.-counter-telescope. They also found that the radiation causing this excess of double coincidences is isotropic. They tried to connect this radiation with the cosmic radiation penetrating to that depth.

We confirmed these observations in our measurements at 540 and 660 m w.e. [5,6] and after the estimation of the efficiency of the telescope for registering coincidences due to low-ionizing radiation, and the measurement of its absorption in lead, we suggested that the effect mentioned above might be due to photons of energies of about 1 MeV, deriving from the radioactive contaminations of the surroundings.

This suggestion has been proved by two of us (M. M. and J. M. M.) [7] in the following way. It has been found that the intensity of this low-ionizing radiation is entirely independent of the

[1] M. Ageno, G. Cortellessa and R. Querzoli *Nuovo Cimento*, **1**, 453 (1955).

[2] J. Barnóthy and M. Forró: *Phys. Rev.*, **55**, 870 (1939).

[3] J. Barnóthy and M. Forró: *Symposium on Cosmic Rays, Kraków* (October 1947).

[4] J. Barnóthy and M. Forró: *Phys. Rev.*, **74**, 1300 (1948).

[5] M. Mięsowicz, L. Jurkiewicz and J. M. Massalski: *Acta Phys. Pol.*, **10**, 69 (1950).

[6] M. Mięsowicz, L. Jurkiewicz and J. M. Massalski: *Phys. Rev.*, **77**, 380 (1950).

[7] M. Mięsowicz and J. M. Massalski: *Acta Phys. Pol.*, **10**, 274 (1950).

intensity of the cosmic radiation, which is a known function of the depth. The intensity of this low-ionizing radiation has been found proportional to the intensity of the local γ-radiation (see Table I), which has been separately registered by means of a single G.M.-counter. The intensity of the local γ-radiation, on the other hand, is defined by the chemical composition of the geological layers where the measurements were made. Because of the changes of the geological layers from place to place the intensity of the local γ-radiation at the same depth in the mine varies within wide limits. We found at the same depth of 313 m w.e. two places 15 m apart, differing in their geological aspect, and their local γ-ray intensity. One of these two places is surrounded by silt and the other by rock-salt. There have been found in these two places different values for the intensity of the low-ionizing radiation giving the excess of the double coincidences over threefold ones. Table I shows the results of our measurements at different depths underground.

The intensity of the local γ-radiation is proportional to the number N given in column 6 of Table I, N being the rate of pulses (per minute) in a single counter caused by γ-radiation of the surroundings. It has been got by subtracting the rate of pulses due to its background and the rate of pulses due to the ionizing component of the cosmic radiation from the observed rate of pulses in this counter. As is seen from Table I (column 7) there is a proportionality between the rate of coincidences caused by low-ionizing radiation and the rate of pulses due to local γ-radiation, but it is not possible to find any proportionality between the rate of coincidences caused by low-ionizing radiation and the rate of coincidences due to cosmic rays (see column 8 of Table I).

Table I.

Depth m w.e.	Surroundings	Threefold coincidences T/h	Double coincidences D/h	$A = D - T$ per hour	Number of pulses above the background N/min	$A/N \cdot 10^2$	A/T
145	silt	42.2 $\pm$0.5	45.3 $\pm$0.5	3.1 $\pm$0.15	301 $\pm$5.5	1.03	0.073
220	rock-salt	16.3 $\pm$0.5	17.1 $\pm$0.5	0.8 $\pm$0.1	301 $\pm$5.5	0.96	0.049
313	»	8.5 $\pm$0.4	10.2 $\pm$0.4	1.7 $\pm$0.2	153 $\pm$6	1.11	0.20
313	silt	8.2 $\pm$0.4	14.3 $\pm$0.5	6.1 $\pm$0.3	543 $\pm$4.5	1.12	0.74
415	rock-salt	3.78 $\pm$0.3	4.65 $\pm$0.2	0.87 $\pm$0.1	99 $\pm$3	0.88	0.23
545	»	1.94 $\pm$0.07	2.70 $\pm$0.1	0.76 $\pm$0.05	82 $\pm$3.6	0.93	0.39
660	»	1.38 $\pm$0.06	1.91 $\pm$0.1	0.53 $\pm$0.04	51 $\pm$3	1.04	0.38

We suggested the following mechanism of registering the double coincidences caused by this radiation in our telescope. The γ-photon going through the first counter discharges it by a Compton electron, and the scattered photon discharges the second counter in the usual way. This mechanism was investigated by Gierula [8] and by Barnóthy and Forró [9]. In the experiments of Gie-

[8] J. Gierula: *Acta Phys. Pol.*, **11**, 36 (1950).

[9] J. Barnóthy and M. Forró: *Midwest Cosmic Ray Group Meeting* (Ann Arbor, 1950).

RULA, carried out in our laboratory, a beam of collimated γ-rays fell on one G.M.-counter and the scattered radiation on a second. The coincidences of pulses from these two counters were recorded. GIERULA investigated the angular dependence of these Compton-coincidences. Integrating the angular distribution of this effect for an isotropic γ-radiation he got a result which might be compared with that which we observed in the mine. In this way GIERULA has demonstrated that there exists an agreement between the efficiency of the telescope registering the double coincidences in the mine and the efficiency of a similar telescope registering the Compton-coincidences due to the γ-radiation emitted by natural radioactive substances.

The Compton-coincidences caused by local γ-radiation must be looked upon as very rare events which are difficult to detect with a G.M.-counter-telescope in a laboratory at ground level, because of the high background of coincidences due to cosmic rays, especially the accidental coincidences. The occurence of these coincidences deep underground is explained by the fact that the rate of accidental coincidences decreases in proportion to the square of the rate of pulses in a single counter, whereas, the rate of Compton-coincidences decreases only in proportion to the first power of the former.

It is also interesting to compare the intensity of the low-energy γ-ray photons recorded in our underground experiments with the intensity of the vertical ionizing cosmic radiation. Taking the efficiency of our counter telescope for registering γ-ray photons of the energy ~ 1 MeV as equal to c. 10^{-5} we get, for the depth of 660 m w.e., c. $4 \cdot 10^5$ quanta per one ionizing cosmic ray particle (in the same solid angle). For photons of energies of 100 keV this number should be still higher because of the lower value of the efficiency for registering them in our telescope. We can compare this figure with that given by AGENO *et al.* –100 quanta per one ionizing cosmic-ray particle.

All these arguments support our former assumption that the photon radiation investigated by us at great depths must be considered as γ-radiation of local origin. This conclusion has been also confirmed by BOLLINGER ([10]) and by RANDALL *et al.* ([11]).

([10]) L. M. BOLLINGER: *Phys. Rev.*, **79**, 207 (1950).

([11]) C. A. RANDALL, N. SHERMAN and W. R. HAZEN: *Phys. Rev.*, **79**, 905 (1950).

Perturbative Expansions.

E. R. Caianiello (*)

CERN Theoretical Study Division - Copenhagen

(ricevuto il 23 Maggio 1955)

We have given, previously, the explicit perturbative expansion of any element of the U-matrix pertaining to a field theory of the type usually envisaged, and, equivalently, that of the corresponding kernel (1). We record here some additional results which complete those already reported, both for future reference and because they may be useful in expediting calculations. The notation is that established in II.

1. – It was shown in II that, for all purposes, it suffices to know the expansions of the purely fermionic kernels, which are given by:

$$(1) \qquad K_{N_0} = K\begin{pmatrix} x_1 \dots x_{N_0} \\ y_1 \dots y_{N_0} \end{pmatrix} = \sum_{n=0}^{\infty} \frac{\lambda^{2n}}{(2n)!} \int \sum \gamma^1 \dots \gamma^{2n} [\xi_1 \dots \xi_{2n}] \begin{pmatrix} x_1 \dots x_{N_0} \; \xi_1 \dots \xi_{2n} \\ y_1 \dots y_{N_0} \; \xi_1 \dots \xi_{2n} \end{pmatrix};$$

or, if the orders of the integrations can be freely exchanged, more simply by:

$$(2) \qquad K\begin{pmatrix} x_1 \dots x_{N_0} \\ y_1 \dots y_{N_0} \end{pmatrix} = \sum_{n=0}^{\infty} \left(\frac{\lambda^2}{2}\right)^n \frac{1}{n!} \int \sum \gamma^1 \dots \gamma^{2n} [\xi_1 \xi_2] \dots [\xi_{2n-1} \xi_{2n}] \begin{pmatrix} x_1 \dots x_{N_0} \; \xi_1 \dots \xi_{2n} \\ y_1 \dots y_{N_0} \; \xi_1 \dots \xi_{2n} \end{pmatrix}.$$

Both expressions have the advantage of maximum formal simplicity, and the disadvantage of expressing kernels which are *not* normalized to unity vacuum-vacuum transition amplitude. This means, of course, that in actual computation one finds, on expanding, say, the determinants of (2), increasingly many uninteresting vacuum-vacuum fluctuation terms, to be dropped on inspection. It is desirable, therefore, to know some simple rule which may avoid automatically the appearence of such terms, yielding directly the expansion of any *normalized* kernel $G_{N_0} = K_{N_0}/K_{N_0=0}$. This task, which would be next to hopeless if one knew only the expansions (1) or (2), becomes easily feasible if one takes as starting point the branching equations (II.51) (or, equivalently, (II.52)). It follows then, indeed, that the branching equations

(*) On leave from Scuola di Perfezionamento in Fisica Nucleare - Roma.

(1) E. R. Caianiello: *Nuovo Cimento*, **10**, 1634 (1953) and **11**, 492 (1954); referred to as I and II.

for the normalized kernels can be written as:

$$(3)\qquad G\begin{pmatrix} x_1 \dots x_{N_0} \\ y_1 \dots y_{N_0} \end{pmatrix} = \sum_{h=1}^{N_0} (-1)^{h-1}(x_1 y_h)\, G\begin{pmatrix} x_2 \dots x_h \quad x_{h+1} \dots x_{N_0} \\ y_1 \dots y_{h-1}\ y_{h+1} \dots y_{N_0} \end{pmatrix} + \\ + (-1)^{N_0}\lambda^2 \int\!\!\int \sum_{1,2} \mathrm{d}\xi_1\, \mathrm{d}\xi_2\, \gamma^1\gamma^2(x_1\xi_1)[\xi_1\xi_2]\, G\begin{pmatrix} x_2 \dots x_{N_0} \quad \xi_1\xi_2 \\ y_1 \dots y_{N_0-1}\ y_{N_0}\xi_2 \end{pmatrix},$$

where now, of course, $G_0 = 1$. On setting

$$G_{N_0} = \sum_{p=0}^{\infty} G_{N_0}^{(p)} \lambda^{2p}; \qquad G_{N_0}^{(p)} = G^{(p)}\begin{pmatrix} x_1 \dots x_{N_0} \\ y_1 \dots y_{N_0} \end{pmatrix},$$

one has for the coefficients $G_{N_0}^{(p)}$ the recursion formulae:

$$(4)\qquad G^{(p)}\begin{pmatrix} x_1 \dots x_{N_0} \\ y_1 \dots y_{N_0} \end{pmatrix} = \sum_{h=1}^{N_0} (-1)^{h-1}(x_1 x_h)\, G^{(p)}\begin{pmatrix} x_2 \dots x_h \quad x_{h+1} \dots x_{N_0} \\ y_1 \dots y_{h-1}\ y_{h+1} \dots y_{N_0} \end{pmatrix} + \\ + (-1)^{N_0} \int\!\!\int \sum_{1,2} \mathrm{d}\xi_1\, \mathrm{d}\xi_2\, \gamma^1\gamma^2(x_1\xi_1)[\xi_1\xi_2]\, G^{(p-1)}\begin{pmatrix} x_2 \dots x_{N_0} \quad \xi_1\xi_2 \\ y_1 \dots y_{N_0-1}\ y_{N_0}\xi_2 \end{pmatrix}.$$

Introduce now the symbol:

$$(5)\qquad \begin{pmatrix} x_1 \dots x_{N_0} \\ y_1 \dots y_{N_0} \end{pmatrix} \begin{vmatrix} \xi_1\xi_2 \\ \xi_1\xi_2 \end{vmatrix} \begin{vmatrix} \xi_3\xi_4 \\ \xi_3\xi_4 \end{vmatrix} \dots \begin{vmatrix} \xi_{2p-1}\xi_{2p} \\ \xi_{2p-1}\xi_{2p} \end{vmatrix} = \\ = \sum_{h=1}^{N_0} (-1)^{h-1}(x_1 y_h) \begin{pmatrix} x_2 \dots x_h \quad y_{h+1} \dots x_{N_0} \\ y_1 \dots y_{h-1}\ y_{h+1} \dots y_{N_0} \end{pmatrix} \begin{vmatrix} \xi_1\xi_2 \\ \xi_1\xi_2 \end{vmatrix} \dots \begin{vmatrix} \xi_{2p1}-\xi_{2p} \\ \xi_{2p-1}\xi_{2p} \end{vmatrix} + \\ + (-1)^{N_0}(x_1\xi_1) \begin{pmatrix} x_2 \dots x_{N_0} \quad \xi_1\xi_2 \\ y_1 \dots y_{N_0-1} y_{N_0}\xi_2 \end{pmatrix} \begin{vmatrix} \xi_3\xi_4 \\ \xi_3\xi_4 \end{vmatrix} \dots \begin{vmatrix} \xi_{2p-1}\xi_{2p} \\ \xi_{2p-1}\xi_{2p} \end{vmatrix} \qquad (N_0 > 2)$$

$$(5')\qquad \begin{pmatrix} x_1 \\ y_1 \end{pmatrix} \begin{vmatrix} \xi_1\xi_2 \\ \xi_1\xi_2 \end{vmatrix} \begin{vmatrix} \xi_3\xi_4 \\ \xi_3\xi_4 \end{vmatrix} \dots \begin{vmatrix} \xi_{2p-1}\xi_{2p} \\ \xi_{2p-1}\xi_{2p} \end{vmatrix} = -(x_1\xi_1) \begin{pmatrix} \xi_1\xi_2 \\ y_1\xi_2 \end{pmatrix} \begin{vmatrix} \xi_3\xi_4 \\ \xi_3\xi_4 \end{vmatrix} \dots \begin{vmatrix} \xi_{2p-1}\xi_{2p} \\ \xi_{2p-1}\xi_{2p} \end{vmatrix} \qquad (N_0 = 1),$$

defined by (5) and (5′), the ultimate products of the reduction being determinants. It is then a straightforward matter to verify that the equations (4) are satisfied if, and only if:

$$(6)\qquad G\begin{pmatrix} x_1 \dots x_{N_0} \\ y_1 \dots y_{N_0} \end{pmatrix} = \sum_{p=0}^{\infty} \lambda^{2p} \int \sum \gamma^1 \dots \gamma^{2n}[\xi_1\xi_2] \dots [\xi_{2p-1}\xi_{2p}] \begin{pmatrix} x_1 \dots x_{N_0} \\ y_1 \dots y_{N_0} \end{pmatrix} \begin{vmatrix} \xi_1\xi_2 \\ \xi_1\xi_2 \end{vmatrix} \dots \begin{vmatrix} \xi_{2p-1}\xi_{2p} \\ \xi_{2p-1}\xi_{2p} \end{vmatrix}.$$

(6) is, thus, the desired expansion. The symbol (5), (5′)—which is, of course, expanded with greater ease than a determinant, since less terms are required, all other rules being the same—contains the prescription for the systematic dropping of the vacuum-vacuum terms in the simple form exhibited by the difference between (5) and (5′).

Interesting relations among the coefficients of (6) can be inferred from other

equations of II; consider, for instance, eq. (II.55):

$$\frac{\mathrm{d}}{\mathrm{d}(\lambda^2)} K\begin{pmatrix} x_1 \dots y_{N_0} \\ x_1 \dots y_{N_0} \end{pmatrix} = \frac{1}{2}\int\int \sum_{1,2} \mathrm{d}\xi_1 \mathrm{d}\xi_2 \gamma^1\gamma^2[\xi_1\xi_2] K\begin{pmatrix} x_1 \dots x_{N_0}\xi_1\xi_2 \\ y_1 \dots y_{N_0}\xi_1\xi_2 \end{pmatrix},$$

which becomes

$$(7) \qquad \frac{\mathrm{d}}{\mathrm{d}(\lambda^2)} G\begin{pmatrix} x_1 \dots x_{N_0} \\ y_1 \dots y_{N_0} \end{pmatrix} = \\ = \frac{1}{2}\int\int \sum_{1,2} \mathrm{d}\xi_1 \mathrm{d}\xi_2 \gamma^1\gamma^2[\xi_1\xi_2] \left\{ G\begin{pmatrix} x_1 \dots x_{N_0}\xi_1\xi_2 \\ y_1 \dots y_{N_0}\xi_1\xi_2 \end{pmatrix} - G\begin{pmatrix} x_1 \dots x_{N_0} \\ y_1 \dots y_{N_0} \end{pmatrix} \cdot G\begin{pmatrix} \xi_1\xi_2 \\ \xi_1\xi_2 \end{pmatrix} \right\}.$$

On expanding according to (6), one finds:

$$(8) \qquad 2pG^{(p)}\begin{pmatrix} x_1 \dots x_{N_0} \\ y_1 \dots y_{N_0} \end{pmatrix} = \\ = \int\int \sum_{1,2} \mathrm{d}\xi_1 \mathrm{d}\xi_2 \gamma^1\gamma^2[\xi_1\xi_2] \left\{ G^{(p-1)}\begin{pmatrix} x_1 \dots x_{N_0}\xi_1\xi_2 \\ y_1 \dots y_{N_0}\xi_1\xi_2 \end{pmatrix} - \sum_{h+k=p-1} G^{(h)}\begin{pmatrix} x_1 \dots x_{N_0} \\ y_1 \dots y_{N_0} \end{pmatrix} \cdot G^{(k)}\begin{pmatrix} \xi_1\xi_2 \\ \xi_1\xi_2 \end{pmatrix} \right\}.$$

This identity, which is by no means obvious a priori, can, of course, be verified by direct evaluation of both sides; it can be iterated at will, most simply by using the same procedure on higher derivatives of K_{N_0} and G_{N_0}.

As has been stated before, (6) is the counterpart of (2); in its derivation it is assumed implicitly that it is legitimate to exchange freely the orders in which the integrations are to be performed. This is certainly allowed in a theory where everything is convergent; it is, conceivably, also true after a renormalization has been carried out with the Dyson-Salam prescriptions: it is important, however, to realize that no ambiguities can ever occur for this reason if one works with the expansions (1). It is well known, indeed, that careless exchange of the order of integration, when dealing with improper or principal-value integrals, leads to wrong results *as a rule and not as an exception*, as is exemplified abundantly in the literature. (1), that is the expression one gets from straigthforward perturbation theory, cannot give rise to troubles of this sort, because all the integrands which appear in it are symmetric functions of their arguments, so that exchanges make no difference. There is no difficulty, though, in passing from (6) to its symmetrized version, which will correspond to (1): it suffices, simply, to replace each non-symmetric integrand with its symmetrizd form, before the integrations are carried out. This is quite obvious, if one reminds the methods followed to derive the results of I and II. The same caution, of course, must apply as well, in any quantitative treatment, to the equations given in II: a point, as relevant as it is simple, which shows that there is no need of postulating rules to resolve such ambiguities, since, in any case, reference to the correct expansions (1) will remove them. Proceeding in this manner one would find, for instance, that the linear divergent contributions to the electron self-energy cancel one another exactly to all orders, or that the photon self-energy vanishes (both well known results), in a direct and unambiguous way.

A quantity of particular interest is $\lg K_0$, because variational differentiations with respect to external fields and sources (which appear, in this formulation, in the

functions (xy) and $[xy]$) permit to derive from it kernels (different from those considered by us) which may find useful applications. Its perturbative expansion is immediately desumed from (II.55), on writing:

$$\frac{1}{K_0}\frac{\mathrm{d}K_0}{\mathrm{d}(\lambda^2)} = \frac{1}{2}\int\int \sum_{1,2} \mathrm{d}\xi_1 \mathrm{d}\xi_2 \gamma^1\gamma^2[\xi_1\xi_2] G\begin{pmatrix}\xi_1\xi_2\\ \xi_1\xi_2\end{pmatrix};$$

this yields

$$\lg K_0 = \sum_{p=1}^{\infty} \frac{\lambda^{2p}}{2p}\int \sum \gamma^1 \dots \gamma^{2p}[\xi_1\xi_2]\dots[\xi_{2p-1}\xi_{2p}]\begin{pmatrix}\xi_1\xi_2 & \xi_3\xi_4 & & \xi_{2p-1}\xi_{2p}\\ \xi_1\xi_2 & \xi_3\xi_4 & \dots & \xi_{2p-1}\xi_{2p}\end{pmatrix}. \tag{9}$$

Comparison of this expression with the familiar one of the Fredholm theory shows most clearly the structural difference between a one-field and a two-field theory.

2. – We touch here upon another point of more general interest. It is not known, at present, whether the expansions here represented have some region of convergence, or should rather be considered as asymptotic, or, worse, as completely devoid of meaning. It is therefore useful, in the hope of future advances of the theory, to obtain compact, though formal, expressions for their remainders, which may be eventually of help in deciding on these questions and in testing the validity of approximative methods. This aim can be achieved in a variety of ways, by using the techniques of II; we shall treat a few typical cases. By iterating (II.55) one finds the exact relation:

$$\frac{\mathrm{d}^n}{\mathrm{d}(\lambda^2)^n} K\begin{pmatrix}x_1 \dots x_{N_0}\\ y_1 \dots y_{N_0}\end{pmatrix} = \frac{1}{2^n}\int \sum \gamma^1 \dots \gamma^{2n}[\xi_1\xi_2]\dots[\xi_{2n-1}\xi_{2n}] K\begin{pmatrix}x_1 \dots x_{N_0}\xi_1 \dots \xi_{2n}\\ y_1 \dots y_{N_0}\xi_1 \dots \xi_{2n}\end{pmatrix}; \tag{10}$$

an equivalent expression is:

$$\frac{\mathrm{d}^n}{\mathrm{d}\lambda^n} K\begin{pmatrix}x_1 \dots x_{N_0}\\ y_1 \dots y_{N_0}\end{pmatrix} = \int \sum \gamma^1 \dots \gamma^n K\begin{pmatrix}x_1 \dots x_{N_0}\xi_1 \dots \xi_n & \\ y_1 \dots y_{N_0}\xi_1 \dots \xi_n & \xi_1 \dots \xi_n\end{pmatrix}. \tag{11}$$

These relations can be considered as equations for K_{N_0}, which are readily solved by using, again, the results of II. One finds, writing $K_{(\lambda)}$ to express the dependence of K on λ:

$$K_{(\lambda^2)}\begin{pmatrix}x_1 \dots x_{N_0}\\ y_1 \dots y_{N_0}\end{pmatrix} = \sum_{p=0}^{n-1}\left(\frac{\lambda^2}{2}\right)^p \frac{1}{p!}\int \sum \gamma^1 \dots \gamma^{2p}[\xi_1\xi_2]\dots[\xi_{2p-1}\xi_{2p}]\begin{pmatrix}x_1 \dots x_{N_0}\xi_1 \dots \xi_{2p}\\ y_1 \dots y_{N_0}\xi_1 \dots \xi_{2p}\end{pmatrix} + \tag{12}$$

$$- \int_0^{\lambda^2} \frac{(\lambda^2-\mu^2)^{n-1}}{(n-1)!}\,\mathrm{d}(\mu^2)\,\frac{1}{2^n}\int \sum \gamma^1 \dots \gamma^{2\mu}[\xi_1\xi_{2\mu}]\dots[\xi_{2n-1}\xi_{2n}] K_{(\mu^2)}\begin{pmatrix}x_1 \dots x_{N_0}\xi_1 \dots \xi_{2n}\\ y_1 \dots y_{N_0}\xi_1 \dots \xi_{2n}\end{pmatrix};$$

$$K_{(\lambda^2)}\begin{pmatrix}x_1 \dots x_{N_0}\\ y_1 \dots y_{N_0}\end{pmatrix} = \sum_{p=0}^{n-1}\left(\frac{\lambda^2}{2}\right)^p \frac{1}{p!}\int \sum \gamma^1 \dots \gamma^2[\xi_1\xi_2]\dots[\xi_{2p-1}\xi_{2p}]\begin{pmatrix}x_1 \dots x_{N_0}\xi_1 \dots \xi_{2p}\\ y_1 \dots y_{N_0}\xi_1 \dots \xi_{2p}\end{pmatrix} + \tag{13}$$

$$- \int_0^{\lambda} \frac{(\lambda-\mu)^{2n-1}}{(2n-1)!}\,\mathrm{d}\mu \int \sum \gamma^1 \dots \gamma^{2n} K_{(\mu)}\begin{pmatrix}x_1 \dots x_{N_0}\xi_1 \dots \xi_{2n} & \\ y_1 \dots y_{N_0}\xi_1 \dots \xi_{2n} & \xi_1 \dots \xi_{2n}\end{pmatrix}.$$

One can infer then without difficulty from (7) that similar, although less simple, expressions hold also for the normalized kernels G_{N_0}.

Finally, we record one more among the host of possible formal expansions, which is non-perturbative and may become of interest if the kernels $K(t_1 \dots t_{P_0})$ turn out to have a simpler structure than the purely fermionic kernels (the proof, which requires some lengthy algebra, is omitted in view of the intuitive character of the result):

$$K\begin{pmatrix} x \\ y \end{pmatrix} = \sum_{p=0}^{\infty} \lambda^p \int \sum \{(x\xi_1)\gamma^1(\xi_1\xi_2)\gamma^2 \dots (\xi_{p-1}\xi_p)\gamma^p(\xi_p y)\} K(\xi_1\xi_2 \dots \xi_p) . \tag{15}$$

3. – In conclusion, and as a justification for our laying so much stress on formal matters, we should like to mention a result, the proof of which will appear in a subsequent paper together with a fuller discussion: if convergence factors are introduced in the momentum expansions of the functions D^F and S^F (or, equivalently and perhaps more significantly, if one works in a lattice space depending upon some fundamental length), then all the series given here certainly converge within a finite range of values of λ (which depends, of course, in a non-renormalized theory, upon the parameters of the convergence factors). Such a thing is not trivial, because finiteness – which one would expect in this case – does by no means imply holomorphy: indeed, this result can only be proved to hold in the case of fermion-boson interactions, but not in the case of a four-fermion or of a quadratic boson-boson interaction.

Sulla radiazione gamma di bassa energia a grande profondità.

M. Ageno

Istituto Superiore di Sanità, Laboratorio di Fisica - Roma

(ricevuto il 25 Maggio 1955)

Nella lettera che precede, Mięsowicz, Jurkiewicz e Massalski [1] dimostrano che la radiazione γ di bassa energia osservata a grande profondità da Barnóthy e Forró [2,3] e da loro [4] non è, per lo meno per la maggior parte, secondaria della radiazione cosmica residua, ma di origine locale, dovuta a radioattività dei materiali circostanti. Essi prendono le mosse da una frase, effettivamente poco chiara, di un nostro lavoro [5], interpretandola nel senso che noi riproponessimo l'ipotesi di una connessione genetica tra i raggi γ di bassa energia da loro osservati e la radiazione cosmica.

In realtà, la nostra frase aveva un'altra intenzione e si riferiva esclusivamente al meccanismo della produzione di uno spettro di raggi γ di energia molto bassa (come quello da noi osservato), a partire dai loro primari. È noto che quando raggi γ di qualunque energia attraversano la materia, in un tratto equivalente a pochi cammini liberi medi per effetto Compton, si stabilisce uno spettro di equilibrio indipendente dallo spettro dei primari e dipendente solo dal numero atomico dei materiali attraversati. Il formarsi di questo spettro di equilibrio è stato studiato teoricamente da Fano e dai suoi collaboratori [6,10] e verificato sperimentalmente da Miss White [11] e da altri. In una serie di esperienze da noi eseguite lo scorso anno e che verranno particolareggiatamente descritte in un prossimo lavoro, noi abbiamo trovato chiara indicazione che la componente ultra-molle di Bernardini e Ferretti [12,13] si forma (con lo spettro da noi osservato) a partire da raggi γ

[1] M. Miesowicz, L. Jurkiewicz and J. M. Massalski: *Nuovo Cimento*, **2**, 152 (1955).

[2] J. Barnóthy and M. Forró: *Phys. Rev.*, **55**, 820 (1939).

[3] J. Barnóthy and M. Forró: *Phys. Rev.*, **74**, 1300 (1948).

[4] M. Miesowicz, L. Jurkiewicz and J. M. Massalski: *Phys. Rev.*, **77**, 380 (1950).

[5] M. Ageno, G. Cortellessa and R. Querzoli: *Nuovo Cimento*, **1**, 453 (1955).

[6] H. A. Bethe, U. Fano and P. R. Karr: *Phys. Rev.*, **76**, 538 (1949).

[7] U. Fano: *Phys. Rev.*, **76**, 739 (1949).

[8] P. R. Karr and J. C. Lamkin: *Phys. Rev.*, **76**, 1843 (1949).

[9] L. V. Spencer and F. Jenkins: *Phys. Rev.*, **76**, 1885 (1949).

[10] U. Fano, H. Hurwitz and L. V. Spencer: *Phys. Rev.*, **77**, 425 (1950).

[11] G. R. White: *Phys. Rev.*, **80**, 154 (1950).

[12] G. Bernardini and B. Ferretti: *Ric. Scient.*, **10** (1), 39 (1939).

[13] G. Bernardini and B. Ferretti: *Nuovo Cimento*, **7**, 173 (1939).

di energia più elevata presenti nella radiazione cosmica, con un meccanismo di questo genere. Era nostra intenzione suggerire un analogo meccanismo di formazione di una componente γ ultra-molle a grande profondità.

Noi accettiamo pertanto completamente le conclusioni di MIĘSOWICZ, JURKIEWICZ e MASSALSKI circa l'origine radioattiva dei loro raggi γ e riteniamo che anch'essi non avranno difficoltà ad accettare come ragionevole la ipotesi di una distribuzione spettrale del tipo di quella da noi osservata, e dovuta allo stesso meccanismo, studiato particolareggiatamente da FANO.

Cross Sections Near Threshold for Charged Photo-Pions from Deuterium.

D. Carlson-Lee, G. Stoppini and L. Tau

Istituto di Fisica dell'Università - Roma
Istituto Nazionale di Fisica Nucleare - Sezione di Roma

(ricevuto il 27 Maggio 1955)

The systematic study of the reactions

$$\gamma + \mathrm{D} \begin{matrix} \nearrow (\mathrm{n}, \mathrm{n}) + \pi^+ \\ \searrow (\mathrm{p}, \mathrm{p}) + \pi^- \end{matrix}$$

has been continued with the same experimental apparatus already described in a preceding work [1]. In the present experiment, however, the use of stripped emulsions rather than plates has permitted a direct determination of the differential cross-sections of the two single processes, in addition to the π^-/π^+ ratio. The same method has been adopted in the parallel experiment on the photoproduction of π^+ in hydrogen [2,3]. The pellicles, (Ilford G5, 500 μm) in groups of three exposed to the angles 45°, 75°, 105° and 150° in the laboratory system, were immersed in large blocks of emulsion so that the number of mesons which stopped in the pellicles was equal (up to rather high energies) to the number of mesons emitted in the solid angle since the out-scattering mesons were compensated by in-scattering mesons. The meson energies were deduced from the total range (corrected for loss of energy in the target, and cooling jacket) and the sign of the mesons was established by distinguishing the π–μ decays from the σ-stars according to the criteria followed in the preceding work; however, the possibility of following the secondaries into the adjacent emulsions permitted the separation of at least 98% of the doubtful cases, π–μ or σ_1 (classification σ) [1]. The pellicles were strongly underdeveloped to reduce the background, but this made it impossible to observe the decay electrons of the μ-mesons and thus to separate the σ_0 from the ρ class. Therefore the total number of π^- was calculated on the basis of the percentage A_0 of stars without ionizing prongs determined in the preceding work [1]. A strong internal check was given by the independent redetermination of the coefficients A_1, A_2, ..., which are in excellent agreement with the preceding values.

The results reported here were obtained by a partial examination of the

[1] M. Beneventano, D. Carlson-Lee, G. Stoppini, G. Bernardini and E. L. Goldwasser: *Nuovo Cimento*, **12**, 156 (1954).

[2] G. Bernardini and E. L. Goldwasser: *Phys. Rev.*, **95**, 857 (1954).

[3] To be published in *Nuovo Cimento*.

central pellicle at each angle. Two independent scannings in volume gave a total efficiency of about 99%, and the total number of mesons found was about 2 500. The data have been corrected for nuclear absorption, decay in flight, and background from the walls of the target, with a maximum correction of less than 10%.

For the calculation of the cross-sections, it has been assumed that the kinematical relation between the energy of the photon and that of the meson emitted is the same as that for the photoproduction of π^+ in hydrogen. This relation, according to the impulse approximation ([4,5]), holds on the average; the modification of the meson spectra due to the nucleon motion has been neglected because the photomeson cross-section does not depend critically upon the photon energy near the threshold.

In Table I are given the values of the cross-sections for the two processes. The errors indicated are only statistical. In the figure are shown the same values averaged over the entire photon energy interval (from ~ 175 to 200 MeV, $\bar{E}_\gamma = 188$ MeV). For comparison, in the same graph are given the cross-sections for the photoproduction of π^- in hydrogen at the same mean photon energy. Aside from an attenuation factor, the two π^+ angular distributions seem to be equal within the error limits. The mean attenuation factor between the two sets of values is $f = 0.81 \pm .04$.

TABLE I.

$(\mathrm{d}\sigma/\mathrm{d}\Omega)_{\mathrm{C.M.}}$ 10^{29} cm^2 (positive mesons)

$\bar{E}_\gamma$ (lab.) \ $\theta_{\mathrm{lab.}}$	45°	75°	105°	150°
180 MeV	.62 ± .07	.61 ± .06	.37 ± .06	—
188	.64 ± .07	.59 ± .06	.78 ± .08	.75 ± .10
196	.69 ± .08	.65 ± .07	1.09 ± .12	.84 ± .10
188 Avg.	.65 ± .04	.62 ± .04	.75 ± .05	—

$(\mathrm{d}\lambda/\mathrm{d}\Omega)_{\mathrm{C.M.}} \cdot 10^{29}$ cm^2 (negative mesons)

$\bar{E}_\gamma$ (lab.) \ $\theta_{\mathrm{lab.}}$	45°	75°	105°	150°
180 MeV	.71 ± .09	.82 ± .08	.86 ± .11	—
188	.89 ± .10	1.02 ± .10	1.17 ± .12	1.14 ± .14
196	.91 ± .11	1.05 ± .10	1.10 ± .12	1.42 ± .16
188 Avg.	.84 ± .06	.96 ± .05	1.04 ± .07	—

A rather straigthforward and significant interpretation can be found both for the similarity of the trend of the two curves and for the attenuation.

This is due to the competing reaction

$$\gamma + \mathrm{D} \rightarrow \mathrm{N} + \mathrm{P} \qquad (2)$$

which has been recently very thorougly investigated by A. H. O. HANSON and coworkers at Illinois and by KECK and TOLLESTRUP at Caltech (A. H. O. HAN-

([4]) G. F. CHEW and H. W. LEWIS: *Phys. Rev.*, **84**, 779 (1951).

([5]) M. LAX and H. FESHBACH: *Phys. Rev.*, **88**, 509 (1952).

son, invited paper at the Thanksgiving Meeting of the A.P.S. Chicago, November 1954; the authors are deeply indebted to Prof. Hanson for a private communication of his data, unfortunately not yet easily available). It has been found that in the region of interest, i.e. between 100 and 200 MeV the reaction (2) has a very slowly varying total cross-section. The value of this cross-section taken between 150 and 200 MeV is $(55 \pm 3) \cdot 10^{-30}$ cm². Considering the averaged value of the π^+/π^- ratio in this energy region given by Table II, i.e.

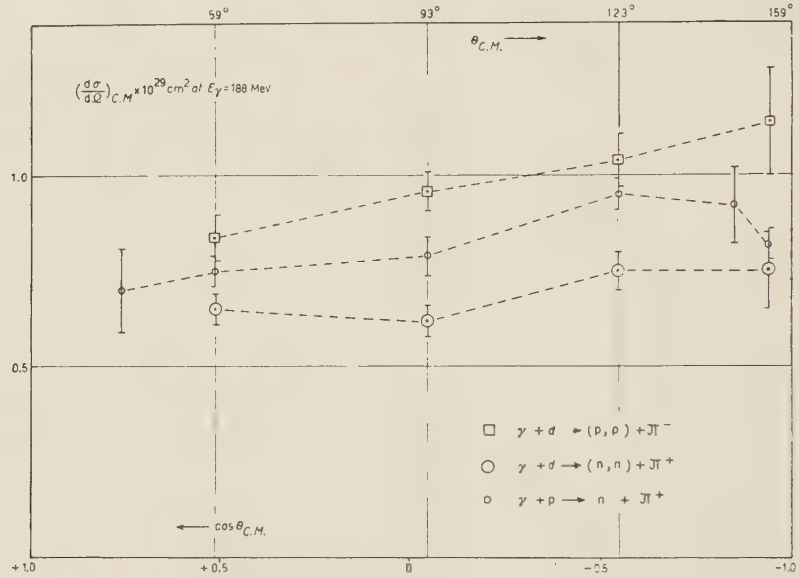

Fig. 1.

Table II.

$\theta_{lab.}$	$\bar{E}_\gamma$	$d\sigma(-)/d\sigma(+)$
45°	187	$1.26 \pm .11$
75°	186	$1.54 \pm .11$
105°	188	$1.43 \pm .13$
150°	200	$1.49 \pm .12$

$\sigma_-/\sigma_+ = 1.43 \pm .06$ and the total cross-section for pion-photoproduction in H in the same energy interval, i.e. $\sigma_H = (104 \pm 20) \cdot 10^{-30}$ cm² with the attenuation factors $f = .81$, one gets for the total photodisintegration cross-section

$$(1 - .81)(1 + 1.42)\sigma_H = (48 \pm 14) \cdot 10^{-30} \text{ cm}^2$$

in good agreement with Hanson's value. It should be noted that this summation property holds in a definite narrow energy interval.

Finally the parallelism of the π^+ angular distributions is in agreement with the result found at this energy for the photopion production in H, i.e., of a prevalent electric dipole absorption of the photon and subsequent S-wave emission of the meson. In this case, in fact, the attenuation at small angles due to the principle of Pauli is negligible ([4,5]).

* * *

It is really a pleasure to thank Prof. G. Bernardini, Prof. A. H. O. and Dr. R. Reitz for having devised and performed the exposure of the pellicles at the 300 MeV Betatron of the University of Illinois.

Sui conteggi dei gruppi di granuli nelle emulsioni nucleari.

I. Iori e A. Roveri

Istituto di Fisica dell'Università - Modena

(ricevuto il 28 Maggio 1955)

Inquadrando nella statistica di Bernoulli lo studio delle fluttuazioni nella distribuzione sia dei granuli singoli, che dei gruppi di granuli, lungo una traccia di particella ionizzante in una emulsione nucleare, sono state dedotte le formule seguenti per i rispettivi scarti quadratici medi [1].

Per i conteggi di granuli singoli:

$$(1) \qquad \sigma_v^2 = np(1-p) = \\ = \nu(1-p) = \nu(1-\nu\, d/L)$$

e per i conteggi di gruppi di granuli:

$$(2) \qquad \sigma_a^2 = a(1-3a/n) = (1-ad/L)\,,$$

essendo n il numero di posti, occupabili ciascuno da un granulo sviluppato, nel quale si pensa, schematicamente, suddiviso, senza soluzione di continuità, un tratto di traccia di lunghezza L (cella), $d=L/n$ il diametro (medio) del granulo sviluppato, p la probabilità per l'evento « granulo sviluppato » in conseguenza del passaggio della particella ionizzante, ν il numero medio di granuli sviluppati in una cella:

$$(3) \qquad \nu = np$$

ed a il numero medio di gruppi di granuli in una cella:

$$(4) \qquad a = np(1-p)\,.$$

Gli scarti quadratici medi σ_ν, σ_a si riferiscono ad un conteggio singolo, del numero di granuli, o di gruppi, in una cella.

Diamo qui i risultati sperimentali dei conteggi di granuli singoli e dei gruppi di granuli effettuati per controllare la validità di impiego delle formule in questione, a complemento dei risultati preliminari già resi noti [1].

I conteggi sono stati eseguiti lungo tracce di particelle ionizzanti osservate in lastre Ilford G5 (spesse 600 μm) che erano state esposte alla radiazione cosmica all'altezza di circa 22 km nella prima serie di lanci in Sardegna, nel 1952.

Le osservazioni sono state eseguite con un microscopio munito di obiettivo 100× ad immersione omogenea e di oculare compensatore 16 micrometrico. La cella impiegata era di 50 μm: sono state scelte tracce che non presentassero un'apprezzabile variazione della densità di granuli da un estremo all'altro del tratto in cui si sono effettuate le misure.

Tenuto conto del fatto che vari fattori, i quali effettivamente intervengono

[1] G. Lovera: *Nuovo Cimento*, **12**, 154 (1954); I. Iori, G. Lovera e A. Roveri: *Atti Sem. Mat. Fis. dell'Univ. di Modena*, **7**, (1954).

nella distribuzione dei granuli (quali le fluttuazioni nelle dimensioni e posizioni dei granuli sensibili originali, le loro variazioni di diametro durante le operazioni di sviluppo, ed altre) non sono contemplate nelle ipotesi schematiche poste a base della presente trattazione statistica, la quale per altro parte dalla considerazione dei granuli già sviluppati, si è ritenuto che la presenza di una lacuna osservabile, quindi di lunghezza non inferiore a quella minima consentita dal potere risolutivo del microscopio nelle condizioni di osservazione, potesse essere considerata, generalmente, come un posto vacante, non occupato da un granulo sviluppato, il quale interrompe la continuità del gruppo di granuli. Nella tab. I (colonne 2^a-5^a) sono raccolti i dati sperimentali medi ottenuti raggruppando opportunamente tracce con caratteristiche prossime tra loro.

Si può osservare, anzitutto, come i valori di σ_ν^2 e di a siano prossimi tra loro, in accordo con le formule (2) e (4).

In fig. 1 e 2 sono tracciate alcune curve calcolate rispettivamente mediante la (1) e la (2), per $L=50$ μm, e per differenti valori del diametro medio d dei granuli sviluppati: $d=0.65$ μm; 0.60 μm; 0.55 μm; 0.50 μm; 0.45 μm (essendo per lo più compreso entro questo intervallo il diametro medio dei granuli sviluppati nelle emulsioni Ilford G5, almeno in condizioni normali di sviluppo), e sono riportati i valori osservati di σ_ν^2 in funzione di ν e di σ_a^2 in funzione di a rispettivamente. Gli errori probabili sono stati calcolati con le formule $\pm 0.674\sigma/\sqrt{N}$ e $\pm 0.674\sigma^2\sqrt{2/N}$ rispettivamente per le medie (ν e a) e per i quadrati degli scarti (σ_ν^2 e σ_a^2), essendo N il numero di celle su cui si sono effettuati i conteggi. Nella fig. 1 è segnata anche la retta $\sigma_\nu^2=\nu$ e nella fig. 2 la retta $\sigma_a^2=a$, che corrispondono alla statistica di Poisson. Dalle due figure risulta che i punti sperimentali si dispongono soddisfacentemente in vicinanza delle curve calcolate secondo la statistica di Bernoulli, mentre appare evidente che la statistica di Poisson non è affatto adeguata a rendere conto dei

Tabella I.

Gruppo di tracce	ν	σ_ν^2	a	σ_a^2	σ_a^2
1	15.25	13.13	12.66	7.62	7.83
2	18.77	14.88	14.49	7.29	7.20
3	20.62	16.37	15.46	7.50	7.60
4	24.84	18.75	17.73	8.36	7.69
5	31.88	20.06	20.72	7.03	6.17
6	37.44	24.24	22.20	7.55	7.13
7	44.13	26.37	23.26	8.45	7.28
8	50.33	25.15	22.19	7.71	6.68

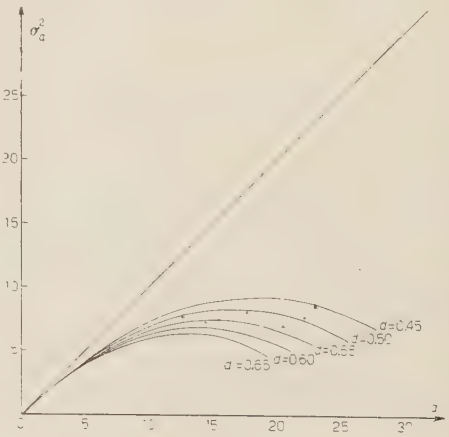

Fig. 1.

valori degli scarti quadratici medi osservati.

Un altro confronto delle formule statistiche in questione con i dati sperimentali, è stato effettuato nel seguente modo: dalle (1), (3), noti ν e σ_ν e dalle (2), (4), vicini a questi, che non a quelli richiesti dalla statistica di Poisson ($\sigma_a^2 = a$). Del resto è opportuno anche rilevare che la trattazione svolta, nell'ambito della statistica di Bernoulli, rappresenta solo una prima approssimazione della effettiva distribuzione dei granuli lungo la traccia, in quanto da un lato il numero dei granuli sviluppabili per la cella non è necessariamente costante, e dall'altro i granuli subiscono variazioni di dimensione durante lo sviluppo, ed intervengono le conseguenze dello sviluppo indotto.

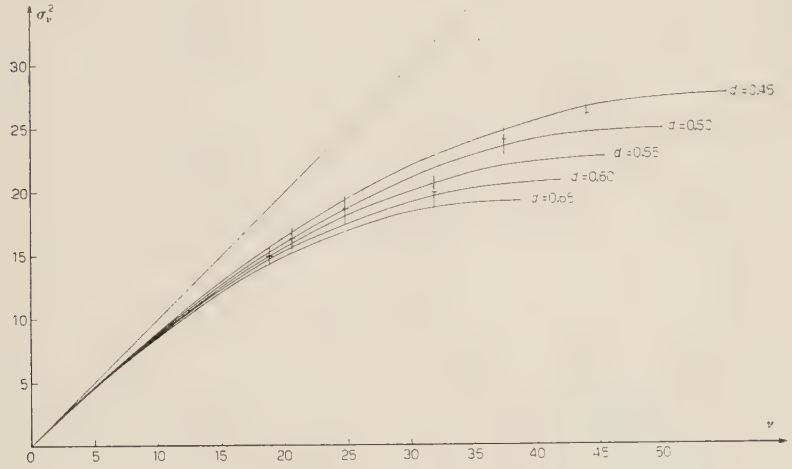

Fig. 2.

noti ν ed a, si può ricavare n:

$$n = \frac{\nu^2}{\nu - \sigma_\nu^2}, \tag{5}$$

$$n = \frac{\nu^2}{\nu - a}, \tag{5'}$$

quindi la (2), dati a ed n, fornisce un valore di σ_a da confrontare con quello sperimentale. Nell'ultima colonna della tab. I sono riportate le medie dei valori di σ_a^2 calcolati, separatamente, per i due valori di n ricavati dalle (5) e (5').

L'accordo con i dati sperimentali è ancora soddisfacente: per lo più, i valori di σ_a^2 osservati sono lievemente superiori a quelli calcolati, però di gran lunga più

C'è da attendersi che queste ulteriori cause di fluttuazioni portino ad un accrescimento dello scarto quadratico medio.

Comunque, dal confronto con l'esperienza, appare che gli scostamenti dalla statistica di Bernoulli sono di modesto rilievo. Si può quindi concludere che i dati sperimentali presi in esame trovano una soddisfacente interpretazione nell'ambito di detta statistica.

Remark on a Previous Note.

E. Corinaldesi
Dublin Institute for Advanced Studies

(ricevuto il 29 Maggio 1955)

In a letter to the Editor of this journal (E. Corinaldesi: *Nuovo Cimento*, **1**, 1289 (1955)), we recently presented a derivation of the equations of the two-body problem of general relativity from Gupta's theory of the quantized gravitational field.

We stated that two terms, of the order of $\varkappa^4$, had not yet been found. These terms might conceivably have been due to radiative corrections to the potential, which were therefore investigated. It soon became clear, however, that they could be traced much more simply to the contribution

$$\ddot{r}_1^i = -[V, [V, r_1^i]] + \dots ,$$

where V is the velocity dependent potential of the order of $\varkappa^2$ (including retardation) described in the previous letter. Though a superficial inspection might suggest that the above double commutator may be responsible only for corrections of the order od $\varkappa^4$ by some power of the velocities, actual calculation shows it to yield

$$\langle \ddot{r}_1^i \rangle = \dots + \varkappa^4 \int \Psi^* (\boldsymbol{r}_1, \boldsymbol{r}_2) \left[-\varphi_{,i} \left(\frac{4m_2}{r} + \frac{5m_1}{r} \right) \right] \Psi(\boldsymbol{r}_1, \boldsymbol{r}_2) \, \mathrm{d}\boldsymbol{r}_1 \, \mathrm{d}\boldsymbol{r}_2 ,$$

with $\varphi \equiv m_2/r$, where the contribution $(-\varphi_{,i}(m_2/r))$ arises from the cross terms which are the product of the Newton part of the potential with the retardation correction, and the remainder from the velocity dependent part of the potential.

Thus the HEI equations are found to hold in their full form for the motion of wave packets, and therefore, in the classical limit of wave mechanics, also for the motion of macroscopic bodies.

An Analysis of Three τ-Mesons.

G. Baroni

Istituto di Fisica dell'Università - Roma
Istituto Nazionale di Fisica Nucleare - Sezione di Roma

(ricevuto il 3 Giugno 1955)

In a batch of Ilford G5 stripped emulsions exposed at 25 000 m during the Sardinia balloon flight expedition in summer 1953, three more positive τ-mesons decaying in the emulsion have been found.

In every case the decay π-meson ends in the emulsion. The more relevant data are collected in Table I. The first part shows the characteristics of the parent star, the energy and the time of flight of the τ-mesons. The prongs of the parent stars have been followed but no associated heavy meson has been found. In the second part of the table the range R, the number n of crossed emulsions, the errors of range measurements (straggling, distortion, fluctuations of emulsion thickness) and the kinetic energy have been collected for the decay π's. The kinetic energy was determined by the range vs. energy curves calculated in this laboratory [1]. In addition the decay process or the interaction of the π-mesons at the end of their range are given. In the last column are listed the Q values.

Since the energy measurements of the decay π's of the τ-mesons found at Rome have been carried out under especially uniform conditions (the stopping power was determined from the range of the μ-mesons, and the range energy relationship was the same for all measurements) it may be useful to give the mean of the Q-values of the 7 τ-mesons found at Rome in stripped emulsions [2], that is:

$$Q = 73.9 \pm 0.4 \text{ MeV} .$$

This value is in agreement with the

$$Q = 74.7 \pm 0.3 .$$

The energy spectrum of the π^- emitted in the decay of τ-mesons is connected with the intrinsic properties of the particles [4,5]. Fabri has suggested a method for checking the different hypotheses on

[1] G. Baroni, C. Castagnoli, G. Cortini, C. Franzinetti and A. Manfredini: preprint.

[2] E. Amaldi, G. Baroni, G. Cortini, C. Franzinetti, and A. Manfredini: *Suppl. Nuovo Cimento*, **12**, 181 (1954).

[3] Report of the Committee on τ-mesons in *Suppl. Nuovo Cimento*, **12**, 419 (1954).

[4] R. H. Dalitz: *Phyl. Mag.*, **44**, 1068 (1953).

[5] E. Fabri: *Nuovo Cimento*, **11**, 479 (1954).

TABLE I.

Particles	Star	$t \cdot 10$ (s)	T (MeV)	R (μm)	n	$\delta R \cdot 10^2/R$			E (MeV)	Decay or capture		Q (MeV)
						Straggling	Distortion	Thickness				
τRo_7	14+8p	1.18	39.9	6 630	11	2.72	1.15	0.63	18.3 ± 0.36	$\pi \to \mu \to e$ therefore	π^+	74.4 ± 0.7
				9 080	9	2.63	1.51	0.24	21.8 ± 0.40	$\pi \to \mu \to e$ »	π^+	
				18 280	6	2.37	0.72	0.03	34.3 ± 0.49	σ_3 »	π^-	
τRo_8	20+5n	0.84	31.1	24 550	20	2.34	0.87	0.12	37.6 ± 0.72	σ_0 »	π^-	72.1 ± 1
				120	1	3.56	—	—	1.9 ± 0.04	$\pi \to \mu \to e$ »	π^+	
				17 440	18	2.42	1.07	0.20	32.6 ± 0.69	$\pi \to \mu \to e$ »	π^+	
τRo_9	15+3n	1.47	47.3	17 580	5	2.42	0.64	0.02	32.8 ± 0.58	$\pi \to \mu \to e$ »	π^+	73.5 ± 1
				15 390	18	2.46	0.86	0.25	30.0 ± 0.62	$\pi \to \mu$ »	π^+	
				2 590	4	2.94	2.31	0.74	10.7 ± 0.37	σ_0 »	π^-	

the spin and parity of τ-mesons. This method consists in giving the number of π^--mesons having energy in the three regions defined as follows:

a) $E_- > E'_+ , \quad E''_+ ;$

b) $E'_+ > E_- > E''_+ ;$

c) $E'_+ , \quad E''_+ > E_- .$

The report of the committee on τ-mesons ([3]) of the Padua Conference of 1954 contains the application of this method to 20 τ-mesons then available. A statistics including these three mesons together with those found in the meantime at Bern, Bombay, Padua and Turin ([6]) gives the following distribution: *a*) 18; *b*) 15; *c*) 15; i.e. almost an isotropic distribution.

This is a rather poor statistics, but it is sufficient to indicate that it is very unlikely that the τ-meson has spin 1.

TEUCHER *et al.* ([7]) have suggested using the possible correlation between the direction of emission of the τ-mesons and the perpendicular to the plane of decay of the τ-mesons for the determination of the spin of the τ.

If the distribution of the angles between these two directions is not isotropic, the spin of the τ should be > 0 and the τ should be polarized in the emission. Similar information could be given by the distribution of the angles between the τ-direction and the π^--meson direction.

The angle values given in Table II for each τ-meson found at Rome refer to:

$\Theta_{N\tau}$ between the direction of emission of the τ-meson and the perpendicular to the plane of decay.

Φ_τ between the direction of emission of the τ-meson and the plane of the emulsion.

Φ_N between the perpendicular to the plane of decay and the plane of the emulsion.

([6]) M. TEUCHER, W. THIRRING and H. WINZELER: *Nuovo Cimento*, **1**, 733 (1955).

([7]) Private communication.

Φ_π between the direction of emission of the unlike π and the plane of the emulsion.

$\Theta_{\pi\tau}$ between the direction of emission of the τ-meson and the direction of the emission of the unlike π.

TABLE II.

Particles	$\Theta_{N\tau}$	Φ_N	Φ_τ	Φ_π	$\Theta_{\pi\tau}$
Ro_3	23°	28°	15°	19.5°	22°
Ro_4	88°	81°	4°	7.5°	5°
Ro_5	66°	54°	9°	34°	67°
Ro_6	45°	30°	17°	38.5°	121°
Ro_7	39°	14°	9°	12.5°	103°
Ro_8	84°	42°	41.5°	33.5°	~95°
Ro_9	61°	41°	16°	37.5°	34°

The data of the three central columns are given for a further analysis as suggested by TEUCHER *et al.*, because some τ-mesons with a small $\Theta_{N\tau}$ may be lost in the scanning.

In the histogram of Fig. 1 the frequency of $\Theta_{N\tau}$ for a given solid angle, for the τ-mesons of Bern and Rome (the only ones now available) is reported.

The percentage of τ-mesons with $\Theta_{N\tau} > 60°$, which for an isotropic distribution must be 50%, is 69%. This is in agreement with the distribution

$$\sin^2 \Theta_{N\tau}\, d\cos \Theta_{N\tau}$$

suggested by the Bern group. However

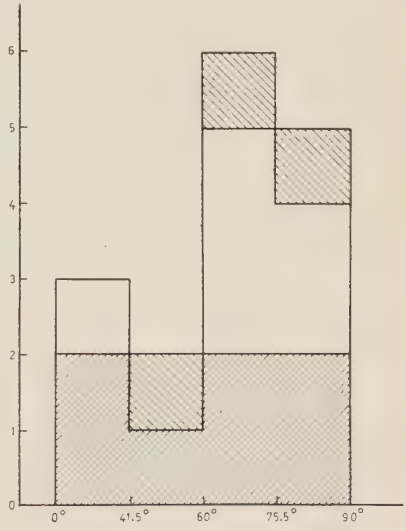

Fig. 1.

more data of other τ-mesons are needed for obtaining more significant results.

* * *

I would like to thank Prof. E. AMALDI for his helpful interest in this work.

On the β^--Decay of ^{171}Tm.

A. Bisi, S. Terrani and L. Zappa

Istituto di Fisica Sperimentale del Politecnico - Milano

(ricevuto il 4 Giugno 1955)

In the neutron-induced activities in erbium, a long lived activity ($T_{\frac{1}{2}}=680$ d) was found to grow from activated Er samples by Ketelle [1] and assigned to ^{171}Tm, daughter of 0.5 h ^{171}Er. The maximum energy of the β-spectrum was reported to be: $E=0.10$ MeV; no γ-rays were detected.

Erbium oxide was irradiated in the Harwell pile; after allowance for the decay of ^{171}Er, the ^{171}Tm sample was found to contain very large impurities of 129 d ^{170}Tm. In order to have a minimum of ^{170}Tm impurity, the β-spectrum was studied fifteen months after the irradiation, by means of an intermediate image β-spectrometer. The sample, 0.5 cm in diameter, was spread, using the method of Schaefer and Harker [2], on an Al foil 0.18 mg/cm² thick; the cut-off energy of the Geiger window, a nylon film, was at about 6 keV. The end point of the β-spectrum came at 103 ± 2 keV. No γ-radiations were detected in the scintillation spectrometer. Our results are in good agreement with the results of Ketelle.

The β transition, $^{171}\mathrm{Tm} \rightarrow {}^{171}\mathrm{Yb}$, occurs between the ground states. By taking into account the measured orbital ^{171}Yb and on the basis of the nuclear shell model the transition can be reasonably classified as first forbidden ($\Delta I=0$; 1; yes). Thus, according to Mayer, Moszkowski and Nordheim [3] the $\log ft$ value must be : $6 < \log ft < 8$. In effect it is: $\log ft=6.4$. A characteristic feature of these transitions is the allowed shape of their spectra. We did not observe appreciable departures from the allowed shape. A detailed investigation of the shape of the spectrum was not made owing to the residual impurities of ^{170}Tm.

[1] J. M. Hollander, I. Perlman and G. T. Seaborg: *Rev. Mod. Phys.*, **25**, 469 (1953).

[2] V. J. Schaefer and D. Harker: *Journ. Appl. Phys.*, **13**, 427 (1942).

[3] M. C. Mayer S. A. Moszkowski and L.W. Nordheim: *Rev. Mod. Phys.*, **23**, 215 (1951).

IL NUOVO CIMENTO Vol. II, N. 1 1° Luglio 1955

On Reduction Formulae in Field Theory.

S. S. Schweber

Brandeis University - Waltham, Massachusetts

(ricevuto il 4 Giugno 1955)

In a recent article Lehmann, Symanzik and Zimmermann [1] have given a formulation of field theory based on certain reduction formulae. It is the purpose of this note to point out that these reduction formulae can easily be derived by an application of Green's theorem:

$$\int_V \frac{\partial F_\mu(x)}{\partial x_\mu}\, \mathrm{d}^4x = \int_S F_\mu(x)\, n^\mu(x)\, \mathrm{d}\sigma(x)\,. \tag{1}$$

In Eq. (1), S is the surface bounding the four-dimensional volume V and n^μ is outward normal to $\mathrm{d}\sigma(x)$. We illustrate the application of (1) to the case of Fermion field operators.

Let $w_n(x)$, $n = 1, 2, \ldots$ be an infinite set of positive energy (wave-packet) solutions of the Dirac equation

$$(i\gamma_\mu \partial^\mu - M)\, w_n(x) = 0 \tag{2}$$

normalized and orthogonal in the scalar product:

$$\int \bar{f}(x)\, \gamma^\mu\, g(x)\, \mathrm{d}\sigma_\mu(x) = (f, g), \tag{2a}$$

which is independent of the space-like surface σ if f and g satisfy Eq. (2). Also

$$\sum_n w_n(x) \overline{w}_n(x') = -\, iS^{(+)}(x - x')\,. \tag{2b}$$

The incoming and outgoing states of the field theoretic scattering problem can then be constructed in a manner similar to the Bose case. Thus

---

[1] H. A. Lehmann, K. Symanzik and W. Zimmermann: *Nuovo Cimento*, **1**, 205 (1955).

(3)
$$\Phi\, p_1 \dots p_n;\, r_1 \dots r_m =$$
$$(n!\, m!)^{-\frac{1}{2}} \int \mathrm{d}\sigma_{\mu_1}(x_1) \int \mathrm{d}\sigma_{\mu_n}(x_n) \int \mathrm{d}\sigma_{\nu_1}(y_1) \dots \int \mathrm{d}\sigma_{\nu_m}(y_m)$$
$$\bar{w}^c_{r_1}(y_1) \dots \bar{w}^c_{r_m}(y_m)\, \gamma^{\nu_1}(y_1) \dots \gamma^{\nu_m}(y_m)$$
$$N(\psi_{\mathrm{in}}(y_1) \dots \psi_{\mathrm{in}}(y_m) \bar{\psi}_{\mathrm{in}}(x_1) \dots \bar{\psi}_{\mathrm{in}}(x_n))$$
$$\gamma^{\mu_1}(x_1) \dots \gamma^{\mu_n}(x_n)\, w_{p_1}(x_1) \dots w_{p_n}(x_n) \Psi_0 ,$$

where N is the normal product operator of WICK ([2]), is an incoming scattering state with n fermions, and m antifermions having properties specified by the eigenvalues $p_1 \dots p_n$, $r_1 \dots r_n$. The superscript c on the amplitudes for the anti-particles denotes that the charge conjugate wave functions are to be used. The symbol $\gamma_\mu(x)$ indicates that γ_μ has indices corresponding to the spinors labelled with the coordinate x. The corresponding outgoing states are obtained by replacing the in-field Heisenberg operators by the out-field ones. Let now $F_\mu(x)$ in (1) be taken as

(4)
$$T[(\psi(y_1) \dots \psi(y_s) \bar{\psi}(x_1) \dots \bar{\psi}(x_t) \psi(x))] \gamma_\mu(x)\, w_n(x) .$$

Then Eq. (1), if V is taken to be the whole of space-time, implies that

(5)
$$(\Psi_0,\, T(\psi(y_1) \dots \psi(y_s) \bar{\psi}(x_1) \dots \bar{\psi}(x_t)(\Phi^{n;}_{\mathrm{in}}) =$$
$$= \int_{\sigma = t = -\infty} \mathrm{d}\sigma^\mu(x) (\Psi_0,\, T(\psi(y_1) \dots \psi(y_s) \bar{\psi}(x_1) \dots \bar{\psi}(x_t) \bar{\psi}(x)) \Psi_0) \gamma_\mu(x)\, w_n(x) -$$
$$= \int_{\sigma = t = +\infty} \mathrm{d}\sigma^\mu(x) (\Psi_0,\, T(\psi(y_1) \dots \psi(y_s) \bar{\psi}(x_1) \dots \bar{\psi}(x_t) \bar{\psi}(x)) \Psi_0) \gamma_\mu(x)\, w_n(x)$$
$$+ i \int_{-\infty}^{+\infty} \mathrm{d}^4x\, (\Psi_0,\, T(\psi(y_1) \dots \psi(y_s) \psi(x_1) \dots \bar{\psi}(x_t) \bar{\psi}(x)) \Psi_0) \cdot (i\gamma^\mu \overleftarrow{\partial}_\mu + M) w_n(x)$$
$$+ i \int_{\infty}^{+\infty} \mathrm{d}^4x (\Psi_0,\, T(\psi(y_1) \dots \psi(y_s) \bar{\psi}(x_1) \dots \bar{\psi}(x_t) \bar{\psi}(x) \Psi_0) \cdot (i\gamma^\mu \overleftarrow{\partial}_\mu - M)\, w_n(x) =$$
$$= i \int_{\infty}^{+\infty} \mathrm{d}^4x\, (\Psi_0,\, T(\psi(y_1) \dots \psi(y_s) \bar{\psi}(x_1) \dots \bar{\psi}(x_t)\, \psi(x) \Psi_0) \cdot (i\gamma^\mu \overleftarrow{\partial}_\mu + M) w_n(x)$$

where we have made use of Eq. (2) and the fact that in the surface integral at $t = -\infty$, $\bar{\psi}(x)$ is later than all the other operators and can therefore be taken outside the T product. But since $\lim_{x^0 \to \infty} \psi(x) = \bar{\psi}_{\mathrm{out}}(x)$ and $\bar{\psi}^{(+)}_{\mathrm{out}}(x) \Psi_0 = 0$, this term

([2]) G. C. WICK: *Phys. Rev.*, **80**, 268, (1950).

vanishes. Similarly

$$(6)\qquad (\Psi_0,\ T(\psi(y_1)\dots\psi(y_s)\bar{\psi}(x_1)\dots\bar{\psi}(x_t))\Phi_{\mathrm{in}}^{r;p}) - i(-1)^t\int_{-\infty}^{+\infty} d^4y\ \bar{w}_p^r(y)(i\gamma^\mu\overleftarrow{\partial}_\mu - M)$$
$$\cdot(\Psi_0,\ T(\psi(y_1)\dots\psi(y_s)\psi(y)\bar{\psi}(x_1)\dots\bar{\psi}(x_t))\Psi_0).$$

Note that (5) vanishes, unless $s=t+1$, and similarly (6) vanishes unless $s+1=t$. The reduction formulae for arbitrary $\Phi_{\mathrm{in}}^{r;p}$ replacing the one particle incoming states in (5) and (6) are easily obtained by induction or from the generalization of (1) to many variables, namely

$$(7)\qquad \int_{V_1} d^4x_1 \dots \int_{V_n} d^4x_n \frac{\partial^n F_{\mu_1\dots\mu_n}(x_1\dots x_n)}{\partial x_{1\mu_1}\dots\partial x_{n\mu_n}} = \int_{S_1} d\sigma^{\mu_1}(x_1)\dots\int_{S_n} d\sigma^{\mu_n}(x_n)\, F_{\mu_1\dots\mu_n}(x_1\dots x_n)\,.$$

The non-linear equations relating the vacuum expectation values of the time-ordered products of Heisenberg operators can be derived in a manner completely analogous to that outlined in reference [1], but attention must now be paid to the factor ± 1 arising from the permutation of fermion operators with the T symbol.

On the Imaginary Part of the Nucleon-Nucleus Potential.

E. Clementel and C. Villi

Istituti di Fisica dell'Università di Padova e di Trieste
Istituto Nazionale di Fisica Nucleare - Sezione di Padova

(ricevuto l'8 Giugno 1955)

The problem of understanding the interactions of neutrons with nuclei led Bohr [1] some twenty years ago to the formulation of the compound nucleus model, where a complete amalgamation is assumed to take place between the incident particle and the nucleons of the target nucleus. The simplest theoretical formulation of this strong interaction model has been given by Feshbach and Weisskopf [2], and it is known as continuum theory of nuclear reactions. In this theory the reaction cross-section, i.e. the cross-section for the formation of the compound nucleus, can be written as a product of the « area » of the incident neutron+target nucleus $\pi^2(\lambda\!\!\!^{-}+R)$ and the transmission coefficient $4kK/(k+K)^2$, where $k=\lambda\!\!\!^{-1}$ and K are the wave numbers of the neutron outside respectively inside the nucleus. Recent experimental results [3] have shown clearly that the cross-sections given by the continuum theory do not agree with experiments. The observed cross-sections are far from being smooth functions of the energy, and they show indeed a rather varied energy dependence, changing in a systematic way from nucleus to nucleus, and some very low and broad maxima and minima.

All these discrepancies happened to be realized at the time when the independent particle model (shell model) was being revived with great success. Since the energy dependence of the observed cross-sections can be fitted by the scattering from a finite potential rather than by the strong coupling picture, it was natural to develop a model with the aim to establish a compromise between the strong interaction of the compound nucleus picture and the complete independent motion of the shell model. Such a model has been developed by Feshbach, Porter and Weisskopf [4] (clouded crystal ball model).

According to this model, the nucleon-nucleus scattering problem is reduced to a one-body problem replacing the nucleus by a complex attractive potential

$$V = V_0 + iV_1 , \tag{1}$$

---

[1] N. Bohr: *Nature*, **137**, 344 (1937).

[2] S. Feshbach and V. F. Weisskopf: *Phys. Rev.*, **76**, 1550 (1949).

[3] H. H. Barshall: *Phys. Rev.*, **86**, 431 (1952). For a review article on these questions see H. H. Barshall: *Am. Journ. Phys.*, **22**, 517 (1954).

[4] H. Feshbach, C. E. Porter and W. F. Weisskopf: *Phys. Rev.*, **96**, 448 (1954).

for $r < R$, otherwise zero, acting upon the incoming nucleon. It is easy to see from the continuity equation (5) that the introduction of a negative imaginary potential energy in the Schrödinger equation describes absorption of particles: in fact Eq. (1) corresponds to an absorption probability $2V_1/\hbar$ per unit time, as long as the particle is within the nucleus. It follows that the target nucleus can act upon the incoming nucleon as a potential well, because the formation of a compound state, described by the potential (1) as an absorption, occurs inside the nucleus with a probability smaller than unity.

The imaginary term V_1 is certainly energy dependent, also assuming V_0 as a constant. In terms of the mean free path L in nuclear matter, the absorption probability per unit time is given by $\beta c/L$, where βc is the velocity of the incident nucleon inside the nucleus. Taking into account the relation $L = 1/\varrho\langle\sigma\rangle$, with ϱ density of nuclear matter, and assuming with GOLDBERGER (5) $\sigma_{pp} = \sigma_{nn} = \sigma_{np}/4$, whe have for a standard nucleus ($\sigma = \sigma_{np}$)

$$V_1(5/16)\beta\varrho\hbar c\langle\sigma\rangle \,. \tag{2}$$

Because of the relation (2), the energy dependence of V_1 is directly related to the energy dependence of the neutron-proton total cross-section. We shall now calculate the average $\langle\sigma\rangle$ by using a Fermi gas model with a maximum kinetic energy $E_F = 25$ MeV and an average binding energy of 8 MeV, i.e. $V_0 = 33$ MeV. Let us denote with $\boldsymbol{p}$ and $\boldsymbol{k}$ the momenta of the incident respectively target nucleon before the collision, with $\boldsymbol{p}'$ and $\boldsymbol{k}'$ the same momenta after the collision and with $\boldsymbol{q}$ and $\boldsymbol{q}'$ the corresponding relative momenta. In the center of mass system, the differential cross-section depends in general on q and the scalar product $\boldsymbol{q}\cdot\boldsymbol{q}'$, i.e. we can write

$$\langle\sigma\rangle = \frac{3}{4\pi k_F^3}\int\frac{|\boldsymbol{p}-\boldsymbol{k}|}{p}\,\mathrm{d}\boldsymbol{k}\int\mathrm{d}\sigma(q, \boldsymbol{q}'\cdot\boldsymbol{q}')\,\delta(q-q')\,\frac{\mathrm{d}\boldsymbol{q}'}{q'^2}\,, \tag{3}$$

where the conservation of energy and momentum has been taken into account. At this stage, to avoid non essential refinements, we shall simplify Eq. (3) neglecting the angular dependence of $\mathrm{d}\sigma$ and we assume $\mathrm{d}\sigma(q, \boldsymbol{q}\cdot\boldsymbol{q}') = \sigma(q)/4\pi$. In fact, although this assumption is somewhat restrictive for neutron-proton scattering, one can have confidence that it is allowed for low energies, where the small-angle scattering is forbidden by the Pauli principle. In this way $\sigma(q)$ can be taken out of the integral over $\boldsymbol{q}'$; the physical meaning of the left integral is now nothing but the solid angle available to the final state $\boldsymbol{q}'$ for a given initial state $\boldsymbol{p}$ and $\boldsymbol{k}$. Choosing as polar axis the direction $\boldsymbol{p}+\boldsymbol{k}$, from the relation $\boldsymbol{p}' = \frac{1}{2}(\boldsymbol{p}+\boldsymbol{k})+\boldsymbol{q}'$ we obtain

$$\int\delta(q-q')\,\frac{\mathrm{d}\boldsymbol{q}'}{q'^2} = \frac{4\pi}{|\boldsymbol{p}-\boldsymbol{k}|\,|\boldsymbol{p}+\boldsymbol{k}|}\int\mathrm{d}(p'^2) = 4\pi\,\frac{p^2+k^2-2k_F^2}{|\boldsymbol{p}-\boldsymbol{k}|\,|\boldsymbol{p}+\boldsymbol{k}|}\,. \tag{4}$$

The lower limit of integration has been fixed according to the Pauli principle $p'^2+k'^2 \geqslant 2k_F^2$; the upper one according to the energy conservation $p^2+k^2 = p'^2+k'^2$.

(5) H. BETHE: *Phys. Rev.*, **57**, 1125 (1940).

In our hypothesis of isotropic cross-section, it follows from Eqs. (3) and (4)

$$\langle\sigma\rangle = \frac{3}{4\pi k_F^3}\,\frac{1}{p}\int \frac{p^2+k^2-2k_F^2}{|\boldsymbol{p}+\boldsymbol{k}|}\,\sigma(q)\,\mathrm{d}\boldsymbol{k}\,. \tag{5}$$

Obviously the lower limit of integration over k is now fixed by the condition $p^2+k^2-2k_F^2 \geqslant 0$, and therefore it is $(2k_F^2-p^2)^{\frac{1}{2}}$ for $p^2 \leqslant 2k_F^2$; whereas it is zero for $p^2 \geqslant 2k_F^2$. In the particular case $\sigma(q)=\sigma_0$; the results are very simple and we get from Eq. (5)

$$\langle\sigma\rangle = \sigma_0\left(1-\frac{7}{5}\,\frac{k_F^2}{p^2}\right) \qquad \text{for} \quad p^2 \geqslant 2k_F^2\,, \tag{6a}$$

$$\langle\sigma\rangle = \sigma_0\left\{1-\frac{7}{5}\,\frac{k_F^2}{p^2}+\frac{2}{5}\,\frac{k_F^2}{p^2}\left(2-\frac{p^2}{k_F^2}\right)^{\frac{5}{2}}\right\} \qquad \text{for} \quad p^2 \leqslant 2k_F^2\,. \tag{6b}$$

The former result has been derived also by GOLDBERGER ([6]) with a different procedure; the formula given by YAMAGUCHI ([7]) for the latter case is incorrect.

More generally, the energy dependence of the neutron-proton total cross-section can be represented ([8]) with a very good approximation up to 200 MeV by the relation $\sigma(E_0)=A/(B+E_0)$, where E_0 is the incident energy (in MeV) in the laboratory system. The values of the constants are $A=8.64$ MeV·barn and $B=1.08$ MeV. Assuming this energy dependence for $\sigma(q)$, we obtain from Eqs. (2) and (5)

$$V_1 = (5MA/16\pi^2\hbar^2)\,\beta pc\,F(p)\,, \tag{7}$$

where

$$F(p) = \int \frac{x(1+x^2-2x_F^2)}{[2(1+x^2+\xi)]^{\frac{1}{2}}}\log\frac{1+3x^2+2\xi+2x[2(1+x^2+\xi)]^{\frac{1}{2}}}{1+3x^2+2\xi-2x[2(1+x^2+\xi)]^{\frac{1}{2}}}\,\mathrm{d}x\,, \tag{8}$$

M being the nucleon mass and having defined $x=k/p$, $x_F=k_F/p$, $\xi=MB/p^2$. It is clear that p is the momentum of the incident nucleon inside the nucleus, and hence it follows in the non-relativistic region from the relation $p=[2M(E_0+V_0)]^{\frac{1}{2}}$. The lower limit of the integral (8) is fixed according to the previous discussion. The potential V_1 goes to zero for $E_0+V_0=E_F$, which is the shell model basic assumption. In Table I we give the dependence of V_1 on E_0 for an attractive potential well $V_0=33$ MeV.

TABLE I.

E_0	0	5	10	20	40	80	100	150	200
V	1.60	3.45	5.38	8.73	11.5	12.5	12.1	10.9	9.58

([6]) M. L. GOLDBERGER: *Phys. Rev.*, **74**, 1269 (1948).
([7]) Y. YAMAGUCHI: *Progr. of Theor. Phys.*, **5**, 332 (1950).
([8]) L. BERETTA, C. VILLI and F. FERRARI: *Suppl. al Nuovo Cimento*, **12**, 499 (1954); see plot VII.

The initial increase of V_1 is due to the fact that the Pauli principle becomes less and less effective increasing E_0, whereas the behavior of $\sigma(E_0)$ is responsible for the decrease at high energies. The dependence of the function $F(\rho)$ on the parameter ξ is sensitive only up to about 20 MeV; this corresponds to the fact that at high energies the cross-section follows practically a E_0^{-1} law, which is contained in Eq. (8) for $\xi=0$. Our results are in satisfactory agreement with the empirical values of V_1 used in interpreting the scattering both of protons [9] and neutrons [10] by nuclei, carried out so far up to about 20 MeV. Generally the values of the real and imaginary part are fixed independently. In our formulation they are connected, and an increase of V_0 implies a decrease of V_1 so far as $E_0+V\leqslant 2E_F$, otherwise an increase. For example, for the choice $V_0=43$ MeV and $E_F=35$ MeV, we obtain $V_1(0)=1.17$, $V_1(10)=4.77$, $V_1(20)=8.59$, and $V_1(40)=13.7$ MeV. The experimental results for 1 MeV neutron scattering are well fitted [4] with the choice $V_0=42$ MeV and $V_1=1.3$ MeV. The slight difference on the real part for proton-nucleus scattering, due to Coulomb effects, does not alter appreciably these conclusions.

The absorption coefficient, given simply by $2V_1/\beta\hbar c$, does not present any minimum for $E_0<50$ MeV, contrary to the result stated by TAYLOR [11]. It is easy to realize that such a minimum would be conflicting with the known experimental behavior of the nucleon-nucleon total cross-sections.

---

[9] R. D. WOODS and D. S. SAXON: *Phys. Rev.*, **95**, 577 (1954).

[10] Y. FUJIMOTO and A. HOSSAIN: *Phil. Mag.*, **46**, 542 (1955); M. WALT and J. R. BEYSTER: *Phys. Rev.*, **98**, 677 (1955).

[11] T. B. TAYLOR: *Phys. Rev.*, **92**, 831 (1953).

Non Linear Integral Equation in Field Theory.

S. Fubini

Istituto di Fisica dell'Università - Torino
Istituto Nazionale di Fisica Nucleare - Sezione di Torino

(arrivato il 9 Giugno 1955)

An approximate non linear integral equation for pion-nucleon scattering has been recently derived by Low [1]. This equation has the main advantage of connecting, in the static approximation, only quantities on the energy shell and of containing only renormalized quantities. The method of derivation used by Low is based on the Heisenberg representation technique developed by Gell Mann and Low [2].

In this paper we want to show a simpler and more general method leading to a set of non linear integral equations whose first approximation coincides with Low's result.

Let us consider a nucleon field ψ interacting with a meson field Φ in the presence of a time dependent external meson field Φ_e. The Hamiltonian of the system may be written, in the Schrödinger representation, as:

$$H = H_f + H_e(t) \tag{1}$$

where H_f is the usual Hamiltonian for two interacting fermion and boson fields and

$$H_e(t) = \int \mathrm{d}^3\boldsymbol{x}\, j^5(\boldsymbol{x})\, \Phi_e(\boldsymbol{x}t) \tag{2}$$

represents the interaction of the fermion field with the fixed external meson field.

If a canonical transformation T is performed in order to diagonalize H_f eq. (1) will become:

$$\widetilde{H} = H_0 + \widetilde{H}_e(t) \tag{3}$$

$$\widetilde{H}_e(t) = -\int \tilde{\jmath}(\tilde{x})\, \varphi_e(\boldsymbol{x}t)\, \mathrm{d}^3x \tag{3'}$$

---

[1] F. Low: *Phys. Rev.*, **97**, 1192 (1955).
[2] M. Gell-Mann and F. Low: *Phys. Rev.*, **84**, 350 (1951).

where $H_0[\psi(\boldsymbol{x})\varphi(\boldsymbol{x})]$ is the usual free particles Hamiltonian in which only the observed masses appear and

$$\tilde{j}_5(\boldsymbol{x}) = T^{-1} j_5(\boldsymbol{x}) T \tag{4}$$

is a very complicated and unknown functional of $\psi(\boldsymbol{x})$ and $\varphi(\boldsymbol{x})$.

Since the « interaction term » is time-dependent, it is convenient to go into an « interaction representation » by means of the transformation $\exp[iH_0 t]$ [3]. As is well known in this representation the operators $\psi(\boldsymbol{x})$ and $\varphi(\boldsymbol{x})$ will become time-dependent and obey the free-field equations with the observed masses. Using this representation the well known $U(t)$ operator is expanded in powers of the external field,

$$U(t) = 1 - i\int_{-\infty}^{t} \tilde{H}(t')\,\mathrm{d}t' + (-i)^2 \int_{-\infty}^{t}\mathrm{d}t' \int_{-\infty}^{t'} \mathrm{d}t''\, \tilde{H}(t')\,H(t'') + \dots . \tag{5}$$

Following the well known techniques of Wick $\tilde{j}_5(x)$ can be developed in normal products as follows

$$j_5(x) = \sum_q [N_0(q) + N_1(q) + N_2(q) + \dots] \exp[iqx] , \tag{6}$$

where:

$$\left\{\begin{aligned} N_0(q) &= \sum_{pp'} : \varphi^*(p')\Lambda_0(pp')\varphi(p) : \delta(p - p' + q) \\ N_1(q) &= \sum_{pp'k} : \varphi^*(p')\Lambda_0(pp'; k)\psi(p)\varphi(k) : \delta(p - p' - q + k) \\ N_2(q) &= \sum_{pp'kk'} : \varphi^*(p')\Lambda_0(pp'; kk')\psi(p)\varphi(k)\varphi(k') : \delta(p - p' - q + k + k') . \end{aligned}\right. \tag{7}$$

The development (6) is introduced in eq. (5). The first order term in eq. (5) will contain normal products of creation and destruction operators of physical meson with only one external field amplitude while the second order term will contain similar normal products multiplied by two external field amplitudes.

It is well known [3] that in a U matrix development the coefficient of normal products:

$$: \varphi(k_1) \dots \varphi(k_n) \dots \psi(p_1) \dots \psi(p_n)\psi(p_1' \dots p_n') ,$$

are unchanged if any of the $\varphi(k_i)$ is replaced by an amplitude $\varphi_e(k_i)$ with the same energy-momentum vector. It follows immediately that $\Lambda_1(p_1 p'; k)$ represents the matrix elements for meson-nucleon scattering (the final meson will have, of course, momentum $\boldsymbol{q} = \boldsymbol{p} - p' + \boldsymbol{k}$); $\Lambda_2 \Lambda_3 \dots$ represent processes with more than two mesons involved [4]. It follows also that equalities exist between the coefficients of the normal products in the first and in the second order terms of eq. (5).

[3] The idea of using such an « interaction representation » is the result of very useful discussions with Prof. M. Cini.

[4] R. P. Feynmann: *Phys. Rev.*, **80**, 440 (1950).

Thus we obtain:

$$(8)\quad \begin{cases} \langle \boldsymbol{p}, \boldsymbol{k} | N_1 | p' \rangle = \sum\limits_q \langle p | O_1(\boldsymbol{q}, \boldsymbol{k}) + O_1(\boldsymbol{k}, \boldsymbol{q}) | p' \rangle \delta(\boldsymbol{p} - \boldsymbol{p}' + \boldsymbol{k} - \boldsymbol{q}) \\ \langle p, kk' | N_2 | p' \rangle = \sum\limits_q \langle p, k' | O_2(\boldsymbol{q}, \boldsymbol{k}) + O_2(\boldsymbol{k}, \boldsymbol{q}) | p' \rangle \delta(\boldsymbol{p} - \boldsymbol{p}' + \boldsymbol{k} + \boldsymbol{k} - \boldsymbol{q}) \end{cases}$$

$$(8')\quad \begin{cases} O_1(\boldsymbol{q}, \boldsymbol{k}) = N_0(\boldsymbol{q}) \dfrac{1}{E_p - H_0 - q_0} N_0(\boldsymbol{q}) + \\ \qquad + N_1(\boldsymbol{q}) \dfrac{1}{E_p - H_0 - q_0} N_1(\boldsymbol{q}) + N_2(\boldsymbol{q}) \dfrac{1}{E_p - H_0 - q_0} N_2(\boldsymbol{q}) + \ldots \\ O_2(\boldsymbol{q}, \boldsymbol{k}) = N_0(\boldsymbol{q}) \dfrac{1}{E_p - H_0 - q_0} N_1(\boldsymbol{k}) + N_1(\boldsymbol{q}) \dfrac{1}{E_p - H_0 - q_0} N_0(\boldsymbol{k}) + \\ \qquad + N_1(\boldsymbol{q}) \dfrac{1}{E_p - H_0 - q_0} N_2(\boldsymbol{k}) + N_2(\boldsymbol{q}) \dfrac{1}{E_p - H_0 - q_0} N_1(\boldsymbol{k}) + \ldots \end{cases}$$

where $q_0 = \omega_q$, $k_0 = -\omega_k$; $\langle p; k_1 \ldots k_i |$ denote the eigenstate of H_0 corresponding to the physical state with one physical nucleon $\boldsymbol{p}$ and physical mesons of momenta $\boldsymbol{k}_1 \ldots \boldsymbol{k}_i$.

These equations have a rather familiar perturbation aspect. It is straightforward to derive from (8) non linear integral equations for the A_i. If all A_i but A_0 and A_1 are neglected the set (8) reduces to the Low equation.

The solution of equations (8) requires the knowledge of A_0. This is not known in the general case. Such a situation is not surprising since eqs. (8) have been deduced with the only assumption of the linearity in the meson field of the interaction Hamiltonian.

In this framework the problem of field theory is split into two different steps. First to derive from an infinite interaction Hamiltonian a finite A_1, secondly to solve the system of equations (8) in which no divergences appear any more. A rather different attitude can also be taken. Instead of taking as a starting point an unphysical interaction Hamiltonian one might start directly by assuming as given A_1 which represents the interaction of a physical nucleon with a physical meson.

***

The author is indebted to Prof. G. Wataghin and Prof. M. Cini for very illuminating discussions and criticism.

(5) The complete development of $\gamma^5(x)$ is more general than (6). For example terms of the type: $\varphi(k)\,\varphi(k')\,\varphi(k'')$: appear corresponding to direct meson-meson interaction. Since these terms do not appear in the lowest orders, we shall disregard them, for the moment.

Masses of the New Particles and the Range-Energy Relation (*).

D. O. Caldwell

Department of Physics and Laboratory for Nuclear Science
Massachusetts Institute of Technology - Cambridge, Massachusetts

(ricevuto il 10 Giugno 1955)

Most of the available methods for measuring the masses of unstable particles depend on a knowledge of the range-energy relation. The accuracy of these measurements is now such that the range-energy relation is the limiting factor in the precision of the mass determinations.

At the energies of interest, the main uncertainty in the range-energy relation arises from a lack of precise knowledge of the mean excitation potential, I, which appears in the energy-loss relation [1],

$$(1) \qquad -\frac{\mathrm{d}E}{\mathrm{d}x} = \frac{4\pi e^4 z^2 N}{mc^2\beta^2} \cdot \left\{ Z\left[\ln\frac{2mc^2\beta^2}{I(1-\beta^2)} - \beta^2\right] - \sum_i C_i \right\},$$

where ez is the charge of the incident particle of velocity βc; m is the electronic mass; N, the number of stopping atoms per unit volume of atomic number Z; and C_i, the correction for nonparticipating electrons of the i-th shell.

There has been some reason to believe that I is not a constant for a given element but is, rather, velocity dependent. Sachs and Richardson [2] showed that the various experimental determinations of I could be reconciled if $I = a - b\log E$, where E is the effective energy, which is 0.6 of the incident energy for a range measurement, and equal to the incident energy for an energy-loss determination of I.

The work of Lindhard a. Scharff [3] gave additional evidence that I is energy dependent. They plotted the stopping number per electron vs. $(\beta^2\hbar c)^2/(e^4 Z)$, and found that data for different elements and different energies lay on a smooth, nonlinear curve, the bulge in the curve corresponding [4] to a maximum value for I at intermediate energies. However, ac-

(*) This work has been supported in part by the joint program of the U.S. Office of Naval Research and the U.S. Atomic Energy Commission.

(1) M. S. Livingston and H. A. Bethe: *Rev. Mod. Phys.*, **9**, 264 (1937).

(2) D. C. Sachs and J. R. Richardson: *Phys. Rev.*, **89**, 1163 (1953).

(3) J. Lindhard and M. Scharff: *Kgl. Danske Videnskab. Selskab. Mat.-fys. Medd.*, **27**, No. 15 (1953).

(4) S. K. Allison and S. D. Warshaw: *Rev. Mod. Phys.*, **25**, 779 (1953).

cording to the LINDHARD-SCHARFF plot, I should not decrease indefinitely with energy, but should level off.

From these two results, the choice of I and hence of the range-energy relation in the region $p/mc \gtrsim 1$ seems very uncertain, and it is desirable to re-examine the available data. The results of the 18 MeV proton energy loss measurements by SACHS and RICHARDSON ([2,5,6]) now can be corrected (C_i) for the partial nonparticipation of electrons bound in the K ([7]), L ([8]), and higher shells. The corrected value for I for copper is 377.5 ± 8 eV, which is plotted against the logarithm of the effective ([2]) energy

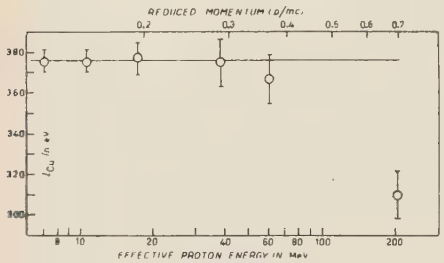

Fig. 1. – Experimental values for the mean excitation potential of copper as a function of the «effective» proton energy (0.6 of the incident energy for range measurements, or the incident energy for energy-loss determinations).

in Fig. 1. Other I values shown include those taken from the range measurements of BLOEMBERGEN and VAN HEERDEN ([9]) (slightly altered), and for the two lowest energy points, from those of BICHSEL and MOZLEY ([10]).

([5]) D. C. SACHS and J. R. RICHARDSON: *Phys. Rev.*, **83**, 834 (1951).

([6]) D. O. CALDWELL and J. R. RICHARDSON: *Phys. Rev.*, **94**, 79 (1954).

([7]) W. C. WALSKE: *Phys. Rev.*, **88**, 1283 (1952).

([8]) W. C. WALSKE: *Phys. Rev.* (to be published) and private communications.

([9]) N. BLOEMBERGEN and P. J. VAN HEERDEN: *Phys. Rev.*, **83**, 561 (1951).

([10]) H. BICHSEL and R. F. MOZLEY: *Phys. Rev.*, **94**, 764(A) (1954) and private communications. Note that their I values and errors as shown here are still preliminary.

It is apparent from the figure that, except for the highest energy point, taken from the range measurement of MATHER ans SEGRÈ ([11]), there is good agreement among the data and no longer any need for assuming that I is energy dependent. The data for aluminium give a very similar plot.

Furthermore, if one adds new or previously unused stopping power measurements ([9,12]) the shape of the Lindhard-Scharff plot is entirely changed, and one gets something closer to a straight line, corresponding to I being proportional to Z and independent of velocity.

Additional evidence against the Mather-Segrè point is furnished by measurements of the mass of the $K_{\mu 2}$ meson made by the Ecole Polytechnique Group. By measuring the momentum and range in Cu of the primary $K_{\mu 2}$; and by using a range-energy curve ([13]) computed for $I_{Cu} = 333.5$ eV, they ([14]) find a mass of 921 ± 16 m_e ([15]). A second mass determination, made by measuring the range in Cu of the μ-meson secondary, gives a mass of 942 ± 8 m ([16]), when using the

([11]) R. MATHER and E. SEGRÈ: *Phys. Rev.*, **84**, 191 (1951).

([12]) E. L. KELLY: *Phys. Rev.*, **75**, 1006 (1949); J. G. TEASDALE: *O N.R. Tech. Rpt.* No. 3, University of California at Los Angeles (1949), T. THOMPSON: *UCRL* -1910, University of California (1951); unpublished; A. B. CHILTON, J. N. COOPER and J. C. HARRIS: *Phys. Rev.*, **93**, 413 (1954); C. P. SONNETT and K. R. MAC KENZIE: *Phys. Rev.*, **98**, 280(A) (1955); and J. E. BROLLEY and F. L. RIBE: *Phys. Rev.* (to be published). The last two sets of authors have very kindly given permission to use their results prior to publication.

([13]) W. A. ARON, B. G. HOFFMAN, and F. C. WILLIAMS: *AECU*, 663 (1949), unpublished.

([14]) R. ARMENTEROS, B. GREGORY, A. HENDEL, A. LAGARRIGUE, L. LEPRINCE-RINGUET, F. MULLER and C. PEYROU: *Nuovo Cimento*, **1**, 915 (1955).

([15]) This value is obtained for those K's which have secondaries of range greater than 45 g/cm², and hence are probably $K_{\mu 2}$'s, and certainly not $K_{\pi 2}$'s, or τ's.

([16]) R. ARMENTEROS, B. GREGORY, A. HENDEL, A. LAGARRIGUE, L. LEPRINCE-RINGUET,

same range-energy curve. If one assumes that I is constant from $p/mc \sim 1$ to 2.2, then in order to make equal the mass values determined by the two methods, one must have $I = 380 \pm 40$, which is in excellent agreement with the low energy measurements, but nearly two standard deviations from the value determined in ref. ([11]) at a somewhat lower p/mc.

Since the only high energy emulsion range measurements ([17,18]) are relative to copper, there is even more uncertainty in emulsion ranges. Since I_{Cu} from ref. ([11]) has generally been used, masses of particles determined in this way are probably in error, and are at least quite uncertain.

While there is clearly need for further absolute range or energy loss measurements at high velocities, if one has to choose a range-energy relation on the basis of information available at present, it seems that it should be one based on the constant I value determined by the low energy work. The masses of some of the K particles computed on this basis will be presented separately ([16]), and a more complete account of this work outlined in the present paper will appear elsewhere.

* * *

The author thanks Prof. BRUNO ROSSI, Dr. HERBERT S. BRIDGE, and Dr. BERNARD GREGORY for helpful discussions, and Dr. CARL WALSKE and Dr. HANS BICHSEL for supplying both their results prior to publication and also much advice.

F. MULLER, C. PEYROU, H. S. BRIDGE, H. C. DESTAEBLER, B. ROSSI and B. V. SREEKANTAN: *Nuovo Cimento* (to be published). This value is an average of the E. P. and M.I.T. results, which are in good agreement.

([17]) O. HEINZ: *Phys. Rev.*, **94**, 1728 (1954).

([18]) H. G. DE CARVALHO and J. I. FRIEDMAN: *Rev. Sci. Instr.*, **26**, 261 (1955).

Non-Perturbative Expansions.

E. R. Caianiello (*)

CERN Theoretical Study Division - Copenhagen

(ricevuto il 16 Giugno 1955)

It has been shown previously that:

a) a given propagation kernel satisfies an integro-differential relation [1,2], which contains the first and second derivatives of the kernel with respect to the interaction strength λ;

b) all the λ-derivatives of a kernel exist and are finite in the point $\lambda=0$, under the hypothesis that the kernel is continuous there [3].

We propose here to show that, as a consequence of *a*) and *b*), it is possible to obtain, in several ways, expansions which are valid under the only assumptions that the kernels exist and are finite with their first and second λ-derivatives (the latter hypothesis may be somehow relaxed, but it would be uninteresting to do it here). While a study of the convergence of perturbative expansions would be only partially conclusive, if the result be negative, a similar investigation on the expansions proposed here (which would present about the same degree of difficulty) would have a direct bearing on the problem of existence, and eventually provide the analytical continuation of the perturbative expansions if these converge within some range of λ. Renormalization presents no special difficulties and will be discussed at the end. Since we only present here a general outline of the method, without any detailed discussion, we use as shortened a notation as possible.

The rôle played by *a*) and *b*) is, intuitively, the following. The result *b*), which gives all the desirable information on the behavior of a kernel in the origin, does not permit any deduction on its behavior in nearby points, since it is not known whether holomorphy holds. An equation *a*), on the other hand, while clearly not sufficient to determine a kernel uniquely if only a finite amount of additional information (initial data) is given, yields however, because of its differential nature, a link between the point $\lambda=0$ and nearby points. Combining *a*) with *b*), therefore, one has an infinite amount of information in $\lambda=0$ (all the λ-derivatives) and a « bridge » connecting the origin with the points near to it, the « crossing » of which is quite independent of any assumption of holomorphy; sufficiency is secured trivially, since it is always possible to revert back, formally, to the perturbative expansion.

It seems most convenient to work

(*) On leave from the Scuola di Perfezionamento in Fisica Nucleare, Università, Roma.

(1,2,3) E. R. Caianiello: *Nuovo Cimento*, **11**, 492 (1954); **12**, 561 (1954); **1**, 337 (1955).

with equations such as given in ref. [2]), and to express all quantities in terms of the new variable $\alpha=\lambda^2$. It will suffice, here, to write the fundamental equation *a*) in the symbolyc form:

$$(1)\quad \mathcal{L}(K) = (L_0\Theta_0 + L_1\Theta_1 + L_2\Theta_2)K = 0\,,$$

where $L_{0,1,2}$ are differential operators in α at most of the second order, and the $\Theta_{0,1,2}$ operate only on the spinor-vector indices (suppressed) and on the space-time variables of K, which we denote, for short, with P: $K=K(\alpha, P)$. The most general expansion one can envisage for $K(\alpha, P)$ is:

$$(2)\qquad K(\alpha, P) = \sum f_n(\alpha)k_n(P)\,,$$

or

$$(3)\qquad K(\alpha, P) = \sum a_{mn}g_m(\alpha)k_n(P)\,,$$

where: $\{k_n(P)\}$ is some prescribed set of functions having the same tensorial character as $K(\alpha, P)$, which is known to be complete with respect to the problem of the linear approximation of functions having the nature of $K(\alpha, P)$; $\{g_m(\alpha)\}$ is a complete set of functions of α relative to some given interval $(0, A)$, conveniently chosen (α must be considered to be real and positive, or else λ would be complex and the interaction Hamiltonian non-Hermitean: the whole formalism should have to be changed); the functions $f_n(\alpha)$, or alternatively the coefficients a_{mn}, are the quantities to be determined.

The usefulness of such an expansion depends upon our *a priori*, knowledge of the set $\{k_n(P)\}$. The theorem *b*) permits to show that we know, indeed, all we need about it. For let $\mathrm{d}^\nu K(\alpha, P)/\mathrm{d}\alpha^\nu|_{\alpha=0} = K_\nu(P)$: then the functions $K_\nu(P)$ must be expandabel, by hypothesis, in terms of the set $\{k_n(P)\}$, so that the latter is linearly related to the set $\{K_\nu(P)\}$. If the functions $K_\nu(P)$ are linearly independent (this we assume without proof, but there can be little doubt as to the validity of this hypothesis), then the set $\{K_\nu(P)\}$ itself or any set

$$(4)\qquad k_n(P) = \sum c_{n\nu}K_\nu(P)$$

are complete and can be used in (2) or (3).

In practice, one shall consider the N^{th} approximation to $K(\alpha, P)$, obtained by neglecting in (2) or (3) all the terms with $m, n > N$. For any finite N:

$$(5)\qquad \frac{\mathrm{d}^\nu K^{(N)}(\alpha, P)}{\mathrm{d}\alpha^\nu}\Big|_{\alpha=0} - K_\nu^{(N)}(P) = \sum_0^N f_n^{(\nu)}(0)k_n(P)\,,$$

or

$$(6)\qquad K_\nu^{(N)}(P) = \sum_0^N a_{mn}g_m^{(\nu)}(0)k_n(P)\,;$$

we need not assume, though, that term-by-term differentiation to all orders is legitimate in the complete series.

The way to follow for the determination of the functions $f_n(\alpha)$ or of the coefficients a_{mn} is quite clear in principle, and will be hinted to only very briefly. As in all such problems, one can ask either that the equation (1) be satisfied exactly by $k^{(N)}(\alpha, P)$ and the initial conditions $K_\nu^{(N)}(P)=K_\nu(P)$ be satisfied only approximately, or viceversa, or that both be satisfied approximately. (In any case, of course, the initial conditions can be satisfied exactly, at most, only for $\nu \leqslant N$. The first instance is not possible if one starts from (3)). A variational procedure consisting in minimizing expressions:

$$(7)\qquad \int_0^A \mathrm{d}\alpha \int \mathrm{d}P\, \varrho(P)\overline{\mathcal{L}(K^{(N)})}\mathcal{L}(K^{(N)})\,,$$

$$(8)\qquad \int \mathrm{d}P\, \varrho(P)|K_\nu^{(N)} - K_\nu|^2\,,$$

where $\varrho(P)$ is some suitable positive tensor weight (to smooth out singularities) may then provide, according to the criterion chosen, the best fit for the $f_n(\alpha)$

or the a_{mn}. The coefficients c_{nv} in (4) are related to the initial values of the $f_n(\alpha)$ and their derivatives.

This outline may be concluded with two remarks. First, the ordinary differential equations one obtains for the $f_n(\alpha)$ are singular in the points $\alpha=0$ and $\alpha=\infty$; this is a feature of general interest, which may throw some light on the nature of the kernels. Second, the equation (1) is satisfied *identically* by the formal power-series expansion; that is, on equating the coefficient of α^n to zero, one obtains a linear identity connecting $\theta_0(K_n(P))$, $\theta_1(K_{n'}(P))$, $\theta_2(K_{n''}(P))$, which is of great help in practical calculations and can be used, conversely, to establish equation (1). The latter point shows also that no troubles arise because *a*) of renormalization, *b*) of normalization to unity vacuum-vacuum transition amplitude (division by K_0). For if renormalization is performed with the standard subtractive technique (as we assume here), then this identity remains true also for quantities calculated in this manner: the renormalized perturbative expansion satisfies, formally, the same equation (1), where now everything is calculated with the subtractive prescriptions. Moreover, FERRETTI [4] has proved, quite generally, that divergencies arising in the calculation of λ-derivatives of kernels are compensated by the same counter terms of the usual theory: this shows, independently of perturbative methods, that the standard subtractive procedure can be legitimately applied in our case. Exactly the same argument shows that the normalized kernels K/K_0 are obtained by simply dropping, throughout, the terms which correspond, in the usual graph terminology, to vacuum-vacuum fluctuations.

A method such as the one proposed here yields, of course, only a formal expansion; however, the conditions for its convergence are much less restrictive than those for the corresponding perturbative expansion. One should prove first that, in the limit $N \to \infty$, both the equation (1) and the initial conditions are satisfied exactly; then investigate the convergence of the expansion: even if only a weighed mean convergence should hold, rather than point-by-point convergence, definite conclusions might then be drawn as to the existence of a solution.

[4] B. FERRETTI: *Nuovo Cimento*, **10**, 3 (1953).

IL NUOVO CIMENTO Vol. II, N. 1 1° Luglio 1955

The " Hodoscope Chamber „: a New Instrument for Nuclear Research (*).

M. Conversi and A. Gozzini

Istituto di Fisica dell'Università - Pisa
Istituto Nazionale di Fisica Nucleare - Gruppo Aggregato di Pisa

(ricevuto il 17 Giugno 1955)

A new instrument, which may be defined as a « hodoscope chamber », has been developed for the detection of events occurring in nuclear or electromagnetic interactions. It is based on the following principle. If a strong electric field is produced soon after the passage of an ionizing particle in a region of space filled with a gas, then a luminous discharge occurs all over this region as a consequence of the processes following the acceleration undergone by the electrons freed by the impinging particle.

The hodoscope chamber that we are going to describe is essentially a parallel plate condenser filled with a large number of thin glass tubes containing neon at a pressure of 35 cm Hg. The condenser is made up of 14 Al plates, 0.3 cm thick, 22×44 cm^2 area, ~ 4 cm apart, every second plate being connected together. Each individual glass tube has an internal diameter of 0.65 cm etxernal diameter ~ 0.7 cm) a length of 22 cm and is shielded against light coming from other tubes by means of thin black paper. A fast ionizing particle crossing one tube in a direction perpendicular to its axis produces on the average 4 to 5 ion-pairs.

The passage of a charged particle through the hodoscope chamber, or the occurrence of a more complex event, is recorded by coincidences among counters placed outside the chamber. The coincidence pulse triggers the networks of Fig. 1, which are of the type employed in modulators for magnetron oscillators, consisting of an open delay line which is short-circuited, through the primary of a pulse transformer, via a hydrogen filled thyratron (a Philips 435). A few tenths of a μs after the passage of the particle or the occurence of an event in the chamber, two square pulses of opposite polarity are thus supplied by the outputs of the pulse transformers to the plates of the condenser. Each pulse lasts 2 μs, can have a maximum size of 20 kV and a maximum power of 250 kW. The intense electric field (up to 10 kV/cm) produced inside the chamber is large enough to accelerate the electrons freed by the ionizing particles, causing a luminous discharge in the neon tubes crossed by the particles, and not in the others. Luminous tracks of the ionizing particles can be recorded photographically without difficulty, as

(*) A more extensive report of this work has been presented by M. Conversi, S. Focardi, C. Franzinetti, A. Gozzini and P. Murtas at the International Conference on Elementary Particles held in Pisa from 12th to the 18th June.

one sees from the examples of events shown in Fig. 2.

For a given pressure, the efficiency of each neon tube depends, of course, on the strength of the electric field, E, and on the delay, τ, between the occurrence of the event and the rise of the pulses generating the field. For $\tau < \sim 1$ μs, the order of 0.1 s. It certainly depends on the nature of the filling gas. However, use of other than inert gases inside the tubes, is contra-indicated because the recombination time is then much shorter, and would require a considerably faster response.

A three-dimensional reproduction of

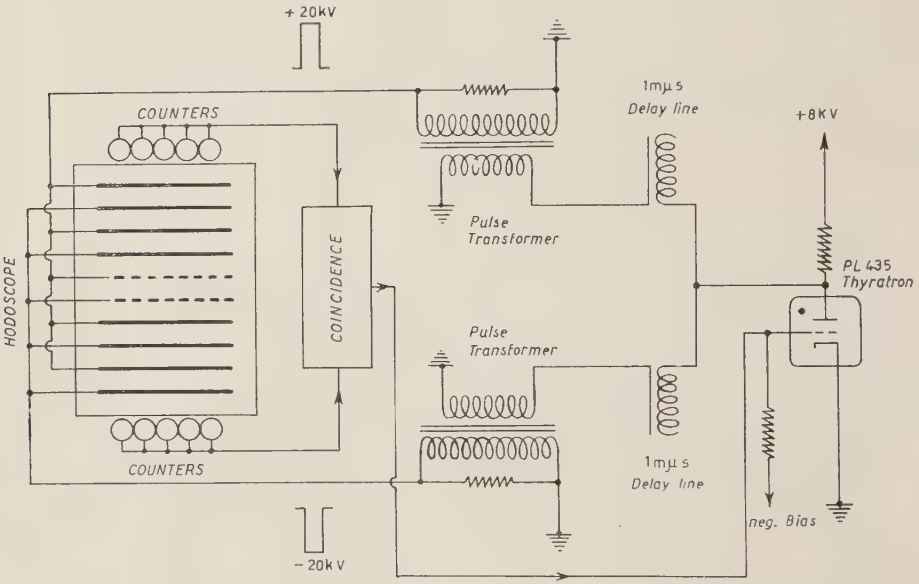

Fig. 1. – Schematic diagram of the hodoscope chamber at the triggering circuits.

no appreciable change has been found experimentally, however, varying E from 5 to 10 kV/cm. This gives an idea of the stability of the device. For $E \approx$ $\approx$ 8 kV/cm, the efficiency starts to decrease when τ exceeds 5 μs. It can be shown that in our conditions the decrease in efficiency with increasing τ_1 is essentially due to diffusion of the free electrons to the glass walls, where they are captured with a high probability.

If a tube is discharged at the instant zero by the pulse produced by a particle crossing it, a second pulse occurring at the instant t will set it alight again, if $t < T$, even if caused by a particle not crossing the tube. For the neon tubes used by us, the recovery time, T, is of

the tracks of ionizing particles can be obtained by arranging the neon tubes in alternating layers perpendicular to each other and taking photographs in two directions at right angles.

The spatial resolution of the instrument can be increased by decreasing the diameter and the wall thickness of the neon tubes. In order to keep the efficiency constant, the gas pressure and the pulse size must be increased when the diameter is decreased. We think, however, that the internal diameter of each tube could be reduced to 2 or 3 mm without difficulty.

The sensitive volume of the instrument here described is $22 \times 44 \times 56$ cm^3. It could be increased by a large factor

A

B

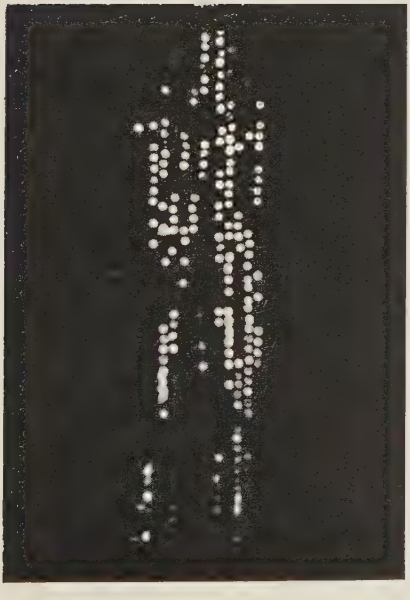

C

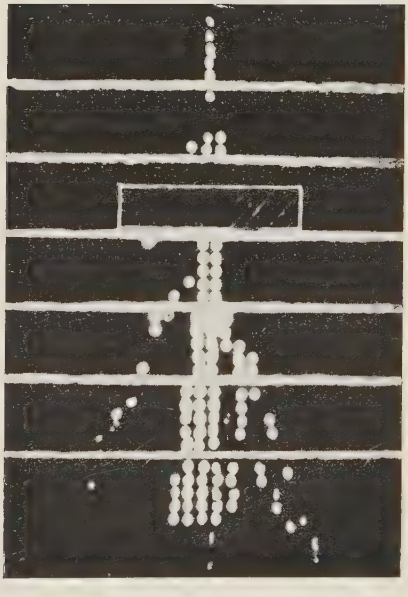

D

Fig. 2. – *A*) Example of a single particle (presumably a μ-meson) crossing the hodoscope chamber; *B*) Example of a shower produced by a neutral particle in one of the Al plates; *C*) Example of an air shower; *D*) Example of a shower produced by an electron and developping in the Pb and Al plates, marked in this photo (the Pb block is placed between the 2nd and 3rd Al plates from the top).

without changing the electronic equipment, since this supplies pulses of such low impendance as to be unaffected by the capacitance of the chamber.

The possibility of making an instrument of comparatively low cost, very small recovery time, with a spatial resolution of a few mm^3 over a volume of the order of one m^3 or more, makes us think that the hodoscope chamber may be of great help in certain types of experiments. Such would be experiments performed in connection with large cosmic ray showers, penetrating showers and underground investigations, as well as in research with accelerators, when the knowledge of angular distributions of particles is essential. If employed in a magnetic field, in conjunction with fast electronics, the instrument may possibly be applied even to look for rare events, since the product of its spatial and time resolutions tends to have a more favorable value then that of the equivalent quantity for other detectors of nuclear events.

Current Density in Heisenberg Representation.

M. Cini and S. Fubini

Istituto di Fisica dell'Università - Torino
Istituto Nazionale di Fisica Nucleare - Sezione di Torino

(ricevuto il 18 Giugno 1955)

In a previous paper [1] a simple method has been sketched in order to derive a set of non linear integral equations between renormalized transition matrix elements. In this paper, starting from a more rigorous reformulation of the method, we obtain some essentially new results concerning the properties of the current density Heisenberg operator $\boldsymbol{j}$ and its relationship to the Low equations [2].

Let us consider the Hamiltonian in the Schrödinger representation:

$$H = H_0 + H' + H_e(t) , \tag{1}$$

where H_0 is the free Hamiltonian with observed masses, H' the interaction Hamiltonian with the appropriate renormalization counter terms [3] and

$$H_e(t) = \int \mathrm{d}^3\boldsymbol{x}\, j(\boldsymbol{x})\, \varphi_e(\boldsymbol{x}t) \tag{2}$$

is the interaction Hamiltonian of the fermion field with an external boson field. The standard interaction representation equation is

$$i\frac{\mathrm{d}U}{\mathrm{d}t} = [H'(t) + H_e(t)]\, U(t) . \tag{3}$$

By setting

$$U(t) = U_0(t)\, O(t) , \tag{4}$$

where $U_0(t)$ is the usual collision operator of the coupled fermion and boson quan-

(1) S. Fubini: *Nuovo Cimento*, **2**, 180 (1955).
(2) F. Low: *Phys. Rev.*, **97**, 1392 (1955).
(3) In the following we will neglect the fermion closed loops and therefore no φ^3 and φ^4 renormalization counter terms are considered.

tized fields, one has for $O(t)$ the equation

$$i\frac{\mathrm{d}O}{\mathrm{d}t} = U_0^{-1}(t)\,H_e(t)\,U_0(t)\,O(t)\,. \tag{5}$$

It is well known that

$$\boldsymbol{j}(x) = U_0^{-1}(t)\,j(\boldsymbol{x}t)\,U_0(t) \tag{6}$$

is the current density operator in Heisenberg representation.

The S matrix of our problem is, obviously

$$S = S_0\,O(+\infty, -\infty)\,. \tag{7}$$

Since $\varphi_e(x)$ is a c-number which can be chosen arbitrarily small we can expand $O(+\infty, -\infty)$ in powers of φ_e in the usual way. Then eq. (6) gives

$$S = S_0 - iS_0\int_{-\infty}^{+\infty}\boldsymbol{j}(x)\,\varphi_e(x)\,\mathrm{d}x + (-i)^2 S_0\int_{-\infty}^{+\infty}\int_{-\infty}^{+\infty}\mathrm{d}x\,\mathrm{d}x'\,\boldsymbol{j}(x)\boldsymbol{j}(x')\,\varphi_e(x)\varphi_e(x')\,\eta(x-x')\,, \tag{8}$$

where:

$$\eta(x-x')\begin{cases} = 1 & x_0 > x_0' \\ = 0 & x_0 < x_0'\,. \end{cases}$$

The essential point of our method is the formulation of the Feynman equivalence principle [4] between the external and the quantized boson fields. The physical meaning of such a principle is that in any S matrix element the emission or the absorption of a boson can be replaced by an interaction with an external field whose Fourier component has the same energy-momentum vector. A simple mathematical formulation of this equivalence is:

$$[S, \varphi(y)] = i\int D(z-y)\,\frac{\delta S}{\delta\varphi_e(z)}\,\mathrm{d}z\,. \tag{9}$$

From eqs. (8) and (9) it is easy to derive the following relations:

$$[S_0, \varphi(y)] = S_0\int \mathrm{d}z\,P(z-y)\,\boldsymbol{j}(z)\,, \tag{10}$$

$$[\boldsymbol{j}(x), \varphi(y)] = \int \mathrm{d}z\,D(z-y)[\boldsymbol{j}(x), \boldsymbol{j}(z)]\,\eta(x-z)\,. \tag{11}$$

Clearly in eqs. (10) and (11) the external field does not appear any longer, and therefore their validity is established quite generally.

---

(4) R. P. FEYNMAN: *Phys. Rev.*, **80**, 440 (1951).

Eq. (10) gives the connection between the current density operator $\boldsymbol{j}(x)$ and the scattering matrix S_0. Applying this operator equation to a one nucleon state $\langle n|$ one gets

$$\langle n, y|\, T = \langle n| \int \mathrm{d}z\, D(z-y)\boldsymbol{j}(z)\,, \tag{12}$$

where $\langle n, y|$ represents a dressed nucleon and a dressed meson at the point y and T is the usual transition matrix $D_0 - 1$. This shows that in the case of one nucleon problems T is immediately deduced from $\boldsymbol{j}$. Eq. (11) is a general non-linear equation for $\boldsymbol{j}$. In momentum space eq. (11) takes the form:

$$[\boldsymbol{j}(\boldsymbol{p}, p_0), a^*(\boldsymbol{k})] = \int \mathrm{d}k_0 \left\{ \frac{\boldsymbol{j}(\boldsymbol{p}, k_0)\boldsymbol{j}(\boldsymbol{k}, p_0+\omega_k-k_0)}{p_0-k_0-i\eta} + \frac{\boldsymbol{j}(\boldsymbol{k}, k_0)\boldsymbol{j}(\boldsymbol{p}, p_0+\omega_k-k_0)}{\omega_k-k_0+i\eta} \right\}. \tag{13}$$

By expressing this operator in terms of normal products of dressed particles creation and destruction operators, and equating their coefficients an infinite set of coupled non linear equations can be obtained. If only normal products $:\bar{\psi}(\boldsymbol{p})\psi(\boldsymbol{p}'):$ and $:\bar{\psi}(\boldsymbol{p})\psi(\boldsymbol{p}')\varphi(\boldsymbol{k}):$ are considered in the developemnt of $\boldsymbol{j}$ one obtains Low's equation ([5]).

An equivalence principle analogous to Eq. (9) holds also for the operator $U(t)$. The equation corresponding to (10) is:

$$[U_0(t), \varphi(y)] = iU_0(t) \int \mathrm{d}z\, D(z-y)\boldsymbol{j}(z)\,\eta(t-z_0)\,. \tag{14}$$

We can introduce a « generalized » Heisenberg operator

$$\boldsymbol{\varphi}_t(y) = U_0^{-1}(t)\varphi(y)U_0(t)$$

in which t is generally different from y_0. Then eq. (14) can be written

$$\boldsymbol{\varphi}_t(y) = \varphi(y) - i\int \mathrm{d}z\, D(z-y)\,\eta(t-z_0)\boldsymbol{j}(z)\,, \tag{15}$$

which obviously reduces to the equation of motion for the Heisenberg operator $\boldsymbol{\varphi}(y)$ when $t = y_0$.

Eq. (11) takes, by making use of eq. (15), the simple form

$$[\boldsymbol{j}(x), \varphi_t(y)] = 0 \qquad \text{for} \quad x_0 = t.$$

We are grateful to Prof. G. WATAGHIN for his kind interest in this investigation.

([5]) The difference in the infinitesimal imaginary term in the denominators arises from the difference between the two Heisenberg operators (defined in F. J. DYSON: *Phys. Rev.*, **82**, 428 (1951) $\boldsymbol{j}(x)$ and $\boldsymbol{j}_F(x)$. Low's equation refers to the matrix elements of the latter).

LIBRI RICEVUTI E RECENSIONI

W. YOURGRAU and S. MANDELSTAM – *Variational Principles in Dynamics and Quantum Theory*; London, Sir Isaac Pitman & Sons, Ltd., 1955.

Gli autori si propongono di coordinare in questo piccolo volumetto gli aspetti storici, matematico-fisici e filosofici dei principi variazionali. Nel primo paragrafo, dal titolo « Prolegomena », vengono ricordate idee e concezioni di PITAGORA, PLATONE, ARISTOTILE, OCKHAM, COPERNICO, KEPLERO, GALILEO, NEWTON, LEIBNIZ, MALEBRANCHE, BACONE, tutte intorno alla solita questione sulla eventuale semplicità della natura e delle sue leggi. Il resto del piccolo volumetto è dedicato all'analisi cronologica dei diversi contributi individuali alla evoluzione dei principi di minimo. Questa analisi dovrebbe mostrare come un canone metafisico si sia andato man mano evolvendo in una legge esatta della natura. Vengono così discussi il principio di Fermat (che nel caso particolare della riflessione su uno specchio piano risale ad ERONE di Alessandria, vissuto un poco prima, c'è chi dice nel I secolo a.C.). il principio di Mapertuis, i successivi sviluppi dovuti ad EULERO e LAGRANGE, le equazioni di Lagrange e di Hamilton, le trasformazioni di contatto, le equazioni canoniche di Hamilton, la forma hamiltoniana delle equazioni della elettrodinamica classica. Infine viene discusso il ruolo che hanno avuto questi risultati nello sviluppo della teoria dei quanti. È opinione degli autori che i principi variazionali non occupino in meccanica quantistica un ruolo preminente quale essi hanno in meccanica classica. Occorre però dire che argomenti come, ad esempio, la recente formulazione della teoria dei campi basata sul principio di azione, restano di gran lunga al di fuori del contenuto di questo volumetto. Il carattere principale della esposizione vuole essere storico-critico.

R. GATTO

A. DAUVILLIER – *Le magnétisme des Corps Célestes - Aurores polaires et luminescence nocturne*; N° 1210 delle « Actualités Scient. et Industr. ». Hermann, Paris, 1954.

Con questo fascicolo, di 143 pagine, 53 figure e una tavola fuori testo, si chiude una interessante sintesi delle attuali conoscenze in quel particolare campo della fisica cosmica che più strettamente si collega al magnetismo celeste.

Questa sintesi, iniziata dall'A. nei fascicoli 1208 e 1209 (già recensiti nel *Nuovo Cimento*, a pag. 959 del vol. XII, 1954), termina ora con lo studio delle aurore polari e della luminescenza notturna.

In un primo capitolo viene fatta una dettagliata descrizione di questi fenomeni, della distribuzione geografica e della frequenza delle aurore polari, e dei vari metodi impiegati nella osservazione e registrazione.

Il secondo capitolo è dedicato ai risultati dello studio spettrografico delle aurore e della luminescenza notturna, e alle deduzioni che se ne possono trarre, specialmente sulla natura e composizione dell'alta atmosfera.

Il problema della altitudine cui i suddetti fenomeni si presentano è quindi discusso nel capitolo terzo, mettendo a raffronto i molteplici, e non sempre concordi, risultati di queste difficili determinazioni.

Il capitolo quarto, che tratta delle periodiche variazioni di intensità e frequenza di apparizione delle aurore è interessante per l'evidenza con cui certe periodicità si possono ricollegare ad analoghe periodicità riscontrate nel nostro sistema solare. Accanto ad una variazione con periodo di 24 ore e ad una con ciclo annuale, se ne notano infatti alcune con periodo di 27 giorni, quindi in evidente connessione colla rotazione solare, ed altre con periodo undecennale.

Alle perturbazioni magnetiche, e a quelle della ionosfera ed hertziane, che appaiono associate alle aurore polari, sono pure dedicate alcune pagine.

Il capitolo quinto passa in rassegna, infine, le varie teorie che dalla fine del secolo scorso sono state sviluppate per spiegare i fenomeni aurorali, e si diffonde in particolare su quella di Birkeland-Störmer e su quelle sviluppate in base alle esperienze di Villard e di altri autori.

Viene pure discussa la natura e l'origine dei corpuscoli aurorali (primari e secondari), cercando di ricavare dei dati sul limite della atmosfera terrestre, che teoricamente dovrebbe estendersi per 5-6 raggi terrestri a partire dalla superficie del globo: questo ultimo risultato è confrontato con quanto trovato a mezzo di razzi V2, fino a 220 km di altezza. Pressione, temperatura e densità di questi alti strati sono presi in considerazione infine per esaminare la consistenza delle ipotesi che localizzano in tali strati alcuni tipici fenomeni di assorbimento sia degli elettroni solari, sia delle radiazioni ultraviolette.

Anche questo volume, come i due precedenti, si presenta ampiamente documentato dal punto di vista bibliografico, così da costituire una messa a punto veramente utile di queste interessanti parti della Fisica cosmica.

A. Drigo

Direttore responsabile: G. POLVANI Tipografia Compositori - Bologna

Questo fascicolo è stato licenziato dai torchi il 28-VI-1955